

THE STRATIGRAPHY AND STRUCTURAL HISTORY  
OF THE MESOZOIC AND CENOZOIC OF THE CENTRAL  
NOVA SCOTIAN SLOPE, EASTERN CANADA

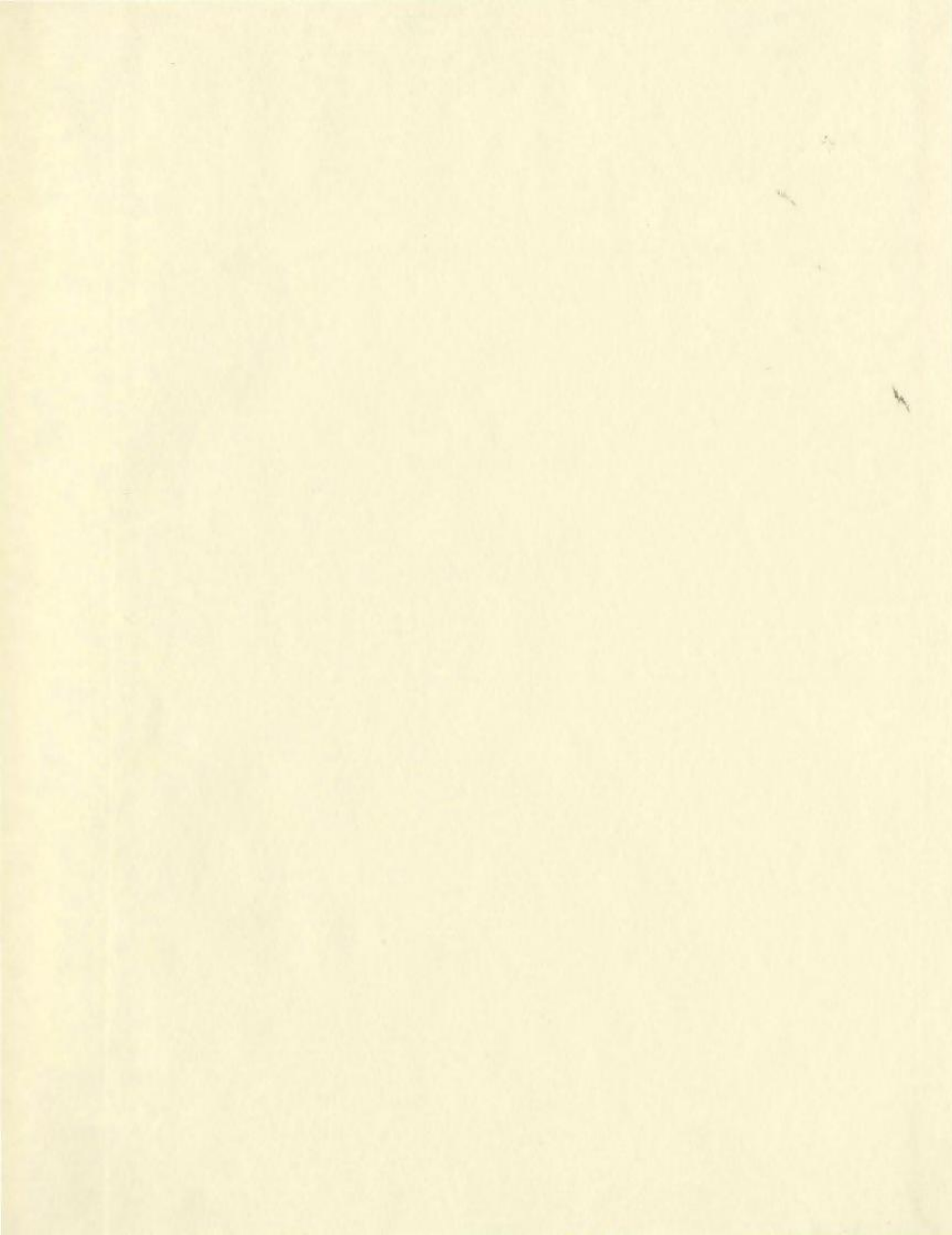
CENTRE FOR NEWFOUNDLAND STUDIES

---

**TOTAL OF 10 PAGES ONLY  
MAY BE XEROXED**

(Without Author's Permission)

JENNIFER LEIGH YOUNG





THE STRATIGRAPHY AND STRUCTURAL HISTORY  
OF THE MESOZOIC AND CENOZOIC OF THE CENTRAL  
NOVA SCOTIAN SLOPE, EASTERN CANADA

by

© Jennifer Leigh Young, B.Sc. (honours)

A thesis submitted to the School of Graduate Studies in partial fulfillment of  
the requirements for the degree of  
Masters of Science

Department of Earth Sciences  
Memorial University  
April 2005

St. John's

Newfoundland and Labrador





Library and  
Archives Canada

Bibliothèque et  
Archives Canada

0-494-06673-3

Published Heritage  
Branch

Direction du  
Patrimoine de l'édition

395 Wellington Street  
Ottawa ON K1A 0N4  
Canada

395, rue Wellington  
Ottawa ON K1A 0N4  
Canada

*Your file* *Votre référence*

*ISBN:*

*Our file* *Notre référence*

*ISBN:*

#### NOTICE:

The author has granted a non-exclusive license allowing Library and Archives Canada to reproduce, publish, archive, preserve, conserve, communicate to the public by telecommunication or on the Internet, loan, distribute and sell theses worldwide, for commercial or non-commercial purposes, in microform, paper, electronic and/or any other formats.

The author retains copyright ownership and moral rights in this thesis. Neither the thesis nor substantial extracts from it may be printed or otherwise reproduced without the author's permission.

#### AVIS:

L'auteur a accordé une licence non exclusive permettant à la Bibliothèque et Archives Canada de reproduire, publier, archiver, sauvegarder, conserver, transmettre au public par télécommunication ou par l'Internet, prêter, distribuer et vendre des thèses partout dans le monde, à des fins commerciales ou autres, sur support microforme, papier, électronique et/ou autres formats.

L'auteur conserve la propriété du droit d'auteur et des droits moraux qui protège cette thèse. Ni la thèse ni des extraits substantiels de celle-ci ne doivent être imprimés ou autrement reproduits sans son autorisation.

---

In compliance with the Canadian Privacy Act some supporting forms may have been removed from this thesis.

Conformément à la loi canadienne sur la protection de la vie privée, quelques formulaires secondaires ont été enlevés de cette thèse.

While these forms may be included in the document page count, their removal does not represent any loss of content from the thesis.

Bien que ces formulaires aient inclus dans la pagination, il n'y aura aucun contenu manquant.

  
**Canada**



## Abstract

The continental shelf and slope of Nova Scotia is underlain by a number of interconnected rift sub-basins that collectively form the Scotian Basin. Petroleum exploration companies have been moderately successful on the shelf region of the basin, close to Sable Island, where several significant hydrocarbon discoveries have led to the development of the Sable Project. This success has sparked interest in exploration of the adjacent frontier slope region within water depths between 200 and 2500m. However, the Scotian Slope Basin has been the focus of only limited regional geologic studies. Present accounts of the slope are largely extrapolated from shelf descriptions and/or modeled after play types and depositional systems typically associated with deep water exploration in other Atlantic margin areas. A discrete study area was defined for this project within the central slope region approximately 125 kilometres southwest of Sable Island. The area is approximately 120 square kilometres and contains five of the ten Scotian Slope exploration wells, three shelf wells and 4 500 kilometres of 2D seismic data.

Scotian Basin development commenced in the Late Triassic - Early Jurassic with rifting of the Pangean Supercontinent and opening of the Atlantic Ocean. Red bed and evaporate deposition characterized the rift phase, while the drift phase was characterized by clastic progradational with periods of carbonate deposition. A prominent carbonate bank developed in the western part of the basin during the Late Jurassic, the eastern extent of which was limited by a Late Jurassic - Early Cretaceous Sable Delta. As relative sea level rose throughout the Late Cretaceous and Tertiary major transgressive sequences were deposited. This overall transgression was punctuated by major sea level drops resulting in the deposition of regressive lowstand sequences partially comprising turbidite deposits.

Seismic stratigraphic analysis of the study area identified ten major sequence boundaries on the basis of reflection character and termination patterns. The sequence boundaries divide the Mesozoic through Cenozoic Scotian Slope Basin fill into nine depositional sequences. There are major changes in depositional style and thickness distribution patterns of the depositional sequence through time. Depositional patterns are closely linked to the tectonic, structural and halotectonic evolution of the basin.

Five fault families were defined within the study on the basis of their regionality, duration of movement and depths of detachment; the Slope Basin-Bounding Fault Family, the Basement-Involved Fault Family, the Listric Growth Fault Family, the Major and Minor Sedimentary Fault Family and the Halokinetically Induced Fault Family. The existence of a sixth fault family, the Transfer Fault Family, is implied by local structural and stratigraphic architecture, however, the signature of this potential transfer fault is not clear enough on the available seismic data to allow for confident mapping.

The complete spectrum of salt structures typical of passive margins has been identified and mapped within the study area. Five halotectonic structural associations with variable areal distributions have been identified. These associations are: the Trough and Swell Association, the Intra-Salt Detachment Association, the Diapiric Association, the Secondary Weld Association, and the Allochthonous Salt Association.

The integration of seismic stratigraphic, structural and halotectonic analysis of the study area allowed for several conclusions regarding implications of a potential Scotian Slope petroleum system to be proposed. Considering all the elements and processes necessary for working hydrocarbon system, the most likely plays within the mapped study area consist of: 1) a reservoir of Cretaceous to Tertiary turbidite channel, levee or lobe sands, 2) a source rock most likely within the Kimmeridgian Verrill Canyon Formation (possible contribution from Jurassic Mohican Formation or Late Triassic to Early Jurassic early Syn-rift and/or Post-rift Lacustrine deposits, 3) a seal of Verrill Canyon Formation, Dawson Canyon or Banquereau shale or allochthonous salt, and 4) structural, tectonic and/or halokinetic traps ranging from Triassic to Cretaceous in age.

Failure to discover hydrocarbons in recent slope explorations wells may point to the limitations of seismic resolution to predict reservoirs within the late Jurassic-Early Cretaceous successions. It also shows that drilling on the Scotian Slope is high risk exploration; more regional and better correlation of seismic with lithologies encountered in the wells are needed.



## Acknowledgements

I would like to start by thanking Andy Pulham for making this project possible. I am very fortunate that he, together with Elliott Burden, Ralph Rudser and Tom Koleszar, thought up this project over a “lively supper” and accepted me as a willing graduate student. Andy has taken care of most of the logistics of this project and provided valuable guidance as well as partial funding. I would like to say thank-you to Tom Calon for his time and guidance, especially with respect to structural interpretation. I would also like to thank Michael Enachescu for his enthusiasm and willingness to share his expertise, speedy and thorough revisions, and general encouragement, all of which I am extremely grateful for.

I would like to acknowledge Kim Abdallah of TGS-NOPEC and Ralph Rudser of BP Canada as being instrumental in facilitating the data access for this thesis. I would like to thank TGS-NOPEC for providing the seismic data set and Landmark for donating to Memorial University the interpretation software used in this study. I would like to acknowledge BP Canada Corporation for partially funding the project and providing digital well data. I am very grateful for the primary funding provided by PanAtlantic Petroleum Systems Consortium. Thank-you to the Geologic Survey of Canada Atlantic for providing access to their Basin Data Base, to EnCana Corporation and John Hogg for providing Figure 2-10, and to Seismic Micro-Technologies and Geo-Logic Systems who donated software.

A very big thank-you is owed to Tony Kocurko who gave so much of his time to loading data and general trouble shooting. A special thanks to Ali Aksu for always

leaving his door open and helping me see the light at the end of the tunnel when things became overwhelming. I would also like to thank a number of people who gave helpful discussions, instructions and/or technical assistance: Ian Atkinson, Sharon Deemer, Rick Hiscott, Rudi Meyer, Ray Pätzold, Darren Smith, Krista Solvason, Jim Wright and Richard Wright. I would also like to thank Gerchard Pfau, Don Tanasichuck and the rest of the 2002 BP Canada East Coast Team for their encouragement, guidance and helpful discussions. Thanks to the many student colleagues that I have met and had the pleasure to work and/or procrastinate with and who have helped to make this experience pleasurable. Thanks to my officemate Rodrigo Sala for stimulating conversations, encouragement, great coffee breaks, and for putting up with me.

Thank you to my mother Marie Young, father and stepmother Richard and Wanda Young and my brother Philip Young who have always believed in me. Without their unconditional support I could never have accomplished what I have. Last but not least, I would like to thank Cory St. Croix whose love, support, and self-sacrifice have been my inspiration.



## Table of Contents

|   |    |
|---|----|
| Title Page  | i  |
| Abstract  | ii |
| Acknowledgements  | iv |
| List of Figures   | ix |
| <br><u>Chapter 1: Introduction</u>                          |    |
| 1.1 Introduction to the Scotian Slope                       | 1  |
| 1.2 Background and Previous Work                            | 4  |
| 1.3 Purpose   | 7  |
| 1.4 Research Objectives                                     | 10 |
| 1.5 Data and Methods  | 10 |
| <br><u>Chapter 2: Geography, Stratigraphy and Structure</u> |    |
| 2.1 Geography   | 18 |
| 2.2 Regional Geology  | 20 |
| 2.3 Stratigraphy and Mesozoic Basin Development             | 21 |
| 2.4 Structural Styles and Geometry                          | 33 |
| 2.4.1 Thick Skin Deformation                                | 33 |
| 2.4.2 Thin Skin Deformation                                 | 37 |
| 2.4.3 Halotectonics   | 39 |
| <br><u>Chapter 3: Seismic Stratigraphy</u>                  |    |
| 3.1 Introduction  | 42 |
| 3.2 Well Control  | 42 |
| 3.2.1 Synthetic Seismograms                                 | 44 |
| 3.2.2 Correlating Seismic Events                            | 44 |
| 3.3 Seismic Stratigraphy                                    | 50 |
| 3.3.1 Top Basement Marker                                   | 53 |
| 3.3.2 Tr1 Sequence Boundary                                 | 55 |
| 3.3.3 Depositional Sequence 1                               | 57 |

|        |                              |    |
|--------|------------------------------|----|
| 3.3.4  | Tr2 Sequence Boundary        | 57 |
| 3.3.5  | Depositional Sequence 2      | 60 |
| 3.3.6  | J1 Sequence Boundary         | 65 |
| 3.3.7  | Depositional Sequence 3      | 68 |
| 3.3.8  | J2 Sequence Boundary         | 69 |
| 3.3.9  | Top Abenaki Formation Marker | 72 |
| 3.3.10 | Depositional Sequence 4      | 73 |
| 3.3.11 | The O Marker                 | 77 |
| 3.3.12 | K1 Sequence Boundary         | 78 |
| 3.3.13 | Depositional Sequence 5      | 79 |
| 3.3.14 | T0 Sequence Boundary         | 82 |
| 3.3.15 | Depositional Sequence 6      | 85 |
| 3.3.16 | T1 Sequence Boundary         | 87 |
| 3.3.17 | Depositional Sequence 7      | 89 |
| 3.3.18 | T2 Sequence Boundary         | 91 |
| 3.3.19 | Depositional Sequence 8      | 91 |
| 3.3.20 | T3 Sequence Boundary         | 95 |
| 3.3.21 | Depositional Sequence 9      | 97 |
| 3.3.22 | Water bottom                 | 99 |

#### Chapter 4: Tectonics

|       |  |     |
|-------|--|-----|
| 4.1   | Introductory Remarks                     | 101 |
| 4.2   | Structural Elements                      | 101 |
| 4.2.1 | Slope Basin-Bounding Fault Family        | 107 |
| 4.2.2 | Basement-Involved Fault Family           | 108 |
| 4.2.3 | Listric Growth Fault Family              | 114 |
| 4.2.4 | Major and Minor Sedimentary Fault Family | 117 |
| 4.2.5 | The Halokinetically Induced Fault Family | 122 |
| 4.2.6 | The Transfer Fault Family                | 124 |

#### Chapter 5: Salt Tectonics

|     |  |     |
|-----|--|-----|
| 5.1 | Mechanics and Geometries of Salt Deformation       | 125 |
| 5.2 | Map Distribution and Style Characteristics of Salt | 132 |



|  |   |     |
|--|---|-----|
| 5.3  | Halotectonic Structural Associations              | 136 |
| 5.3.1  | The Trough and Swell Association                  | 136 |
| 5.3.2  | The Intra-Salt Detachment Association             | 137 |
| 5.3.3  | The Diapiric Association                          | 142 |
| 5.3.4  | The Secondary Weld Association                    | 155 |
| 5.3.5  | The Allochthonous Salt Association                | 158 |
| 5.4  | Kinematic Analysis of Salt Structures             | 170 |
| 5.4.1  | Introduction                                      | 170 |
| 5.4.2  | Salt Movement and Sedimentation                   | 173 |
| <br><u>Chapter 6: Evolution of the Scotian Slope Basin: Discussion</u> |   |     |
| 6.1  | Evolution of the Scotian Slope Basin              | 184 |
| 6.1.1  | Pre-Mesozoic                                      | 184 |
| 6.1.2  | Late Triassic to Early Jurassic                   | 190 |
| 6.1.3  | Middle to Late Jurassic                           | 193 |
| 6.1.4  | Cretaceous  | 196 |
| 6.1.5  | Tertiary  | 198 |
| 6.1.6  | Quaternary  | 200 |
| 6.2  | Implications for a Scotian Slope Petroleum System | 202 |
| <br><u>Chapter 7: Conclusions and Recommendations for Future Work</u>  |   |     |
| 7.1  | Justifications for the Study                      | 214 |
| 7.2  | Key Conclusions                                   | 215 |
| 7.3  | Recommendations for Future Work                   | 220 |
| <br><u>References</u>  |   | 221 |

## List of Figures (Short Titles)

|      |   |    |
|------|---|----|
| 1-1  | Bathymetry, political boundaries, petroleum exploration licenses and study area of the Nova Scotia continental margin | 2  |
| 1-2  | Comparative stratigraphic chart of Scotian Basin and Atlantic margin analogs  | 9  |
| 1-3  | Basemap of TGS-NOPEC seismic data used in study   | 11 |
| 1-4  | Example TGS-NOPEC seismic line  | 13 |
| 1-5  | Basemap of Lithoprobe seismic data used in study  | 14 |
| 1-6  | Basemap of exploration wells located on the Scotian Slope and those within study area                                 | 16 |
| 2-1  | Regional Tectonic Elements of Atlantic Canada   | 19 |
| 2-2  | Schematic cross-section A-A' through Scotian Basin  | 22 |
| 2-3  | Lithostratigraphy of the Scotian Shelf  | 23 |
| 2-4  | Cross-section B-B' of Glooscap C-63, Moheida P-15, Mohican I-100 and Acadia K-62 wells                                | 26 |
| 2-5  | Generalized facies distribution of the Abenaki and equivalent formations  | 28 |
| 2-6  | Multibeam bathymetric image of central Scotian Slope  | 32 |
| 2-7  | Basement structure of the Scotian Basin   | 34 |
| 2-8  | Tectonic reconstruction of Orpheus and Scotian basins   | 36 |
| 2-9  | Regional geologic cross-section C-C' across the Scotian Shelf and Slope   | 38 |
| 2-10 | Scotian Margin basemap showing bathymetry, lease block boundaries, study area and salt body distribution              | 41 |
| 3-1  | Seismic profile showing key seismic surfaces (1-10) and other significant surfaces                                    | 43 |
| 3-2  | Synthetic seismogram of the Oneida O-25 well  | 45 |

|      |   |    |
|------|---|----|
| 3-3  | Lithoprobe 88-1a seismic profile  | 47 |
| 3-4  | Generalized Scotian Basin stratigraphy, M.Sc. sequence boundaries or seismic markers, name and correlation confidence, depositional sequences and Deep Sea Drilling Project seismic markers | 49 |
| 3-5  | Seismic profile showing reflection termination patterns of sequence boundaries  | 51 |
| 3-6  | Seismic profile showing example of Top Basement Marker  | 54 |
| 3-7  | Seismic profile and schematic showing relationship between top basement marker, Tr1 and Tr2 sequence boundaries and Depositional Sequence 1   | 56 |
| 3-8  | Time structure map of the Tr2 Sequence Boundary   | 59 |
| 3-9  | Seismic profile D-D' showing seismic tie with Moheida P-15 well   | 61 |
| 3-10 | Seismic line E-E' showing seismic tie with Glooscap C-63, Oneida O-25 and Evangeline H-100 wells  | 62 |
| 3-11 | Seismic section showing typical reflection character of salt  | 64 |
| 3-12 | Time structure map of the J1 Sequence Boundary  | 67 |
| 3-13 | Isochron map of Depositional Sequence 3   | 70 |
| 3-14 | Time structure map of the J2 Sequence Boundary  | 71 |
| 3-15 | Time structure map of the top Abenaki Formation marker  | 74 |
| 3-16 | Isochron map of Depositional Sequence 4   | 76 |
| 3-17 | Seismic line showing relationship between sequence boundaries K1, T0, T1, T2, T3 and depositional sequences 5-9   | 80 |
| 3-18 | Isochron map of Depositional Sequence 5   | 81 |
| 3-19 | Seismic profile showing seismic tie with Shubenacadie H-100 well  | 83 |
| 3-20 | Time structure map of the T0 Sequence Boundary  | 84 |
| 3-21 | Isochron map of Depositional Sequence 6   | 86 |



|      |   |     |
|------|---|-----|
| 3-22 | Time structure map of the T1 Sequence Boundary  | 88  |
| 3-23 | Isochron map of Depositional Sequence 7   | 90  |
| 3-24 | Time structure map of the T2 Sequence Boundary  | 92  |
| 3-25 | Isochron map of Depositional Sequence 8   | 94  |
| 3-26 | Time structure map of the T3 Sequence Boundary  | 96  |
| 3-27 | Isochron map of Depositional Sequence 9   | 98  |
| 3-28 | Time structure map of the water bottom  | 100 |
| 4-1  | Time structure map of the Tr2 Sequence Boundary showing spatial distribution of the Basin-Bounding Fault Family and the Basement-Involved Fault Family  | 103 |
| 4-2  | Seismic profile A-A' with examples of: Basin-Bounding Fault Family, Basement-Involved Fault Family, Listric Growth Fault Family, Major and minor Fault Family, and the Halokinetically induced Fault Family | 105 |
| 4-3  | Seismic profile B-B' showing structure typical of the Basement-Involved Fault Family  | 110 |
| 4-4  | Portion of seismic profile A-A' showing anomalous pre-Mesozoic reflector configuration, and example of similar structure from the Jeanne d'Arc Basin  | 113 |
| 4-5  | Seismic profile with example of Listric Growth Fault Family   | 115 |
| 4-6  | a) Seismic profile with example of a group of related listric faults soling into a common level of detachment, and b) Example of listric growth fault with salt-cored anticline                             | 116 |
| 4-7  | Seismic strike line with example of two major faults detaching on salt  | 118 |
| 4-8  | Close-up of seismic profile A-A' showing major and minor faults   | 121 |
| 4-9  | Seismic strike line showing examples of minor faults associated with pock marks   | 123 |

|      |  |     |
|------|--|-----|
| 5-1  | Block diagram showing schematic shapes of salt structures by structural maturity and size  | 128 |
| 5-2  | Schematic diagram of typical stress and strain domains in a clastic passive continental margin   | 130 |
| 5-3  | Tectono-stratigraphic provinces of the northern Gulf of Mexico Basin   | 131 |
| 5-4  | Time structure map of the top of salt horizon  | 133 |
| 5-5  | Map distribution of halotectonic structural associations and their broad domianial distribution  | 135 |
| 5-6  | A) Section of seismic profile showing example of salt trough and swell,<br>B) Schematic diagram showing relationship between basement faulting and swell formation | 137 |
| 5-7  | Two seismic profile sections showing examples of salt structures typical of the Intra-Salt Detachment association  | 140 |
| 5-8  | Stages of diapir initiation and growth during extension  | 144 |
| 5-9  | Salt structure geometries as controlled by salt supply and sedimentation   | 145 |
| 5-10 | SW-NE seismic strike line A-A' with examples of salt structures typical of the Diapiric association  | 147 |
| 5-11 | SW-NE seismic strike line B-B' with examples of salt structures typical of the Diapiric association  | 148 |
| 5-12 | SW-NE seismic profile C-C' with examples of salt structures typical of the Diapiric association  | 150 |
| 5-13 | SW-NE seismic profile D-D' with examples of salt structures typical of the Diapiric association  | 151 |
| 5-14 | Diapir rejuvenation during contraction   | 153 |
| 5-15 | Portion of NW-SE seismic profile with example of rejuvenated "hourglass" shaped diapir with vertical secondary weld at middle stem                                 | 156 |
| 5-16 | Portion of NW-SE seismic profile with example of inclined secondary weld as feeder to a basinward tilted diapir  | 157 |

|      |   |     |
|------|---|-----|
| 5-17 | End member geometries of allochthonous salt systems   | 160 |
| 5-18 | Seismic strike line E-E' with examples of salt structures typical of the Allochthonous Salt association   | 162 |
| 5-19 | Seismic strike line F-F' with examples of allochthonous salt stocks, coalesced out of the plane of section  | 163 |
| 5-20 | A) Seismic profile G-G' with example of allochthonous stepped counterregional salt tongue, B) Schematic evolution of a stepped counterregional salt tongue system   | 165 |
| 5-21 | Schematic evolution of an allochthonous roho salt tongue system   | 167 |
| 5-22 | Seismic profile H-H' with example of questionable roho salt tongue system   | 168 |
| 5-23 | Seismic profile from the west map area with temporal kinematic stages of diapir evolution highlighted   | 179 |
| 5-24 | Seismic strike line from the western portion of the central slope region with temporal kinematic stages of diapir evolution highlighted   | 181 |
| 5-25 | Seismic strike line from the eastern portion of the central slope region with temporal kinematic stages of diapir evolution highlighted   | 183 |
| 6-1  | Seismic profile from the western map area with 6 tectono-stratigraphic mega-sequences highlighted   | 186 |
| 6-2  | Tectono-stratigraphic compilation chart of the Scotian Basin summarizing lithology, lithostratigraphy, sequence boundaries and depositional sequences, tectono-stratigraphic mega-sequences and structural styles   | 188 |
| 6-3  | Schematic block diagram of the Early Jurassic structure of the study area   | 191 |
| 6-4  | Structuring of salt walls by four types of stress regimes   | 194 |
| 6-5  | A) Portion of seismic profile with example of channel levee, B) Spectrum of turbidite channels contrasting the geometric and depositional attributes of erosional and depositional types as a function of texture and sediment transport, C) Geomorphic elements of a turbidite channel/lobe complex. | 204 |



|     |   |     |
|-----|---|-----|
| 6-6 | Burial history for the western-central Scotian Slope. | 207 |
| 6-7 | Isochron map of Sequence Boundary J2 to Water Bottom. | 208 |

# Chapter 1

## Introduction

### 1.1 Introduction to the Scotian Slope

The Nova Scotian Continental Slope of south-eastern Canada has recently become an attractive frontier region for hydrocarbon exploration (Hogg, 2000). The slope lies southeast of the Nova Scotian Shelf where successful hydrocarbon discoveries and subsequent production have spurred the search for new resources in the adjacent deeper water. The Scotian Slope is approximately 850 kilometers in length and 100 kilometres in width and, therefore, represents a very large exploration region (Figure 1-1). To date, ten exploration wells have been drilled on the slope.

The passive continental margin of Eastern Canada is characterized by a series of deep sedimentary basins above a wide zone of significantly thinned continental crust. Faulting style and basin geometry vary laterally along the margin. The margin evolved subsequent to the Late Triassic rifting of the Pangean super-continent (Tankard and Balkwill, 1989). In the area off Nova Scotia, rifting resulted in a series of interconnected sub-basins that collectively form the Mesozoic Scotian Basin. Ensuing basin development and sediment accumulation created conditions suitable for the generation and preservation of hydrocarbons.

In the Scotian Basin, red bed and evaporite deposition characterized the rift phase, while the drift phase was characterized by typical clastic progradational sequences with periods of carbonate deposition (Kidston et. al., 2002). A prominent carbonate bank

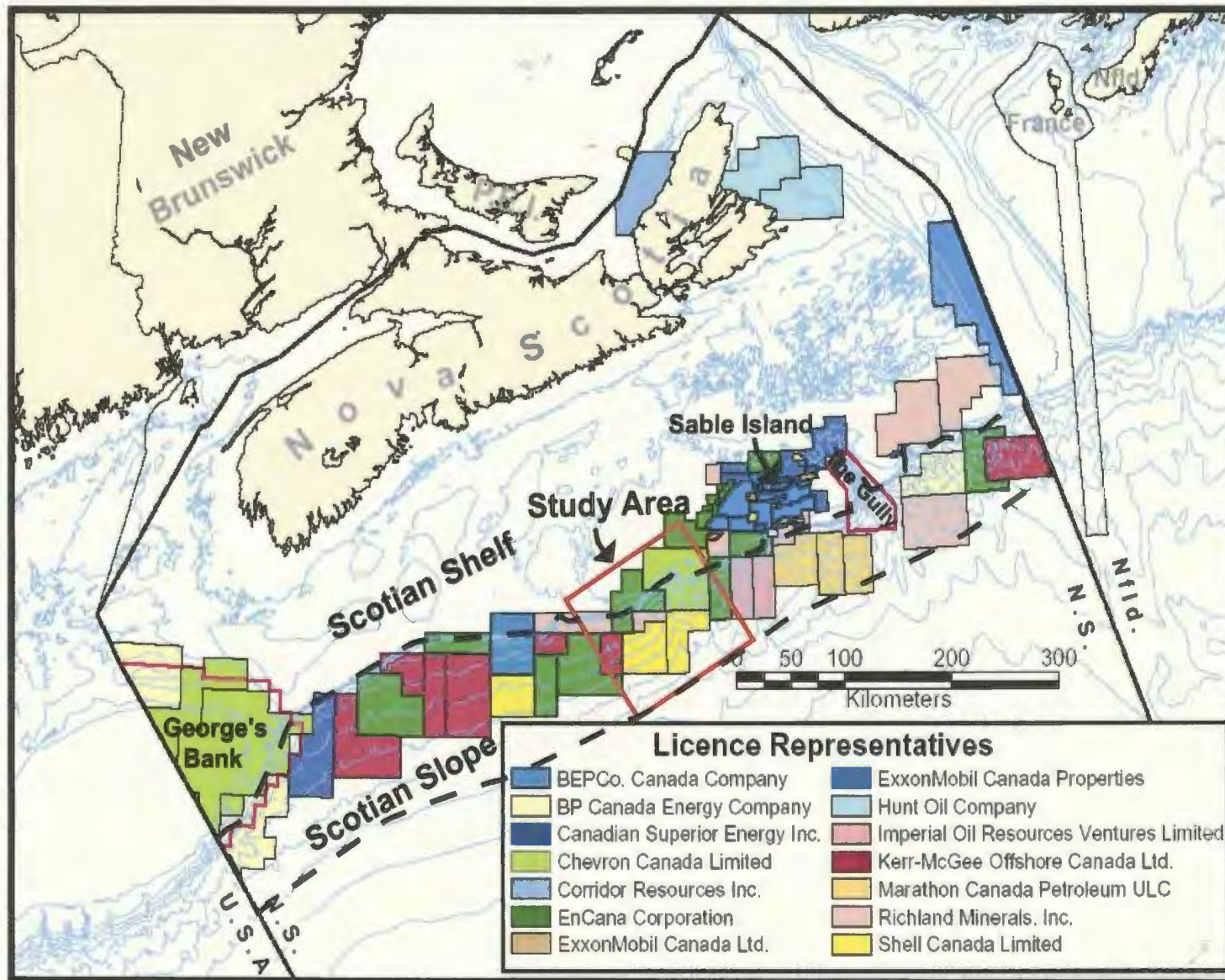


Figure 1-1: Bathymetry, political boundaries, petroleum lease blocks and study area of the Scotian Margin. Figure modified from Canada-Nova Scotia Offshore Petroleum Board (2004).



developed in the western part of the basin during the Late Jurassic, the eastern extent of which was limited by a major deltaic depocenter located in the Sable Island area during the Late Jurassic to Early Cretaceous. Major transgressive sequences were deposited as relative sea level rose throughout the Late Cretaceous and Tertiary (Wade and MacLean, 1990). This overall general transgression was punctuated by major sea level falls resulting in the deposition of regressive lowstand sequences (Kidston et. al, 2002). These potential reservoir sediments were deposited as submarine channels, lobes and fans in areas of accommodation on the slope or basin floor. Movement of Late Triassic- to Early Jurassic-aged salt largely controlled the creation and distribution of accommodation space through the formation of salt withdrawal minibasins. Sediment loading continued to drive halokinesis during the Tertiary resulting in the configuration of salt swells, walls, ridges, and domes seen today.

A regional 2D grid of high quality reflection seismic data has recently been acquired over the Scotian Slope. The detailed analysis of this seismic grid and the integration of seismic stratigraphy with well data are in the early stages and are mostly being undertaken by exploration groups of oil and gas companies and the government regulatory board (Canadian-Nova Scotia Offshore Petroleum Board). The current exploration emphasis is on an improved understanding of the slope seismic stratigraphy, petroleum systems of the region and definition of prospective plays.

## 1.2 Background and Previous Work

There is limited government and academic literature that discusses the Scotian Slope area and setting based on recent drilling information and seismic data. However, there are specific papers that describe and discuss the adjacent Scotian Shelf and regional basins. In recent years exploration groups of several oil and gas companies have produced the majority of publicly available information pertaining to the slope region, mostly as short articles or conference presentations.

Modern exploration of the Scotian Shelf commenced in 1948 when ships of the Lamont Geological Survey, under the direction of Maurice Ewing, carried out seismic refraction surveys across much of Canada's southeastern continental shelf (Sherwin, 1973). The results of this study, and those of two subsequent voyages in 1950 and 1951, were first published in 1954 by Drake et al., Officer and Ewing, and Press and Beckmann. These studies provided evidence that Eastern Canada's Continental Margin was comprised of a thick sedimentary succession overlying a basement complex of high velocity igneous and metamorphic rocks (Sherwin, 1973).

The Canadian Government first became involved in geological investigation of Canada's eastern continental margin in 1955 when the Nova Scotia Research Foundation and Dominion Observatory conducted seismic refraction studies in the Sable Island area. Results of these studies were published by Willomore and Tolmie (1956). In 1964 and 1965 Dalhousie University carried out deep refraction surveys on the Scotian Shelf, continental slope and rise beyond (Barrett et al., 1964; Keen and Loncarevic, 1966).

Areomagnetic surveys of the North Atlantic continental shelf were first conducted by Lamont Geological Survey in 1955 and 1957 and extended by the Geological Survey of Canada (G.S.C) in 1958, 1959 and 1960 over the Scotian Shelf (Sherwin, 1973).

Aeromagnetic mapping and interpretation was reported by Bhattacharyya and Raychaudhuri (1967). Sea magnetometer programs were conducted over the Scotian Shelf by the G.S.C in 1960 and 1963 and described by Bower (1962) and Hood (1966a, 1966b).

The petroleum industry first become actively interested in the petroleum potential of Eastern Canada's continental shelf in 1959, when Mobil Oil Canada conducted both aeromagnetic and seismic surveys of the Sable Island area (Sherwin, 1973). In 1960 Mobil Oil filed in a small block of federal oil and gas permits on and around Sable Island. The situation remained static until 1963, when Shell Canada filed in 20 million acres of federal permits, covering most of the Scotian Shelf (Sherwin, 1973). In 1967, Mobil Oil Canada's Sable Island C-67 was the first well spudded on the Scotian Shelf. It was drilled on Sable Island to a depth of 4 600 m and found minor amounts of oil and gas (GSC Basin Database, 2004). The stratigraphic succession of well C-67 was described by Magnusson (1973).

The continental slope, rise and abyssal plain of Nova Scotia were investigated by Uchupi (1965, 1968, 1969) and Emery and Uchupi (1965) and Emery et al. (1970), using seismic reflection gravity and magnetic data collected by Woods Hole Oceanographic Institute and the United States Geological Survey. In 1970 two publications, one by



Emery et al. and the other by King and MacLean reported the presence of diapiric structures beneath the continental slope off the Scotian Shelf.

McIver (1972), in a major contribution based on information from exploratory wells and processed seismic data, proposed a stratigraphic framework and described the succession underlying the Scotian Shelf. Sherwin (1973) later discussed the geology and hydrocarbon potential of the Scotian Shelf and Grand Banks. Subsequently, through analysis of commercial seismic and well data, the geological framework of the Scotian Shelf was refined by Hardy (1975), Jansa and Wade (1975), Wade and McLean (1990), and Wade et al. (1995). In 1990 Bell and Campbell reexamined the petroleum potential of offshore Eastern Canada, including the Scotian Shelf and slope.

Sea floor bathymetry, sediment instability and other process that are currently shaping the Scotian Slope are the subjects of considerable past and current research by the Geological Survey of Canada (GSC), e.g. (Keen et al., 1991), (Keen and Kay, 1991), (Keen and Potter, 1995), (Pickrill, et. al, 2001), (Piper et. al, 1985, 1999), (Swift, 1987) and Dalhousie University e.g. (Hill and Bowen, 1983), (Berry and Piper, 1993), and (Gauley, 2001).

The GSC, as part of the East Coast Basin Atlas Series (1991), compiled a collection of geological and geophysical studies relating to the Scotian Shelf. An excellent synopsis of the geology and hydrocarbon potential of the deep water Scotian Slope was produced by the Canadian-Nova Scotia Offshore Petroleum Board (Kidston et. al, 2002). Research on the source rock potential of the Scotian Slope is being conducted

by Mukhopadhyay and Wade (1990), Williamson and Smyth (1992), Mukhopadhyay (1995), and Mukhopadhyay et al., (2002)

Commercial 2D reflection seismic collected by various contractors now covers over 30 000 km of the basin, extending from the Georges Banks to the South Whale Basin. Proprietary 3D seismic surveys have been acquired by petroleum exploration companies in localized areas of interest. The detailed analysis of newly acquired seismic and well data is mostly being undertaken within exploration groups of oil and gas companies. EnCana Corporation, formally PanCanadian Petroleum Ltd., has been especially active in exploration and promotion of the Scotian Slope (e.g. Hogg, 2000, 2003); (Hogg et. al., 2001); (Dolph et. al., 2001).

### 1.3 Purpose

There have been few academic studies that concern the geological setting of the Scotian Slope area. Present accounts of the Scotian Slope are largely extrapolated from shelf descriptions and/or modeled after play types and depositional systems typically associated with deep water exploration in other Atlantic margin areas such as the Gulf of Mexico and West Africa.

Exploration within the Scotian Basin has historically focused on the shelf region where play types include rollover anticlines and deep-seated geopressured structures within the clastic rich Mesozoic section (Hogg, 2000; Dolph et. al., 2001). In contrast, unproven play types within the slope will focus primarily on salt-related structures with clastic reservoirs of Cretaceous and Early Tertiary-aged subaqueous channel, channel

levee, submarine fan and turbidite deposits (Dolph et. al., 2001). Explorationists have looked to other Atlantic-facing passive margins to help model the frontier Scotian Slope petroleum system (Figure 1-2). The three primary analogs, the Gulf of Mexico (GOM), offshore Brazil and offshore West Central Africa, all share common geologic history to the Scotian Basin; a pull-apart margin followed by thermal sag and a prograding shelf with a carbonate bank, major river delta and mobile salt substrate. However, these analogs often fail to consider the finer details such as the number of basin sediment input points and resulting impact on the basin development.

Improving the understanding of the regional Petroleum System of the Scotian Slope requires both the detailed analyses of the Late Mesozoic and Tertiary depositional history and the interaction of Late Triassic-Early Jurassic salt and subsequent sediment deposition. A key technical challenge with respect to the construction of new hydrocarbon plays is therefore the construction of predictive models of slope sedimentation and coeval salt tectonics.

Within the central region of the Scotian Basin, the Sable sub-basin and adjacent slope provide an excellent opportunity for analysis of the petroleum system of the Scotian Slope. This central area lies in the axis of the important Mesozoic sedimentary system, but is not overly complicated by salt structures.

A discrete study area has been defined within the central slope region approximately 125 kilometers southwest of Sable Island. The area is approximately 120 square kilometres and contains five of the ten Scotian Slope exploration wells, three shelf wells and 4 500 kilometres of 2D seismic data.



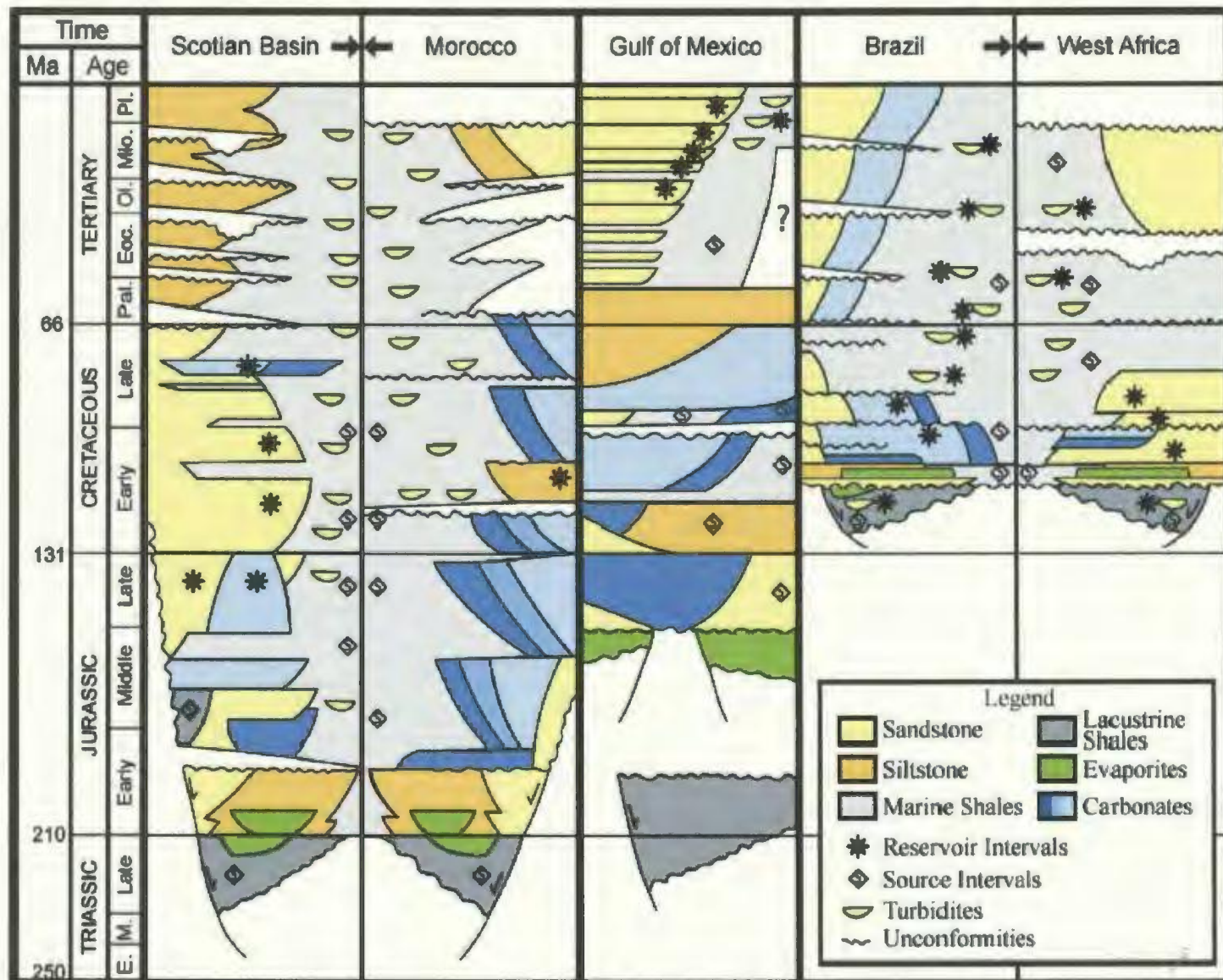


Figure 1-2: Comparative stratigraphic chart of the Scotian Basin and Atlantic Margin Analogs. Source rock and reservoir intervals either confirmed or speculative (figure modified from Kidston et. al., 2001)



## 1.4 Research Objectives

This thesis has three main objectives.

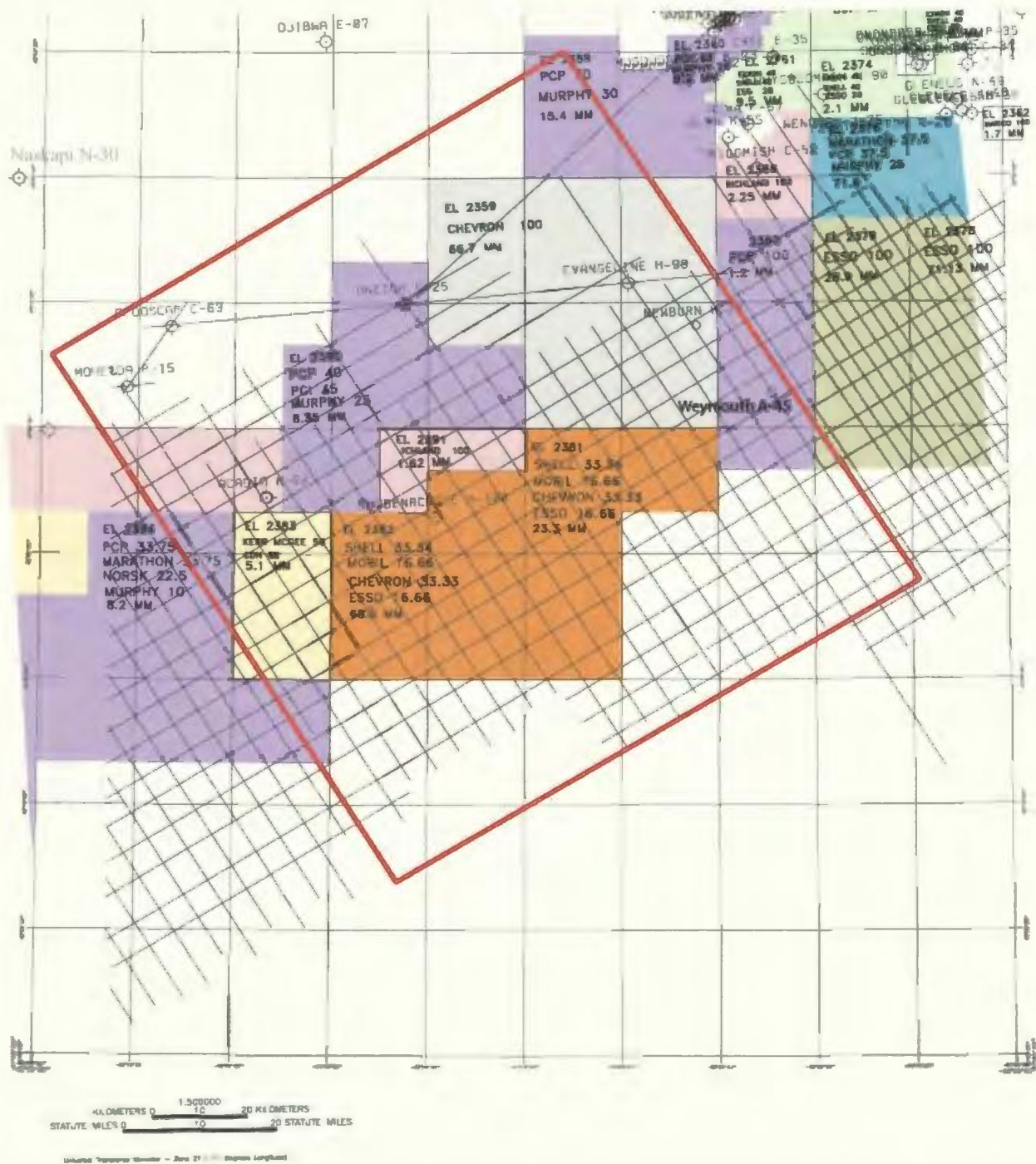
Firstly, a seismic stratigraphic analysis of the Mesozoic and Cenozoic stratigraphy, definition of seismic sequences, tying these sequences to available well data and publicly available information, and developing a framework for the description and interpretation of the depositional history of the slope within the study area.

Secondly, an analysis of the tectonic elements that deform pre-Mesozoic through Quaternary stratigraphy, with particular emphasis on the timing of tectonic deformation in relation to defined seismic stratigraphy packages, and the analysis of the related growth stratal architecture.

A third objective of the research is an analysis of the salt tectonics with reference to the seismic stratigraphy, in order to provide a more integrated stratigraphic analysis of the area. This provides a method for assessment of the importance of salt-sediment interactions across the study area.

## 1.5 Data and Methods

At the request of BP Canada, TGS-NOPEC of Houston, Texas, provided to me a digital data set of approximately 4 500 kilometers of high quality seismic data located over the central Scotian Slope (Figure 1-3). The data included a grid of forty 80-fold 2D seismic lines, each approximately 80-120 kilometers in length, with an average line spacing of approximately six kilometers. The seismic data is of 1998-99 vintage.



The post stack time-migrated seismic data were received in SEG-Y format on 4 mm DAT tapes. Processing of the data was completed by TGS-NOPEC. The data was loaded onto a Sun Microsystems SunFire V880 server housed at Memorial University and interpreted using Landmark® software. Data were recorded to a depth of 14 seconds TWT. Resolution is excellent to a depth of approximately 8 sec TWT above salt and in non-salt areas (Figure 1-4). Where salt was present the expected raypath distortion was profound and not fully compensated for by the post-stack time-domain migration.

Two 60-fold deep crustal seismic lines, 88-1 and 88-1a of the Geological Survey of Canada Lithoprobe dataset, located in or near the thesis study area were also incorporated in the study (Figure 1-5). The lines run northwest-southeast slightly oblique to the TGS-NOPEC dip lines. Line 88-1 is approximately 175 kilometers long, extending far beyond the upper limit of the study area onto the shelf. Line 88-1a extends from the shelf break approximately 200 kilometers, to the abyssal plane. Line 88-1 was particularly useful in this study as it extends past the slope salt province, imaging deep basement structures that are not well resolved when situated below salt.

Using seismic stratigraphic principles (e.g. Vail et al., 1977a, b) key seismic surfaces and events were identified and defined in terms of their reflection termination patterns. The mapping and regional interpretation of sub-salt stratigraphy was limited by poor data quality.

Mapping was based on time migrated seismic data. Thicknesses are therefore described as isochronous and measured in two way travel-time. In order to accurately image geometries, depths and thicknesses, the seismic data would have to be depth



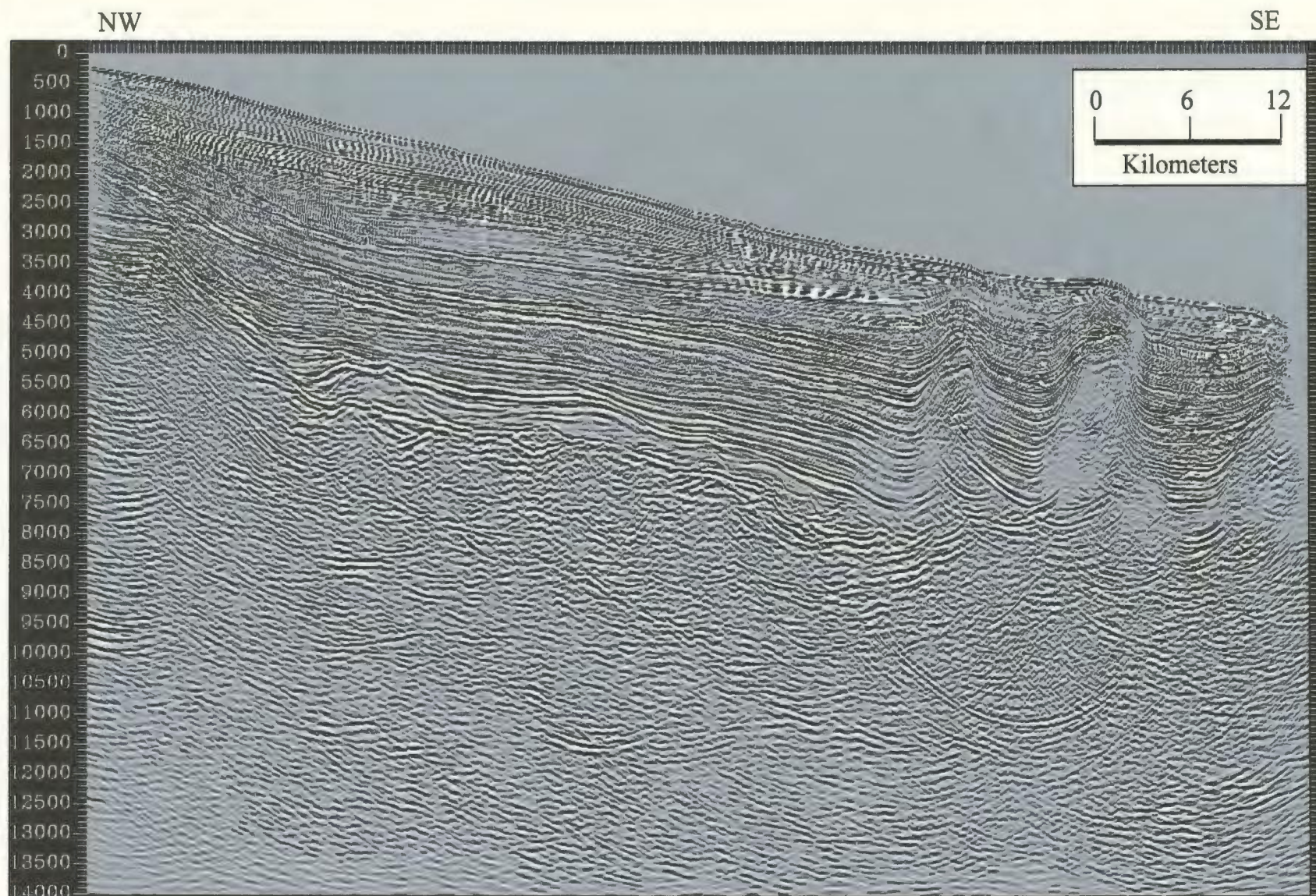


Figure 1-4: Example TGS-NOPEC '98-99 2D seismic dip line. Vertical scale is two way travel time (ms).



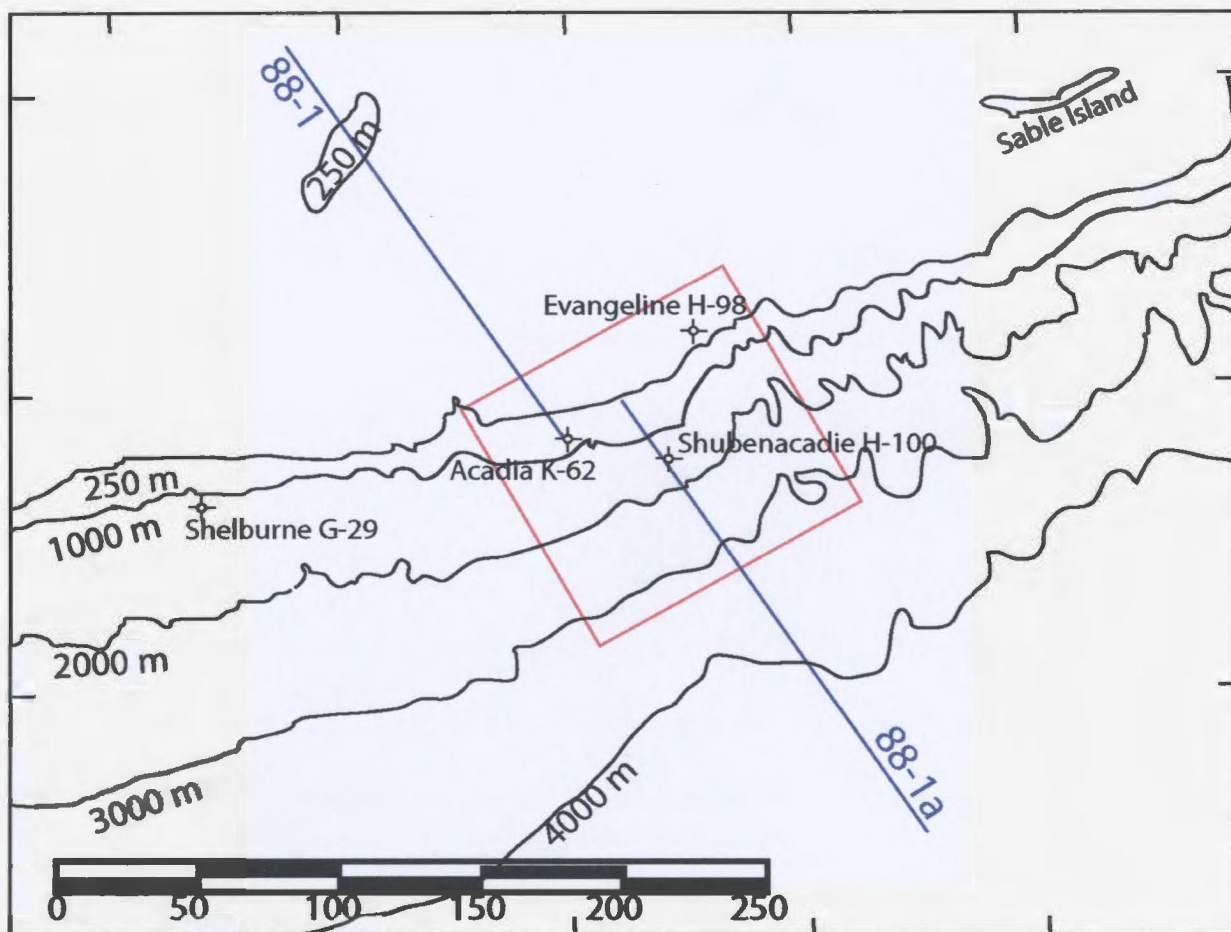


Figure 1-5: Central Scotian Slope basemap showing gross seafloor bathymetry, select exploration wells, Lithoprobe deep seismic lines 88-1 and 88-1a, and study area (red).

converted and migrated using velocity information from wells. This processing was not done as it was outside the objectives of the thesis. The use of time migrated seismic is, however, a standard within both academia and the petroleum industry and, as long as its limitations are acknowledged, is an acceptable means of interpretation.

Guidelines for the interpretation of salt structures and surrounding strata were obtained from salt tectonic and structural models established in works by Jenyon (1986), Jackson and Cramez (1989), Venderville and Jackson (1992a, 1992b), Jackson and Venderville (1994) Letouzey et al. (1995), Ge et al. (1997) and others.

Eight exploration wells are located within the thesis study area: three on the shelf and five on the slope (Figure 1-6). Two of the slope wells, Newburn H-23 and Weymouth A-45, were drilled within the past two years during the completion of this study. Thus, according to regulations, information pertaining to these two wells was held proprietary by the operating companies, Chevron et al. and EnCana et al. respectively, and was not available for public use. BP Canada provided digital density, sonic and checkshot data for five of the remaining wells: Moheida P-15, Glooscap C-63 and Oneida O-25 all located on the shelf, Evangeline H-98 located on the shelf break, and Acadia K-62 located on the slope (Figure 1-6). Digital density and sonic data were provided by BP Canada for the slope well Shubenacadie H-100.

Synthetic seismic sections were created in order to tie seismic and well data. Lithostratigraphic and biostratigraphic data posted on the GSC Atlantic Basin Database (2004) was used to identify and date key seismic surfaces. These surfaces were then used

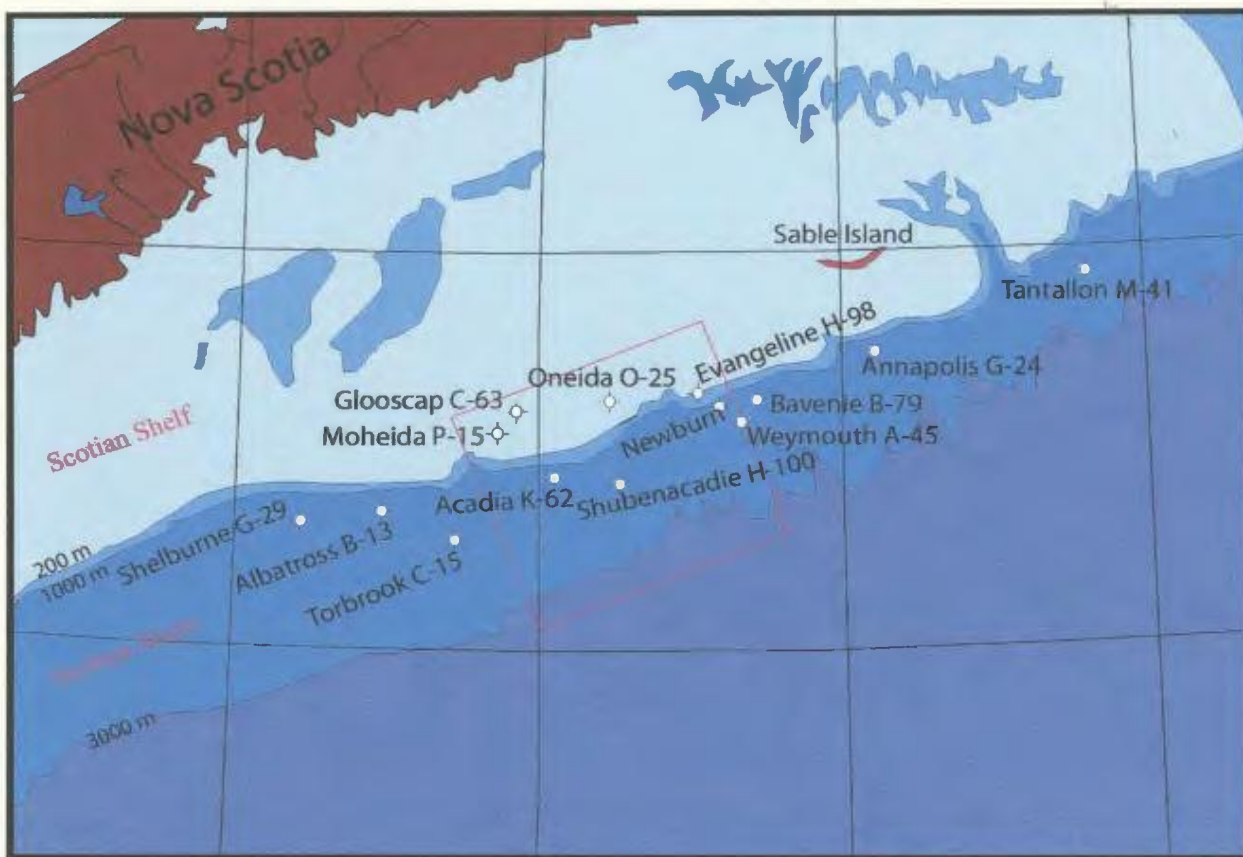


Figure 1-6: Basemap of Scotian Margin showing gross bathymetry, study area (red), Scotian Shelf wells located within study area and location of wells that have tested Scotian Slope targets.

to date the effects of salt tectonics as preserved in the stratigraphic record, thereby providing potential constraints on models of margin evolution.

The results of the study and particulars of research undertaken are presented in Chapters 3, 4, and 5. A discussion is presented in Chapter 6, conclusions and recommendations for further work are presented in and 7. Chapter 2 contains a review of the published regional geological knowledge and structural and stratigraphic understanding of the Scotian Slope. This review provides the necessary framework for the original geoscience work done during the study.



## Chapter 2

### Geography, Stratigraphy and Structure

#### 2.1 Geography

The Scotian Basin extends 1200 kilometers along Atlantic Canada's eastern seaboard from the Yarmouth Arch and the United States border in the southwest to the Avalon Uplift on the Grand Banks of Newfoundland in the northeast (Figure 2-1). The primary structural elements of the Scotian Basin region are typical of a passive continental margin with a shallow basement platform and ridges flanking deep marginal sedimentary basins and farther seaward, beyond the continental shelf and slope, a deep water oceanic basin.

The Scotian Basin has an average width of 250 kilometres and a total area of approximately 300,000 square kilometers. Half of the basin is situated below the present day continental shelf while the other half lies beneath the present continental slope. The Scotian Shelf is defined as the part of the continental margin contained in water depths less than 200 m. The Scotian Slope, representing the transition from the continental shelf to the abyssal plain, extends from the 200 m isobath to depths exceeding 4000 m (Kidston et. al., 2002). The average declivity of the central slope is 2.5° (Sherwin, 1973). Below the slope lies the Slope Diapiric Province, a distinct geological area containing autochthonous and allochthonous salt that trends along the margin of Nova Scotia and into the western Grand Banks. The area north of the Laurentian Channel and the Newfoundland Transfer Fault has geologic affiliation with the Scotian Basin but

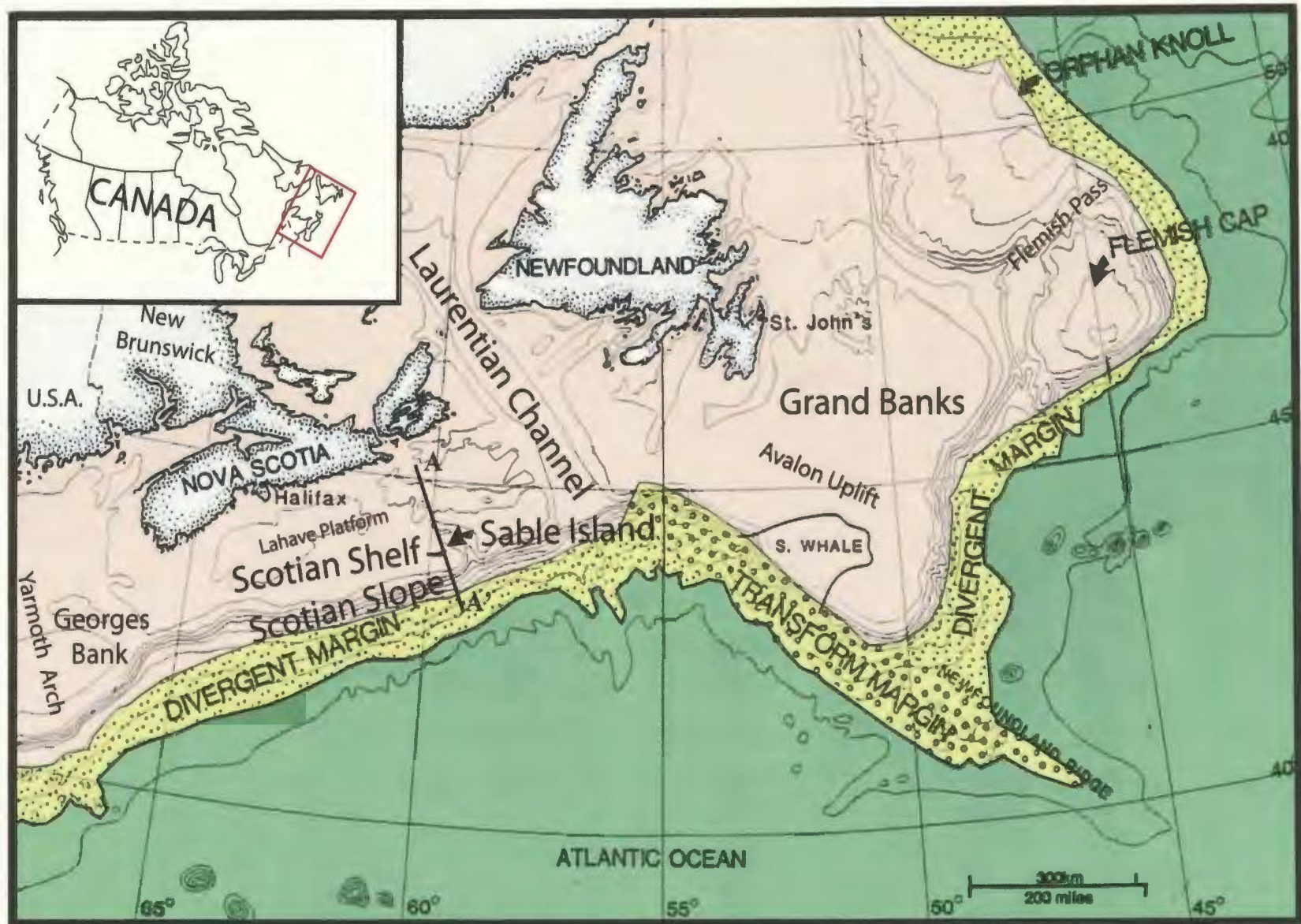


Figure 2-1: Bathymetry and regional plate tectonic setting of the Atlantic Canadian continental margin. Peach represents continental crust underlying the shelf, yellow represents transitional crust, and green represents oceanic crust (figure modified from Enachescu, 1987). Approximate location of cross-section A-A' shown.



is considered part of the Newfoundland continental margin (Enachescu, 1987 and 2004).

## 2.2 Regional Geology

The southeastern seaboard of Canada and its continental margin are underlain by a suite of accretionary terrains and sedimentary basins that record a long history of Paleozoic convergence and Mesozoic extension. Accretion of island-arc and continental terrains to the North American craton began in the Ordovician. By the Permian the Pangean supercontinent had formed about the Appalachian-Caledonide mountain belt (Williams, 1984). The Appalachian orogen was built on an early Paleozoic Atlantic-type margin (Williams, 1984), the shape of which profoundly influenced the pattern of orogenesis and subsequent extension.

The evolution of the North Atlantic Ocean commenced with Triassic rifting resulting in the separation of Africa and North America in the Middle Jurassic (Tankard and Balkwill, 1989). The eastern boundary of this rift is defined by the East Coast Magnetic Anomaly (ECMA); a narrow linear highly magnetic trend of interpreted subareal extrusive volcanism of approximate Bajocian age, believed to mark the boundary between continental and oceanic crust (Dehler and Keen, 2001, 2002). North America and European separation spread northwest between Iberia and the Grand Banks region of offshore Newfoundland in the Early Cretaceous, and finally between the European, Greenland and North American plates in the latest Cretaceous (Enachescu, 1987; Tankard and Welsink, 1989).

Within the area of the Scotian Basin, Late Triassic-Early Jurassic continental extension resulted in a suite of half grabens and intervening basement ridges. Extension was followed by Jurassic-Tertiary ocean spreading and passive margin development (Welsink et al., 1989). During this time the Nova Scotian coastal margin underwent significant postrift or thermal subsidence resulting in deposition of a seaward thickening wedge up to 20 kilometres in thickness (Figure 2-2). This thick sedimentary cover masks much of the underlying rift basin structure (Tankard and Welsink, 1989).

### 2.3 Stratigraphy and Mesozoic Basin Development

During the early Triassic, present day Nova Scotia and the then adjacent Morocco were situated slightly north of the equator as part of the Pangean supercontinent. By the Middle Triassic, approximately 225 Ma, rifting of the super-continent commenced, resulting in a series of narrow, interconnected rift sub-basins separating North America and Africa. On the Nova Scotia margin, the pre-rift basement is formed by Precambrian metamorphic, Paleozoic metasedimentary and igneous rocks of the Meguma Terrane of the Appalachian Orogen (Williams, 1984). The first synrift sequences to be deposited on the evolving irregular basement surface were the fluvial-lacustrine red beds of the Eurydice and equivalent formations (Welsink et al., 1989; Figure 2-3). More than 1.5 kilometers of Eurydice Formation have been drilled in a well on the LaHave Platform, northwest of the study area (well Sambro I-29).



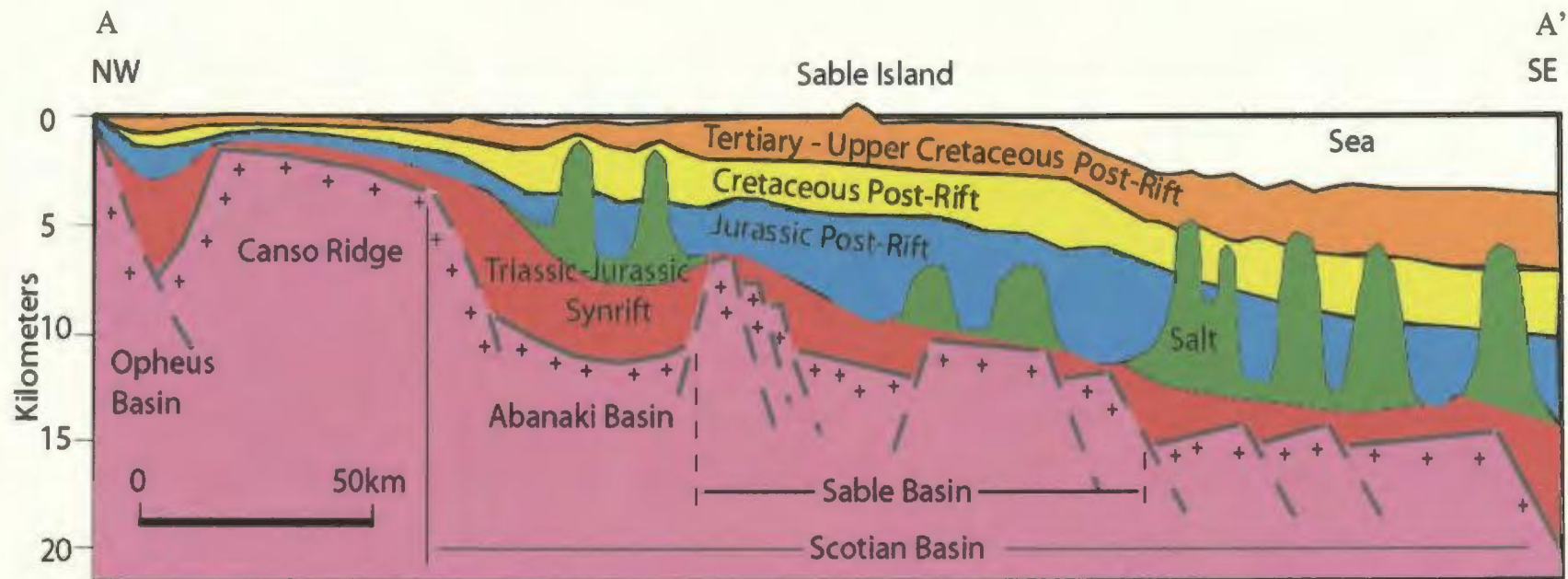


Figure 2-2: Schematic cross-section A-A' through the Scotian Basin showing seismic-stratigraphic sequences from Orpheus Basin through the Abenaki and Sable basins. Vertical exaggeration is 1:5. Various colours represent different mega-sequences that are predominately terrigenous clastics; green represents salt; pink is basement (modified from Welsink et. al., 1989). See Figure 2-1 for approximate location.

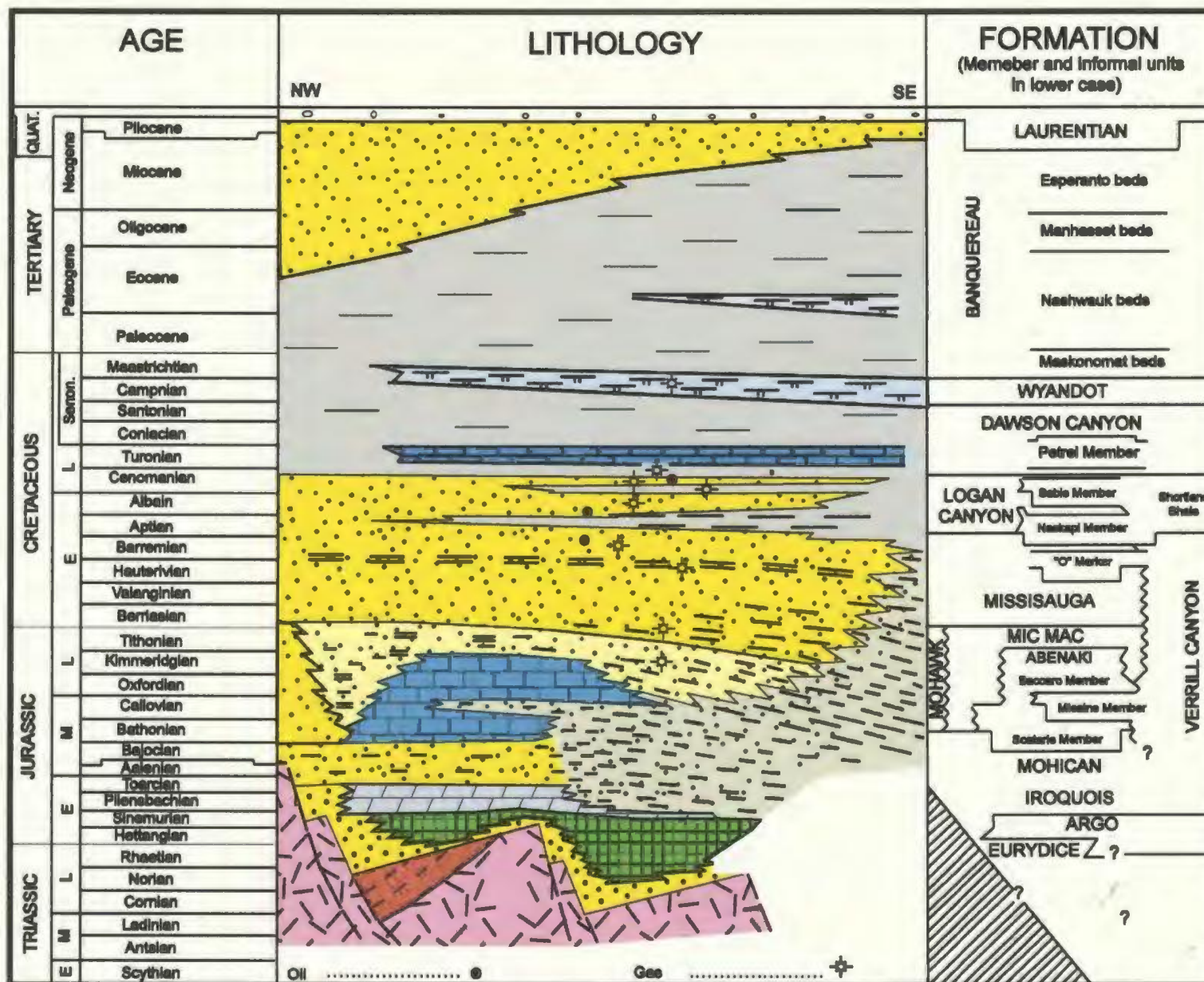


Figure 2-3: Generalized lithostratigraphy of the Scotian Shelf (after Wade et. al., 1989)

By the latest Triassic, the North American and African plates in the Scotian region had drifted northward to approximately 10-20° paleo-latitude, a relatively arid sub-equatorial climatic zone (Kidston et. al, 2002). Renewed rifting to the north in the Grand Banks/ Iberia area breached topographic barriers to the proto-Atlantic ocean and permitted the first incursion of marine waters from the Tethys oceanic realm to flood the interconnected syn-rift basins. Restricted shallow marine conditions were established at this time. Due to the hot dry climate and sub-sea level elevation, these waters were repeatedly evaporated, resulting in the accumulation of extensive salt and anhydrite deposits of the Argo Formation. Estimations on the thickness of the Argo Formation range from two kilometers thick in central rift sub-basins (Kidston et. al, 2002) to in excess of five kilometers in parts of the Orpheus Graben and Abenaki Subbasin (MacLean and Wade, 1992). The Argo Formation overlies the Eurydice Formation in the basin center and interfingers with it near basin margins (MacLean and Wade, 1992).

Renewed tectonism during the Sinemurian resulted in complex faulting and some erosion of Late Triassic and Early Jurassic sediments and older rocks (Wade and MacLean, 1990). This phase of erosion is known as the Break-Up Unconformity (BU) and marks a time of tectonic adjustment related to plate separation and associated ocean spreading. Within the study area the Breakup Unconformity forms an easily mappable seismic horizon that marks the top of Late Triassic-Early Jurassic synrift strata. The southwest-northeast trending series of platforms, ridges, and depocenters that were created on the Nova Scotia margin as a result of the Sinemurian breakup are defined by



the landward extensions of regularly spaced oceanic fracture zones rooted onto continental crust (Welsink et al., 1990).

Shallow marine dolostones of the Iroquois Formation and tidally influenced siliclastics of the Mohican Formation overlie the Breakup Unconformity. The Iroquois Formation attains a maximum thickness of approximately 800 m on the LaHave platform where it is coeval with the lower Mohican Formation (Wade and MacLean, 1990). Siliclastics of the Mohican Formation form a very thick late-Early to early-Middle Jurassic molasse sequence that was deposited into an actively subsiding sub-basin (MacLean and Wade, 1992). The Mohican Formation is widespread on the Scotian Shelf. Over 400 m of Mohican section was drilled in the study area in the Glooscap C-65 and Moheida P-15 wells (MacLean and Wade, 1993, Figure 2-4). Seismic data indicates that the formation may be as much as 4 kilometers thick in the Abenaki Sub-Basin. In some areas, salt flow occurred coeval with deposition of the Mohican Formation resulting in formation thicknesses as great as 5.5 kilometers in salt withdrawal synclines (MacLean and Wade, 1992).

The combination of sea-floor spreading, basin subsidence and global sea level rise in the Middle Jurassic caused the North Atlantic Ocean to become broader and deepen to approximately 1000 m (Kidston et. al, 2002). A complex suite of shelf carbonates of the Scatarie Member, Abenaki Formation formed along the basement hinge zone in the relatively stable marine environment. Equivalent deepwater deposits at this time are the marls and muds of the Verrill Canyon Formation. Continued subsidence and relative sea level rise during the Callovian resulted in flooding of the carbonate bank and deposition



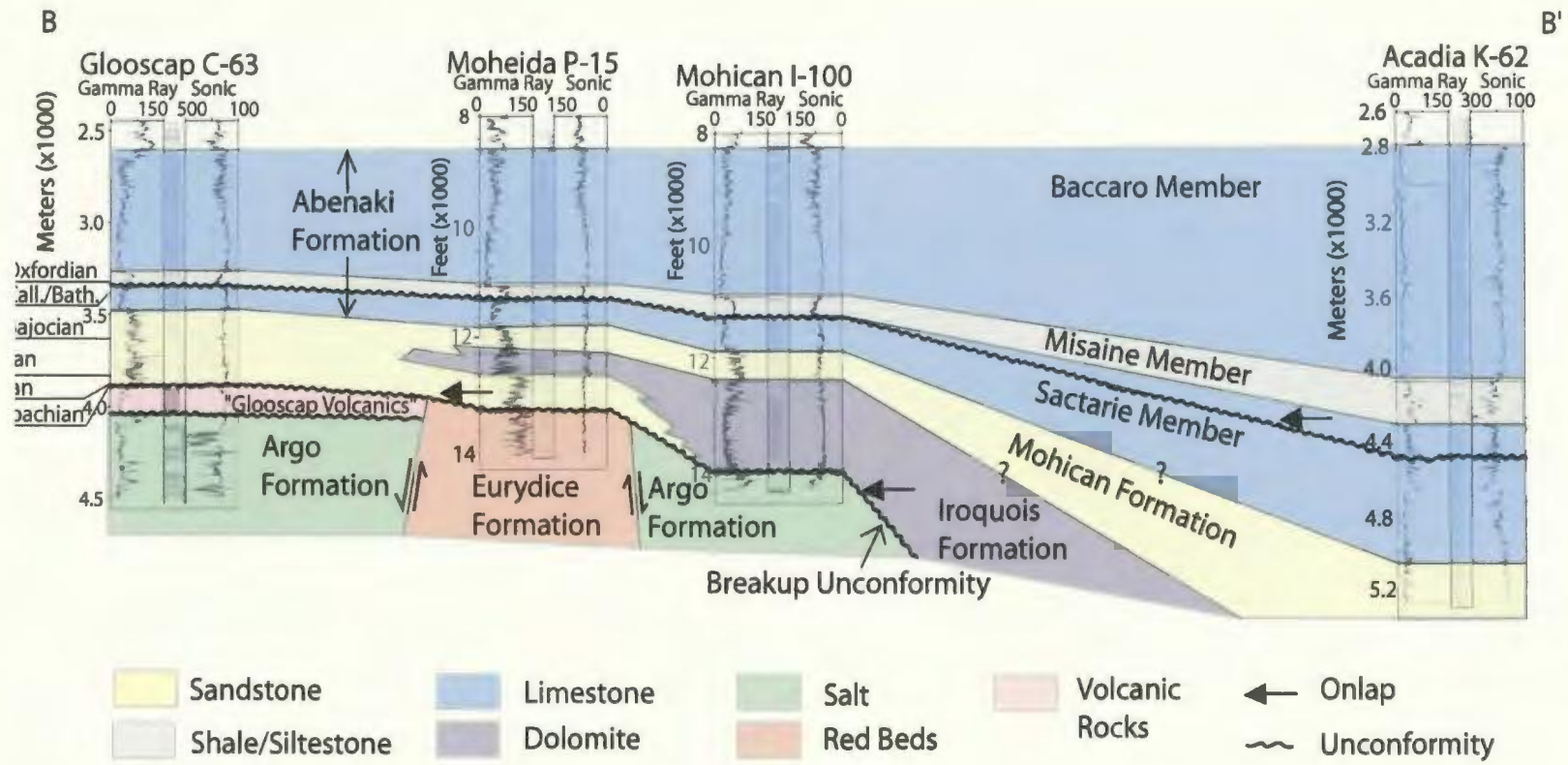


Figure 2-4: Geological cross-section B-B' showing details of the Mohican and Iroquois formations. Red box in location map represents study area (Modified from Keen and MacLean, 1990b).

marine shales of the Misaine Member of the Abenaki Formation (Kidston et. al., 2002).

During the Oxfordian to Kimmeridgian carbonate reef, bank and platform environments again flourished along the basin hinge line on the La Have Platform resulting in the deposition of the carbonate deposits of the Baccaro Member of the Abenaki Formation. Marine mud, shale and limestone of the Verrill Canyon Formation continued to represent coeval deep-water sedimentation. Concurrent with carbonate deposition, regional uplift to the west resulted in an influx of clastic sediments and the establishment of three major mixed energy (current and tidal) deltas. These deltas are from east to west; the Laurentian Delta, the Sable Delta and the Shelburne Delta (Figure 2-5). The Mic Mac Formation records the first phase of delta progradation, represented by distributary channel and delta front fluvial sands cyclically interfingered with prodelta and shelf marine shales of the Verrill Canyon Formation (Kidston et. al., 2002).

The onset of major deltaic deposition in the Mid-Late Jurassic, particularly at the shelf edge resulted in shelf instability south of the basement hinge zone, initiating subsidence and development of seaward dipping growth faults. The associated half grabens acted as traps for sediment accumulation (Kidston et. al., 2002). During the Late Jurassic river systems cut deeply into the outer shelf during lowstand sea-level conditions, possibly forming shelf-edge delta complexes (Kidston et al, 2002). Turbidity currents, mass sediment flows and large slumps carried significant volumes of clastic sediment derived from the Mic Mac Formation into the deep water. The sediment loading that resulted from this period of deepwater deposition mobilized salt resulting in sinks

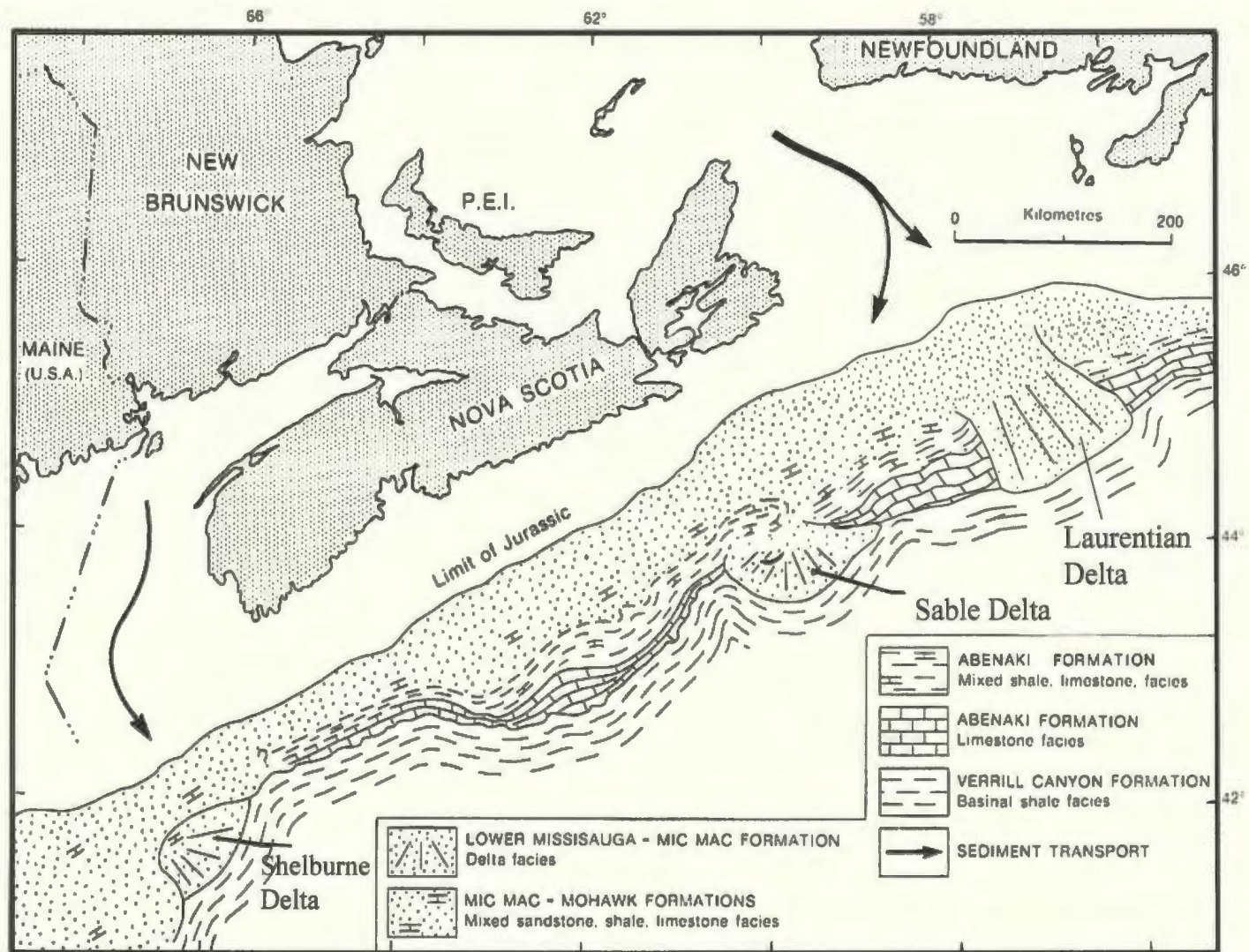


Figure 2-5: Generalized facies distribution, Abenaki and equivalent formations, Scotian Shelf (modified from Keen and MacLean, 1990b and from Kidston et. al., 2002)



and positive relief structures on the seafloor. This process was accentuated in areas such as the Sable and Shelburne deltas where sedimentation rates were particularly high.

By the Early Cretaceous regional surface and deep-water circulation patterns had developed in the newly opened Atlantic Ocean. The ancestral St. Lawrence River was well established delivering an increasing supply of clastic sediments into the Scotian Basin resulting in a third thick postrift clastic succession, the Missisauga Formation. The Missisauga Formation is comprised of a series of thick sand rich deltaic, strandplain, carbonate shoal and shallow marine shelf successions (Welsink et. al., 1989). It is subdivided into three informal members; the lower member extends from a Kimmeridgian-age limestone bed marking the top of the Mic Mac Formation to the top of a predominant shaley sequence dated as Berriasian-Valanginian. The middle member extends from this shale unit to the base of a series of limestone beds of Hauterivian to Barremian age, known as the "O" marker, a regional lithologic and seismic marker. The upper member extends from the top of the "O" Marker to the base of the Logan Canyon Formation. (Wade and MacLean, 1990).

During the Early Cretaceous, the Sable Delta migrated southwest into the Laurentian and Sable sub-basins. The rapid deposition and increased sediment load that resulted from this deltaic migration initiated new and renewed growth faulting that stepped progressively seaward as the delta prograded (Kidston et. al., 2002). In adjacent deepwater settings, fine grained sediments of the Verrill Canyon Formation continued to dominate. Periods of relative falls in sea level resulted in large volumes of deltaic sands being transported through and redeposited from shelf margin settings and ultimately



deposited in the deepwater. As with previous periods of high rates of deposition into the deepwater, the increased sediment load in the Early Cretaceous initiated renewed salt motion, resulting in salt withdrawal mini-basins that formed negative relief structures on the seafloor in which turbidite channel and fan sediments were focused and deposited (Kidston et. al., 2002). Further south the Shelburne Delta became abandoned due to exhaustion and/or redistribution of the fluvial sediment supply (Kidston et. al., 2002).

Deltaic sedimentation ceased along the entire Scotian margin during the Late Cretaceous and was followed by a period of slow relative sea level rise and deposition of a thick succession of coastal plain and shallow marine shelf sand and shale of the Logan Canyon Formation. No regional seismic markers are contained within the Logan Canyon Formation (MacLean and Wade, 1992). The distal equivalent of the Logan Canyon Formation is the Shortland Shale. Within the study area drilled thickness of Logan Canyon Formation (or equivalent) range from 776.3 m in well Moheida P-15 to 2220.0 m in well Evangeline H-98 (MacLean and Wade, 1993).

Continued relatively high sea level conditions combined with low relief hinterland, resulted in a reduction of sediment supply to the basin during the Late Cretaceous (Kidston et. al., 2002). Marine shales, chalks and minor limestones of the Dawson Canyon Formation were deposited throughout the Scotian Basin at this time. The Petrel Member, a persistent series of thin Turonian age limestones, forms a regional lithologic and seismic marker within the Dawson Canyon Formation (Wade, 1991). The Dawson Canyon Formation was intersected in all six wells used in this study and has a

formation thickness consistently in the  $250 \pm 30$  m range except for well Evangeline H-98, where it is 809.5 m in thickness (MacLean and Wade, 1993).

The Wyandot Formation overlies the Dawson Canyon Formation. It is composed of chalks, chalky mudstones, marls and minor limestones (MacLean and Wade, 1992). Within the study area the top of the Wyandot Formation is unconformably overlain by Tertiary sediments. The unconformity surface forms an easily recognizable regional seismic marker considered to mark the base of Tertiary stratigraphy. Within the study area the drilled thickness of the Wyandot Formation ranges from 19.0 m in well Oneida O-25 to 158.5 m in well Evangeline H-98 (MacLean and Wade, 1993).

In the Scotian Basin the entire Tertiary sedimentary succession is included in the Banquereau Formation. An overall regression of the sedimentary systems through the Tertiary is reflected in an upward coarsening succession from marine shelf mudstones at the base of the Banquereau Formation to sandstones and conglomerates in the top. Three predominant seismic reflections within the Tertiary section are correlated with erosional surfaces within the Eocene, Oligocene and Miocene epochs (MacLean and Wade, 1992). Quaternary erosion in parts of the Laurentian Channel has removed the Tertiary section completely (MacLean and Wade, 1992). The increased deepwater Tertiary sediment load again resulted in renewed salt movement.

During the past two million years, several hundred metres of glacial and marine sediments were deposited on the outer shelf and upper slope. Quaternary glacial runoff resulted in major incisions on the slope (Kidston et. al., 2002), forming the rugose water bottom seen today in the eastern portion of the study area (Figure 2-6).

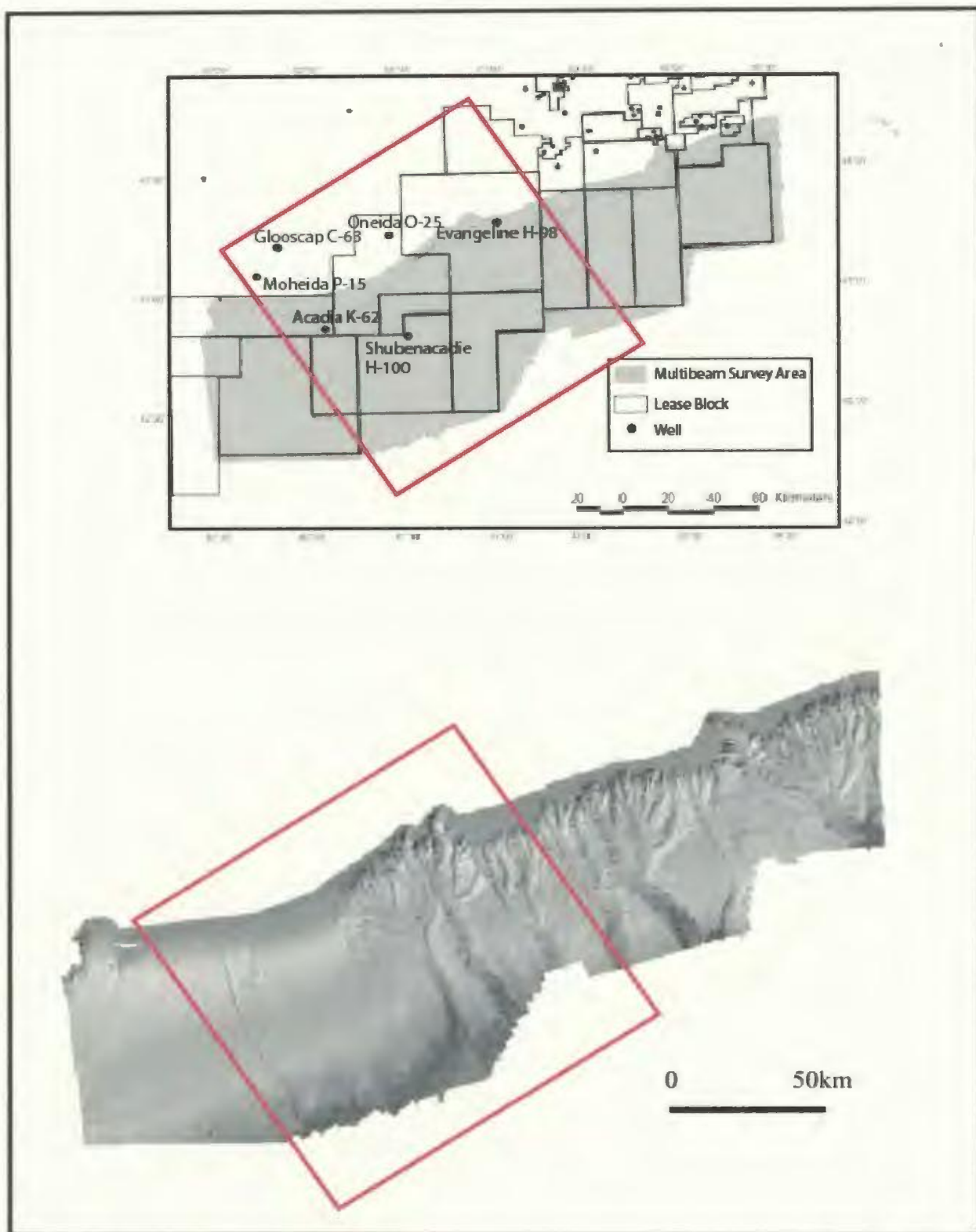


Figure 2-6: Top; index map of Scotian Slope showing lease blocks, wells, and area of multibeam bathymetric survey. Bottom; multibeam bathymetric image of central Scotian Slope. Note, M.Sc study area shown in red (modified from Pickerill et. al., 2001)



## 2.4 Structural Styles and Geometry

The rifted margin off Nova Scotia is the best understood of the rifted margins of eastern Canada. The margin was formed within the Appalachian Meguma Zone as the result of Late Triassic to Early Jurassic rifting was between Africa and North America. Normal faulting accompanied this rifting (Keen et. al., 1990). The margin has a well-developed hinge line, a thick sedimentary wedge consisting of both syn- and post-rift sediments, numerous salt diapirs (particularly beneath the slope) and carbonate build-ups that probably represent the position of an earlier Jurassic shelf edge. After the rift phase, both fault and thermally controlled subsidence occurred as the basin settled through Mid-Jurassic to Recent.

Two principal classes of faults are recognized within the Scotian Basin: (1) those that involve basement (thick skin); and (2) those that detach within the cover sequence (thin skin). Both styles contribute to the gross structural framework of northeast trending normal faults, and subordinate northwest trending transfer faults (Welsink et al., 1989).

### 2.4.1 Thick Skin Deformation

Basin forming faults of the composite Scotian Basin are long and sinuous. Large amounts of extension were accommodated by dip-slip and oblique slip movement along a system of en echelon and intersecting faults and relay ramps (Tankard and Welsink, 1989; Figure 2-7).

The distribution and geometries of Mesozoic Scotian rift basins are controlled largely by tensional stress fields within pre-existing crustal structure. Metasedimentary

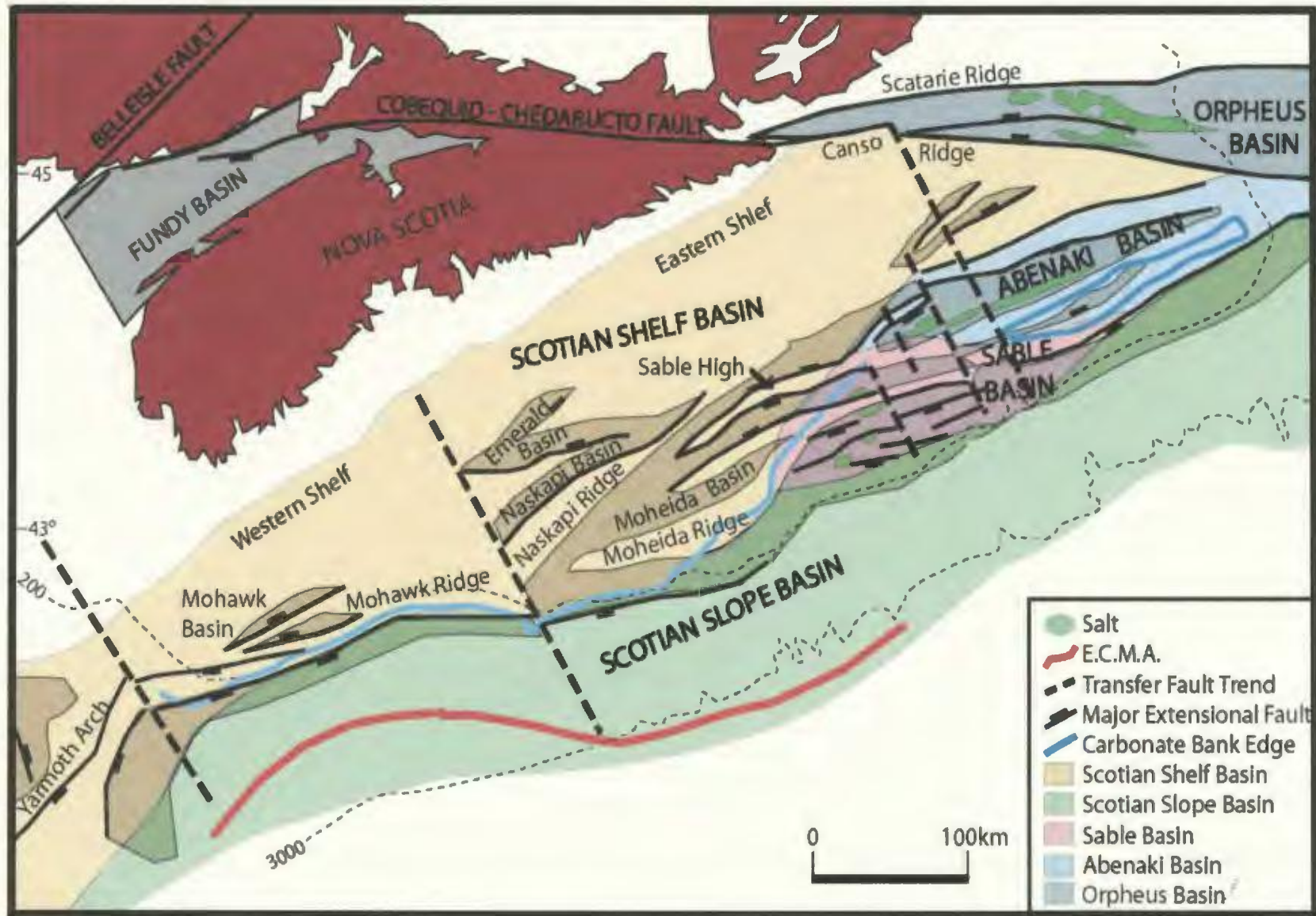


Figure 2-7: En echelon arrangement of crustal-scale listric faults, subbasins, and intervening horsts beneath the Scotian Basin (modified from Welsink et. al., 1989)



and igneous rocks of the Meguma Terrain underlying the Scotian Basin contain structural fabrics induced by Caledonian and Hercynian deformation (Williams, 1984). Listric and planar normal basin-forming faults and transfer faults that accommodated crustal extension during the Late Triassic-Early Jurassic, are seated within Meguma basement and are believed to be reactivated pre-existing structural fabrics (Welsink et al., 1989).

Each subbasin in the collective Scotian Basin is bordered on one side by a major extensional fault and on the other side by a multiply faulted horst (Figure 2-8), (Tankard and Welsink, 1989). Two levels of intracrustal detachment have been interpreted by Welsink et. al., (1989) and Tankard and Balkwill (1989). Many of the eastern Scotian Basin subbasins, including the Orpheus, Abenaki and Sable, are interpreted to have major basin bounding faults that dip seaward, exhibit 6 - 8 kilometers of structural relief and detach at a similar depth. Section balancing techniques suggest that these faults have a common depth of detachment in basement between 15 to 19 kilometers below the Early Jurassic breakup unconformity (Welsink et. al., 1989). The breakup unconformity is used as a reference datum to compensate for the very large and variable amounts of post rift subsidence to which the Scotian Basin was subjected, permitting comparison between basins and construction of tectonic models

Landward dipping normal listric faults form the seaward boundary of a number of the Scotian Basin's subbasins, including the Emerald, Naskapi and Mohican sub-basins in the central Scotian Basin and the Mohawk sub-basins in the south-west. Depth to detachment calculations indicate that these faults sole into the same level of detachment,



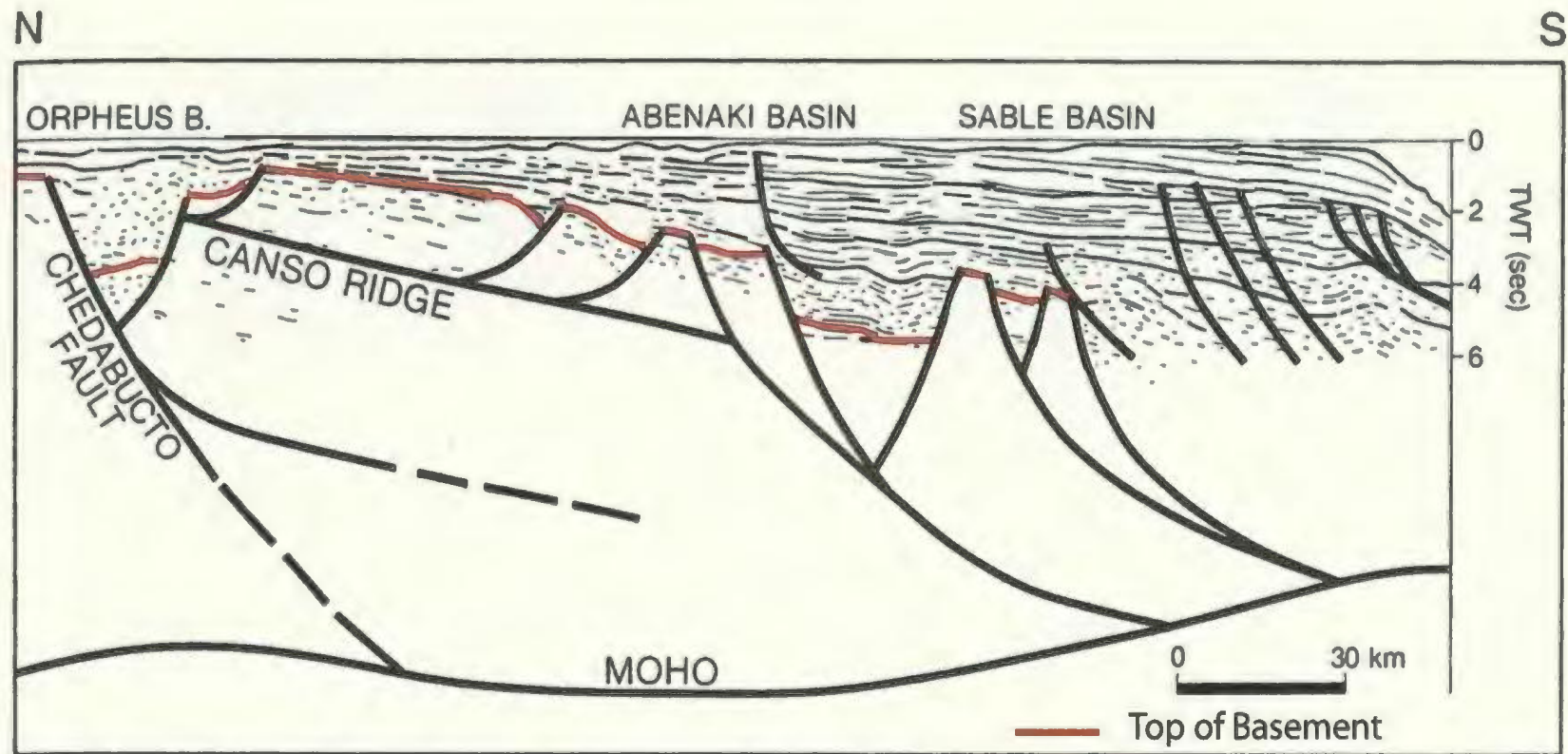


Figure 2-8: Tectonic reconstruction of the Orpheus and Scotian basins on balanced-section techniques and Lithoprobe deep seismic line 86-5B across the Orpheus basin. The broad tract and basin depth are related to two levels of intracrustal detachment at 15-18 km and approximately 7km, restored to mid-Jurassic "breakup" unconformity datum to avoid effects of substantial and asymmetrical postrift subsidence. Top of basement reflector in red.

approximately 6 to 7 kilometers below the Early Jurassic breakup unconformity (Welsink et al., 1989) thus indicating that a common extensional system apparently links these landward-dipping basin-forming faults.

Transfer fault zones are conspicuous off Nova Scotia where they accommodate distinct extensional tracts within the collective Scotian Basin, but are less predominant within subbasins. The lack of internal transfer trends and the en echelon arrangement of the major basin-forming faults suggest that extensional strain was transmitted across linked relay structures (Larson, 1988; Tankard and Welsink, 1989).

#### 2.4.2 Thin Skin Deformation

Within the Scotian Basin postrift structural modification was largely accommodated by seaward-dipping listric faults and associated synthetic and antithetic faults that detach within the sedimentary cover. Their occurrence is directly related to, but does not involve, underlying basement geometry. Two sets of postrift faults are recognized by Welsink et al. (1989); those restricted to the Jurassic postrift sequence and those that deform Cretaceous sediments (Figure 2-9). Although generally detaching at similar depths, these faults tend to extend to progressively higher stratigraphic levels in a seaward direction. Where syn-depositional, these faults are associated with rollover anticlines and growth strata.

Syn-sedimentary growth faults set up one of the primary play types of the Scotian Shelf and are also predicted to play a similar role in the frontier Scotian Slope.



Figure 2-9: Regional Geological cross section C-C' across the Scotian Shelf and Slope east of the study area (red) showing interpreted thin skin deformation style. Vertical exaggeration of 1.25:1. Figure modified from Wade and MacLean, 1990b.



### 2.2.3 Halotectonics

In addition to a complex extensional tectonic history, other structural complications on the Nova Scotia margin were caused by salt mobilization and multistage growth. Within the Scotian Basin salt is generally associated with the larger and deeper sub-basins (e.g., Orpheus and Abenaki), those seaward of the Jurassic carbonate bank in the Slope Diapiric Province (Figure 2-12).

Over the past 200 Ma the Argo Salt has responded to differential loading due to down-dip gravity sliding caused by sediment instability. This is primarily observed on the prograding shelf, especially around the Sable Delta. As a result the salt was mobilized, forming the complete spectrum of salt structures typical of extensional margins described by Jackson and Talbot (1991). Salt related structures imaged on Scotian Basin seismic sections include: welds, pillows and anticlines, rollers, diapirs in different stages of maturity, and allochthonous salt sheets. Other local structural complications are related to salt withdrawal accompanied by collapse and faulting.

Salt bodies, including rooted diapirs, detached diapirs, and canopies, commonly intersect the Sub-Tertiary Unconformity, and may even reach water bottom. Salt bodies tend to trend parallel to the major basement-involved faults, implying a structural or tectonic control on halokinetics (Welsink et al., 1989). Listric faulting associated with salt mobility is restricted to the postrift sedimentary wedge (Welsink et al., 1989).

Sedimentation patterns in the Scotian Basin were locally affected by salt movement. In the peripheral sinks of salt structures the sedimentary column is thickened, while in areas over active diapirs the column is locally thinned. Moreover, local facies

variation of the siliclastics likely took place around mounded salt features, similar to that described by Winker (1996) in the Gulf of Mexico.

In the Scotian slope, early descriptions considered structured salt to be deeply rooted to its original strata of origin (autochthonous). Through drilling and improved seismic processing techniques such as pre-stack depth migration, it has been demonstrated that much of salt is non-rooted (allochthonous) (Kidston et al., 2002). Its position within the sedimentary column is highly variable both vertically and laterally.

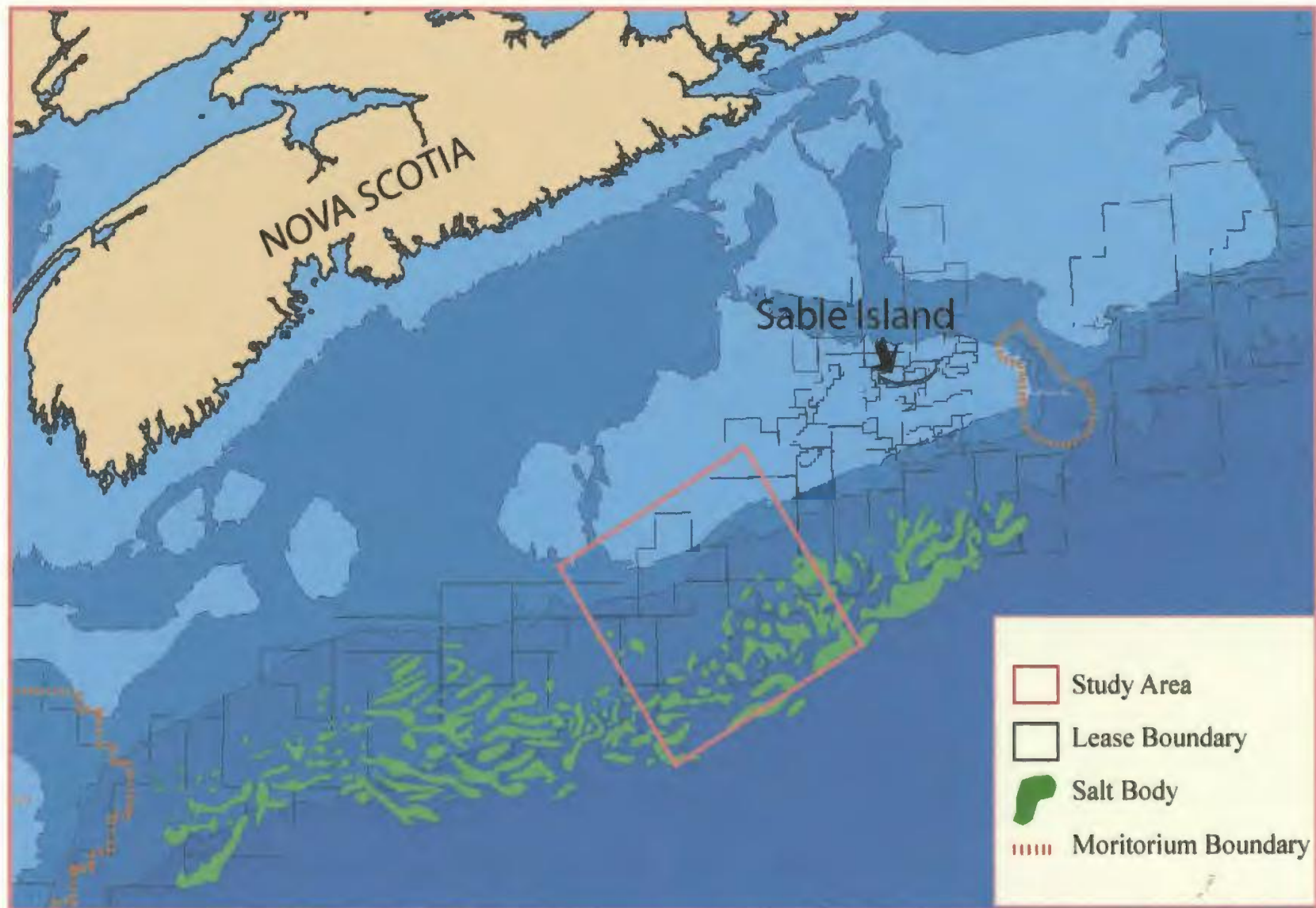


Figure 2-10: Scotian Margin basemap showing bathymetry, lease block boundaries, study area and salt body distribution. Map provided by EnCana Corporation, modified from Hogg, 2004.



## Chapter 3

### Seismic Stratigraphy

#### 3.1 Introduction

Using well control, regional correlation and seismic stratigraphic principles (e.g. Vail et al., 1977a, b) key seismic surfaces and events were identified and defined. Within the project area a top of basement reflector, ten regional seismic stratigraphic surfaces (i.e. sequence boundaries or seismic markers), top salt, top carbonate bank and the seafloor have been defined and mapped in time (TWT) (Figure 3-1).

The depth and age of each key seismic surface was determined by using synthetic seismograms in exploration wells and comparison to published biostratigraphic and lithostratigraphic picks.

#### 3.2 Well Control

Wireline logs and biostratigraphic information from the Moheida P-15, Glooscap C-63, Oneida O-25, Shubenacadie H-100, Acadia K-62 and Evangeline H-98 wells were used to depth-convert seismic data at well locations, to date the seismic markers and to correlate them with regional lithostratigraphy defined by Wade et al. (1989).

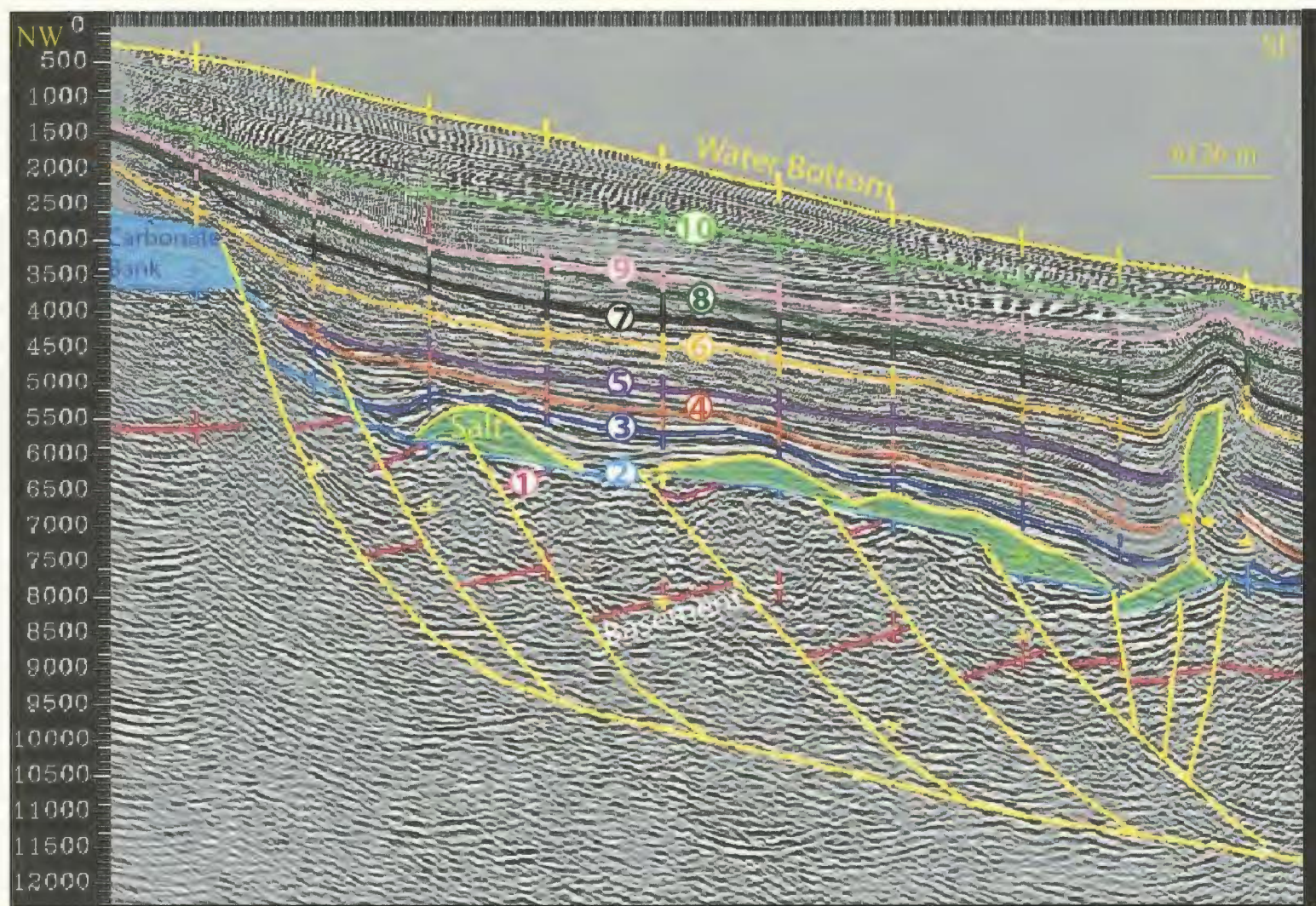


Figure 3-1: Representative NW to SE seismic profile from the central map area showing key seismic surface (1-10) and top of basement reflector, salt, carbonate bank and seafloor.

### 3.2.1 Synthetic Seismograms

Synthetic seismograms were generated using checkshot, sonic and density logs for the Acacia K-62, Evangeline H-98, Glooscap C-63, Moheida P-15, and Oneida O-25 wells. Wavelets used to create the synthetic seismograms were extracted from a 500 to 1200 ms window around the base Tertiary unconformity, an easily identifiable and well documented regional sequence boundary identified and described by King and MacLean (1976), Wade (1977), Wade et. al. (1989), and Welsink et al. (1989). The seismic grid used in this study had been processed to 0° phase, however, wavelets extracted range from near 0° to ~ 30°. The synthetic seismograms generated tie moderately to very well with the seismic reflection profiles (Figure 3-2). The best correlations obtained were those of the top Abenaki Formation marker and the base Tertiary unconformity marker.

There was no checkshot survey available for the Shubenacadie H-100 well. The synthetic seismogram for this well was created using density and sonic logs and hung on the base Tertiary unconformity.

### 3.2.2 Correlating Seismic Events

Seismic events were dated using the biostratigraphic and lithostratigraphic picks posted on the Geological Survey of Canada Basin Database (2004). Biostratigraphic reports used in this study include Ascoli (1988), Bujak Davies Group (1988), and Thomas (2001).



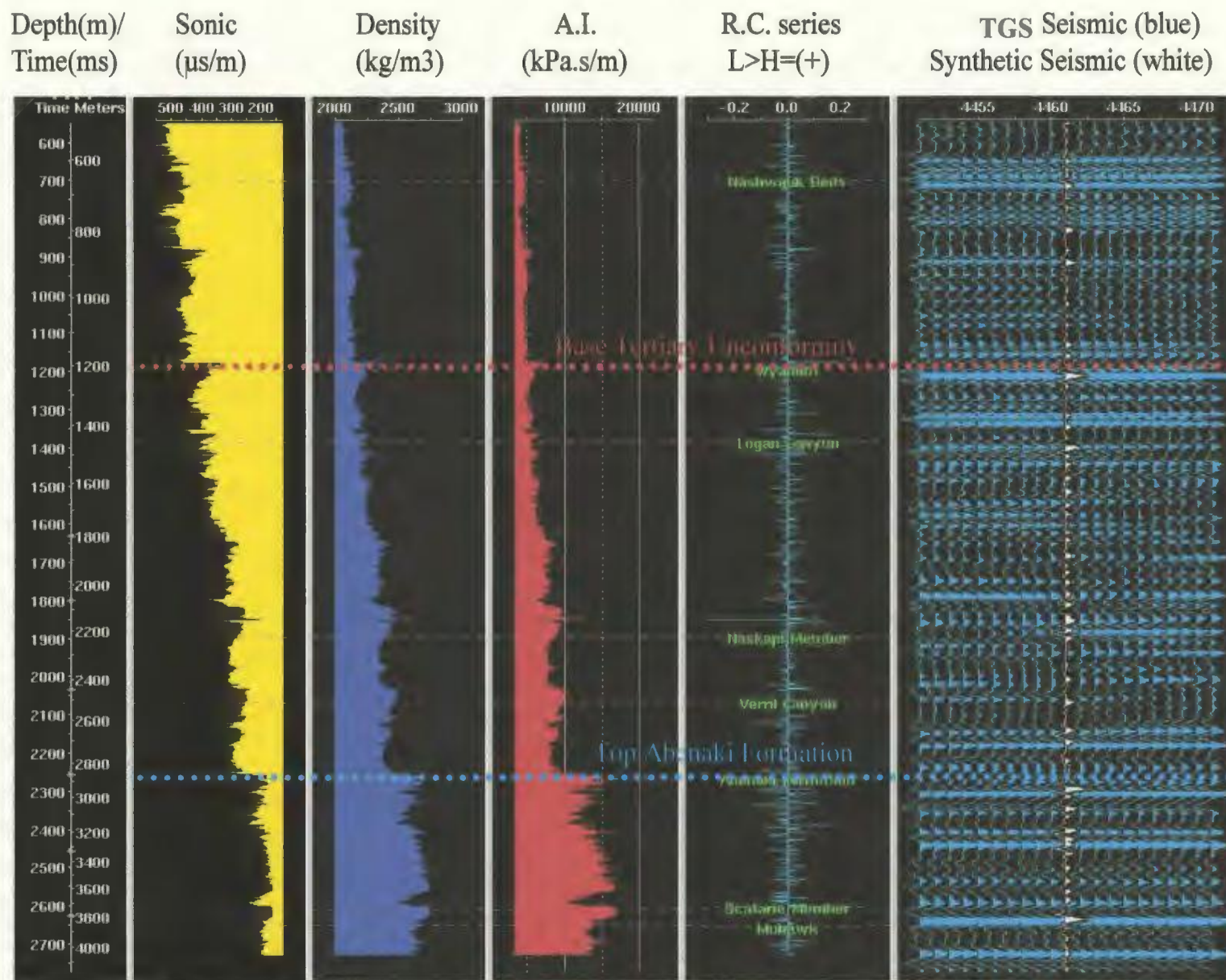


Figure 3-2: Synthetic seismogram of the Oneida O-25 well.

For consistency, the work of MacLean and Wade (1993) was the primary reference used for correlating lithostratigraphic picks. This was the most recent publicly available report at the time of writing, and was the only report that included all the wells used in this study. Due to an overall lack of lithostratigraphic information pertaining to Tertiary stratigraphy, other references were also incorporated into the study including Hardy (1975), and Wade and Sherwin (1990).

In instances where no well intersected a particular marker (as was the case with some of the deeper markers) or where the regional extrapolation of a well correlation proved highly uncertain (such as under the slope break or through the diapiric province) the marker was dated by comparing the TGS seismic data to previously published interpreted sections (Figure 3-3). References that were used as an approach to interpret the data set in this way include Wade and MacLean (1990), Keen et al. (1991), Geological Survey of Canada (1991), Kidston et al. (2002), and Loudon (2002).

A summary of the ages and the lithostratigraphic affinities of each significant seismic event and the general degree of confidence in the ability to regionally map these markers are presented in Figure 3-4. A description of each of the events summarized in Figure 3-4, including the age, seismic character, reflection termination patterns, correlation confidence, stratal geometry and geologic significance, ordered from oldest to youngest, is presented in Section 3.3 of this chapter.

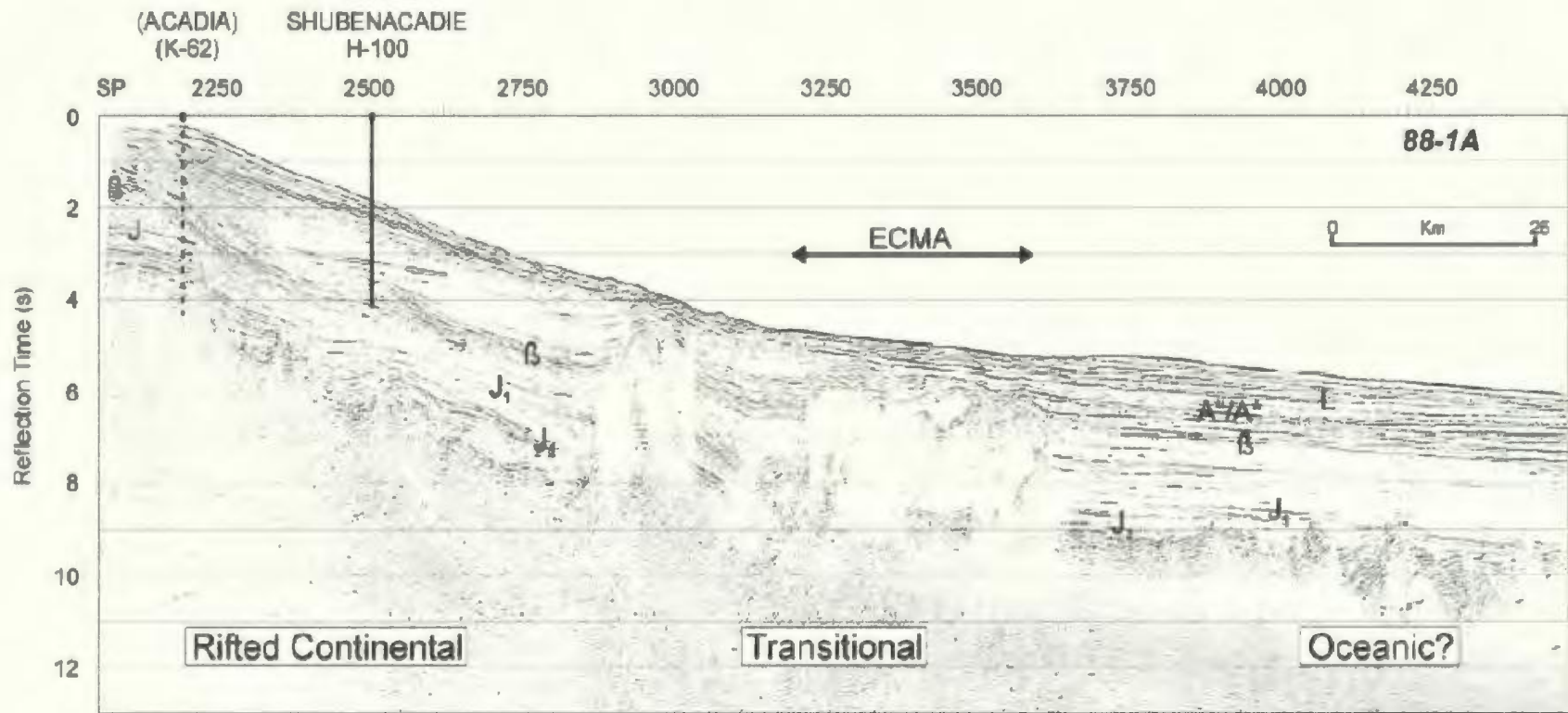
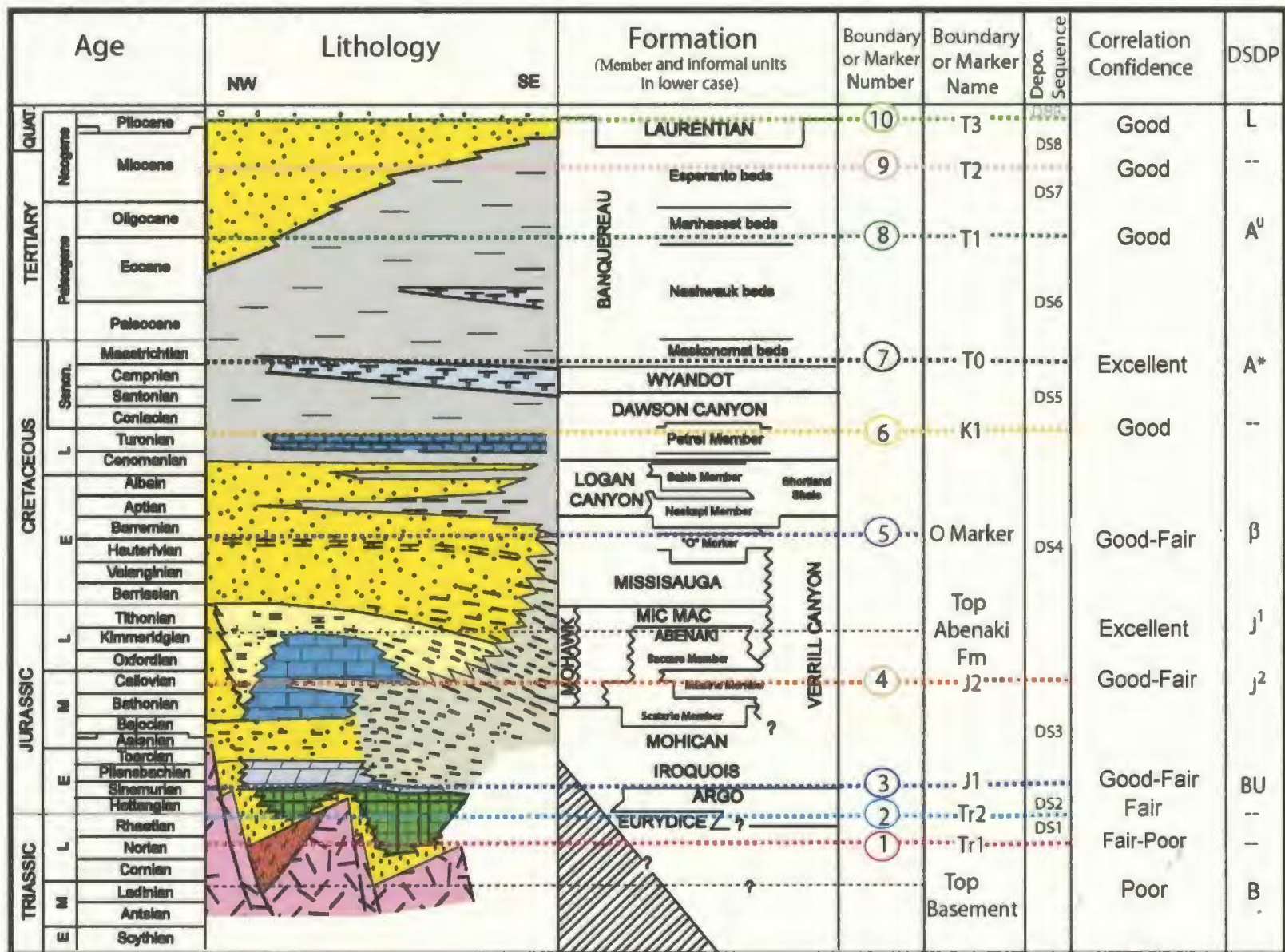


Figure 3-3: Lithoprobe seismic reflection profile 88-1a and location of coincident Shubenacadie H-100 well and adjacent Acadia K-62 well. Seismic markers are Pliocene (L); A<sup>u</sup>/A\* (Oligocene and top Cretaceous); Early Cretaceous (β); top Jurassic (J); and Late Jurassic (J<sub>1</sub>, J<sub>2</sub>). Basement crustal types are defined by changes in reflection pattern. ECMA marks zone of East Coast Magnetic Anomaly. See Figure 1-5 for location. Reprinted from Loudon (2002)



Figure 3-4: Generalized Scotian Basin stratigraphy (Wade et al., 1989), M.Sc. sequence boundaries or seismic markers by number (Figure 3-1), M. Sc. boundary or marker name and correlation confidence, M. Sc. depositional sequences, and Deep Sea Drilling Project (DSDP) seismic markers.



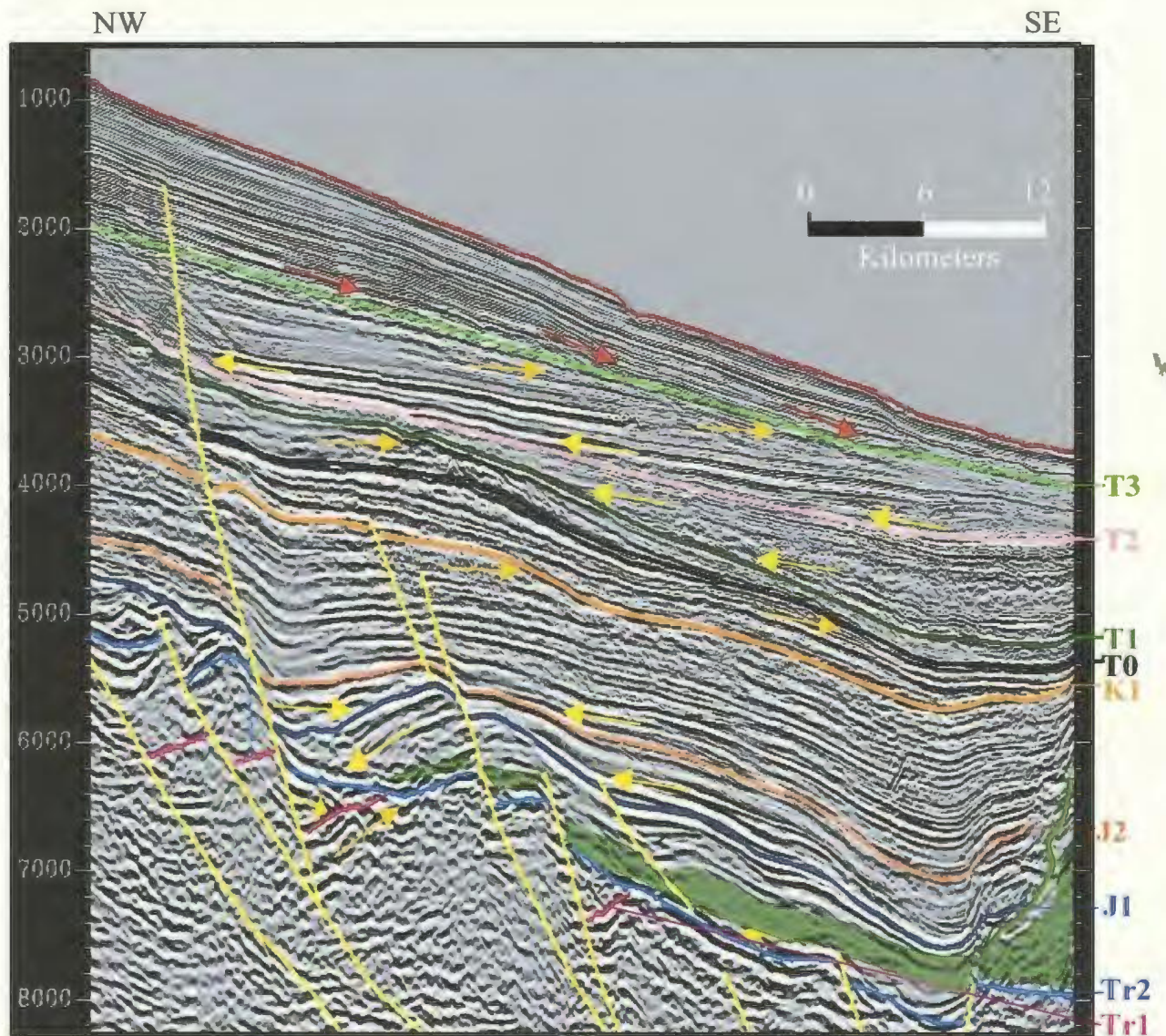
### 3.3 Seismic Stratigraphy

The term “sequence” has been widely used (and abused) in its application to describe successions of sedimentary rocks deposited during discrete and definable episodes of basin fill. Mitchum et al. (1977) first defined a depositional sequence as “a stratigraphic unit of a relatively conformable succession of genetically related strata bounded at its top and base by unconformities or their correlative conformities”. Initial confusion was caused by the ambiguity surrounding the use of the word unconformity. As a result, Van Wagoner et al. (1990) more rigidly defined an unconformity as “a surface separating older from younger strata along which there is evidence of subareal truncation or subareal exposure, with significant hiatus indicated”.

The geometry and internal characteristics of an idealized sequence was first proposed by Van Wagoner et al (1988). The model divided a depositional sequence into three system tracts representing cycles of sea-level rise and fall. The seismic expression of a systems tract is a unit of conformable reflections bounded by surfaces of reflection termination (“seismic stratigraphic units” of Brown and Fisher, 1977; “seismic sequences” of Mitchum et al., 1977). Reflection termination patterns include onlap, downlap and erosional truncation (Figure 3-5).

A detailed analysis of the sequence stratigraphic architecture of map area is not one of the objectives of this thesis. Seismic stratigraphy has been here used as a means to identify and date packages of related, conformable seismic sequences and their bounding seismic surfaces, therefore the seismic stratigraphic definitions





→ Onlap
 ← Downlap
 → Erosional Truncation

Figure 3-5: Seismic profile from the central map area illustrating typical reflection termination patterns that define each seismic sequence boundary. Green shaded area represents salt unit. Vertical scale given in TWT (ms).

proposed by Mitchum et al (1977) have been used. The term depositional sequence has been used throughout the text to refer to the seismic expression of conformable reflections bounded by surfaces of reflection termination. The surfaces of reflection termination are here referred to as sequence boundaries. The term sequence boundary used here is not meant to be interpreted as a surface over which there has been any specific change in sea-level (ie. Van Wagoner et al (1988) define sequence boundary as surfaces of erosion resulting from a fall in relative sea-level). Rather, I have used sequence boundary to represent the seismic surface bounding a package of conformable seismic reflections. Depositional sequence is here used to refer to the package of conformable seismic reflections.

Once defined, seismic sequence boundaries and recognized seismic markers were regionally mapped using loop-tying procedure with reference to seismic examples by other authors from the Scotian Slope or published from other salt basins. When loop tying, the sequence boundary or marker was interpreted at a point where it was easily defined and well imaged, then traced through a number of intersecting seismic lines in a loop ending at the point of origin. In areas where poor quality of events, complex faulting or salt structures, out-of line events or noise obstructed seismic loop-tying correlation, jump correlations based on characteristics of the sequence and attributes of the marker were employed. Best judgments were used when everything else failed.

### 3.3.1. Top Basement Marker

Within the Scotian Basin very few exploration wells have penetrated pre-Mesozoic basement. Those basement wells are restricted to the LaHave Platform and Canso Ridge. None of the wells used in this study penetrated the basement, however, two wells northwest of the map area, the Ojibwa E-07 and the Naskapi N-30 wells (Figure 1-3), bottomed in Cambro-Ordovician metasedimentary rocks of the Meguma Group and coarse grained biotitic granite (359 ± 12 Ma) respectively (Wade and MacLean, 1990).

A weak event imaged deep in the seismic data has been interpreted as the top basement marker (Figure 3-6). The marker does not yield strong reflections, but is characterized by a change in seismic character from highly reflective, often stratified reflections above to a generally non-reflective zone below, indicating a small impedance contrast at the top of basement.

The top basement seismic marker is considered to represent the top of the pre-Mesozoic metasedimentary and igneous rocks of the Meguma Group. Due to the low impedance contrast at the top of basement and the stratified nature of the Meguma Group metasedimentary basement, the exact top of basement is often difficult to define and may locally represent an intrabasement pick. In relatively unstructured areas with stratified cover, local correlation confidence in the top basement pick is moderate. However, in structurally complex areas or in regions where seismic resolution has been reduced due to overlying salt, correlation confidence in picking the top basement is low.



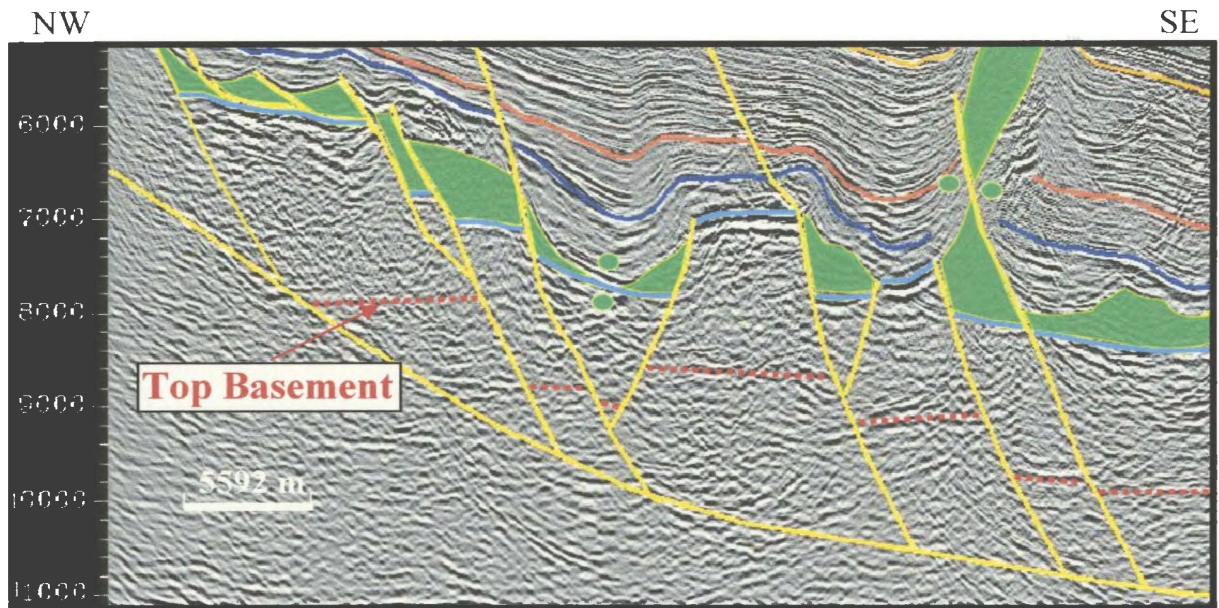


Figure 3-6: Section of a seismic profile through the central map area. Yellow reflections represent planes of discordance (faults) in seismic reflections, green overlay represents the evaporite unit, paired green circles represent areas where evaporites have evacuated (welds). Red dashed lines represent the top of basement seismic marker, pale blue the Tr2 Sequence Boundary, dark blue the J1 Sequence Boundary, dark orange the J2 Sequence Boundary and light orange the J2 Sequence Boundary. Vertical scale is in TWT (ms).

### 3.3.2. Tr1 Sequence Boundary

The Tr1 Sequence Boundary is defined as an angular unconformity surface marked by the onlap of shallowly-dipping overlying reflections (Figure 3-7). The boundary is mapped as the top of a series of sub parallel seismic reflections that are concordant with the top basement marker.

The Tr1 Sequence Boundary is cut by a number of basement faults. The boundary commonly dips steeply northwest when contained within rotated basement fault blocks, but is locally near horizontal within basement horst and graben blocks. Reflections overlying the lower portions of the dipping Tr1 Sequence Boundary commonly have a divergent reflection pattern. Upper portions of the dipping Tr1 Sequence Boundary are commonly eroded by the Tr2 Sequence Boundary (Figure 3-7).

The Tr1 Sequence Boundary was not penetrated by any of the wells in this study. The boundary marks the top of a package of reflections that are concordant the top basement marker, and therefore the Tr1 Sequence Boundary marks the top of prerift stratigraphy. stratigraphy that regionally occurs in the Late Triassic of the Scotian Basin (Wade et al., 1989).

Correlation confidence in the in the Tr1 Sequence Boundary is low over most of the map area, especially where overlying salt structures have caused a decrease in underlying seismic resolution. This is particularly true near the base of the slope in the south-eastern part of the seismic project. Locally, however, where onlapping syn-rift sediments can be observed the correlation confidence is fair to good.



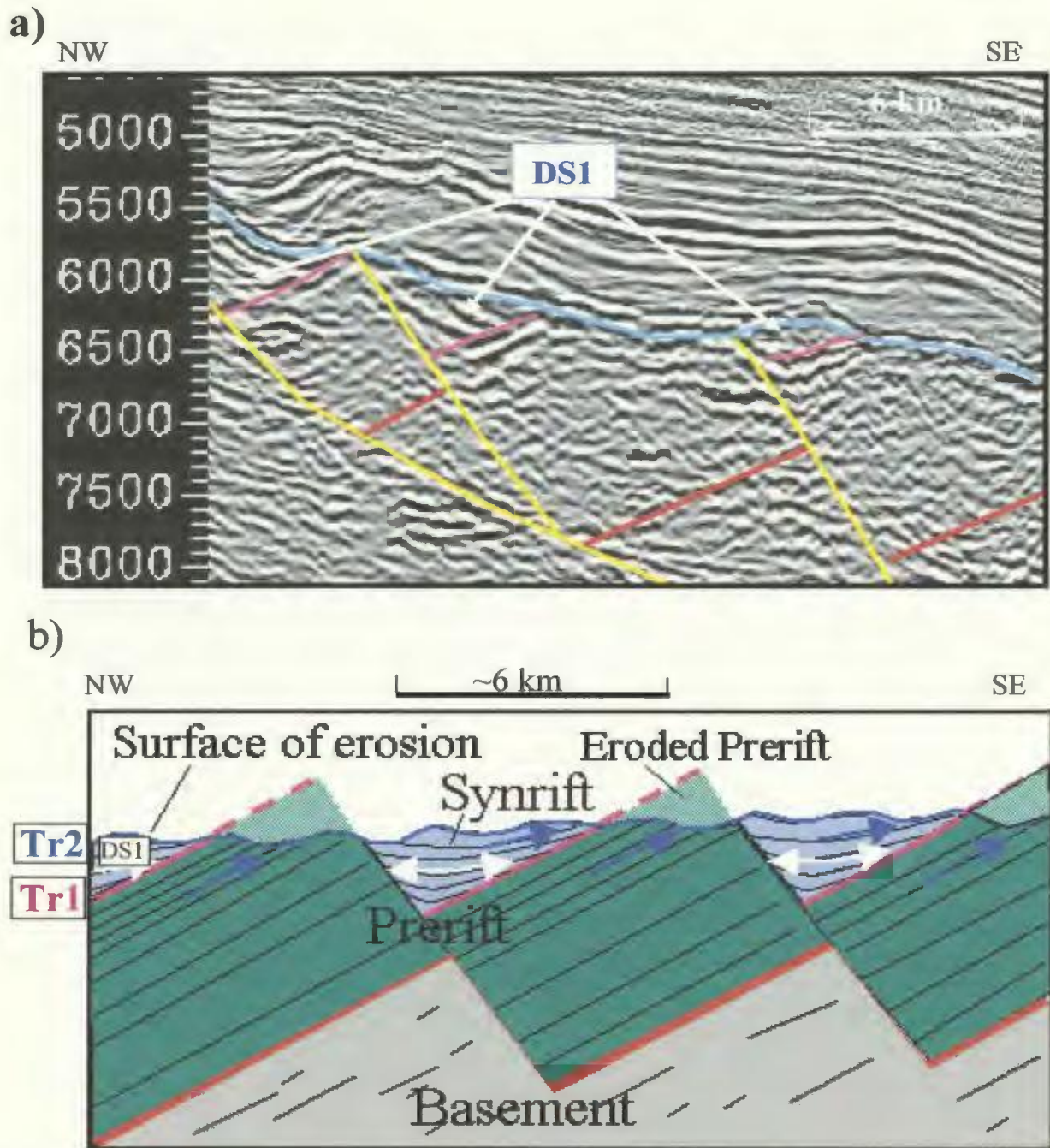


Figure 3-7: a) Section of seismic profile from the central map are showing top of basement seismic marker (red), Tr1 (pink) and Tr2 (blue) sequence boundaries and Depositional Sequence 1 (DS1). Yellow lines represent planes of discordance in seismic reflections. b) Schematic diagram showing relationship Tr1, Tr2 and DS1. Note white arrows represent onlap, blue arrows represent erosional truncation.



### 3.3.3 Depositional Sequence 1

Depositional Sequence 1 is the sedimentary package bounded by sequence boundaries Tr1 and Tr2. The sequence has moderate to low seismic reflectivity and directly overlies prerift stratigraphy. Depositional Sequence 1 consists of a series of horizontal to shallowly dipping, sub parallel, divergent and convergent reflections. Reflections within this depositional sequence commonly onlap the tilted Tr1 Sequence Boundary and are erosionally truncated by the Tr2 Sequence Boundary (Figure 3-7).

Depositional Sequence 1 has limited areal extent, largely due to erosion by Sequence Boundary Tr2. The sequence is only preserved locally and displays significant thickness variations, from approximately 1000 ms TWT at its thickest, to 0 ms where the Tr1 and Tr2 sequence boundaries merge. Depositional Sequence 1 is most often preserved within half grabens formed by rotated basement blocks.

Depositional Sequence 1 has been interpreted as synrift stratigraphy on the basis of its architecture (divergent reflections or growth strata), location directly overlying prerift stratigraphy, and onlapping relationship with the top of prerift sequence boundary (Tr1).

### 3.3.4. Tr2 Sequence Boundary

The Tr2 Sequence Boundary is an erosional unconformity surface that is marked by a coherent, high-amplitude reflector formed by a positive impedance contrast. The unconformable surface is defined by the truncation of both sub parallel,

steeply dipping, prerift reflections and/or shallowly dipping, convergent or divergent synrift reflections (Figure 3-7). Reflections overlying the Tr2 Sequence Boundary have variable frequency, variable reflection amplitude or are acoustically transparent.

Correlation confidence in the regional mapping of the Tr2 Sequence Boundary is overall fair. In the upper and western slope, the boundary is easily identifiable and can be mapped with high confidence. The extrapolation of the Tr2 Sequence Boundary, as defined on the slope, on to the shelf is difficult due to the poor seismic resolution underlying the shelf break. Seafloor multiples in this area and the destruction of primary reflections during processing are particularly bad. In the southeastern map area complex salt structures result in poor seismic resolution. As a result, local correlation confidence in this region is low.

A time structure map of the Tr2 Sequence Boundary is presented in Figure 3-8. The sequence boundary was contoured over most of the map area, except in the southeast corner where data is aliased by poor seismic resolution. Within this region of poor seismic resolution, the sequence boundary was imaged in only local select areas. The location and depth of these local picks were mapped, but not contoured, and are shown in the southeastern corner of the Tr2 time structure map (Figure 3-8). The general trend of the contours on the Tr2 time structure map is south-southwest to north-northeast. This trend is slightly oblique to the strike lines of the regional seismic grid. The contour map shows that the sequence boundary has a shallow southeasterly sheet dip. There are local areas where the seaward dipping trend of the

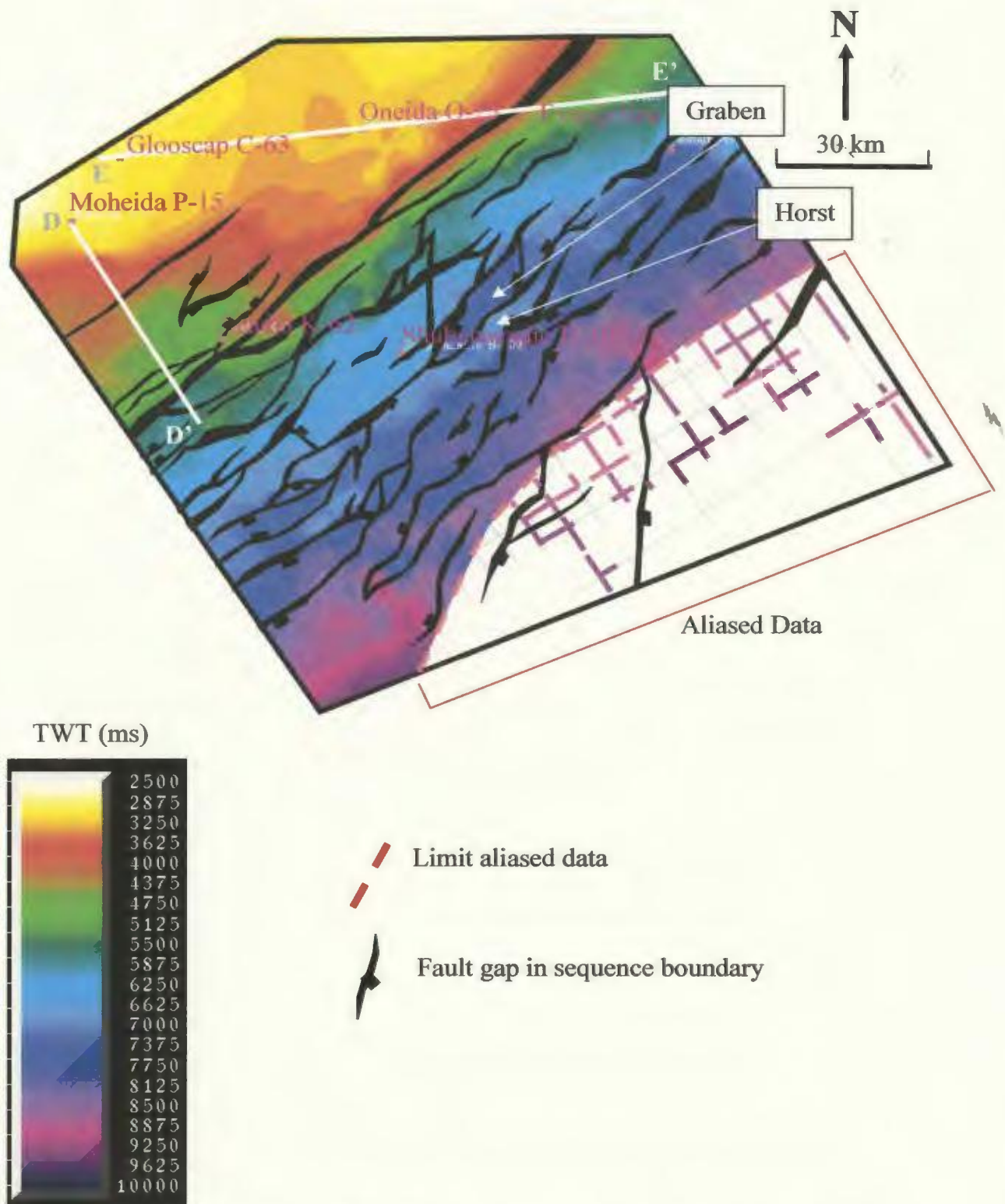


Figure 3-8: Time structure map of the Tr2 Sequence Boundary. Note that area of aliased data has not been contoured. Colour bar shows depth in TWT (ms). Well names and locations shown in pink, seismic grid shown in gray. Location of sections D-D' and E-E' shown in gray.



Tr2 Sequence Boundary is not observed. One such area is south west of the Shubenacadie H-100 well. Here, a local south-southwest to north north-east trending structural low (graben) and associated structural high (horst) are imaged. The time structure map the Tr2 Sequence Boundary shows numerous fault gaps trending approximately parallel with the time structure contours. The significance of these structural features will be discussed in Chapter 4.

### 3.3.5 Depositional Sequence 2

Depositional Sequence 2 (DS2) is structurally complex and characterized by variable frequency and reflection amplitude or is in places opaque. The sequence is bounded at its base by the Tr2 Sequence Boundary and at its top by the J1 Sequence Boundary. Correlation with exploration wells show that Depositional Sequence 2 is composed of Late Triassic to Early Jurassic sediments. Rocks contained within this sequence include red bed deposits of the Eurydice Formation and evaporites of the Argo Formation (Figures 3-9 and 3-10).

Evaporites of the Argo Formation commonly overlie red bed deposits of the Eurydice Formation, and are overlain by dolomites of the Iroquois Formation. The type section of the Eurydice Formation is from 2393-2965 m in the Eurydice P-36 well located in the Orpheus Basin. At this location the formation consists of 45% red to red-brown silty shale with minor green shale, 45% thin red sandstone and siltstone beds, and 10% limestone and evaporite (Wade and MacLean, 1990). At its type section between 2305-3085 m in the Argo F-38 well, Orpheus Basin, the Argo

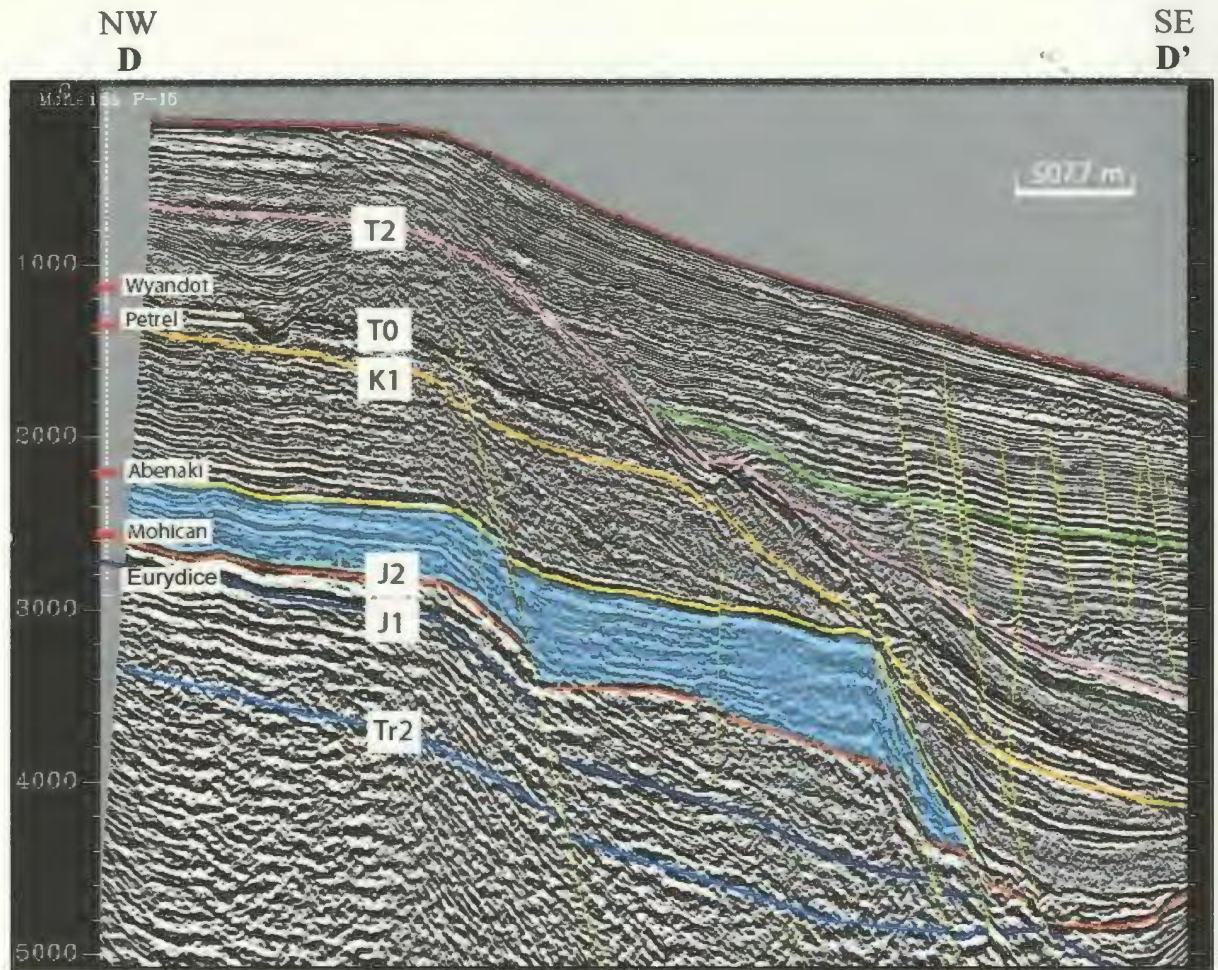


Figure 3-9: Seismic profile D-D'. Moheida P-15 well with lithostratigraphic ties shown. Area of Jurassic carbonate bank shown with blue transparency, top Abenaki Formation in Yellow. Vertical to near vertical yellow lines mark planes of discordance in seismic reflections. Vertical scale is in TWT (ms). See Figure 3-8 for location.



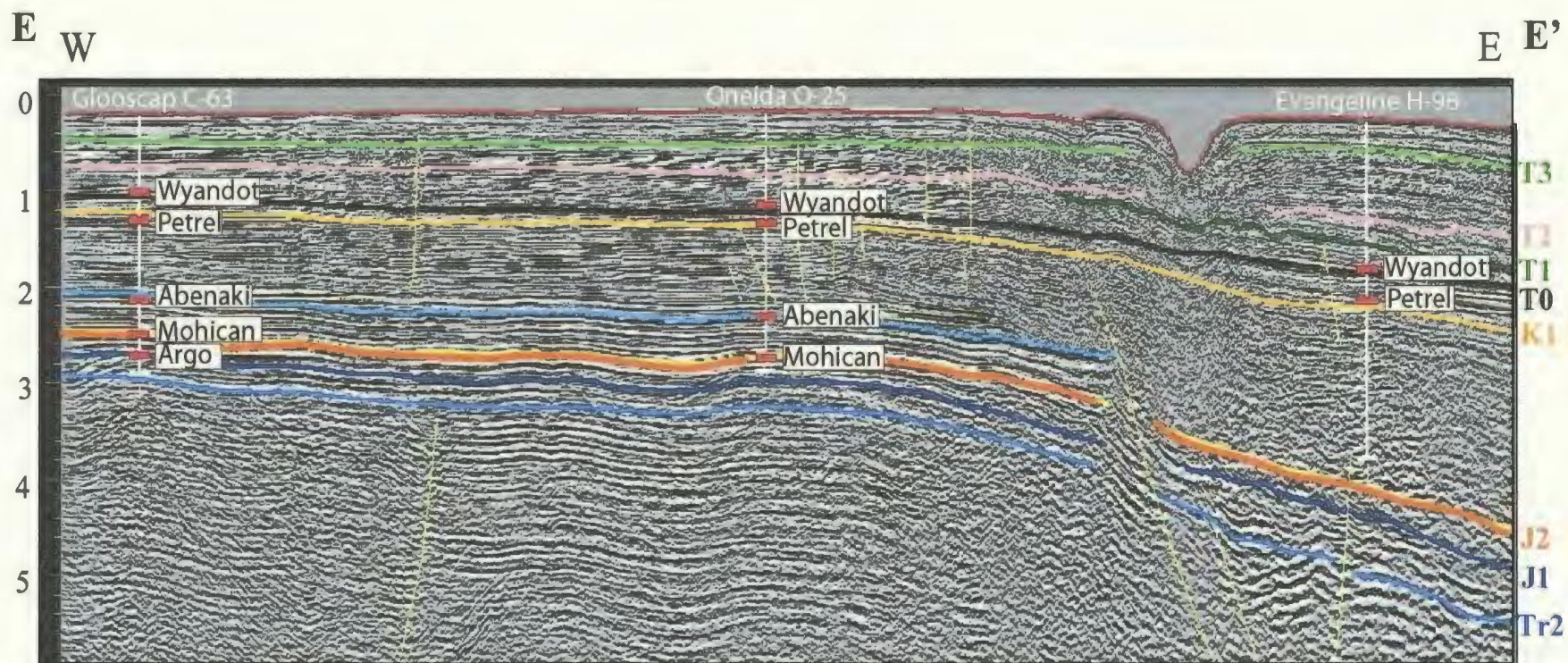


Figure 3-10: West -East seismic strike line E-E' showing lithostratigraphic correlations of Glooscap C-63, Oneida O-25, and Evangeline H-98 wells (see Figure 1-5 for location). See Figure 3-8 for location. Vertical scale in TWT (s).



Formation consists of a series of massive beds of colourless to pale orange salt, coarsely crystalline and separated by zones of red shale. The lithologic variation suggests brief periods when massive salt was deposited, interspersed with extended periods when there was little or no deposition (Wade, 1981).

Neither the thickness of undeformed salt nor the original distribution of the Argo Formation are known with certainty (Wade and MacLean, 1990). This is largely due to the depth of the formation and the extensive flowage of salt.

The only well to penetrate the Eurydice Formation within the study area is Moheida P-15 (Figure 3-9). At this location the seismic reflection character of the Eurydice Formation is strong and continuous. Glooscap C-63 was the only well used in this study that penetrated the Argo Formation (Figure 3-10). At this location, seismic reflection character of the Argo Formation is weak and discontinuous. Within the study area the seismic expression of the Argo and Eurydice formations vary considerably and the boundary between the two is commonly indistinguishable on seismic data. The seismic expression of the Argo Formation ranges from a sequence of strong parallel reflections to series of discontinuous, varying amplitude seismic reflections, to classic examples of reflection free seismic character (Figure 3-11). When salt deposits are *in situ* (autochthonous), thin, and a relatively small component of the total section, adjacent beds are less prone to disturbance and are generally concordant with the top of the salt unit. Thick salt packages (allochthonous) contain few coherent reflections and are associated with halokinesis (Figure 3-11). Locally weak to moderately strong reflections may be imaged within the evaporite formation.

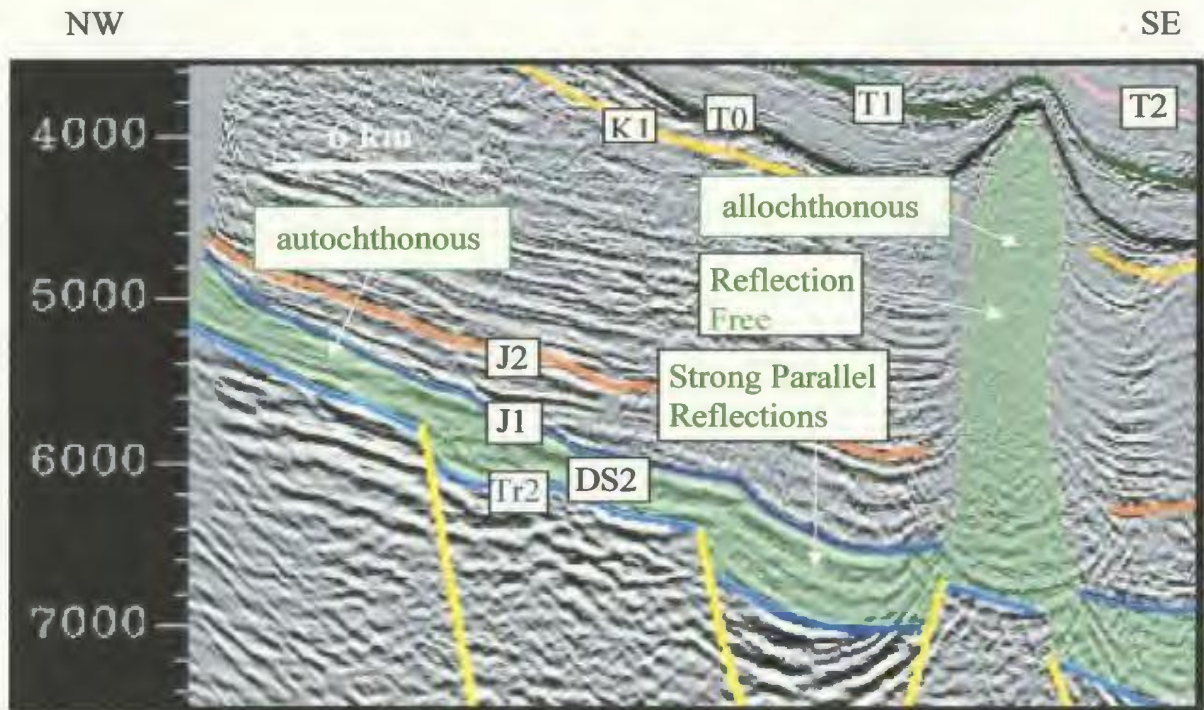


Figure 3-11 Seismic reflection profile from the eastern map area. Yellow lines represent faults. Sequence boundaries represented by remaining coloured lines. Depositional Sequence 2, the evaporite unit, is marked by green transparent overlay. Note variable seismic character of salt, from reflection free to containing strong parallel reflections. Vertical scale is TWT (ms).

These reflections may represent intervals where red beds of the Eurydice Formation are interbedded with the Argo Formation.

Due the strong seismic reflector produced at the salt sediment interface, the top salt seismic reflector was picked with a high degree of confidence. However, in areas of complexly deformed overlying sediments it remained highly interpretive. The base of salt reflector and inter-salt welds are even more speculative, but there is significant evidence to show overall allochthonous nature of the salt.

The Argo Formation has significant presence on the Scotian slope, the extent of which, including stratal and temporal distribution will be further discussed in Chapter 5.

### 3.3.6 J1 Sequence Boundary

Wade and MacLean (1990) state that the breakup unconformity is generally unrecognizable within subbasins of the Scotian Basin, but assumed to occur at approximately the top of the Argo Formation. Within the study area Sequence Boundary J1, the breakup unconformity, has been defined on the shelf as the Norian to Hettangian-Sinemurian unconformity marking the top of the Argo Formation and/or Eurydice Formations as identified in the Moheida P-15 and Glooscap C-63 wells (Figures 3-9 and 3-10). None of the other wells used in this study penetrate the breakup unconformity.

On the slope, the breakup unconformity is marked by a coherent, high amplitude reflector formed by a positive impedance contrast. The unconformity



marks a major seismic character change from overlying coherent, sub-parallel, divergent or convergent reflections that commonly onlap onto the boundary, to variable amplitude reflections of the underlying evaporite unit. Where reflections are imaged in the evaporite unit, they are commonly concordant to the breakup unconformity.

Figure 3-12 is a time structure map of the J1 Sequence Boundary. The general trend of the TWT contours is southwest to northeast with an overall southeasterly dip. The J1 Sequence Boundary is cut by a number of faults and interrupted by a number of salt structures. Locally there are a number of anomalous regions where depth of the J1 Sequence Boundary has been elevated or depressed in relation to the regional trend. These anomalous zones are concentrated in the mid- to lower-slope region and directly mimic the thickness of underlying *in situ* salt (autochthonous) or occur in proximity to salt structures. They have been interpreted as salt withdrawal synclines.

The coherent high amplitude reflector that marks Sequence Boundary J1 can be mapped regionally across the slope with a high degree of confidence, except in the southeast where it has been structurally complicated by salt tectonics or is poorly imaged due to overlying allochthonous salt. The correlation between the sequence boundary picked on the slope and on the shelf is somewhat speculative due to poor seismic quality in the region of the shelf break where seafloor multiples are present in the data. However, the pick presented here correlates to previously published interpretations that represent the approximate top of autochthonous salt or coeval formations. As such the J1 Sequence Boundary represents the breakup unconformity

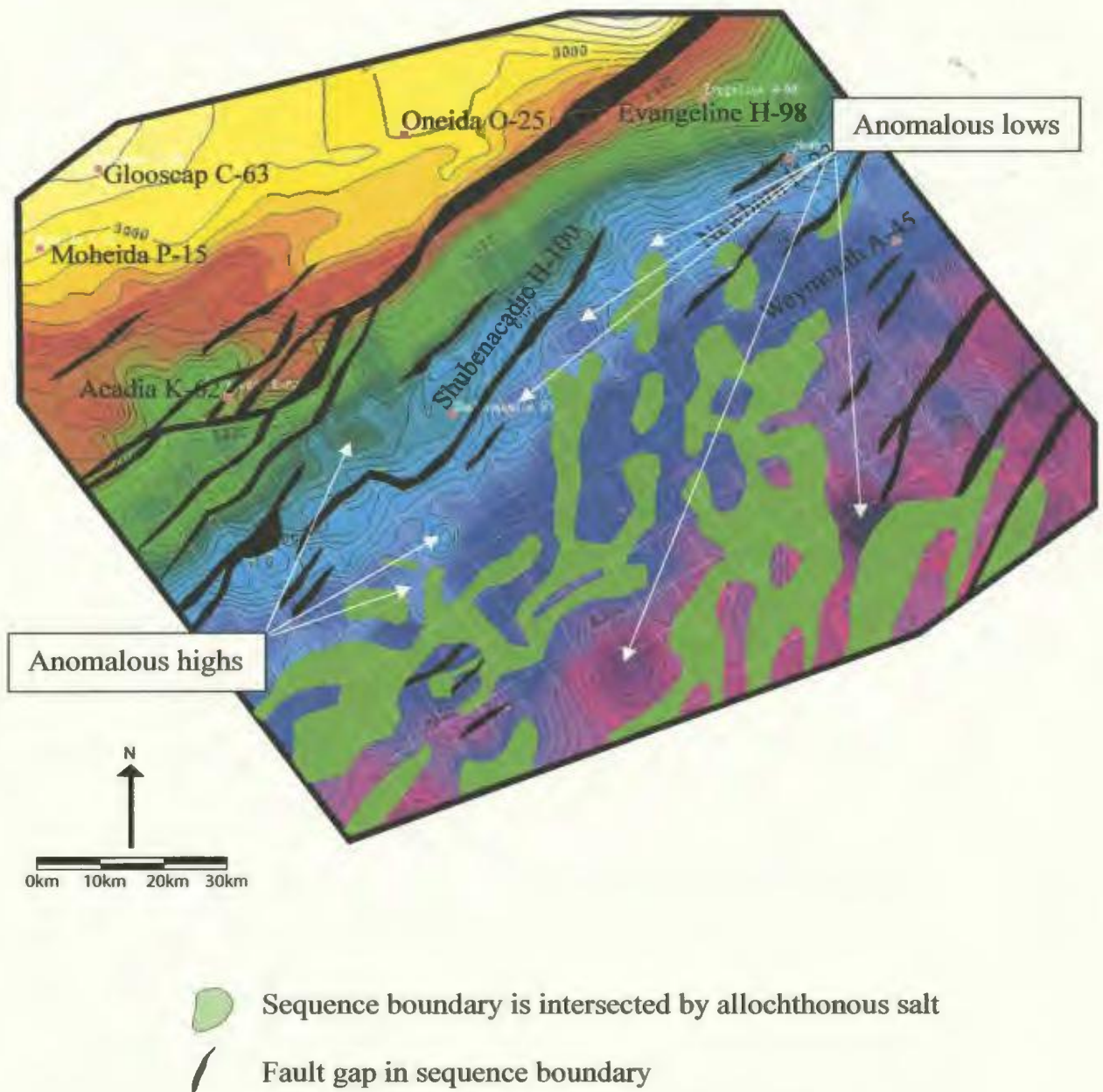


Figure 3-12: Time structure map of the J1 Sequence Boundary that separates depositional sequences 2 and 3. Contour interval of 125 ms with annotation every 1000 ms. Contour intervals given in TWT (ms). Seismic basemap in white, well locations in pink.

as defined in the Glooscap C-63 and Moheida P-15 wells (King and MacLean, 1974; Enachescu, 1987; Welsink et. al., 1989; Keen, et. al., 1990; Keen and MacLean, 1990b; Jackson and Talbot, 1991; Keen and Potter, 1995; Kidston et. al., 2002).

### 3.3.7 Depositional Sequence 3

Depositional Sequence 3 (DS3) is the sedimentary package bounded by sequence boundaries J1 and J2. Seismic reflections within DS3 are typically continuous with moderate amplitude and high frequency and commonly onlap the underlying J1 Sequence Boundary where it has positive structural relief. Locally, where the J1 Sequence Boundary has not been affected by faulting or salt movement, reflections of DS3 are concordant with it.

Depositional Sequence 3 characteristically contains divergent and convergent reflections (thickening and thinning of the sedimentary package). Divergent reflections (thickened growth packages) generally occur above the hanging wall of listric sedimentary faults, above salt evacuation structures and/or above basement lows. Conversely, convergent reflections (thinned packages) generally occur above the footwall of listric sedimentary faults, above positive (thickened) salt structures, or above basement highs. Thickness variation within Depositional Sequence 3 is largely random. Although there is a general thickening trend toward the southeast, changes in thickness are not always gradational, and rapid variations tend to occur in small or local areas. Thickened packages commonly extend 2 to 20 kilometers in length, and may be up to 1800 ms thick TWT (ms). Thinned packages tend to be circular to oval



in shape, 1 to 12 kilometers in diameter and as little as 90 ms thick TWT (Figure 3-13).

Reflections of DS3 are commonly truncated by the overlying J2 Sequence Boundary. Truncation is not uniformly distributed, but occurs locally toward underlying basement structural highs or salt-related highs. Truncated reflections commonly display a convergent reflection pattern (thin) toward the direction of erosion, and a divergent reflection pattern (thick) away from the direction of erosion. Correlations with exploration wells show that DS3 is composed of texturally immature clastics of the Mohican Formation (Figures 3-11 and 3-12). At its type section in the Oneida O-25 well, the Mohican Formation consists of dolomitic siltstones, fine grained sandstones and interbedded red, red-brown and green shale (Wade and MacLean, 1990).

### 3.3.8 J2 Sequence Boundary

On the Scotian Shelf, the J2 Sequence Boundary is a coherent, high amplitude, reflector formed by a negative impedance contrast. It is defined as the minimum value of a trough on a seismic display. This sequence boundary has been interpreted as an unconformity surface defined by the truncation of underlying reflections.

Figure 3-14 is a time structure map of the J2 Sequence Boundary. The figure shows the relatively uniform gentle southwesterly dip of the boundary except for local disturbances in proximity to salt structures. In the middle to lower slope region,

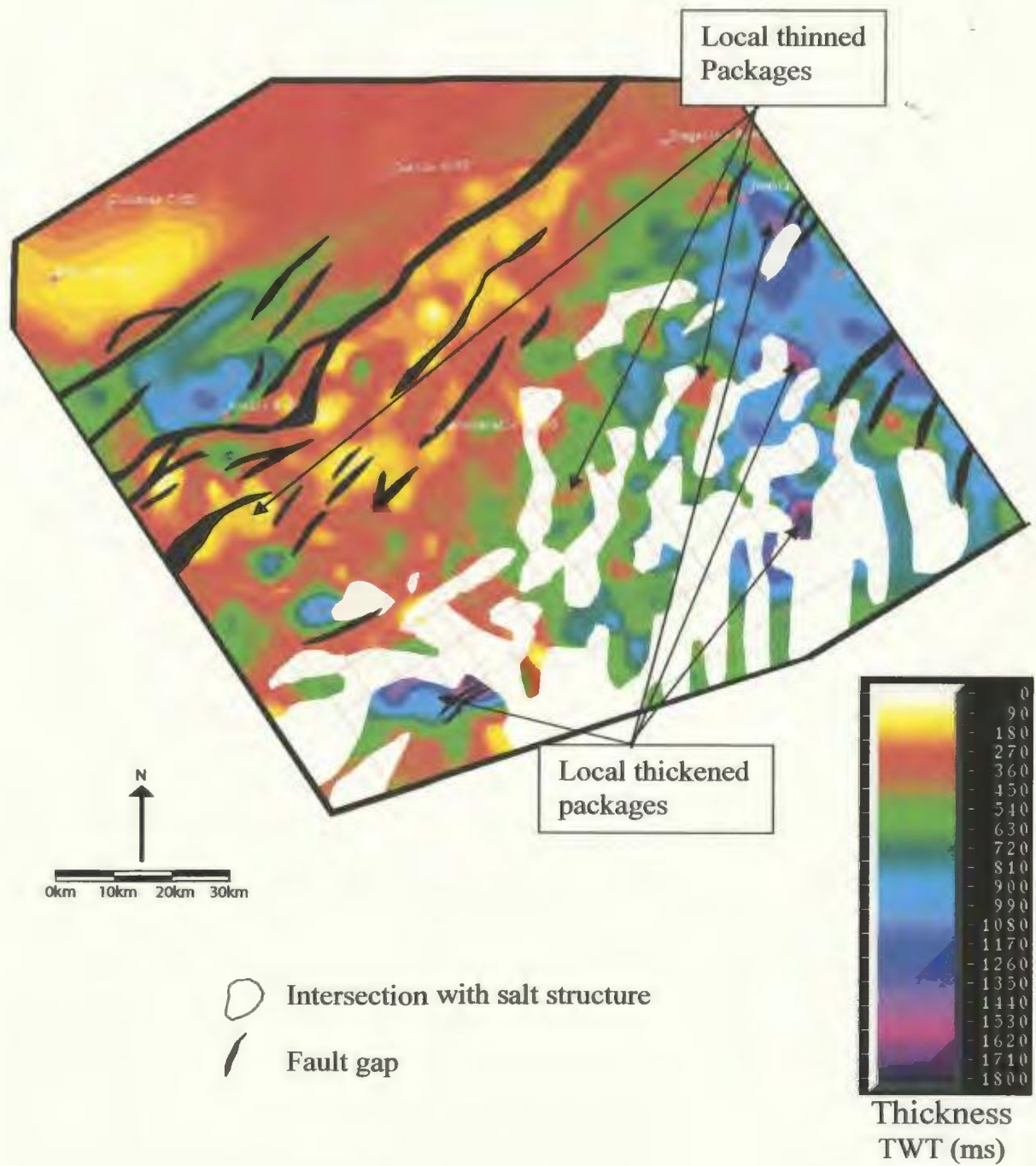


Figure 3-13: Isochron map of Depositional Sequence 3, Sequence Boundary J1 to Sequence Boundary J2. Thickness given in TWT (ms).

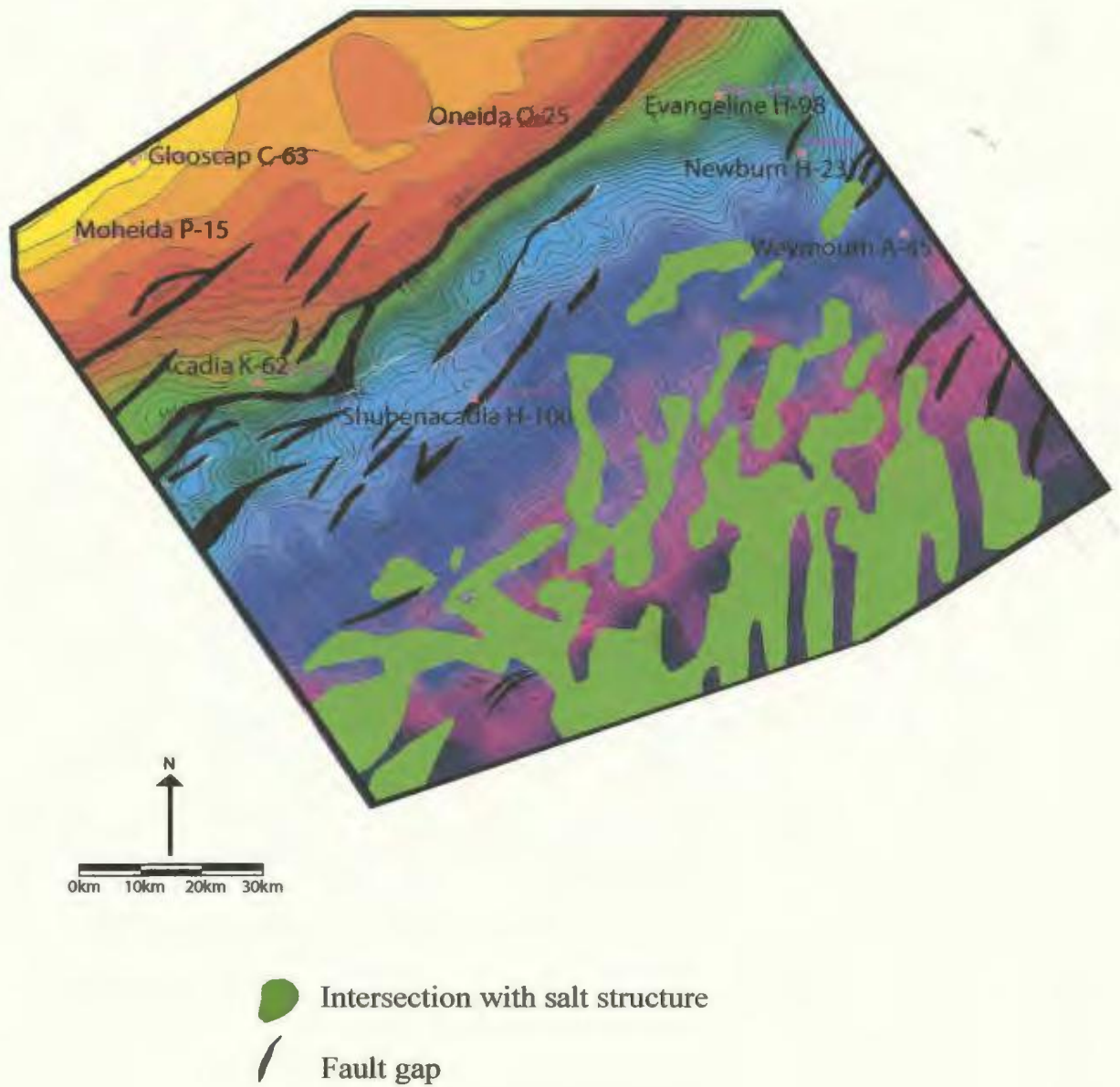


Figure 3-14: Time structure map of the J2 Sequence Boundary. Vertical scale is TWT (ms). Contour interval of 100 ms with annotation every 1000 ms.



overlying reflections are commonly concordant with the J2 sequence boundary. On the upper slope, reflections successively onlap the J2 sequence boundary at a very low angle in a landward direction.

Within the map area the J2 unconformity marks a major change in mini-basin style. The packages of reflections of underlying Depositional Sequence 3 are contained in local, relatively deep and narrow, mini-basins largely formed by salt movement or tectonics (Figure 3-13), where as overlying Depositional Sequence 4 reflections are contained in relatively wide and shallow minibasins. Further discussion of DS4 is presented in section 3.3.10.

Correlations with exploration wells show that the J2 Sequence Boundary marks the top of texturally immature, Aalenian-Bajocian, clastic deposits of the Mohican Formation (Figure 3-9 and 3-10). The strong coherent reflector that marks the J2 sequence boundary is easily recognizable, resulting in good regional correlation confidence. Correlation confidence decreases to fair in areas where the boundary is overlain by allochthonous salt.

### 3.3.9 Top Abenaki Formation Marker

The marker representing the top of the Abenaki Formation is a crisp, strong amplitude peak marking the interface between Early Cretaceous clastics and Jurassic carbonates. The Abenaki Formation is defined as a Bajocian to Tithonian limestone at its type section between -2858 m to -3821 m in the Oneida O-25 well (Figure 3-9). Three other wells used in this study, the Moheida P-15, Glooscap C-63 and Acadia K-

62, also intersected the Abenaki Formation.

The Abenaki Formation has limited areal extent, as it is present on the shelf and extends only locally onto the slope in the western map area near the Acadia K-62 well (Figure 3-15). The southern boundary of the formation is a tectonic lineament of en échelon basement rooted faults.

Due to the pronounced seismic character of the top Abenaki Formation marker, and the robust well control, correlation confidence in the seismic marker is excellent.

#### 3.3.10 Depositional Sequence 4

Depositional Sequence 4 is bounded at its top by the K1 Sequence Boundary. Two distinct boundaries make up the base of this sequence. Where the Jurassic carbonate bank is present, the top Abenaki Formation marker forms the base of Depositional Sequence 4. Over the rest of the map area, the base of the sequence is marked by the J2 Sequence Boundary (Figure 3-9).

Seismic reflections within Sequence Boundary 4 are primarily weak, continuous, evenly spaced and parallel to sub parallel, with a shallow southeasterly sheet dip. On the shelf, DS4 reflections are generally concordant with both the top Abenaki Formation marker and Sequence Boundary K1. Immediately landward of the paleo-carbonate bank DS4 reflections successively downlap onto the top Abenaki Formation marker. Near the Jurassic slope break, at the seaward limits of the paleo-carbonate bank, reflections of DS4 successively onlap the top Abenaki Formation

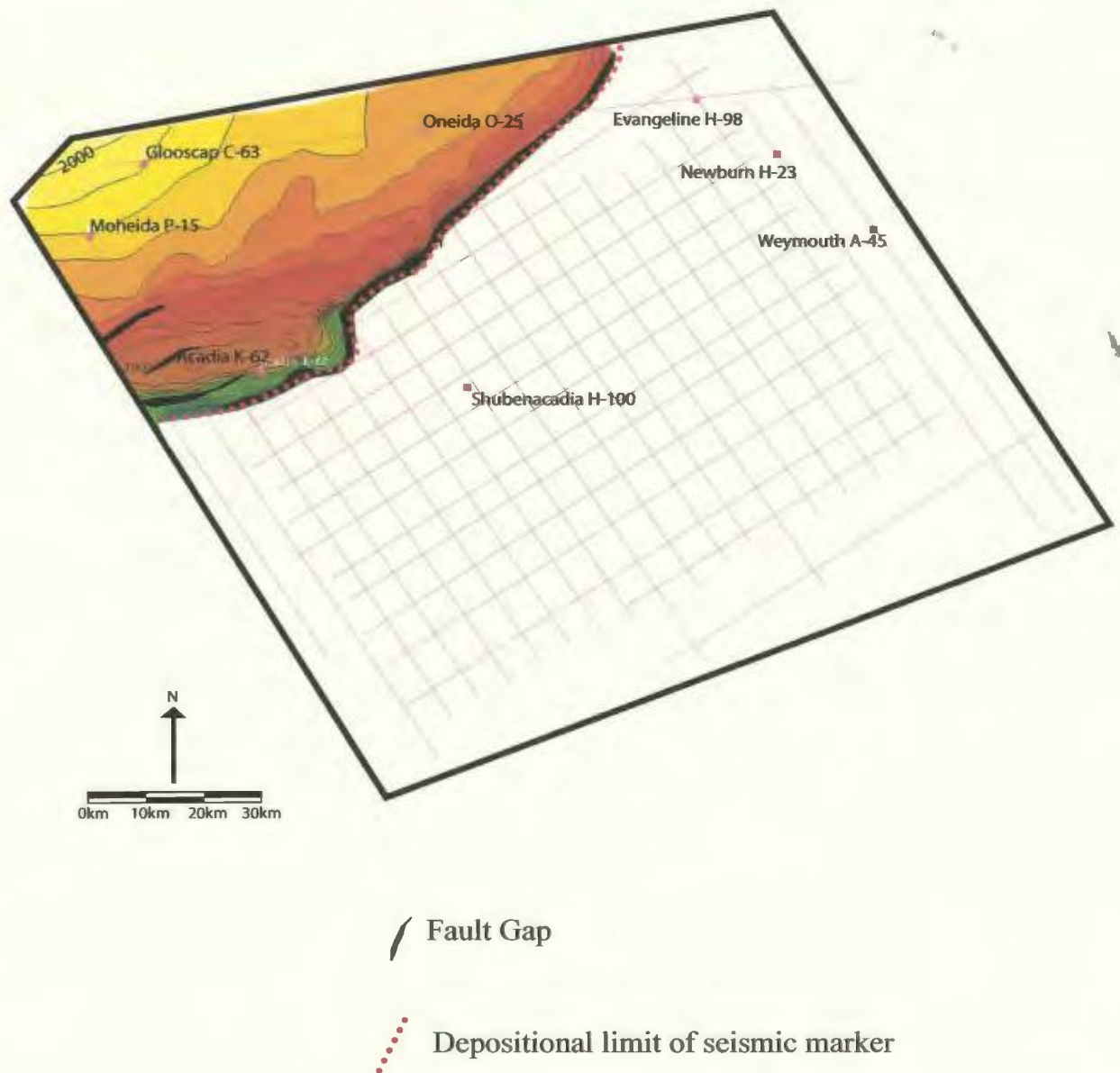


Figure 3-15: Time structure map of the top of the Jurassic carbonate bank, Abenaki Formation. Contour interval of 100 ms with annotation every 1000 ms. Contour interval given in TWT. Seismic basemap shown in pink, well locations marked by pink squares.



marker in a landward direction (Figure 3-9).

On the slope, reflections within Depositional Sequence 4 are commonly concordant with the overlying K1 Sequence Boundary. In local areas, generally within close proximity to salt structures, the K1 Sequence Boundary truncates DS4 reflections at a very low angle, causing minor local thinning in the sequence. In the lower slope region, DS4 reflections are often concordant with the J2 sequence boundary. Towards the middle to upper slope region DS4 reflections may be concordant with or successively onlap J2 at a very low angle. Seismic profiles from the slope show very little thickness variation within in Sequence Boundary 4.

Correlations with exploration wells show that Depositional Sequence 4 is comprised of Albain to Callovian age clastic deposits of the Logan Canyon, Mississauga, Mic Mac and Verrill Canyon formations. Due to the gradational contact between the Mississauga and Mic Mac formations, and the fact that the Verrill Canyon Formation is considered to be the distal facies equivalent of both (Wade and MacLean, 1990), it was not possible to differentiate between these formations on seismic data. However, a thin Hauterivian to Barremian aged limestone marker within the Mississauga Formation, the O Marker recognized by Jansa and Wade (1975), was identified and used as an age constraint within this depositional sequence.

Figure 3-16 is an isochron map of Depositional Sequence 4. The map shows a general thickening of the sequence towards the east, and inversely, a thinning of the sequence towards the west. There is little variation in the thickness of DS4 in a north-

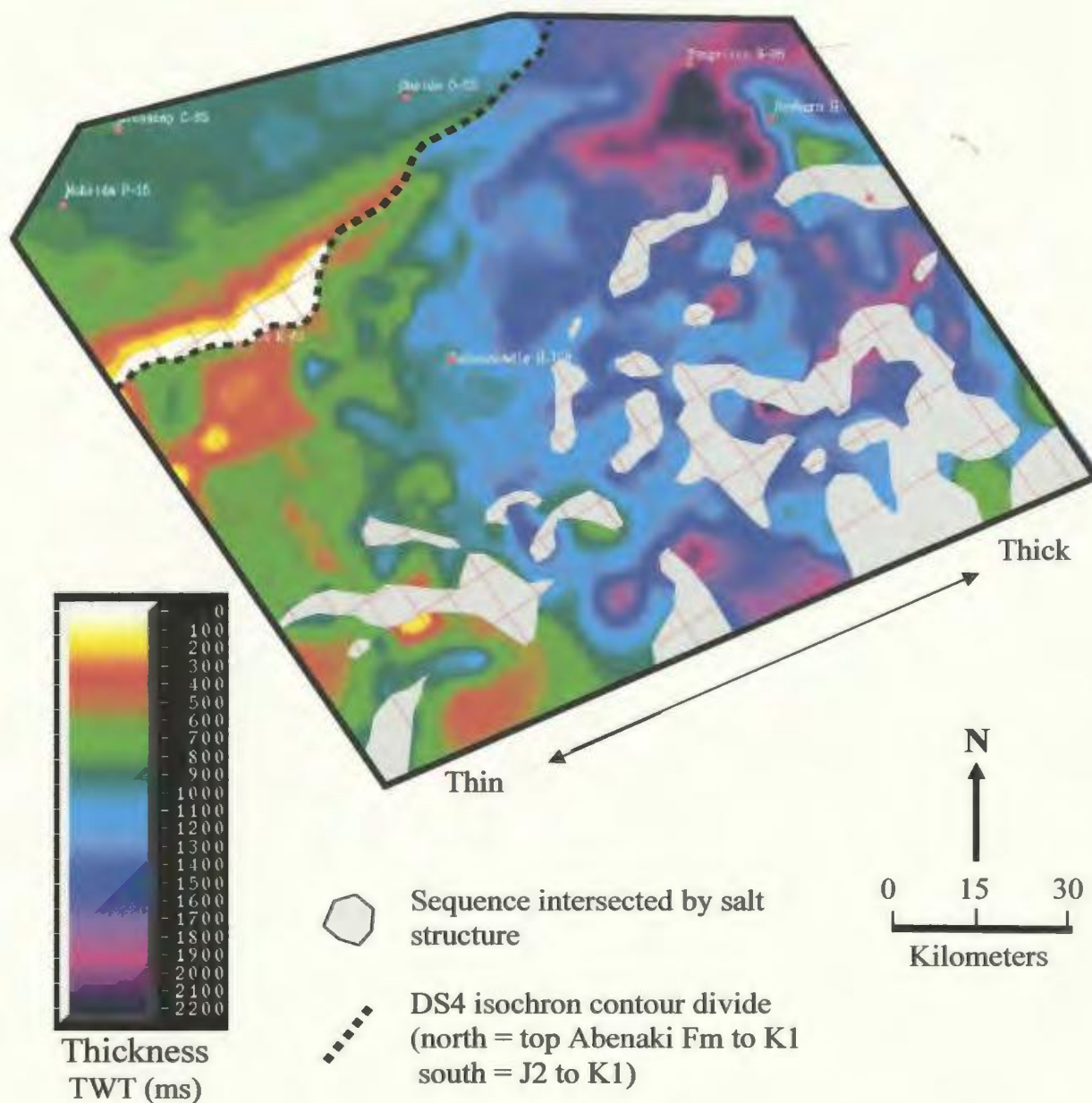


Figure 3-16: Isochron map of Depositional Sequence 4. Area north of black dashed line is Top Abenaki Formation to Sequence Boundary K1, area south of black dashed line is Sequence Boundary J2 to Sequence Boundary K1. Thickness given in TWT (ms), well locations in pink, seismic grid in pink. Note that sequence thickens to the east, thins to the west, and has fairly consistent thickness in a north-south trend on the slope.

south (slope-parallel) direction. The thickening trend of large shallow mini-basin of DS4 is in stark contrast to the deep local mini-basins of DS3.

The general easterly thickening trend of DS4 is likely due to the proximity of this portion of the study area to the Cretaceous Sable Delta. Inversely, western thinning trend of the sequence is likely a result of the distal position of this area to the Delta.

### 3.3.11 The O Marker

The O marker, a Barremian aged limestone bed contained within the Missisauga Formation, is a well-established seismic horizon in Scotian Shelf literature and easily recognizable seismic data (Wade and MacLean, 1990). This marker intersects three of the shelf exploration wells within the study area, the Moheida P-15, Glooscap C-62 and Oneida O-25 wells. The O Marker is imaged on seismic data as the only strong reflector contained within Depositional Sequence 4. The marker can only be mapped, with high correlation confidence, across the shelf portion of the study area.

The O Marker is not a sequence boundary as seismic reflections are concordant both above and below it. However, the O Marker represents an easily mappable seismic marker that ties well with shelf wells and can be used as an age check for Depositional Sequence 4. The O Marker has a high correlation confidence on the shelf in proximity to the wells in which it was intersected.



Time structure mapping of the O Marker shows a relatively undeformed and uniformly southwesterly dipping horizon.

### 3.3.12 K1 Sequence Boundary

Sequence Boundary K1 is a minor unconformity surface defined by the local low angle truncation of underlying reflections and local onlap of overlying reflections. The boundary is imaged on seismic data as a coherent and high amplitude reflector formed by a positive impedance contrast.

Within the study area, the K1 Sequence Boundary marks a significant change in seismic character from underlying low amplitude reflections of DS4 to overlying reflections with distinctive very high amplitude.

In map view, the K1 Sequence Boundary dips fairly uniformly south-southeast. Contours trend southwest to northeast, approximately parallel with seismic strike lines. Minor deviations in the sheet dip occur locally in proximity to salt structures.

Correlations with exploration wells show that this minor unconformity is approximately Turonian to Coniacian in age (Figure 3-9 and 3-10), and corresponds to the Petrel Member Marker (Jansa and Wade, 1975). Confidence in the seismic correlation of this pick is excellent. The boundary has been intersected in all six wells used in this study, and constitutes an easily recognizable seismic marker.

### 3.3.13 Depositional Sequence 5

Depositional Sequence 5 (DS5) consists of a series of strong, high amplitude reflections bounded by the K1 and T0 sequence boundaries. Correlations with exploration wells show that the sequence contains Late Cretaceous shales of the Dawson Canyon Formation, and Campanian to Maastrichtian aged chalk deposits of the Wyandot Formation (Figure 3-9 and 3-10). The high amplitude reflections characteristic of DS5 are in stark contrast to the low to moderate reflectivity typical of most of the Mesozoic siliclastic basin fill (Figure 3-17). Thus, DS5 is easily identifiable on seismic data. McIver (1972) described the Wyandot Chalk as “the most distinctive and widely recognized lithologic unit on the (Scotian) shelf”.

Seismic reflections within Depositional Sequence 5 are very strong, continuous, evenly spaced, and parallel to sub parallel. On the shelf, DS5 reflections downlap the K1 sequence boundary at a low angle. On the slope DS5 reflections are concordant with K1 (Figure 3-17).

On the western slope DS5 is erosionally truncated by three large canyons. These canyons measure up to 15 kilometers in width and have up to 300 ms of erosional relief (Figure 3-17 and 3-18). The canyons extend, parallel to the slope dip, from the shelf break to the diapiric province of the lower slope region. Due to this erosion, local thickness of Depositional Sequence 5 varies greatly throughout the map area. However, a general trend of thickening toward the west and thinning toward the east can be observed on both the shelf and slope (Figure 3-18). This thickening trend

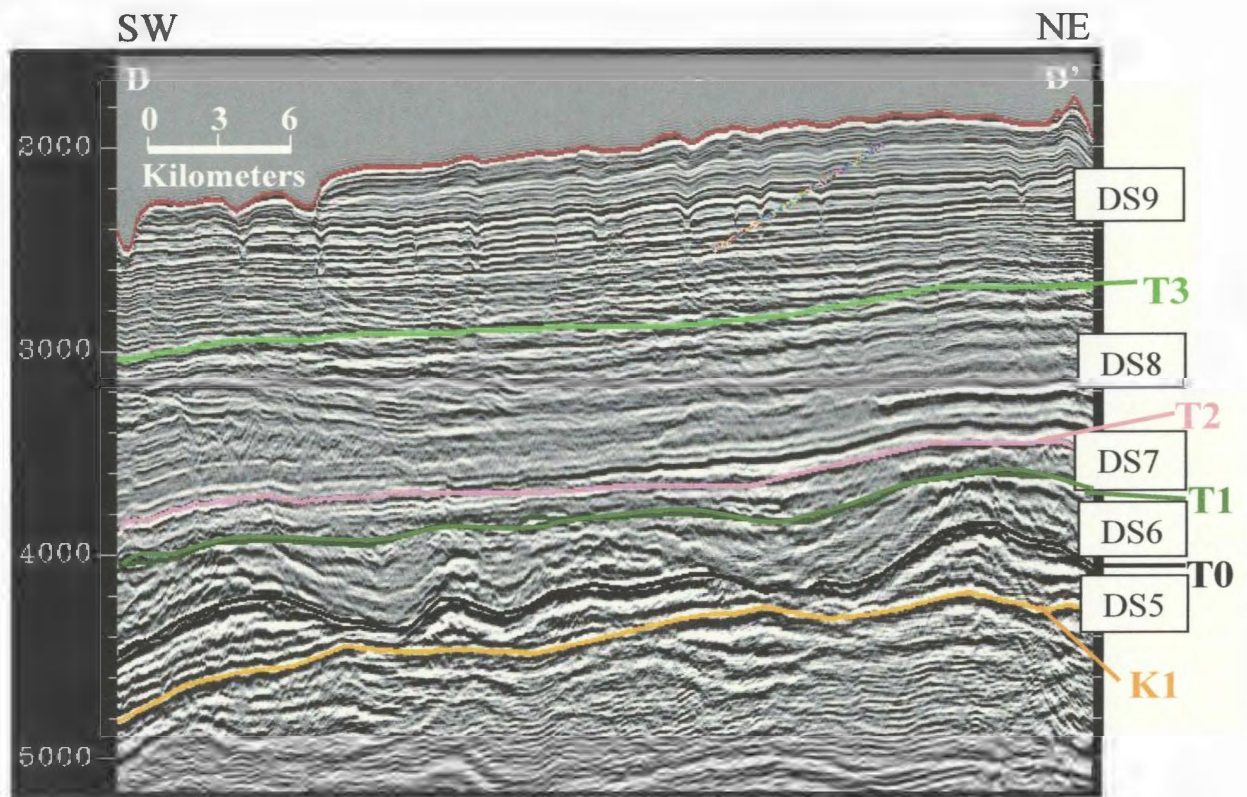


Figure 3-17: Seismic strike line D-D' from the western map area, central slope. Depth given in TWT (ms). See Figure 3-18 for location.



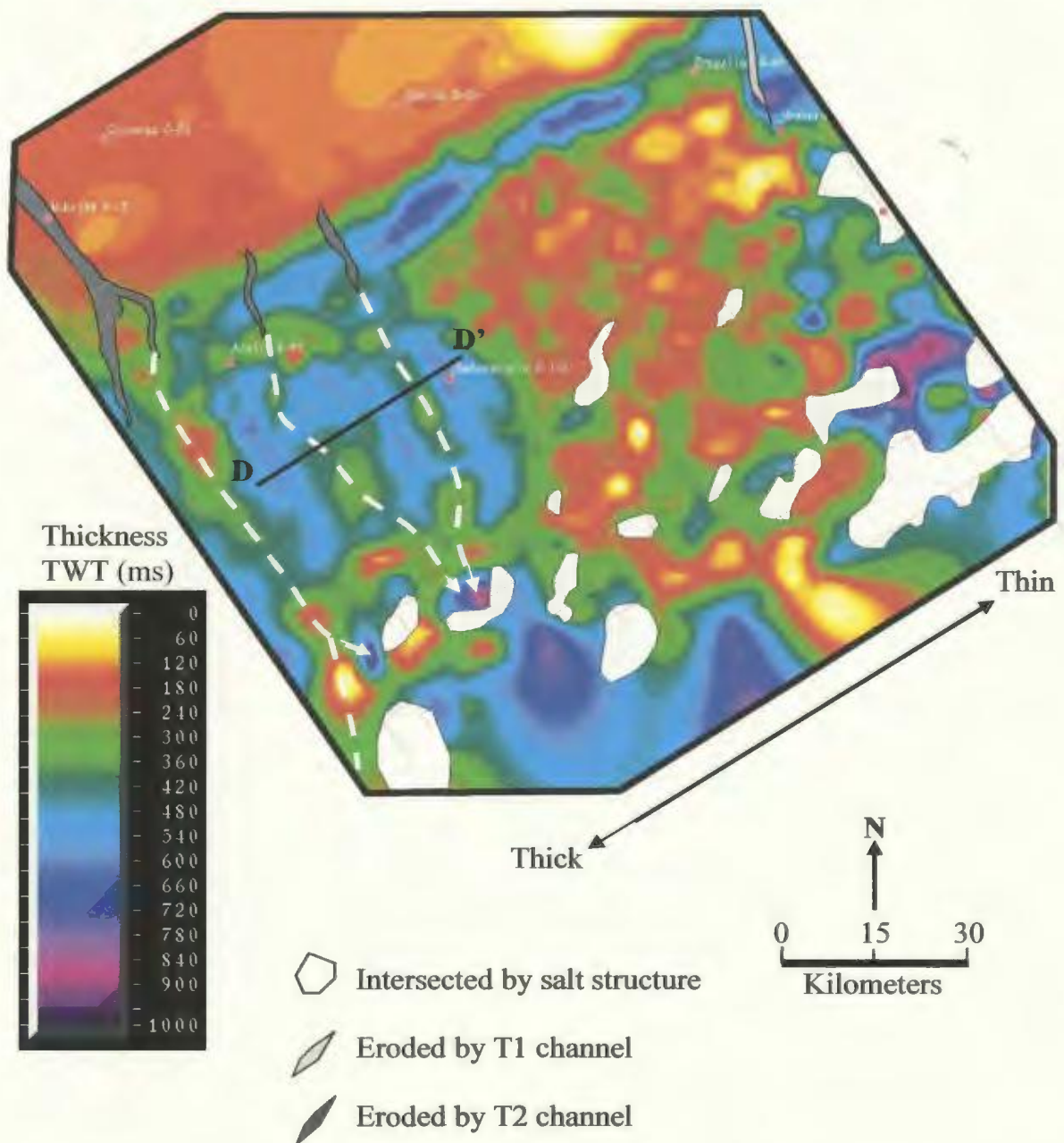


Figure 3-18: Isochron map of Depositional Sequence 5, Sequence Boundary K1 to Sequence Boundary T0. Thickness given in TWT (ms). Well locations in pink, seismic grid in pink.

is the exact opposite of that of underlying DS4, which thickens to the east and thins to the west (Figure 3-16).

Sedimentation rates for the Wyandot Formation are among the lowest in the Scotian Basin. Average thickness of the formation is 135 m which was deposited over 15 Ma (Wade and MacLean, 1990).

#### 3.3.14 T0 Sequence Boundary

Sequence Boundary T0 is a coherent a high amplitude reflector formed by a positive impedance contrast. It is defined as the maximum value of a peak on a seismic display. Correlations with exploration wells show that this major unconformity marks the top of Campanian to Maastrichtian chinks of the Wyandot Formation (Figures 3-9, 3-10 and 3-19). It is therefore correlated with the base Tertiary unconformity of Wade et al. (1989).

The T0 Sequence Boundary is an undulating surface of erosion with significant relief and a slope dip parallel (north-west to south-east) orientated fabric. (Figure 3-20). Overlying reflections drape sequence boundary on slope and onlap onto boundary in a landward direction near shelf break

In the basal slope region, the T0 Sequence Boundary has been intersected by a number of salt structures. Overlying reflections successively onlap T0 toward these salt structures.

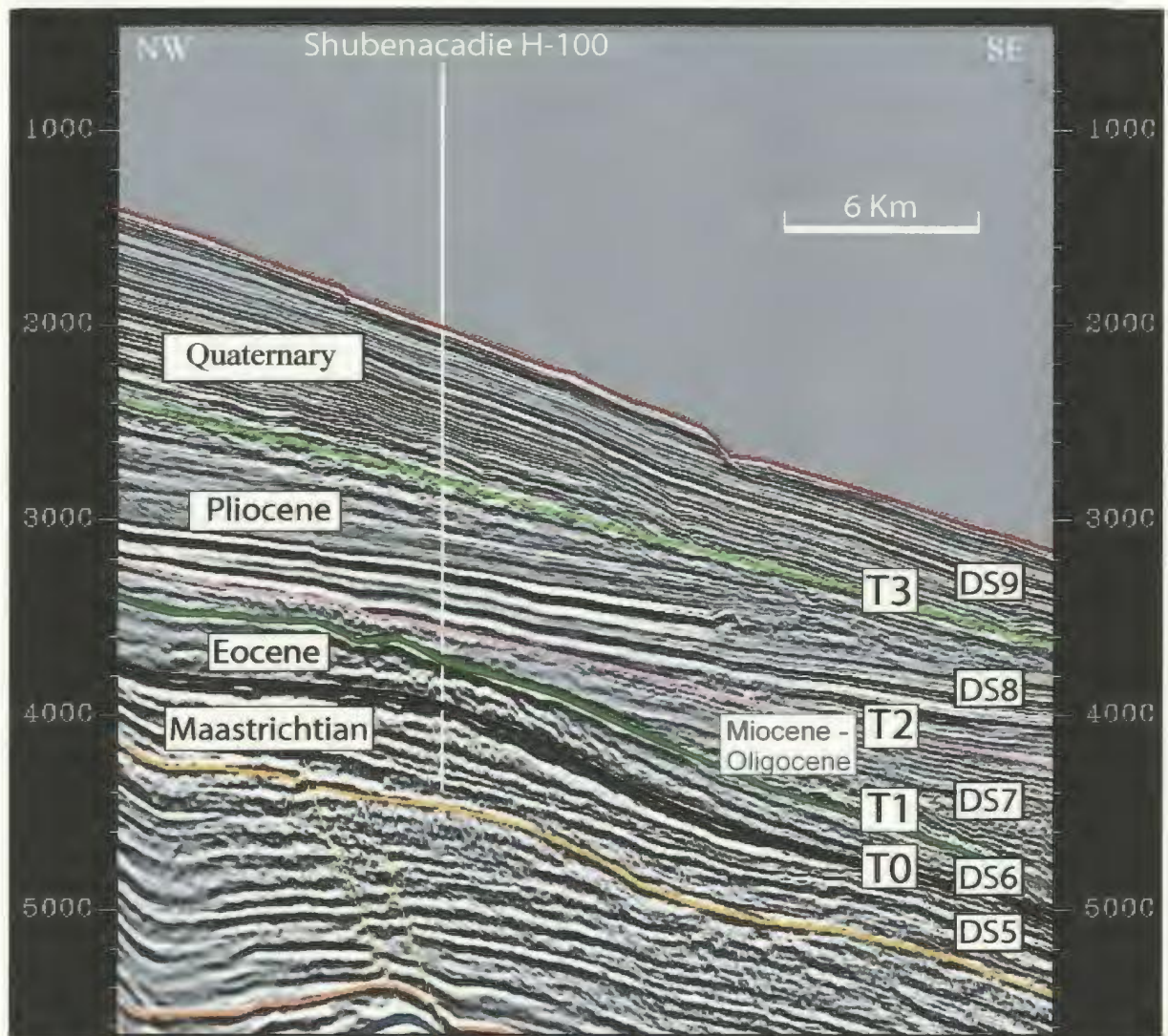
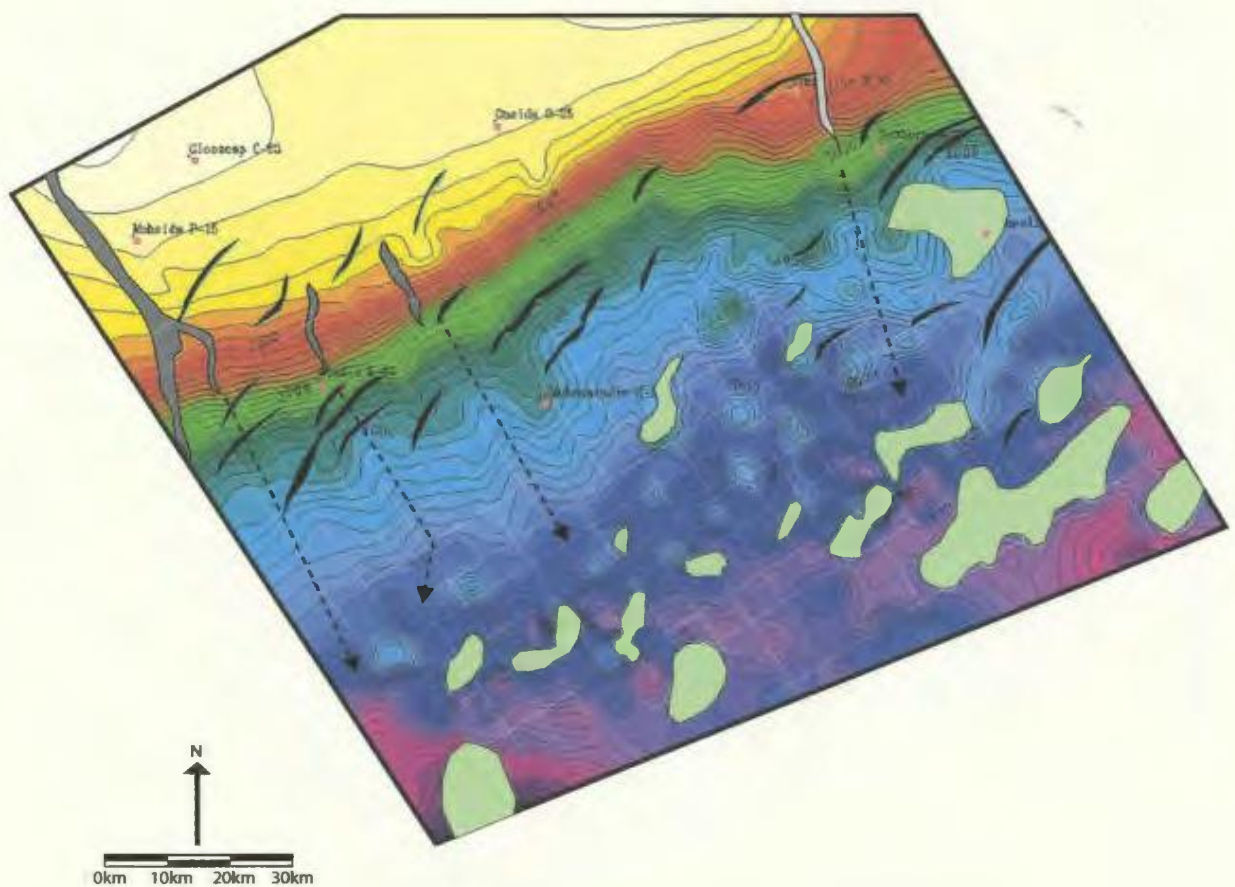


Figure 3-19: Northwest-southeast seismic profile from the Scotian Slope near the Shubenacadie H-100 well showing Tertiary sequence boundaries (T0-T3), depositional sequences (DS5-DS9) and ages. Depth given in TWT (ms)










-  Sequence boundary is intersected by salt structure
-  Fault gap
-  Sequence boundary is truncated by Sequence Boundary T2
-  Sequence boundary is truncated by Sequence Boundary T1
-  Direction of erosion

Figure 3-20: Time structure map of the T0 Sequence Boundary separating depositional sequences 5 and 6. Contour interval of 125 ms with annotation every 1000 ms. Seismic grid in white, well locations in pink. Time intervals given in TWT (ms). White arrows represent interpreted paleo channels.

Due to the consistently high amplitude and continuity the correlation confidence in reflector marking the T0 Sequence Boundary is excellent. The unconformity has been intersected by all wells within the study area.

### 3.3.15 Depositional Sequence 6

Depositional Sequence 6 (DS6) is a low reflectivity package of sediments delimited on the slope by sequence boundaries T0 and T1 and on the shelf by sequence boundaries T0 and T2. Reflections within this sequence are generally concordant with (drape) the undulating T0 Sequence Boundary (Figure 3-17). Commonly, the overlying T1 sequence boundary sequentially truncates reflections of DS6 over DS5 highs and in a landward direction (Figure 3-5 and 3-17).

On the shelf and lower slope, seismic reflections within DS6 are commonly evenly spaced and parallel to sub parallel. On the upper to central slope, reflections are often broken and rotated by minor faults or chaotic. Such reflection patterns are interpreted as gravity faulting and debris flows respectively and indicate periods of slope instability (Galloway, 1986). Within the lower slope region, local unconformities related to episodes of salt movement and subsequent growth strata have been mapped within DS6.

Local thickness distributions of Depositional Sequence 6 are largely oriented in a slope dip parallel (north-west to south-east) pattern (Figure 3-21). The location of thickened and thinned DS6 packages coarsely correspond to areas of high and low erosional relief of Sequence Boundary T0 respectively.

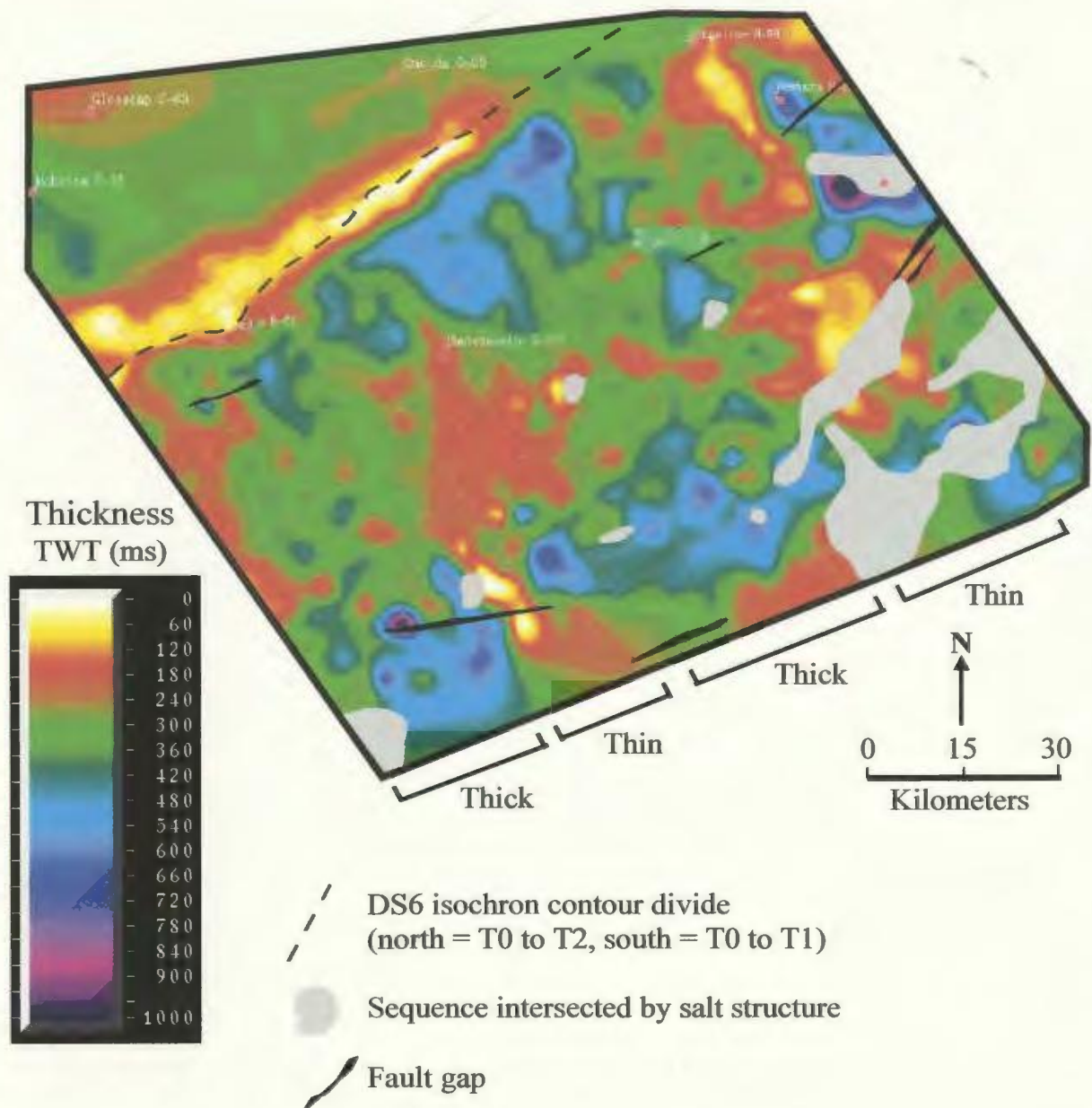


Figure 3-21: Isochron map of Depositional Sequence 6. Area north of black dashed line is Sequence Boundary T2 to Sequence Boundary T0, area south of black dashed line is Sequence Boundary T1 to Sequence Boundary T0. Note the slope parallel thickness distribution pattern. Thickness given in TWT (ms), well locations in pink, seismic grid in white.



Correlation with the Shubenacadie H-100 well has dated Depositional Sequence 6 as Eocene.

#### 3.3.16. T1 Sequence Boundary

Sequence Boundary T1 is defined as an angular unconformity. Reflections underlying T1 are either concordant to or angularly truncated by it with minor erosional relief in a landward direction. Locally, near salt induced structures, underlying reflections are successively truncated towards the structure. Reflections overlying T1 successively onlap on to it toward the shelf, except locally where onlapping reflections are directed towards salt structures.

The dip angle of the T1 Sequence Boundary is moderate and to the south-southeast in the upper slope region, and decreases to shallow in the central and lower slope region. The boundary is relatively planar over the much of the slope, with the exception of the lower slope region in proximity to the slope diapiric province. In the western map the T1 boundary undulates slightly, mimicking the structure of the underlying T0 Sequence Boundary (Figure 3-18). The T1 boundary is truncated in the region of, and near parallel with, the shelf break by Sequence Boundary T2 (Figure 3-22)

Correlation with the Shubenacadie H-100 well has dated Sequence Boundary T2 as late Eocene to Oligocene.

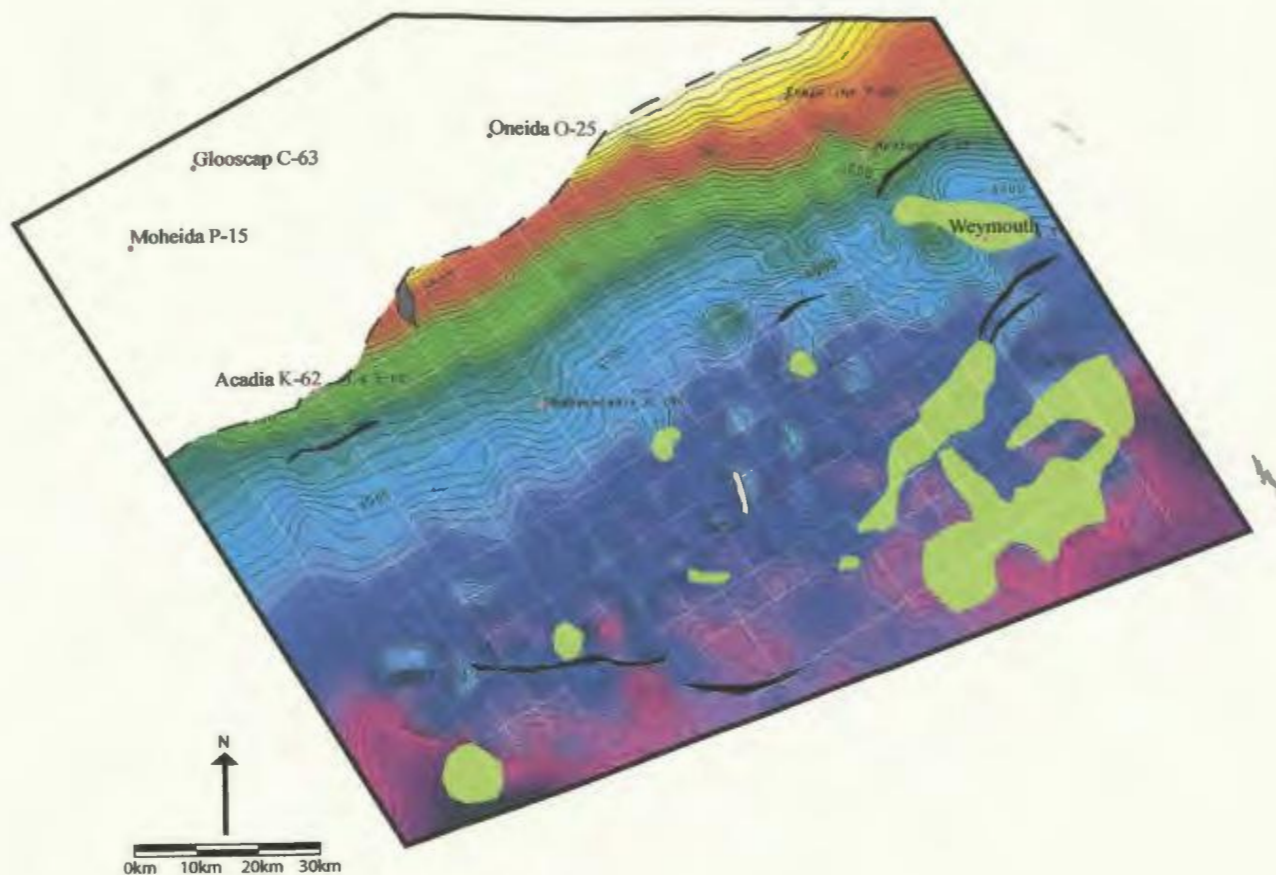


Figure 3-22: Time structure map of the T1 Sequence Boundary. Contour interval of 100 ms with annotation every 1000 ms. Seismic grid in white, well locations in pink. Time interval given in TWT (ms).

### 3.3.17 Depositional Sequence 7

Depositional Sequence 7 (DS7) is a series seismic reflections bounded at the base by Sequence Boundary T1, and at the top by Sequence Boundary T2. Through comparison with data from the Shubenacadie H-100 exploration well, the sequence has been dated Miocene to Oligocene.

Reflections within DS7 successively downlap Sequence Boundary T1 at a low angle in a basinward direction. Sequence Boundary T2 successively truncates DS7 reflections in a landward direction. Slightly basinward of the slope break is a lineament marking the landward limit of DS7 where Sequence Boundary T1 is truncated by Sequence Boundary T2 (Figure 3-23). The lineament trends southwest-northeast. Basinward and parallel to lineament the DS7 thickens in a basinward direction. In the proximity of salt structures, the general thickening trend is commonly disrupted by local areas of thickening and thinning. Within DS7, local sequence boundaries related to episodes of salt movement and subsequent growth strata have been mapped.

The seismic character of DS7 is variable throughout the study area. Frequency and amplitude of reflections both decrease from moderate in the western study area to low in the east. Reflector configuration is generally parallel to sub-parallel in the east and west of the study area. In the central region reflection patterns are commonly chaotic to wavy, suggesting slope instability in this area.



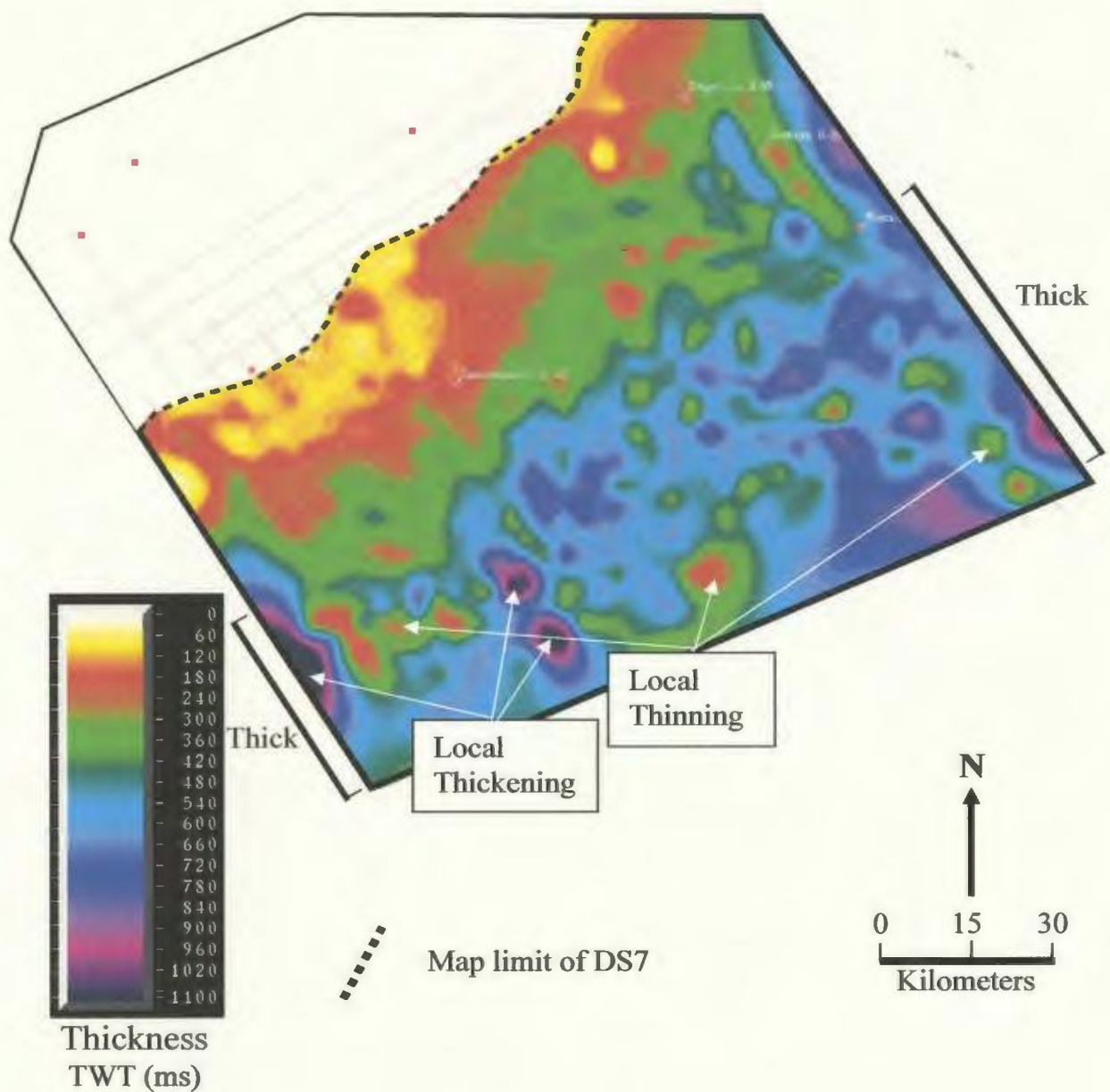


Figure 3-23: Isochron map of Depositional Sequence 7 (DS7), Sequence Boundary T1 to Sequence Boundary T2. Dashed black line represents area where T2 erosionally truncates T1. Thickness given in TWT (ms). Well locations in pink, seismic grid in white.

### 3.3.18. T2 Sequence Boundary

The T2 Sequence Boundary is characterized by the seaward divergence of reflections on the slope. Overlying near horizontal to very shallowly southwest dipping reflections successively onlap the T2 Sequence Boundary towards the shelf break. These reflections become concordant with T2 in the basal slope region.

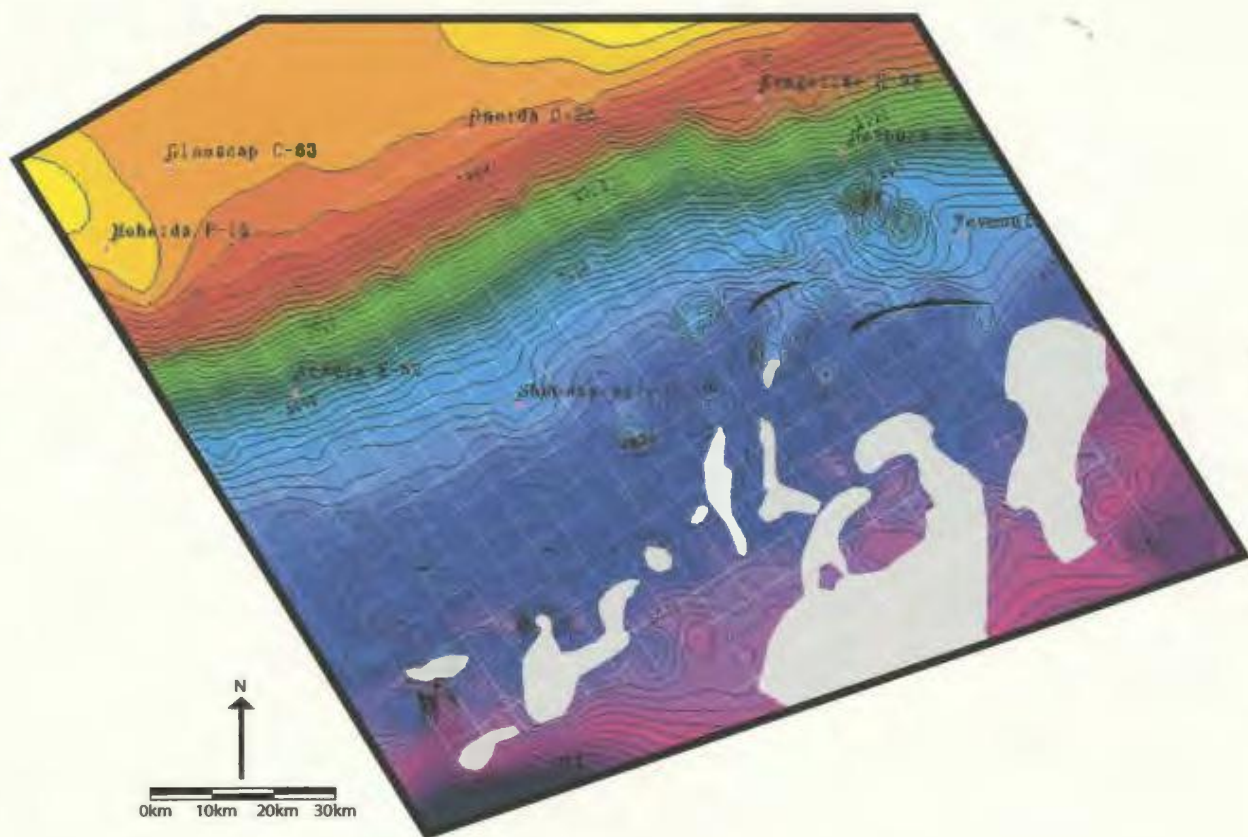
Underlying reflections dip moderately to shallowly seaward and are sequentially truncated by T2 in a landward direction.

The T2 Sequence Boundary dips moderately south-southeast in the upper slope region. In the central and lower slope region the dip angle decreases significantly (Figure 3-24). In the central slope region, sequence boundary T2 is locally eroded by a large surface channel. In the lower slope region, relatively large portions of Sequence Boundary T2 have been eroded by Sequence Boundary T3. This type of erosion occurs exclusively over large salt bodies where T2 has been elevated above its regional dip.

Correlation with the Shubenacadie H-100 well has dated the T2 Sequence Boundary as Miocene-Pliocene.

### 3.3.19 Depositional Sequence 8

Depositional Sequence 8 (DS8) is a series of near horizontal low amplitude reflections bounded at the base by Sequence Boundary T2, and at the top by Sequence Boundary T3. Through comparison with data from the Shubenacadie H-100 exploration well, the sequence has been dated Pliocene.






-  Sequence boundary truncated by T3 over salt structure
-  Fault Gap
-  Sequence boundary truncated by bathymetry

Figure 3-24: Time structure map of Sequence Boundary T2. Contour interval of 100 ms with annotation every 1000 ms. Seismic grid in white, well locations in pink. Interval time in TWT (ms)



Reflections within DS8 are commonly parallel to sub parallel, continuous and evenly spaced. Chaotic reflection patterns are locally observed within DS8 over the upper and central slope and have been interpreted as gravity flows, and indication of slope instability. Locally, in the northeastern map area reflections within this sequence are eroded by bathymetric channels (Figure 3-25).

On the western shelf and slope break, large paleo-channels are contained within the lower portions of DS8. These channels are up to 3 kilometers wide and 1000 ms deep. They locally truncate all underlying Tertiary section. Depositional Sequence 8 has a fairly consistent thickness of approximately 150-200 ms over most of the shelf, except in the west where it is truncated by the T3 Sequence Boundary. On the slope T3 truncates DS8 reflections, at a moderate angle, in a seaward direction resulting in successive seaward thinning of DS8. The area of thickest DS8 accumulation (700 to 800 ms) is a southwest-northeast trending band situated in central slope region. The sequence gradually thins down slope to approximately 300ms. In the lower slope region, thickness of DS8 is highly variably and does not follow the southwest-northeast trend observed on the central slope. In the basal slope region, large salt structures have uplifted overlying Tertiary stratigraphy. In such areas large portions and sometimes the entirety of DS8 has been eroded by the T3 Sequence Boundary.

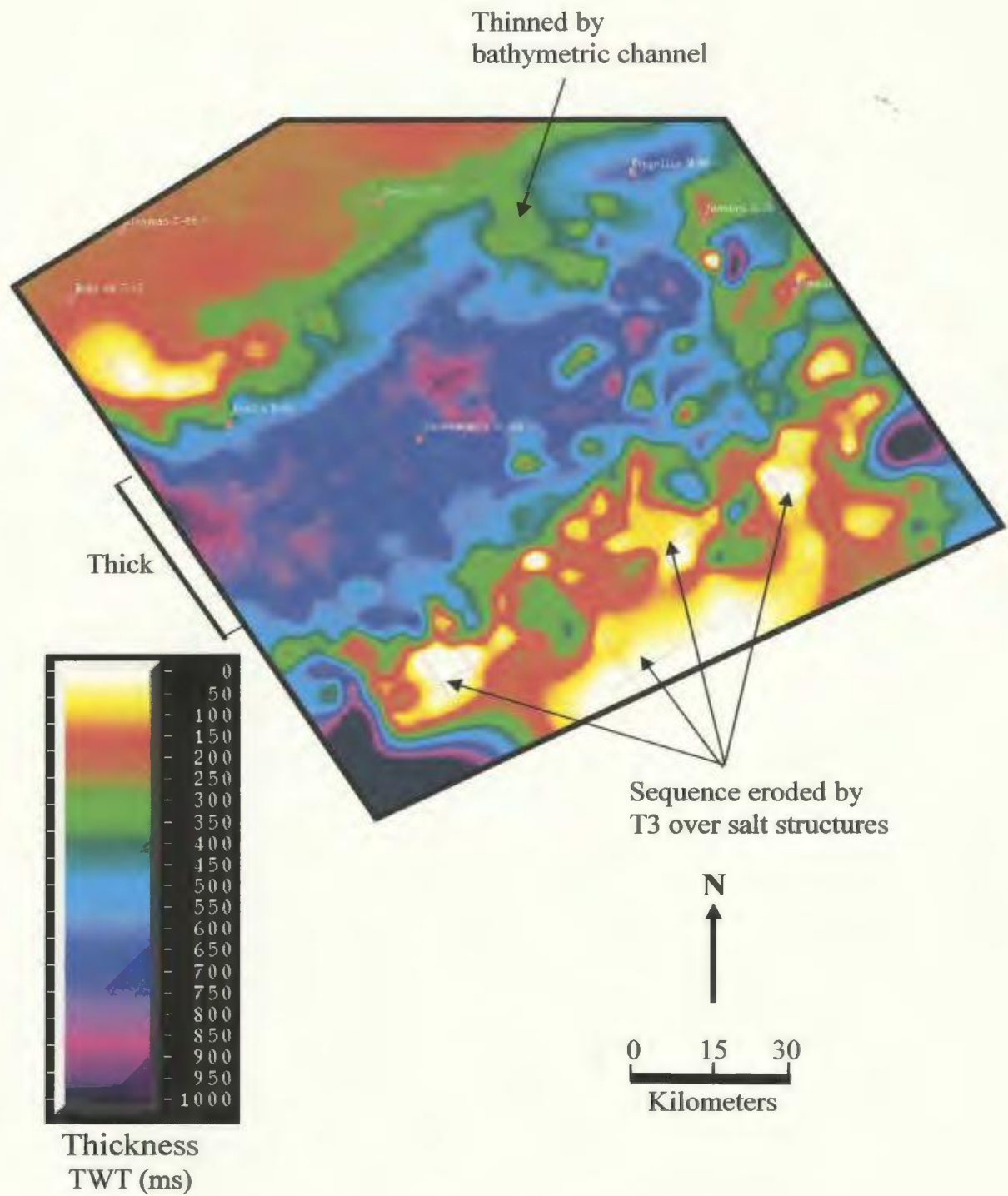


Figure 3-25: Isochron map of Depositional Sequence 8 (DS8), T2 Sequence Boundary to water bottom.

### 3.3.20 T3 Sequence Boundary

The T3 Sequence Boundary is observed to be an angular unconformity. On the slope, overlying and underlying seismic reflections converge in a seaward direction to the T3 Sequence Boundary. Shallowly southeasterly dipping overlying reflections successively downlap onto this unconformity in a seaward direction, while underlying near horizontal reflections are successively truncated in a seaward direction. On the shelf, both overlying and underlying reflections are generally concordant with the T3 Sequence Boundary.

On the slope the T3 Sequence Boundary dips at a shallow angle fairly uniformly southwest (Figure 3-26). The boundary is largely planar with the exception of few local areas of uplift on the lower slope caused by underlying salt structures. The T3 Sequence Boundary has been eroded in the east by large Quaternary and bathymetric channels that run down slope from shelf to base of the map area.

The correlation confidence in mapping this sequence boundary is excellent over the majority of the slope. In the eastern study area, where seafloor bathymetry is particularly rugose, correlation confidence in T3 is good. Here, the extreme seafloor incision, presence of stacked channels, and moderate quality seismic data (due to velocity "push downs" and seafloor multiples) introduces a level of uncertainty in the correlation of this boundary that is not present elsewhere in the study area.

Using foraminifera, Piper et al. (1987) dated the T3 Sequence Boundary as Late Pliocene to Early Pleistocene in the Acadia K-62 exploration well.



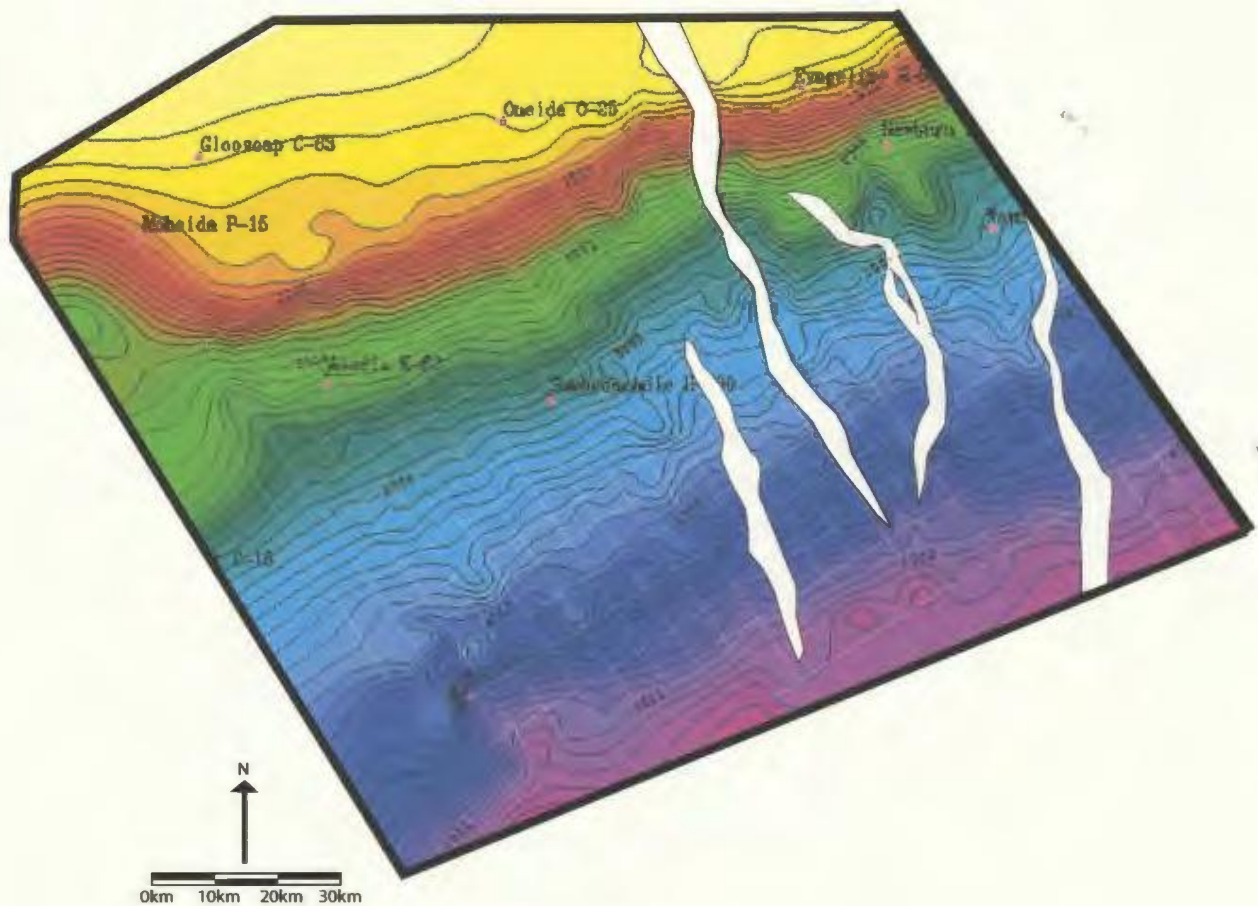


Figure 3-26: Time structure map of Sequence Boundary T3. Contour interval of 100 ms with annotation every 1000 ms. Seismic grid in white, well locations in pink. Time interval given in TWT (ms).

### 3.3.21 Depositional Sequence 9

Depositional sequence 9 is the sedimentary package bounded by the T3 Sequence Boundary and the seafloor. Correlation with exploration wells indicates this sequence consists of unconsolidated Quaternary muds and tills of the Laurentian Formation and Late Pliocene siliclastics of the upper Banquereau Formation. Reflections within this sequence generally dip shallowly seaward, concordant with the T3 Sequence Boundary. Reflections are evenly spaced and parallel to sub-parallel with high amplitude and frequency.

A number of stacked channels are contained within DS9 in the western map area. These channels underlie bathymetric canyons on the modern seafloor in the western map area. This consistent position indicates that drainage patterns have not significantly changed location since the Late Pliocene. Some of the channels within DS9 are up to 1.5 kilometers wide and 1000 ms deep, truncating most of the underlying Tertiary section.

Figure 3-26 is an isochron map of Depositional Sequence 9. The map pattern shows a fairly consistent thickness of approximately 300 ms on the shelf. On the western slope this sequence is thickest just seaward of the shelf break (east of the Acadia K-62 well) and thins to the south. This depositional pattern is not preserved in eastern map area where Depositional Sequence 9 has been completely eroded by large bathymetric canyons with up to 1200 ms of erosional relief (Figure 3-27).

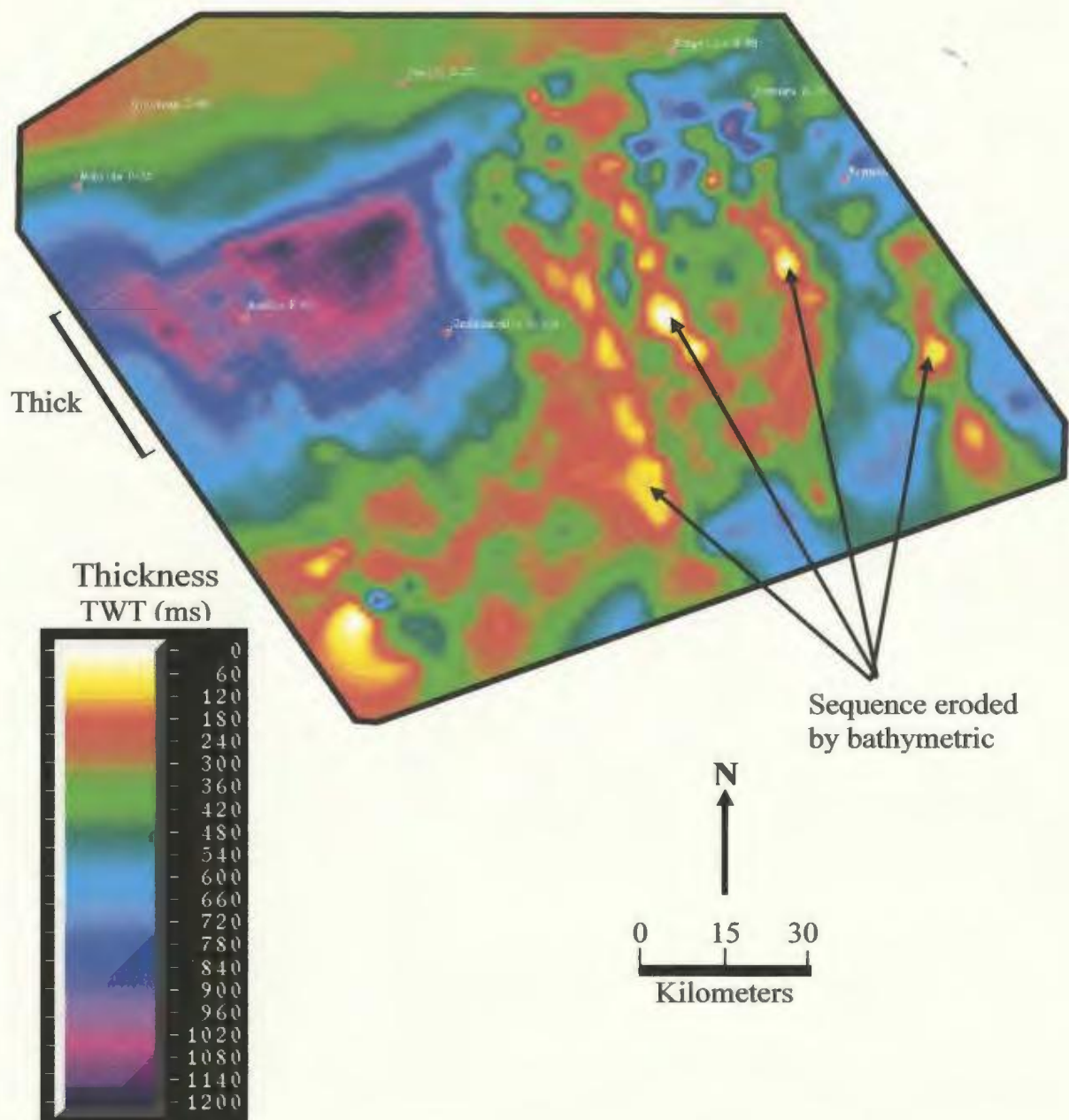


Figure 3-27: Isochron map of Depositional Sequence 9 (DS9), T3 Sequence Boundary to water bottom. Thickness given in TWT (ms). Seismic basemap in white, well names and locations in pink.



### 3.3.22 Water Bottom

The uppermost reflector imaged on all seismic sections in this study is interpreted as the water bottom horizon. This horizon is a continuous, high amplitude, positive acoustic impedance reflector, with significant bathymetric relief primarily related to erosion (Figure 3-28). The water bottom slope gradient is interrupted by three major bathymetric canyons located between the Oneida and Evangeline wells, and two minor canyons, one south of the Weymouth and the other south of Acadia.

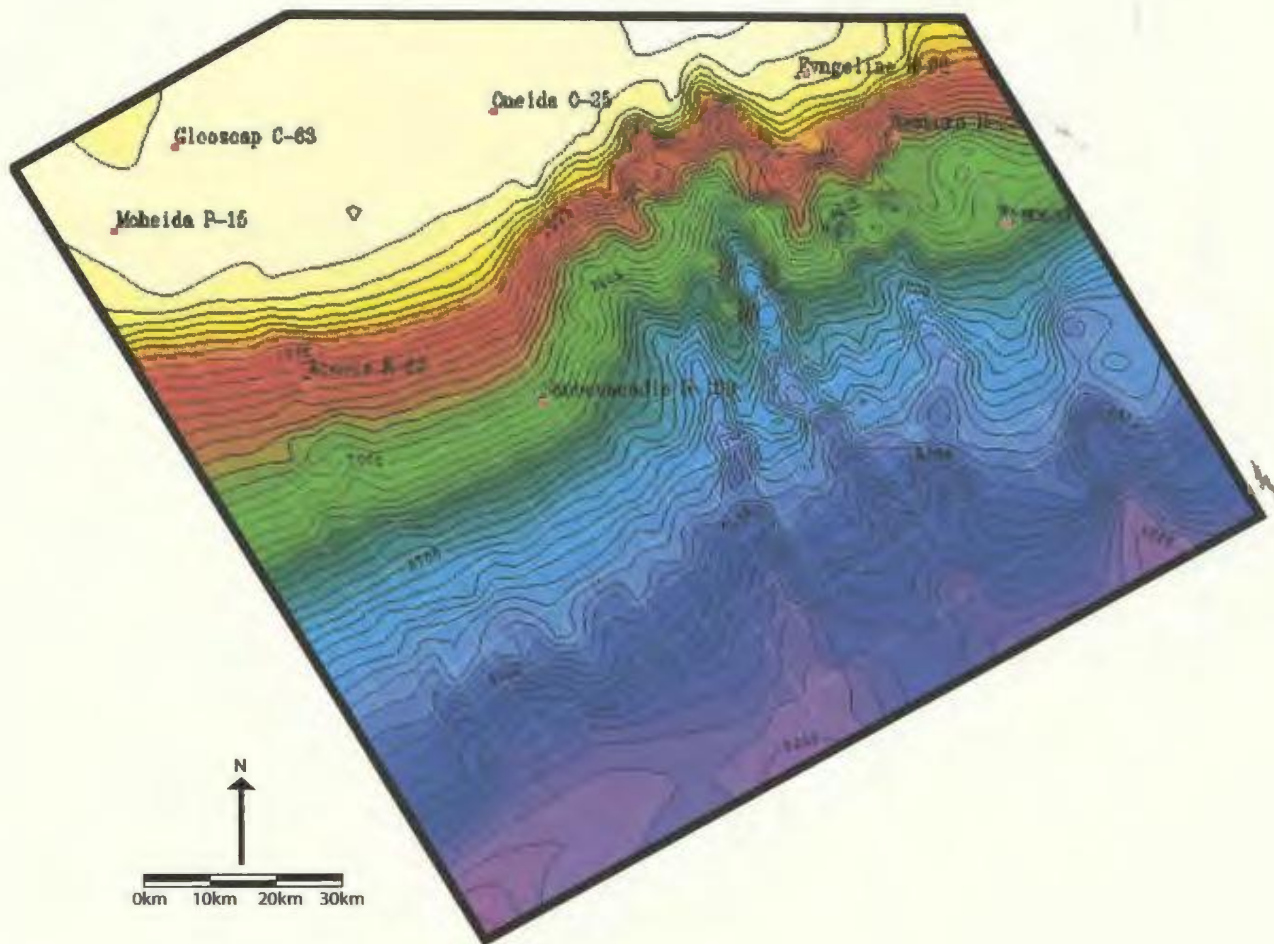


Figure 3-28: Time structure map of Water Bottom. Contour interval 100 ms with annotation every 1000 ms. Seismic grid in white, well locations in pink. Time interval given in TWT (ms).

## Chapter 4

### Tectonics

#### 4.1 Introductory Remarks

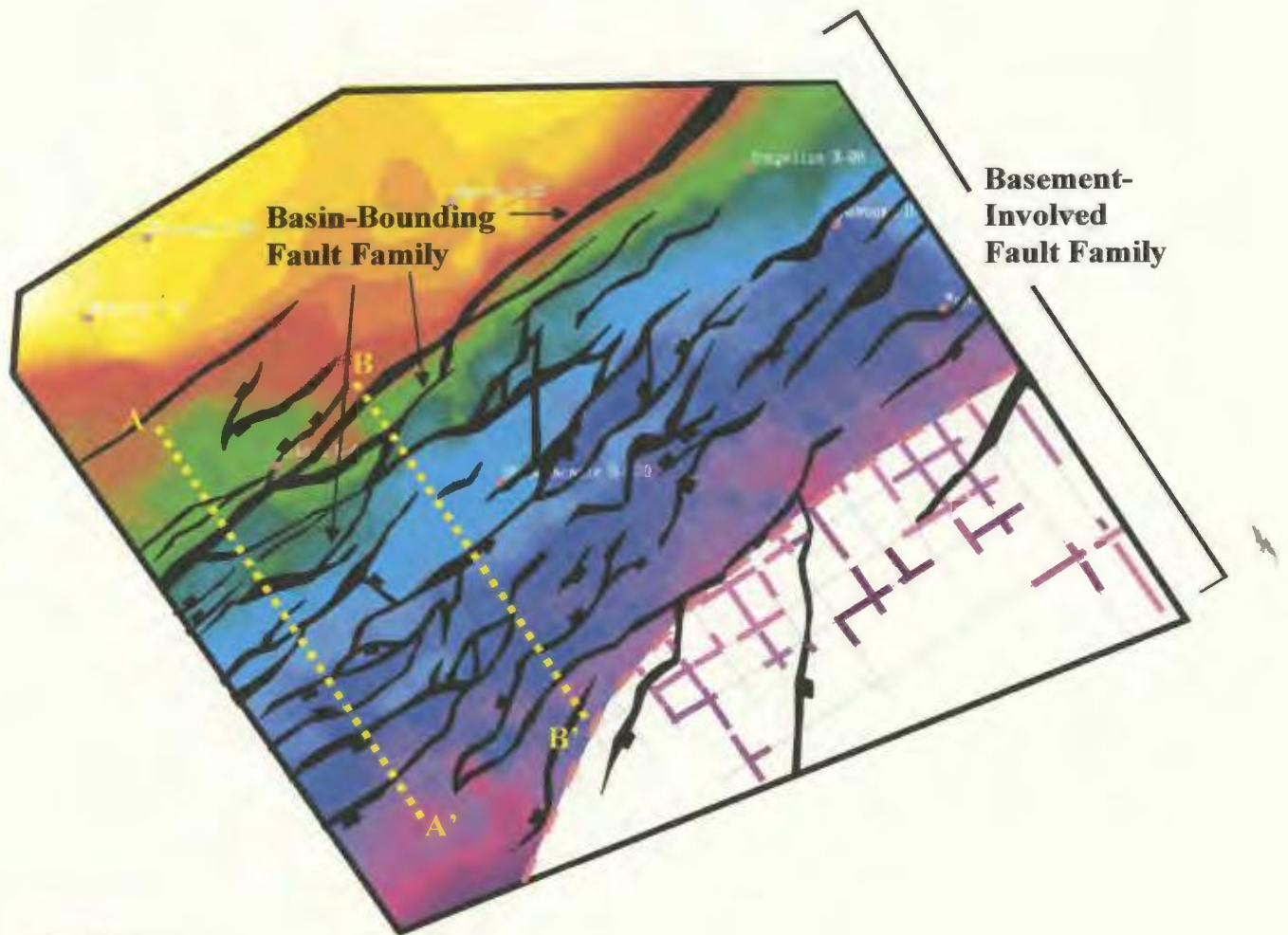
Late Triassic to Early Jurassic (~230-190 Ma) rifting on the Scotian Margin resulted in the formation of a number of southwest-northeast trending basement normal faults and northwest-southeast trending transfer faults which define the boundaries of a set of sub-basins (Figures 2-7 and 4-1). Initial rifting was followed by post-rift basin subsidence which occurred during three main periods: the Jurassic, Cretaceous and Tertiary. The timing of post-rift subsidence events may be related to the general progressive south to north opening of the North Atlantic Ocean (Louden, 2002) as follows: North America separated from Iberia to form the Southern Newfoundland margin (125 Ma); North America separated from Europe to form the Northern Newfoundland margin (120 Ma); North America separated from Greenland to form the Labrador margin (70 Ma); Greenland separated from Europe (55 Ma). During the post-rift stages, the development of syn-sedimentary listric normal faults characterized the evolution of the margin.

#### 4.2 Structural Elements

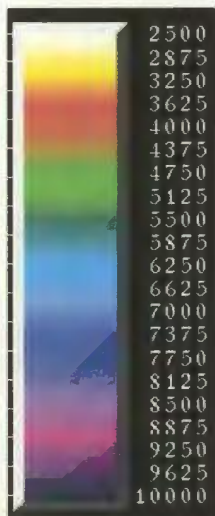
All faults defined within the study area show normal sense dip separation on stratigraphic markers in various parts of the succession, and are interpreted to be normal extensional in nature (Figure 4-1 and 4-2). The style of the faults is, however, highly



Figure 4-1: Time structure map of the Tr2 Sequence Boundary showing spatial distribution of the Slope Basin-Bounding Fault Family and Basement-Involved Fault Family. Colours represent vertical scale in TWT (ms). Location of profiles A-A' and B-B' is shown. Seismic grid base map in gray, well locations in pink. Dashed line represents limit of confident map correlation. Time structure contours were not constructed in area of low confidence. Coloured lines represent Vertical distance in TWT (ms) to the Tr-2 Sequence Boundary where imaged between salt structures in area of low map confidence.



(TWT ms)



Normal Fault, with fault gap



Limit of high map confidence

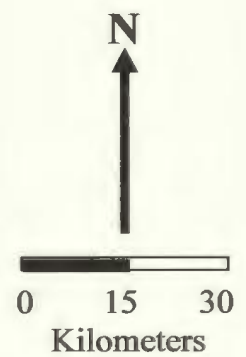
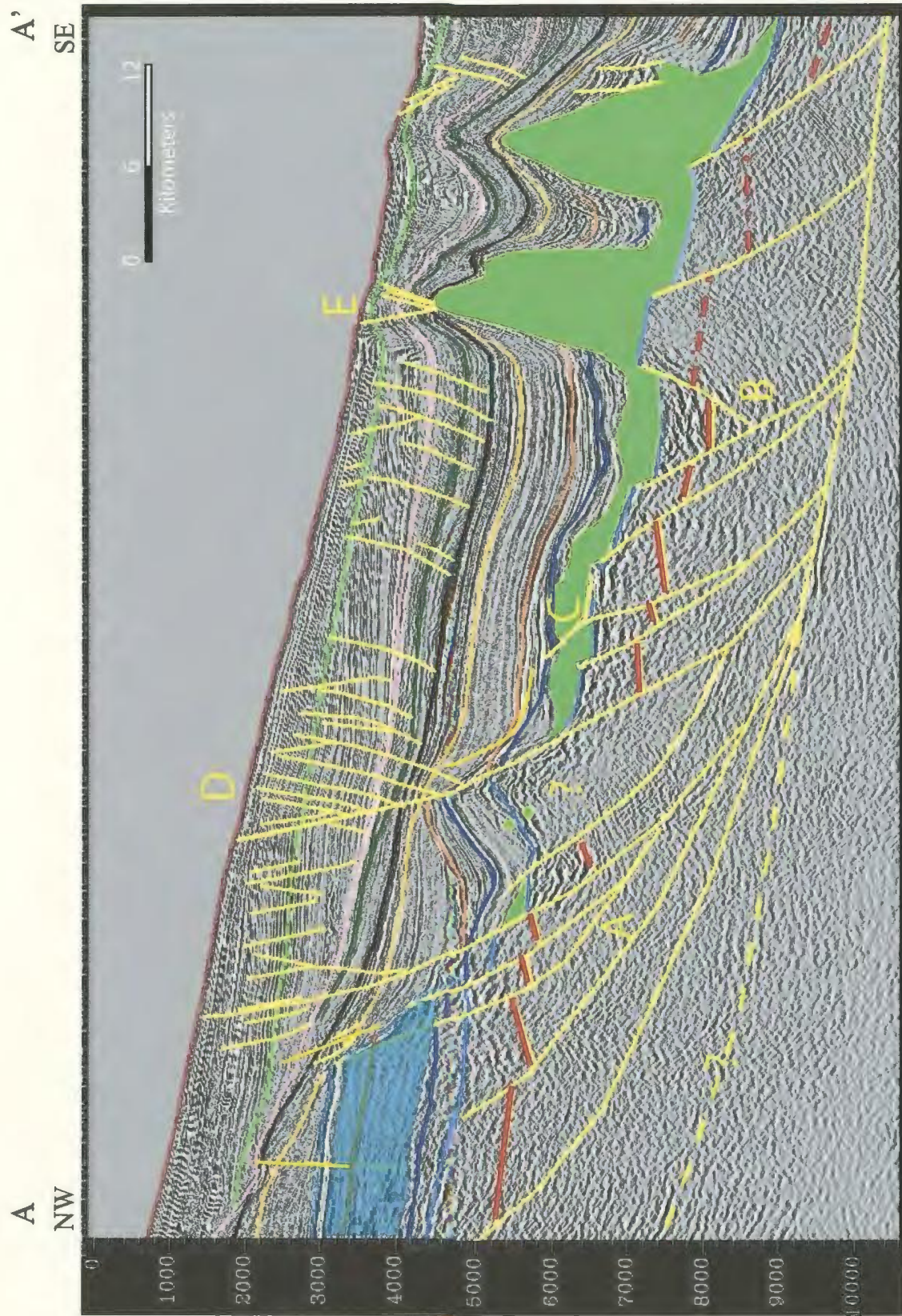


Figure 4-2: Seismic profile A-A' of the Scotian Slope, western map area. See Figure 4-1 for location. Fault assemblages (yellow) labeled. A = Slope Basin-Bounding Fault Family; B = Basement-Involved Fault Family; C = Listric Growth Fault Family; D = Major and Minor Sedimentary Fault Family; E = The Halokinetically Induced Fault Family. Note that Assemblages A and B detach within Basement, C and E detach within salt or between overburden and salt, and D within clastics or between carbonates and clastics. Green shaded areas represent salt, blue represents the Jurassic carbonate bank. Paired green circles represent salt welds. See Figure 3-6 for seismic horizon colour key. Vertical scale is two way travel time (ms).





variable; fault shapes range from planar to listric, and fault plane dips range from low- to high-angle. Three main zones of detachment are recognized: 1) within the basement; 2) within salt or between salt and the overlying sedimentary section, including salt welds between the basement/sedimentary infill; 3) between carbonates and clastics or within clastics (Figure 4-2).

Five major fault assemblages or families are defined within this study on the basis of differing structural styles and depths of detachment. These fault families are: the Slope Basin-Bounding Fault Family, the Basement-Involved Fault Family, the Listric Growth Fault Family, the Major and Minor Sedimentary Fault Family, and the Halokinetically Induced Fault Family (Figure 4-2). Indirect evidence suggests the presence of a sixth fault family, the Transfer Fault Family. These faults have not been identified with certainty on individual seismic lines, but their presence may be inferred from regional map patterns.

As a consequence of the relatively coarse six kilometer grid-spacing of the seismic data used in this study (Figure 4-1), fault aliasing occurs, as numerous alternative fault correlations were possible in the construction of time structure maps. The fault-pattern interpretations in plan view presented in this study are, therefore, not unique or definitive solutions. 3D data is needed for more accurate fault mapping. However, I feel that the 2D interpretation presented here is acceptable as it is based on structural style considerations, along strike continuity of major faults and their associated half-graben fills, the amount of throw on the faults and along strike continuity of salt diapirs associated with major extensional faults.

#### 4.2.1 Slope Basin-Bounding Fault Family

The Slope Basin-Bounding Fault Family consists of a series of extensional basement-involved faults located beneath the outer edge of the shelf. The faults are easily identifiable on seismic lines and have been described in regional basin studies by Tankard and Balkwill (1989), Tankard and Welsink (1989), Welsink et al. (1989), Keen et al. (1990), Wade and MacLean (1990), and others. Faults of this family have normal sense separations with downthrow into the basin (A in Figure 4-2).

The Slope Basin-Bounding Fault Family started forming during the Late Triassic. The faults accommodated the extension associated with initial rifting, and evolved into a dominant listric basement-involved (thick-skinned) fault fan system. This fault family accounts for the bulk of the crustal extension on the margin (Welsink et al., 1989).

Within the study area faults of the Slope Basin-Bounding Fault Family are listric in shape and sole deep within the pre-Mesozoic basement. They dip shallowly southeast and appear to link with leading branch points to a gently southeasterly dipping detachment within the lower crust, at depths between 9,000 and 11,000 ms TWT (Figure 4-2). In the western map area, the Slope Basin-Bounding Fault Family defines a zone of tip lines in the upper portion of the listric fan. The fan is the primary control on the local distribution of the Jurassic carbonate bank. The most predominant faults within the fan mark the seaward limit of the bank and generally tip at the Top Abenaki Formation seismic marker (Figure 4-2). The fault fan trends west-southwest to east-northeast in the eastern and western portion of the study area (Figure 4-1). In the central map area the



fault fan merges into a south-southwest to north-northeast orientated master fault (Figure 4-1).

A deep-seated fault is imaged in the footwall of the most inboard faults of the Slope Basin-Bounding Fault Family (Figures 4-2). Below the slope break, this fault is imaged as a low-angle lineament occurring at approximately 7000 to 9000 ms depth TWT. The fault merges with the sole of the Slope Basin-Bounding Fault Family. Due to limited seismic coverage over the outer shelf region, the upper portion of the footwall fault is not imaged in the TGS NOPEC seismic data set. However, this fault can be easily traced onto the shelf in the Lithoprobe 88-1 deep seismic line. The fault links with the regional seaward-dipping Scotian Basin bounding fault system recognized and described by Welsink et al. (1989).

#### 4.2.2 Basement-Involved Fault Family

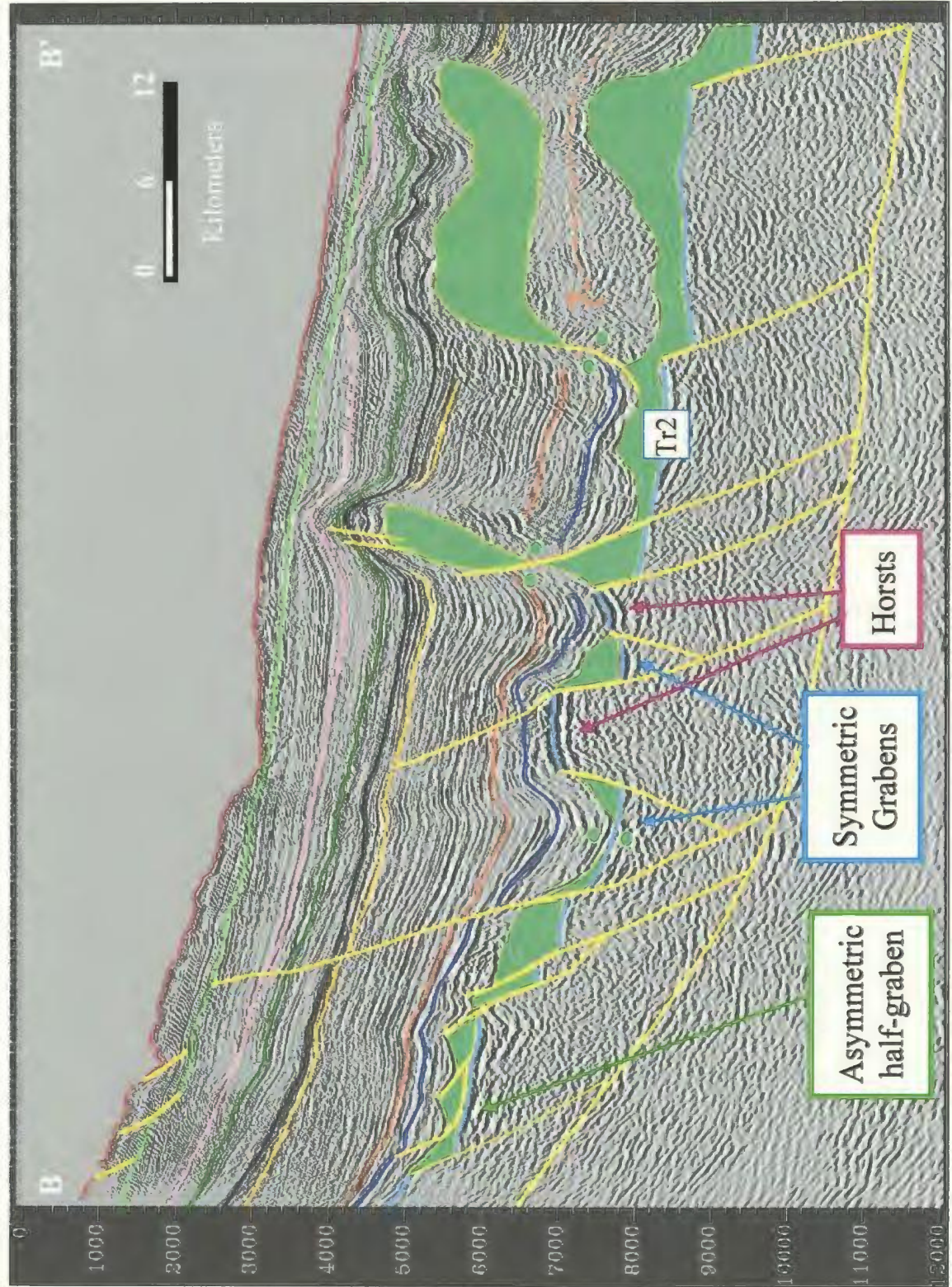
Within the map area faults of the Basement-Involved Fault Family are located in the hanging wall of, and sole into the Basin-Bounding Fault Family (B in Figure 4-2). They form a listric fan of synthetic and antithetic faults that affect the pre-Mesozoic basement and synrift successions, and to a lesser extent the postrift succession. The faults of this family delineate the major structural units in the map area by sub-dividing the hanging wall side of the Basin-Bounding Fault Family into: a) asymmetric half-grabens filled with syn-rift sediments, b) symmetric grabens filled with syn-rift sediments, and c) horsts, bounded by onlapping sediments (Figure 4-3). The faults here grouped in the Basement-Involved Family have previously been described as “higher” faults by

Figure 4-3: Seismic Profile B-B' showing part of the Basement-Involved Fault Family dividing the hanging wall of the basal detachment of the Slope Basin-Bounding Fault into major structural units: a) asymmetric half-grabens filled with syn-rift sediments, and b) symmetric grabens and horsts. Location of profile is shown in Figure 4-1. See Figure 3-6 for seismic horizon colour key. Vertical scale is TWT (ms).



SE

NW





Wernicke (1981) or “second-order” by Angelier (1985), who together with Gibbs (1983, 1984) give a thorough account of the role of these faults in creating the complexity of the structural architecture of rift zones.

Throughout the majority of the map area, where seismic resolution is good to excellent, faults of the Basement-Involved Fault Family are easily identifiable on seismic profiles based on discontinuities in the Tr2 Sequence Boundary (Figures 4-1, 4-2 and 4-3), or on the basis of the presence and geometries of associated growth strata successions.

In the southeastern map area extensive salt structures result in poor seismic resolution of the architecture in the sub-salt sections. Structural interpretation of the crustal structure from dip separations of seismic markers and reflectors in this area is generally not possible. In this case basement-involved faults were inferred through the location and geometry of overlying salt bodies, a relationship described by Jackson and Vendeville (1994) (Figure 4-2). The occurrence of significant discrepancies in the depth to Sequence Boundary Tr2 where imaged in small windows between salt structures, also justified the inference of basement-involved faults (Figure 4-1), and their extrapolation on seismic sections.

Faults of the Basement-Involved family that are synthetic to the Slope Basin-Bounding Fault Family trend west-southwest to east-northeast, have normal sense separations, and dip steeply southeast. In most profiles these faults delineate fairly regularly spaced rotated fault blocks, or form the seaward-bounding fault in basement-involved horst blocks (Figure 4-3). Faults that are antithetic to the Slope Basin-Bounding Fault Family trend west-southwest to east-northeast, have normal sense separations and

dip steeply northwest. These faults constitute the landward-bounding faults in basement-involved horst blocks (Figure 4-3).

Locally, there are anomalous geometries associated with the Basement Involved Fault Family. One such structure is presented in Figure 4-4. Here, basement reflectors located within a “rotated fault block” have a domed, rather than rotated reflection pattern typical of rotated fault blocks. The structure in question appears to be uplifted relative to adjacent section, this is also not typical of rotational faulting. The geometry of this structure is very similar to that of the Flying Foam salt associated-structure of the Jeanne d’Arc Basin, another Eastern Canadian rift basin located northeast of the Scotian Basin (Figure 4-4). The local presence of a second, older (Paleozoic) salt body contained within pre-Mesozoic basement stratigraphy is one possible explanation for the anomalous structural architecture of this section. Although pre-Mesozoic salt has not been recognized within the Scotian Basin, there are numerous Paleozoic basins within the eastern Canadian continental margin where pre-Mesozoic salt has been documented. For example, Wade and MacLean (1990) speculate the presence of upper Paleozoic evaporites in the Georges Banks region, southwest of the Scotian Basin. Abundant Carboniferous salt has been mapped in outcrop on Cape Breton Island, and offshore in the Magdalen Basin, situated immediately northeast of the Scotian Basin (Howie and Barss, 1975). Although interesting, the analysis of the potential pre-Mesozoic salt is outside the objectives defined for this project and thus, was noted but not pursued.

The Basement-Involved Fault Family primarily disrupts Paleozoic basement, pre-rift and syn-rift successions. The Tr2 Sequence Boundary marks the top of the



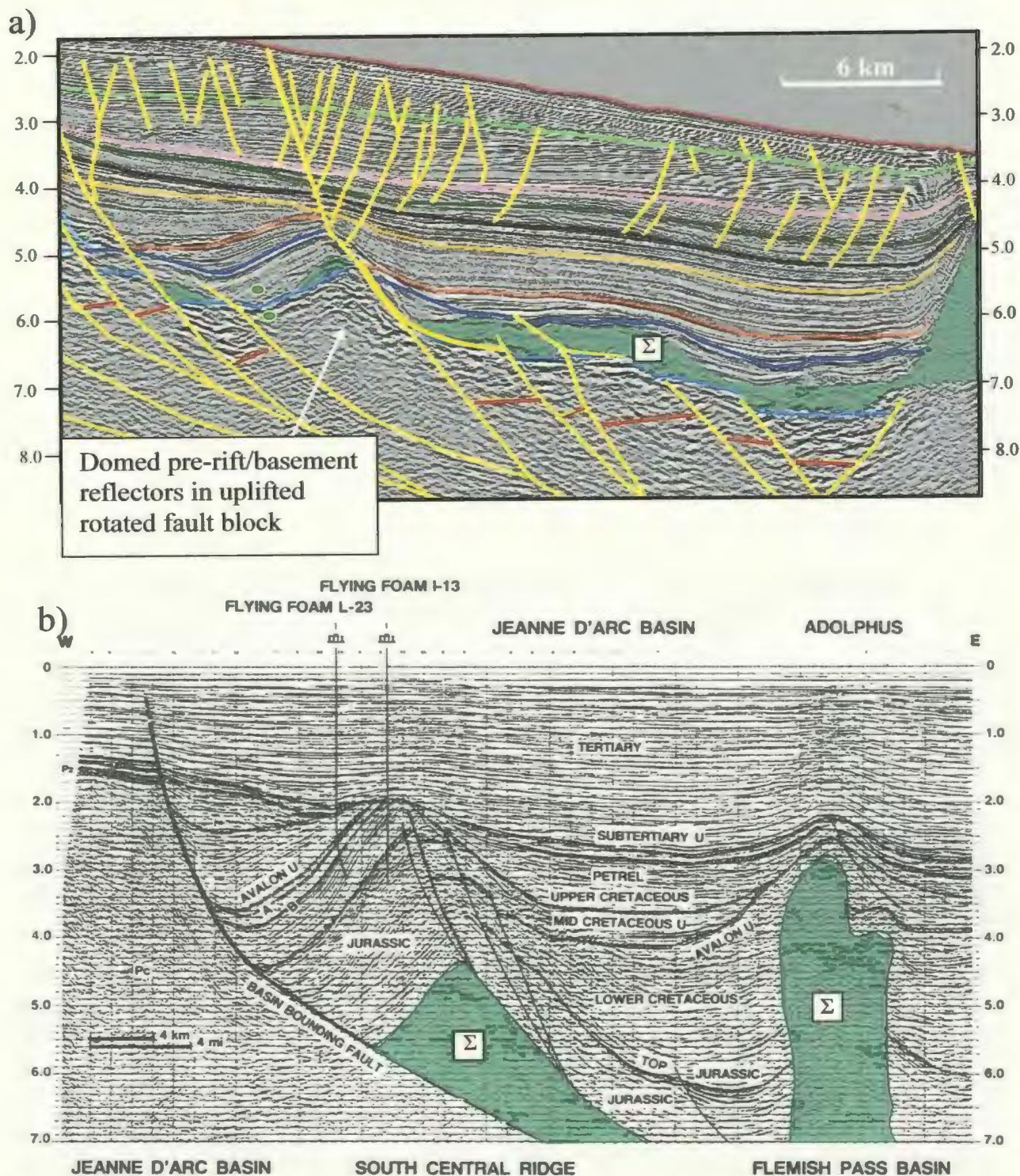


Figure 4-4: a) Portion of seismic profile A-A' (Figure 4-1) showing anomalous domed prerift and basement reflector configuration (not typical of rotated fault blocks). Structure has similar style to b) the Flying Foam salt-related structure of the Jeanne d'Arc Basin (Enachescu, 1987). Vertical scales are TWT (s).



stratigraphic succession most affected by this fault system. In local areas faults do penetrate Mesozoic basin fill and may affect Jurassic, Cretaceous, and even Tertiary sections. Bathymetric relief related to reactivated basement-involved faults suggests that in some local areas this fault family may be active today.

#### 4.2.3 Listric Growth Fault Family

Faults of the Listric Growth Fault Family are shallow, curvilinear, concave-upwards surfaces which commonly sole, usually at a low angle, into the top of or within the autochthonous evaporite unit (C in Figure 4-2 and Figure 4-5). They display normal sense apparent dip separations. These faults exclusively deform seismic reflectors within depositional sequences 2 and 3. Although faults of the Listric Growth Fault Family commonly penetrate the top evaporite horizon, they do not affect the Tr2 Sequence Boundary, nor do they penetrate above the J2 Sequence Boundary. The location of faults of this family is thus restricted to Late Triassic to Jurassic stratigraphic successions.

In map pattern, the listric growth faults have curvilinear fault traces with an overall strike of west-southwest to east-northeast, parallel to the shelf break. The faults occur either singularly or as parallel groups that sole into a common detachment surface (Figure 4-6). All faults of this family dip to the southwest. Considerable roll-over is often associated with listric growth faults. The roll-over structure is often further accentuated by the existence of a salt core (Figure 4-6, Chapter 5.3.3). Sedimentary packages in the hanging walls of the faults characteristically exhibit growth-related asymmetric

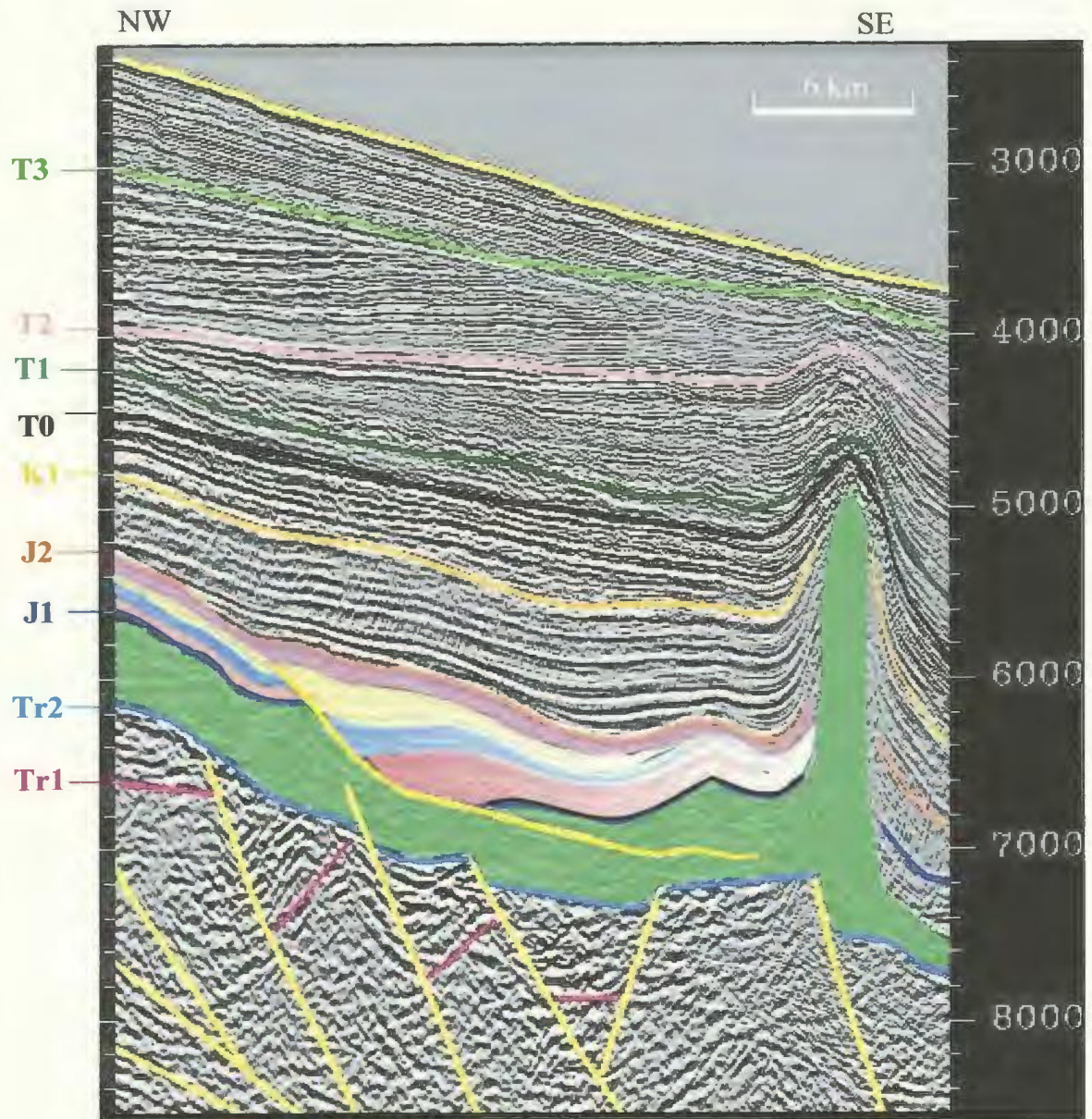


Figure 4-5: Example of listric growth fault activity in Jurassic aged strata of the western map area. Pink, blue and yellow represent syn-growth strata, purple post-growth strata. Note local growth above post-growth strata related to salt withdrawal into diapir in the southeast, not to listric faulting. Vertical scale is TWT (ms).



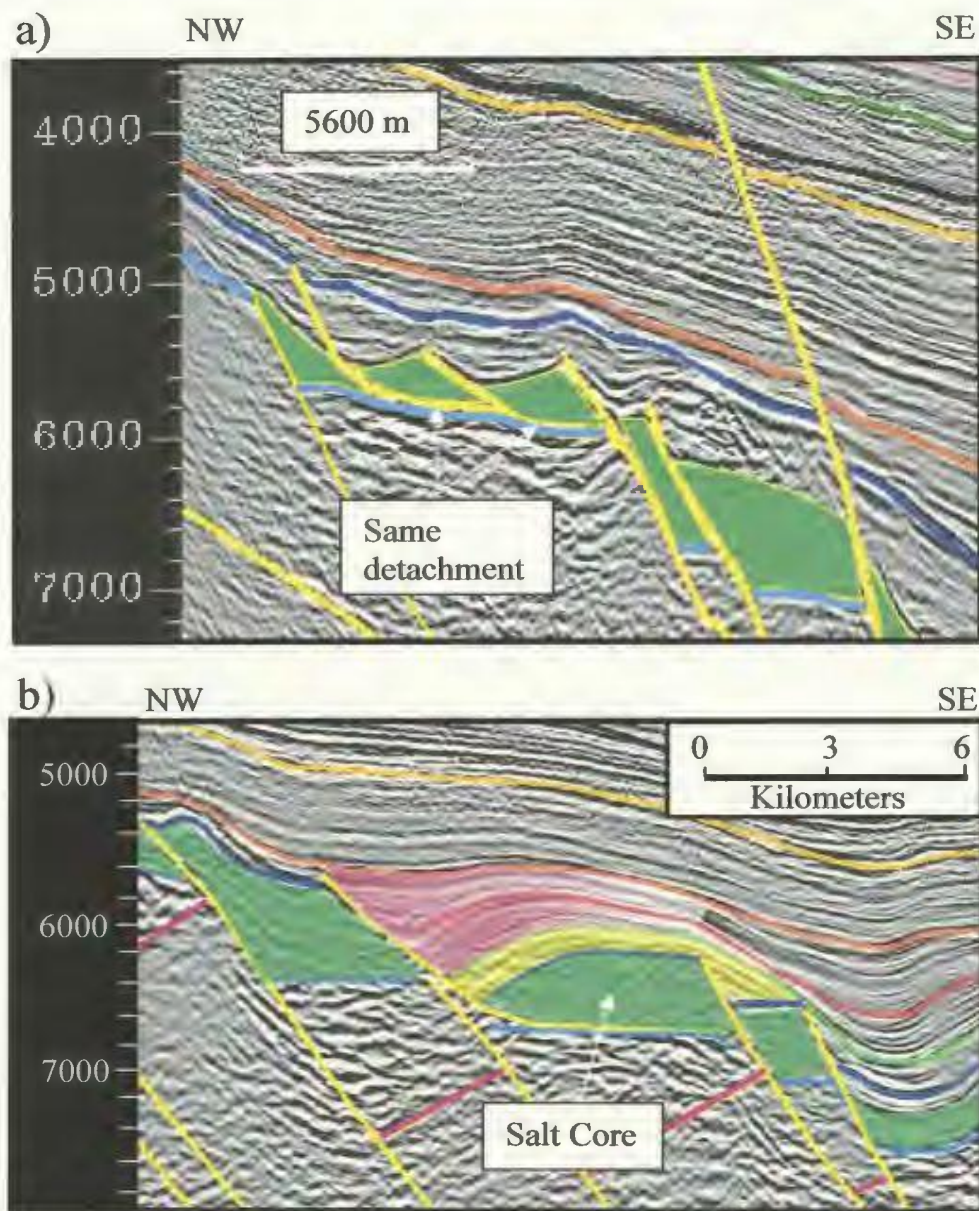


Figure 4-6: a) Section of NW to SE seismic profile from the upper slope of the central map area showing example of a group of related faults of the Listric Growth Fault Family soling into a common level of detachment within salt, and b) Example of listric growth fault with accentuated rollover due to salt core. Listric fault related growth highlighted in pink, “pre-fault” strata with no thickness variation in yellow. Vertical scale is TWT (ms).



thickening, resulting in distinct wedge-shaped geometries of the syn-growth packages (Figure 4-5 and 4-6).

An intimate association is observed between the faults of the Listric Growth Fault Family and those of the Basement-Involved Fault Family. The distribution of listric growth faults appears spatially related to, but does not involve, basement-involved faults. The syn-sedimentary listric growth faults generally trend parallel to the basement-involved faults and often occur in the Jurassic sequence situated in the hanging wall of the basement-involved faults (Figure 4-6).

Various types of salt structures also occur in association with the Listric Growth Fault Family (Figure 4-5 and 4-6). These structures are described in Chapter 5.

#### 4.2.4 Major and Minor Sedimentary Fault Family

Typical major sedimentary faults are slightly curved to listric, strike southwest-northeast, and dip either basinward or landward, depending on underlying crustal structure (D in Figure 4-2). These faults are commonly spatially associated with, and trend parallel to, basin-bounding and basement-involved faults. Major sedimentary faults typically detach on top of, or within, the evaporite unit (Figure 4-7), or link with underlying basement-involved faults (Figure 4-2). They typically exhibit approximately 100 ms of throw, but do not have associated growth strata that are clearly imaged seismically (Figure 4-2). Major sedimentary faults cut sequence boundaries J1 through T3 (Figure 4-2). Their movement has thus been dated as ranging from Jurassic to

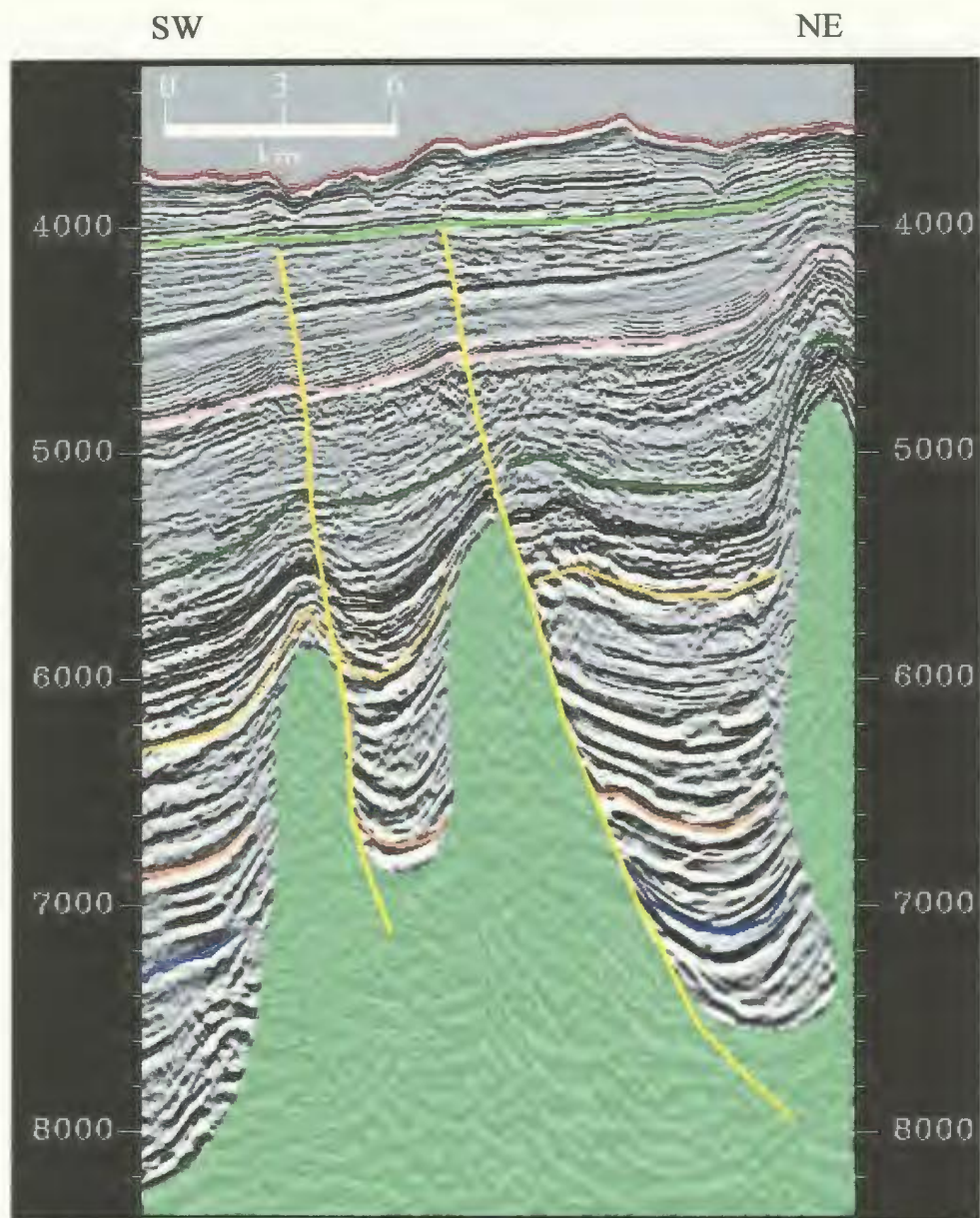


Figure 4-7: Seismic strike line with example of two major sedimentary faults both detaching on salt diapirs. Vertical scale is TWT (ms).

Tertiary. In the northwest some major faults have structural relief on the sea floor suggesting that these faults are still active in certain areas of the basin.

The major faults have curved traces in plan view with a west-southwest to east-northeast strike in the western portion of the map area and a south-southwest to north-northwest strike in the central and western map area (Figure 3-16). The two orientations of fault sets appear to merge near the center of the map area, but connectivity of the fault sets remains undetermined due to the wide spacing of the seismic grid.

Minor sedimentary faults occur in all stratigraphic units from Jurassic to Quaternary, but are most common in Tertiary to Quaternary strata. They show a wide range of shapes and forms varying from curved and listric to planar and domino-style. Most commonly they constitute the synthetic and antithetic faults associated with the development of the major sedimentary faults (Figures 4-2, 4-8). Minor faults commonly form local half grabens, symmetrical horsts and graben structures, and arrays of tilted small domino fault blocks (Figure 4-8).

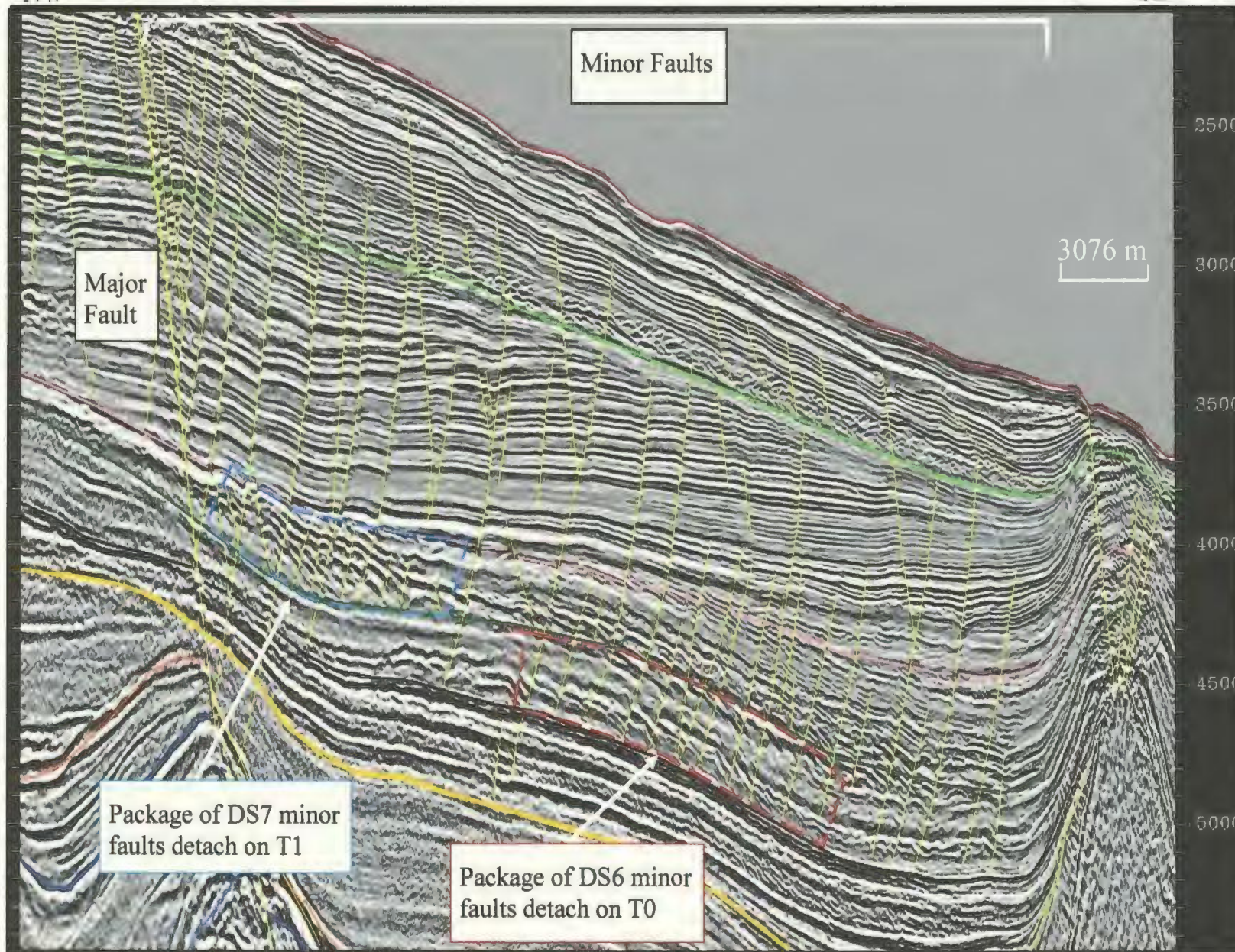
Within Tertiary and Quaternary strata, Minor faults commonly occur in discrete fault packages that detach on distinct bedding parallel slip surfaces (Figure 4-8). Fault style and dip patterns change between across slip surfaces, reflecting differences in mechanical behavior of lithology during the development of the fault systems. These faults appear to occur as a result of gravitational tension. They often form in blocks bounded by canyons which have deeply eroded the youngest successions.



Figure 4-8: Close-up portion of seismic profile A-A' (Figure 4-1) showing major and minor faults (yellow). Minor faults constitute the synthetic and antithetic faults associated with the development of the major sedimentary fault. Minor faults commonly form local half grabens, symmetrical horsts and graben structures, and arrays of tilted small domino fault blocks. Note the presence of distinct packages of minor faults (highlighted in red and blue) with unique fault style and differing levels of detachment on bedding parallel slip surfaces. Vertical scale is TWT (ms).

NW

SE





Minor faults are often associated with triangular depressions at the tip point of the fault (Figure 4-9). The depressions are up to 400 m wide, and 75 ms TWT deep and are concentrated on one Quaternary seismic horizon, but may also show on the sea floor. One interpretation of this association is that it is a series of pock-marks controlled by the presence of a network of syn-sedimentary minor faults acting as potential conduits for fluid flow. The spatial distribution of the pockmarks is impossible to determine due to the coarse seismic grid spacing. However, in view of their association with minor faults it is likely that in plan view, these pock-marks are either linear anomalies caused by leakages along faults or circular anomalies caused by point leakages at the intersection of two faults. The geometry of the suspected pockmarks is comparable to those described by Carvalho and Kuilman (2003) in deep water offshore Angola, where these features vary in diameter from 25 to 400 m and can be up to 80 m deep.

#### 4.2.5 The Halokinetically Induced Fault Family

Within the Scotian Basin the protracted movement of salt has resulted in numerous halokinetically induced faults. These characteristically developed adjacent to or above the crests of evaporite structures. The geometry, spatial distribution and association between Halokinetically Induced Faults and salt structures are discussed in Chapter 5.



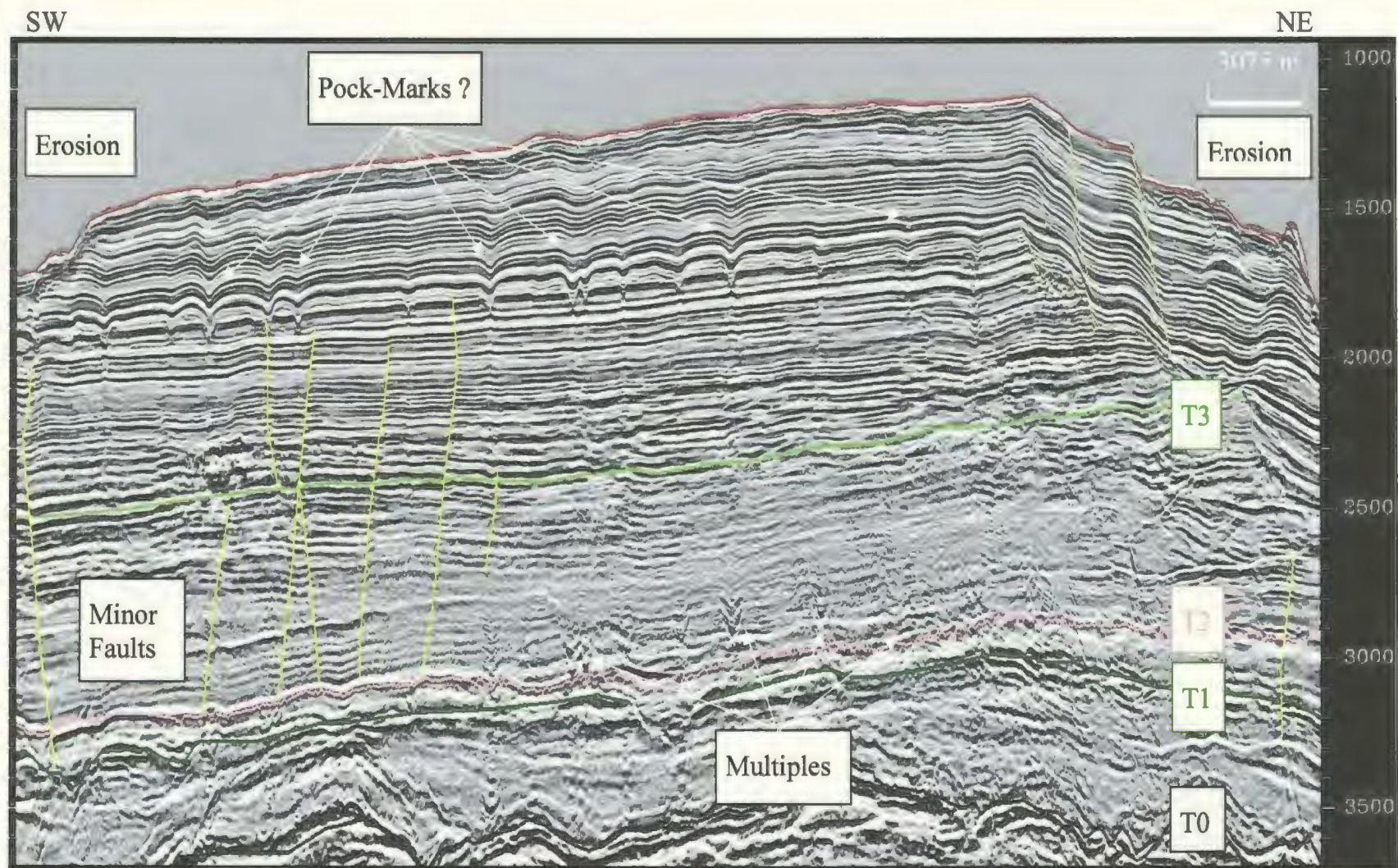


Figure 4-9: Southwest-Northeast seismic strike section from the upper slope, central map area. Minor faults (yellow) associated with Quaternary pockmarks. Vertical scale is TWT (ms).

#### 4.2.6 The Transfer Fault Family

Transfer faults are a different type of fault associated with regional extensional fault systems (Gibbs, 1984; Lister et al., 1986). They are the cratonic equivalent of transform faults, which are associated with mid-oceanic ridges and oceanic crust. These transfer faults are characteristic of all extensional terrains, allowing displacement transfer between extensional basement faults with differing slip rates (Gibbs, 1984; Lister et al., 1986).

Transfer faults are identifiable on seismic sections only when deformation style and lithology varies across the fault plane. Transfer faults are not simple strike slip faults in the classical sense, because they often have a rotational component and, therefore, are of the so-called scissor fault type (e.g., Enachescu, 1987).

Within the map area no transfer faults were identified. However, the existence of a secondary transfer zone is a possible explanation for: 1) the change in major fault orientation through the center of the map area, and 2) the offset of the landward limit of diapiric salt structures across the central map area (see section 5.3.5). The signature of this potential transfer fault, however, is not clearly enough defined on the available seismic data to allow for confident mapping of it.



## Chapter 5

### Salt Tectonics

#### 5.1 Mechanics and Geometries of Salt Deformation

The generic term 'salt' is used for successions including a wide range of evaporite lithologies, amongst others, pure halite, gypsum and anhydrite. On a local scale the various types of evaporites may react differently to applied stresses, but, on the regional scale as resolved in seismic sections these differences are generally considered minimal (Rowan, 2002). Salt tectonics, or halotectonics, is the term given to any tectonic deformation involving salt as a substratum or source layer. Halokinetics is a form of salt tectonics whereby the movement of salt is entirely powered by gravity in the absence of significant lateral tectonic forces (Jackson and Talbot, 1991)

A number of important aspects need to be considered in studies of salt tectonics, including the trigger for diapirism, the stages of diapir rise and fall, the coupling and/or decoupling of sedimentary overburden and evaporites, decoupling of salt from the subsalt strata, and the nature of the causative stress fields. Also important is the relative timing and influence of salt movement in relation to sedimentation. These relationships can be identified through various indicators of salt and sediment movement that can be observed in the region of the salt body.

There has been an enormous revolution in our understanding of salt tectonics in the past decade. Our increased knowledge of the geometry and kinematics of salt bodies and associated strata is due, in large, to the fortuitous convergence of advances in the



areas of seismic imaging, experimental and numerical modeling, and structural restoration. Excellent reviews of modern salt tectonics are by Jackson and Talbot (1991), Vendeville and Jackson (1992 a and b), Rowan (1993, 2002), Jackson and Vendeville (1994), Jackson (1995), Ge et al. (1997), and Alsop et al. (2000).

Rock salt is very different from other sedimentary rock types. Its behavior is primarily dictated by two key factors: its constant density of  $2.2 \text{ g/cm}^3$  and its relative weakness under both tension and compression as compared to other sedimentary rocks (Jackson and Vendeville, 1994). The strength of salt as a function of depth is essentially zero, causing salt to mainly deform as a viscous material. Salt flow is a combination of Poiseuille flow due to overburden loading, and Couette flow due to overburden translation (Rowan, 2002). The viscous nature of salt means that evaporite-dominated successions form very weak layers between other sedimentary strata. Thus, salt serves as an excellent ductile detachment into which faults in the sedimentary overburden sole.

In contrast to other types of sedimentary rocks that become compacted and thus denser during burial, salt has a constant density of  $2.2 \text{ g/cm}^3$ . Salt is denser than most surrounding strata when it is near the surface, but less dense once buried beneath 1000-1500 m of sediment. The low density of buried salt was historically used as a rationale for models in which salt punches its way through denser overburden until it reaches a level of neutral buoyancy. This model would be valid if the overburden also acted as a viscous fluid, but in fact, the overburden is a brittle material with real strength (Vendeville and Jackson, 1992a). The strength and brittle nature of overburden means that density contrast plays only a limited role in salt tectonics. Instead, salt can be viewed

as a pressurized fluid with differential fluid pressure acting as the primary control governing salt flow (Vendeville and Jackson, 1992a). According to Rowan (2002), "It does not matter whether overburden is of lesser, equal or greater density than the salt, if there is a place to go salt will flow". Salt generally cannot push its way into surrounding strata and for salt flow to occur: (1) there must be an open path to a near surface salt body; (2) the overburden must be thin and weak enough for the differential fluid pressure to overcome its strength, in which case it will deform the overburden; or (3) some other process (e.g., tectonics) must create space. In other words, "salt does not drive salt tectonics; instead, salt merely facilitates and reacts passively to external forces" (Rowan, 2002).

The geometry of salt structures is a fundamental indicator of the movements of salt within a basin. When evaporites are deposited, their upper boundary is a relatively flat to gently curved continuous surface regardless of basement topography. Upon deformation, salt will commonly rise up to form bulbous or linear salt structures such as pillows, swells, diapirs, and walls. The presence of such structures is an indication that salt has moved since deposition. The relative maturity of a salt structure can be inferred from the geometry of that structure. The wide variety of salt structure geometries as a function of their relative maturities is shown in Figure 5-1.

In passive slope margins and/or rapidly prograding systems, up-slope extension induced by gravity gliding is common. Extension is balanced by a shortening zone located at the toe-of-slope region that is often associated with under-compacted

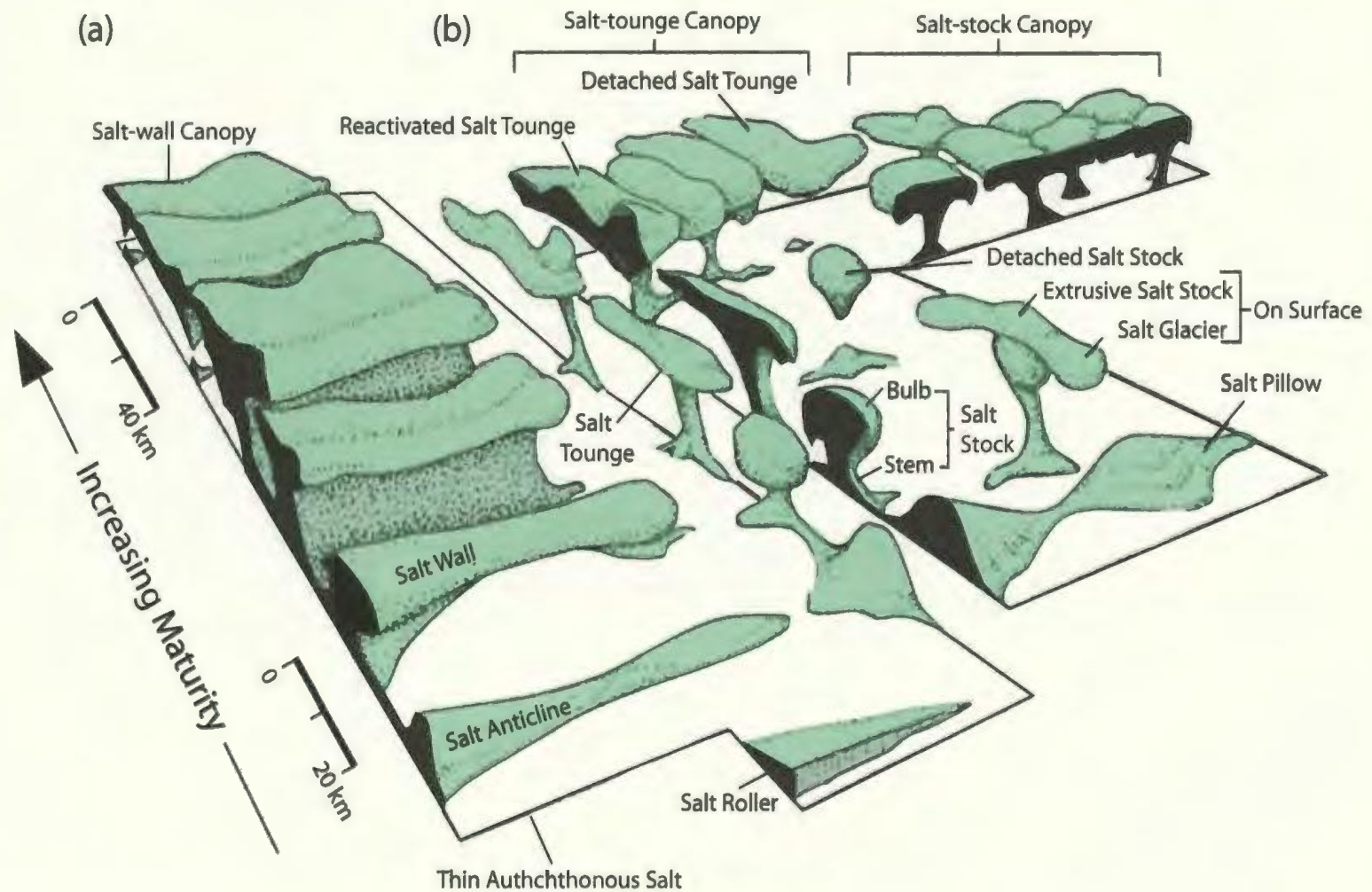


Figure 5-1: Block diagram showing schematic shapes of known classes of salt structures. Structural maturity and size increase toward the composite, coalesced structures in the background. Panel (a) shows elongated structures rising from line sources. Panel (b) shows structures rising from point sources. Modified from Jackson and Talbot (1991).



shales related to rapid progradation (e.g. Niger delta, Tarakan delta offshore eastern Borneo, and offshore northeastern Brazil), or salt (e.g. Mississippi fan, Sable Delta (Cretaceous), Perdido fan (Gulf of Mexico, Middle Jurassic), West Africa (Angola, Gabon, Lower Cretaceous) and the Nile delta (Mediterranean, upper Miocene)).

Contraction is driven by gravity gliding associated with progressive tilting of the margin and by gravity spreading of the under-compacted shale or salt layer under the differential loading related to progradation (Letouzey et al., 1995).

Where shortening is associated with gravity gliding and/or spreading, the slope can be divided into three gravity driven tectonic stress domains: an upper slope extensional domain, a middle slope transitional domain, and a lower (toe of) slope compressional domain (Figure 5-2). The type, maturity and shape of salt structures and associated growth stratal architectures differ significantly between these stress domains.

The best studied passive margin with an up-dip prograding delta and down-dip salt is the Gulf of Mexico. Numerous researchers (e.g., Diegel et al. (1995), Peel et al. (1995), and Rowan (1995)) have mapped the structural associations of the Gulf Coast Continental Margin documenting the relationship between location in a slope to base-of-slope system and style of salt deformation. In general, salt dome/minibasin diapiric, and detachment associations characterize the upper slope extensional domains, while diapiric, tabular (allochthonous) salt, associated minibasins and fold belts are typical of the lower slope compressional domains (Figure 5-3). The middle slope transitional domain typically contains structures typical of both extension and compression.

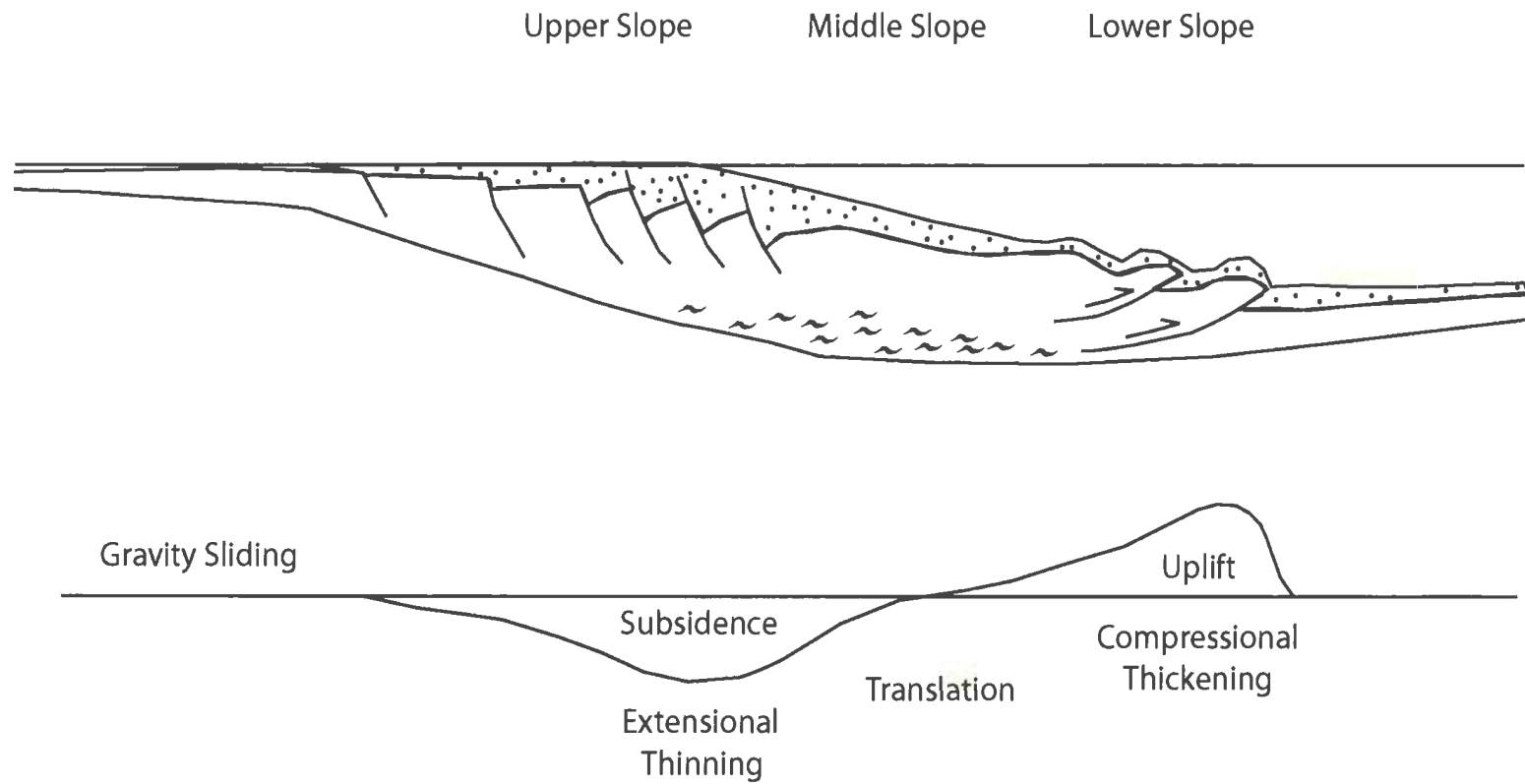


Figure 5-2: Schematic diagram of typical stress and strain domains in a clastic passive continental margin. Modified from Galloway (1986).

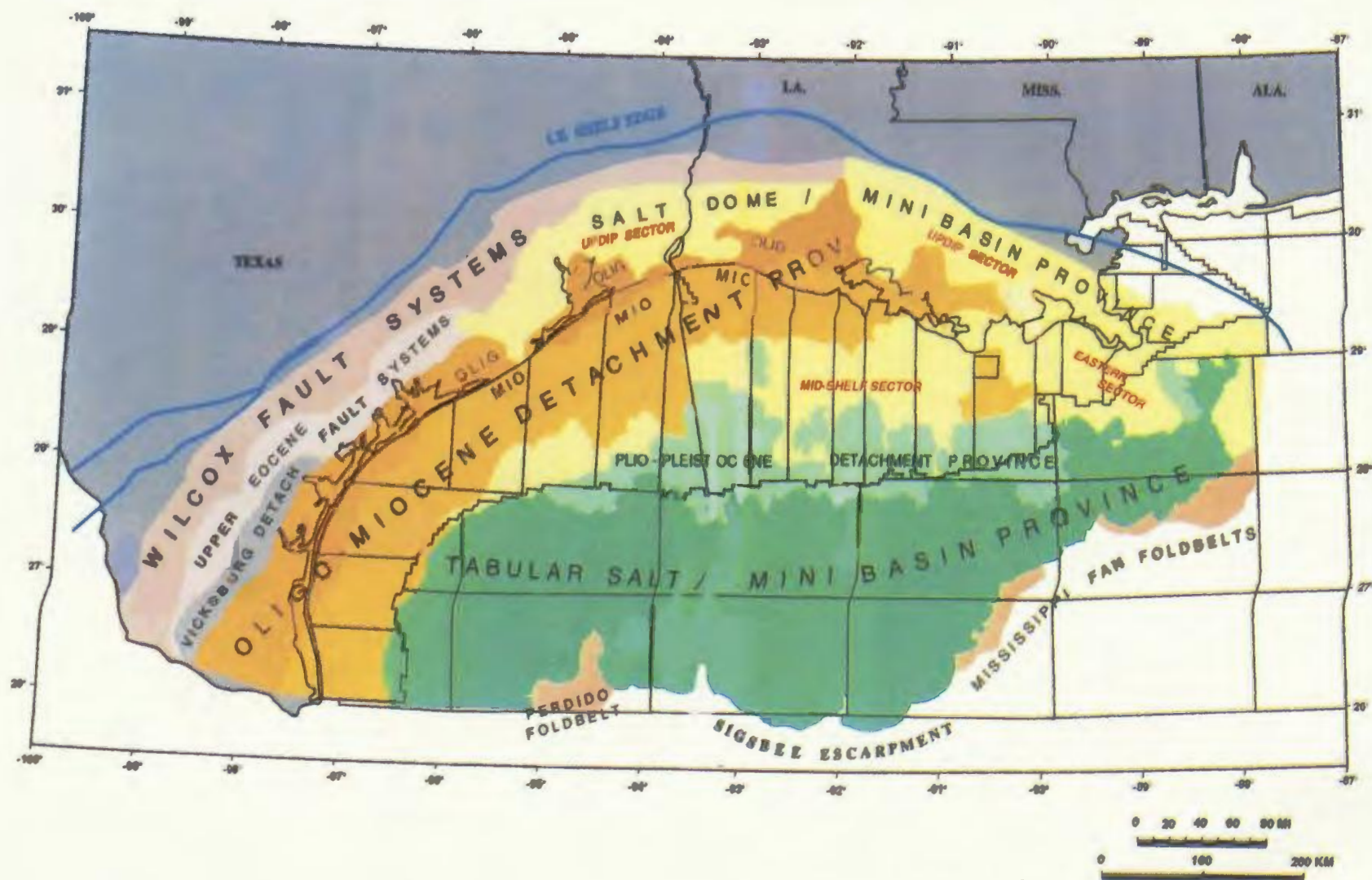


Figure 5-3: Tectono-stratigraphic provinces of the northern Gulf of Mexico Basin. Modified from Diegel et al. (1995).



## 5.2 Map Distribution and Style Characteristics of Salt

Within the mapped area on the Scotian Margin, there is considerable variation in structural style of salt deformation, and no one seismic strike or dip line is representative of the regional structure of the area. The present configuration of salt structures within the study area is a result of the collective geological process that shaped the area, thus, the variation in salt structural style is directly associated with variability of controlling geological factors.

There are a number of tectono-stratigraphic features that are common to the entire study area: 1) a rifted pre-Mesozoic basement characterized by symmetric and asymmetric grabens and horsts with an overall southwest-northeast oriented fabric, 2) the presence of abundant salt, 3) a thick Triassic to Recent basin fill, and 4) a high volume of Mesozoic sediment deposited by the prograding Sable Delta. Features that vary within the map area include: 1) the original thickness of autochthonous salt, with thicker deposits located within grabens, and thinner deposits located over horsts, 2) the extent and timing of salt movement, 3) the thickness of Mesozoic Sable Delta deposits, with thickening to the east in proximity to the delta and thinning to the west, distal to the delta, 4) the inherent stress regimes produced by a delta prograding over a shelf and slope, and 5) the location and severity of Early Tertiary to Recent channeling.

The contemporary distribution of salt structures within the study area, and the major synclinal and anticlinal trends are illustrated in Figure 5-4, which is a time

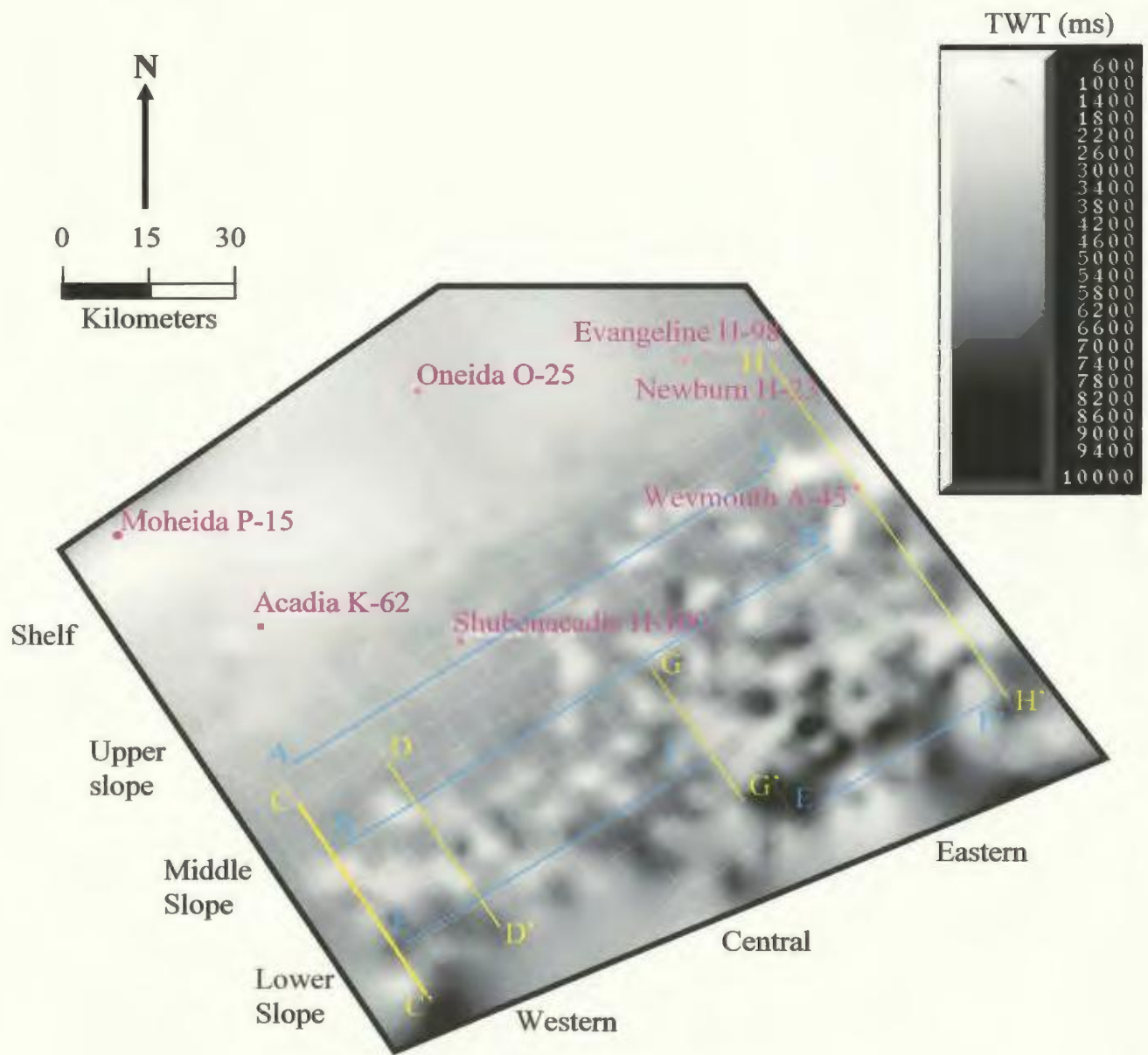


Figure 5-4: Time structure map of top of salt, with location of shelf and the three structural domains on the slope. The upper slope region is the extensional domain; the middle slope region is the transitional domain, and the lower slope region the compression domain. Vertical scale is TWT (ms). Seismic grid in white, well names and locations in pink.

structure map of the top of salt horizon. The complete spectrum of salt structures typical of passive margins, such as those described by Jackson and Talbot (1991; Figure 5-1) has been identified and mapped within the study area. Five halotectonic structural associations with variable domianal distributions have been identified (Figure 5-5). These associations are: the Trough and Swell Association, the Intra-Salt Detachment Association, the Diapiric Association, the Secondary Weld Association, and the Allochthonous Salt Association.

The map distribution of these structures is somewhat generalized as the boundaries between different associations are commonly diffuse zones rather than sharp boundaries. The six-kilometer seismic grid spacing does not allow the structural complexity of salt to be precisely defined, particularly in the structurally complex middle and lower slope region where several reasonable subdivisions may be interpreted to reflect some of the significant changes in structural style.

Within the map area, the only structural association of the shelf is the Trough and Swell association. The upper slope is subdivided into two associations: the Trough and Swell and the Intra-Salt Detachment associations. The middle slope region contains examples of structural styles typical of all structural associations. The lower slope region contains only three structural associations: the Secondary Weld association, the Diapiric association and the Allochthonous Salt association. Further descriptions of the map patters, structural style and spatial relations of each structural association are presented in the following text sections.



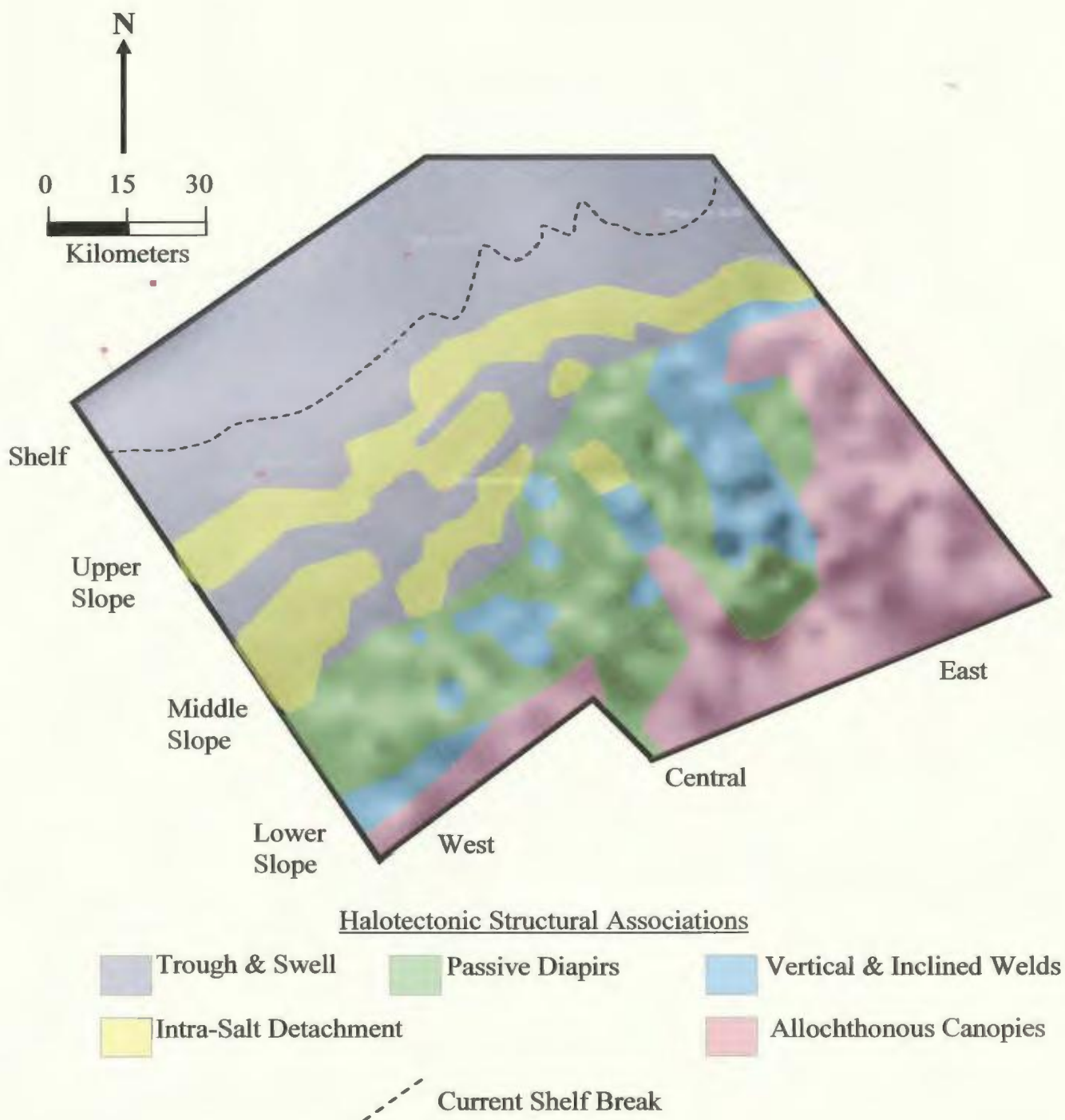


Figure 5-5: Map distribution of halotectonic structural associations and their broad domainal distribution. See Figure 5-4 for well locations.

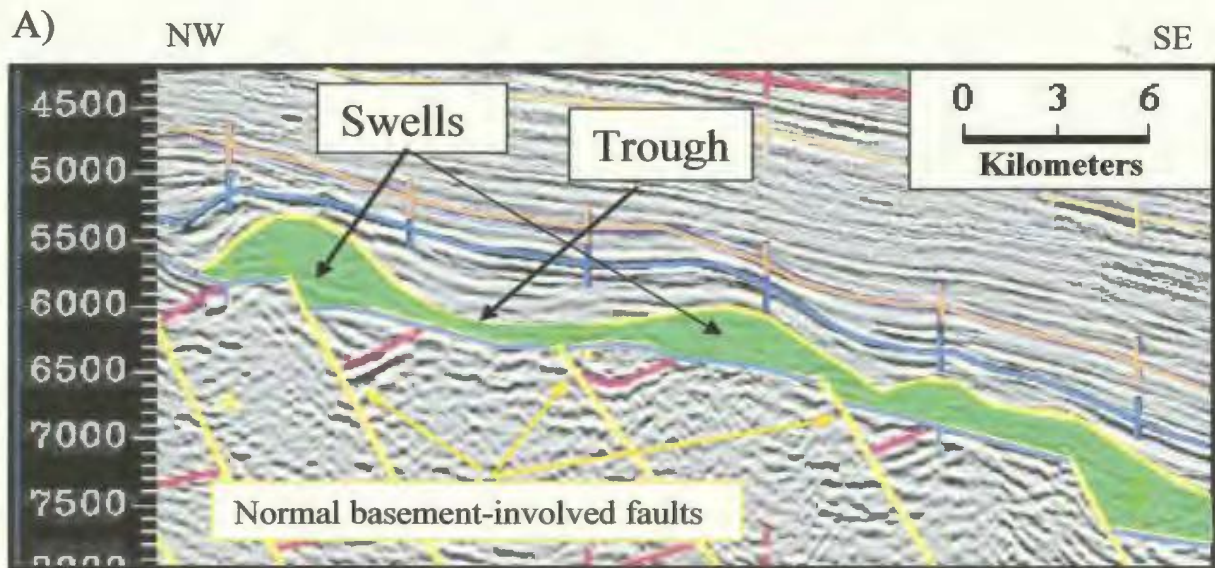
## 5.3 Halotectonic Structural Associations

### 5.3.1 The Trough and Swell Association

The Trough and Swell association is developed over the entire shelf region, and onto the upper slope (purple in Figure 5-5), where it commonly occurs in close proximity to the Intra-Salt Detachment association. It is characterized by its structural simplicity relative to the rest of the map area. Salt in the Trough and Swell association is always autochthonous in nature. The only salt structures typical of this association are salt pillows, salt anticlines, and their associated troughs (e.g. Figure 5-1).

Autochthonous salt refers to any salt body resting on the original strata or surface on which it was accumulated by evaporation. Within the map area autochthonous salt has been intersected in two shelf exploration wells (see Section 3.3.5). Salt swells are formed during the first stages of salt tectonics. They are gentle upwellings of autochthonous salt that form through differential loading or in response to crustal adjustment to extensional faulting (Jackson and Talbot, 1991). The result is an undulating top salt surface formed by local minor concentration of salt in the swells and corresponding evacuation of salt from regions adjacent to the swells creating the troughs. If the swell forms from a point source it is termed a salt pillow, and if it forms from a line source it is termed a salt anticline.

Salt of the Trough and Swell association characteristically has a horizontal to irregular undulating top surface. Adjacent stratigraphy is commonly concordant with or onlaps the top of salt. Salt swells range in profile width from 3 to 12 kilometers, and in strike length from 3 to 30 kilometers (Figure 5-6). Associated troughs range in profile



B)

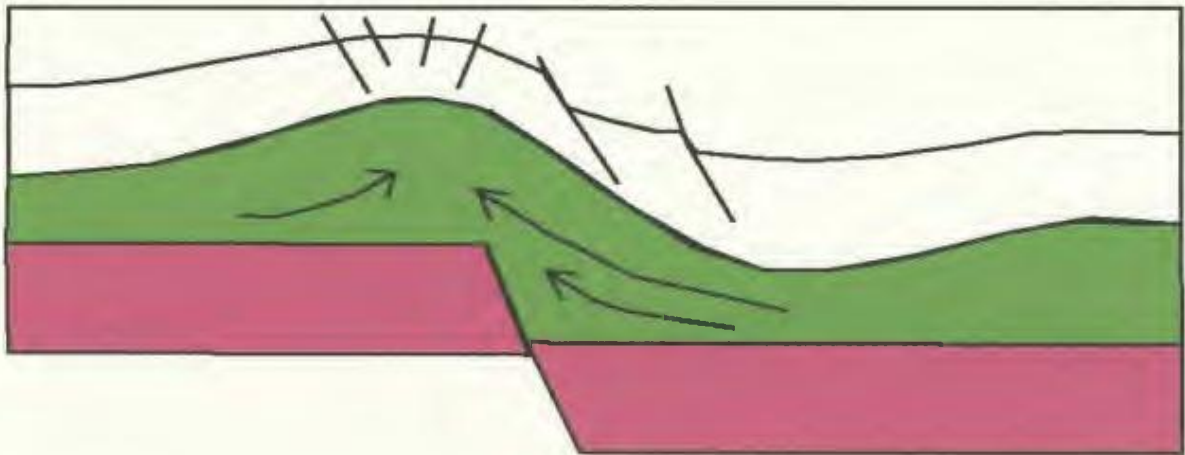


Figure 5-6: A) Section of seismic profile from the western upper slope region of the map area showing example of salt and trough swell. Notice location of swells over basement-involved faults, but not every fault has an associated swell. Vertical scale is TWT (ms). B) Schematic diagram showing relationship between normal basement faulting and swell location (swells are located over normal faults). Differential loading and tectonic stress result in salt flow. The footwall of the normal basement fault forms a baffle to flow causing salt to rise into pillow (or salt anticline if linear source) with an associated trough formed by evacuation.



width from 2 to 12 kilometers, and in strike length from 3 to 30 kilometers. The structural relief from the top of a swell to the top of an associated trough ranges from 100 ms to 600 ms TWT. Swells are restricted to Late Triassic to Early Jurassic stratigraphy, with no salt swells intersecting the J1 break-up unconformity sequence.

There is a close association between salt swells and basement-involved faults. Most swells are located directly above the faults. Linear swells (anticlines) trend southwest-northeast in map view, parallel to basement-involved faults and dominate the upper slope region. However, not all basement-involved faults have an associated overlying salt swell, thus indicating that although these faults have a strong control in the location and orientation of salt swells, basement structure was not the only influence in salt swell formation. In areas where overlying seismic reflectors onlap the top of salt, salt evacuation and subsequent accumulation were likely driven by differential loading. Salt swells with onlapping reflectors are less common than swells with concordant reflectors.

### 5.3.2 The Intra-Salt Detachment Association

The Intra-Salt Detachment association is located within the upper and middle slope regions of the study area (yellow on Figure 5-5). It is contained in southwest-northeast trending zones that are typically interfingered with the Trough and Swell association. The Intra-Salt Detachment Association is characterized by seaward dipping normal faults that are part of the Listric Growth Fault Family (Section 4.2.3), and detach on or within salt. There are a number of related salt structures that characterize the Intra-

Salt Detachment Association including: salt rollers, salt cored anticlines, fault welds, and rafts.

Salt rollers are defined in cross sectional view as low amplitude asymmetrical salt structures with a gently dipping flank in conformable stratigraphic contact with the overburden, and one more steeply dipping flank in normal faulted contact with the overburden (Jackson and Talbot, 1991). They form as a result of gravitational gliding on a decollement surface in or at the base of salt during extensional faulting, and are an unequivocal sign of regional thin-skinned extension perpendicular to the strike of the rollers (Vendeville and Jackson, 1992a).

Within the Intra-Salt Detachment Association, salt rollers are located in the footwall of extensional faults of the Listric Growth Fault Family. They trend southwest to northeast parallel to the strike of the faults and the shelf break, indicating thin-skinned extension perpendicular to this trend in a down-slope, basinward direction. Salt rollers are composed exclusively of Late Triassic to Early Jurassic salt of DS2 and have associated growth strata restricted to DS3.

The geometry of the salt rollers varies greatly. Smaller rollers up to approximately 400 ms TWT in height, have a very repetitive and predictable “horn” shape, and often occur in pairs or groups with regular, relatively short spacing of approximately 2-2.5 km (Figure 5-7). Larger rollers, up to 800 ms TWT in height, tend to occur singularly or in widely spaced pairs; their conformable flank is often less regular than that of smaller rollers. The spacing of rollers within a group is a function of the thickness of the overburden being extended (Rowan, 2002). The smaller, tightly spaced rollers likely



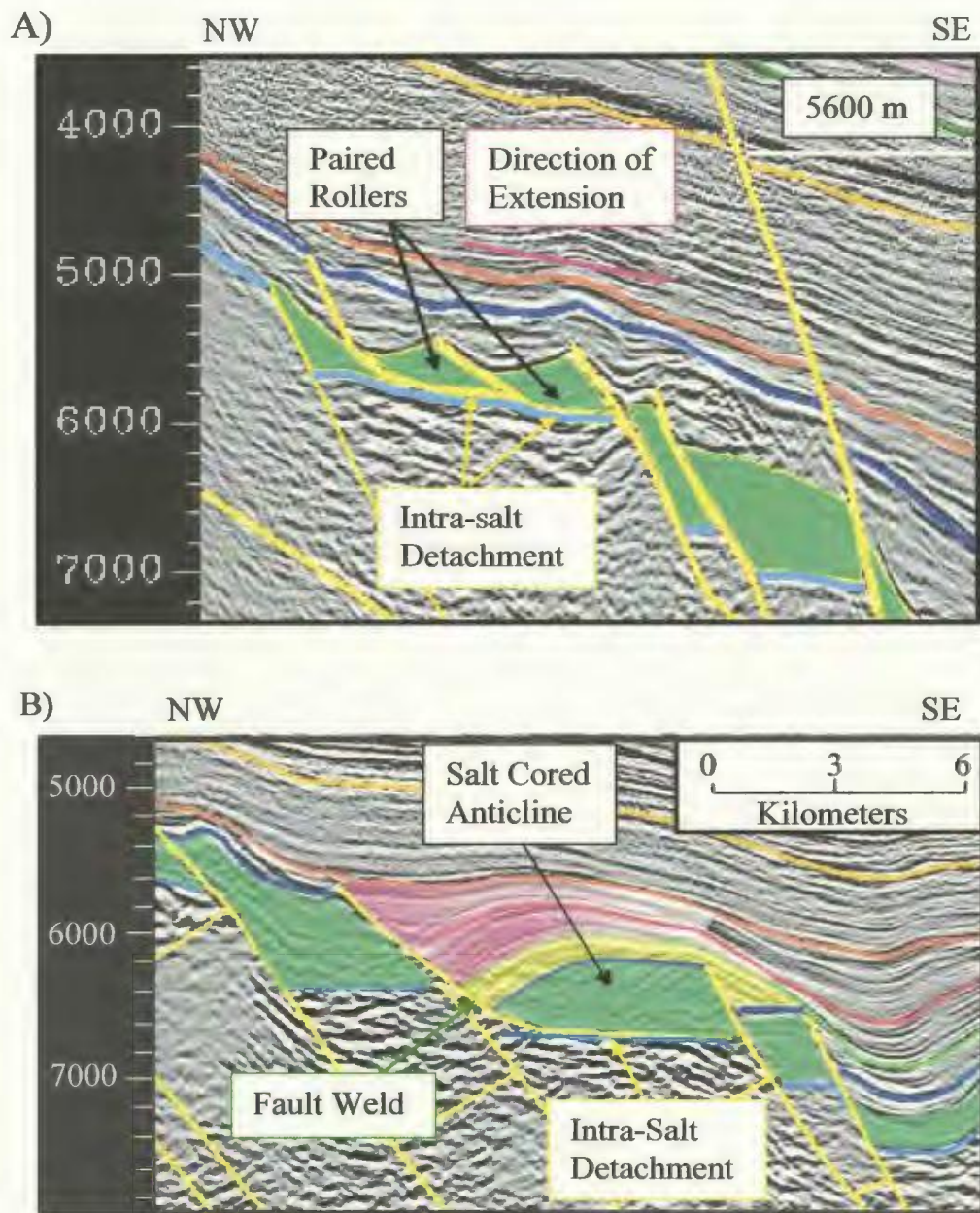


Figure 5-7: NW to SE portions of seismic profiles showing example of some of the associated structures typical of the Intra-Salt Detachment association A) Section from the upper slope, central map area showing normal listric seaward dipping faults with a common level of detachment within salt, and salt rollers in their footwalls. B) Section from the middle slope, western map area showing normal seaward dipping listric growth fault that detaches within salt and has an associated salt cored roll-over anticline. Note that the portion of the fault between the bottom salt footwall cutoff and the top salt hanging wall cutoff is a fault weld, and the overall geometry is that of a raft system. Yellow shaded section represents pre-kinematic strata relative to faulting, pink represents growth strata related to faulting. Vertical scales are TWT (ms).



formed shortly after autochthonous salt deposition when there was relatively little overburden. Larger, wider spaced rollers formed comparatively later, when the thickness of overburden was greater.

Roll-over anticlines are characteristically associated with normal listric growth faults. They occur in the hanging wall of such faults and accommodate extension associated with the concave upward scoop shape of the fault. Within the Intra-salt Detachment association the amount of extension and related rollover of the hanging wall anticline in listric faults is often accentuated by the presence of a salt core of the anticline (Figure 5-7).

A salt weld is a surface joining strata that were originally separated by autochthonous or allochthonous salt (Jackson and Talbot, 1991). The weld is a “negative” salt structure resulting from the complete or near complete removal of intervening salt. Salt welds are identified on seismic sections as discontinuous, high-amplitude reflectors, often with angular discordance between strata on either side. Their seismic character reflects the presence of “pods” of remnant salt in the weld because the overlying and underlying surfaces (or either side in the case of vertical welds) do not have perfectly matching geometries (Rowan, 2002). Residue of non-evaporite material contained within the evaporite unit may also contribute to the “rubbly” seismic character of the weld (Jackson and Cramez, 1989).

Salt welds have variable geometries. Welds will have a horizontal orientation when formed along the original autochthonous salt layer, and are referred to as primary. Welds can be inclined due to evacuation above a dipping base salt surface, or vertical if a

salt wall or diapir is squeezed shut due to shortening. In both cases the welds are referred to as a secondary. A fault weld is considered any type of salt weld along which there has been significant fault slip or shear.

Fault welds are infrequently contained within the Intra-Salt Detachment association where they represent shear along primary welds (Figure 5-7 b). They are formed where movement on listric growth faults causes rotation and extension, so that the hanging wall top salt cut-off on the fault is located basinward of the footwall bottom salt cut-off. In extreme cases of thin-skinned extension, where the offset between adjoining fault blocks is so great that these fault blocks uncouple and separate from each other (hanging wall does not overlie footwall), these isolated fault blocks are known as rafts. Within the study area there are a few examples of raft systems.

### 5.3.3 The Diapiric Association

The Diapiric association predominates the architecture of the middle and lower slope regions (green in Figure 5-5). It is also the only salt association that borders with all other salt associations. The Diapiric association is characterized by two salt structures: primary welds and diapirs, which show a great diversity in shape and size. There is also diversity in the character and geometry of associated growth strata and deformed overburden associated with the diapirs.

A salt diapir is any vertical to sub-vertical salt body with overlapping adjacent strata. A salt wall is a linear mass of diapiric salt and commonly occurs in sinuous parallel rows. Experimental modeling by Vendeville and Jackson (1992 a, b) and Jackson

and Vendeville (1994) shows that there is a close association between salt diapirism and regional extension movement, both in time and space. Temporally, diapirism is generally preceded by extension. Spatially, diapirs are often located in proximity to extensional faults. There are three main successive stages in the formation and evolution of a diapir in an extensional domain: reactive, active and passive diapirism (Vendeville and Jackson, 1992a; Figure 5-8). Reactive diapirism is the initial stage in the growth of a diapir. It occurs during extension when the sedimentary overburden is lengthened and thinned, resulting in the formation of a graben at the surface and an “inverse graben” at the salt-sediment interface. Salt reacts to the thinning by filling the space in the inverse graben. The result is a relatively immature triangular diapir (elongate in the strike direction) that has flanking growth faults that get younger toward the diapir.

Once the overburden has become thin and weak enough and/or the differential fluid pressure between the salt and overburden great enough, the diapir will punch through the overburden to reach the surface. This process is known as active diapirism (Figure 5-9) and is a relatively short-lived process in the evolution of the diapir.

If the diapir reaches the seafloor it will passively grow there as long as there is adequate salt in the source layer to feed it. During this process, known as passive diapirism, the diapir's crest essentially remains at the seafloor while surrounding strata subside into the source layer. During passive growth, the steepness of the flanks of a diapir is primarily a function of the ratio of the rate of salt flow to the rate of sedimentation (Figure 5-9). When the two are balanced the diapir grows vertically; when sedimentation is relatively slower than the rate of salt flow the diapir will progressively



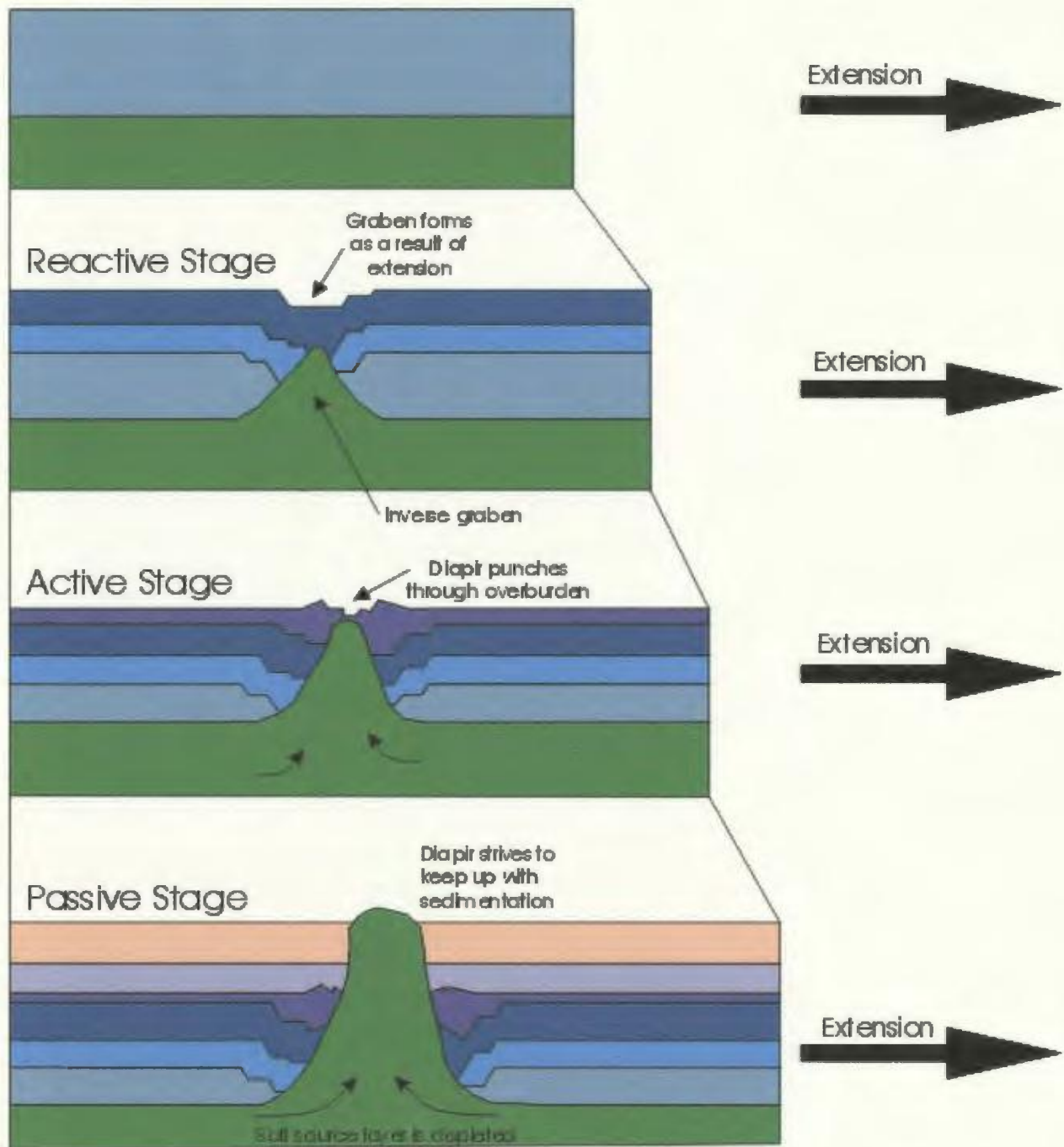


Figure 5-8: Stages of diapir initiation and growth during extension (Vendeville and Jackson, 1992a)

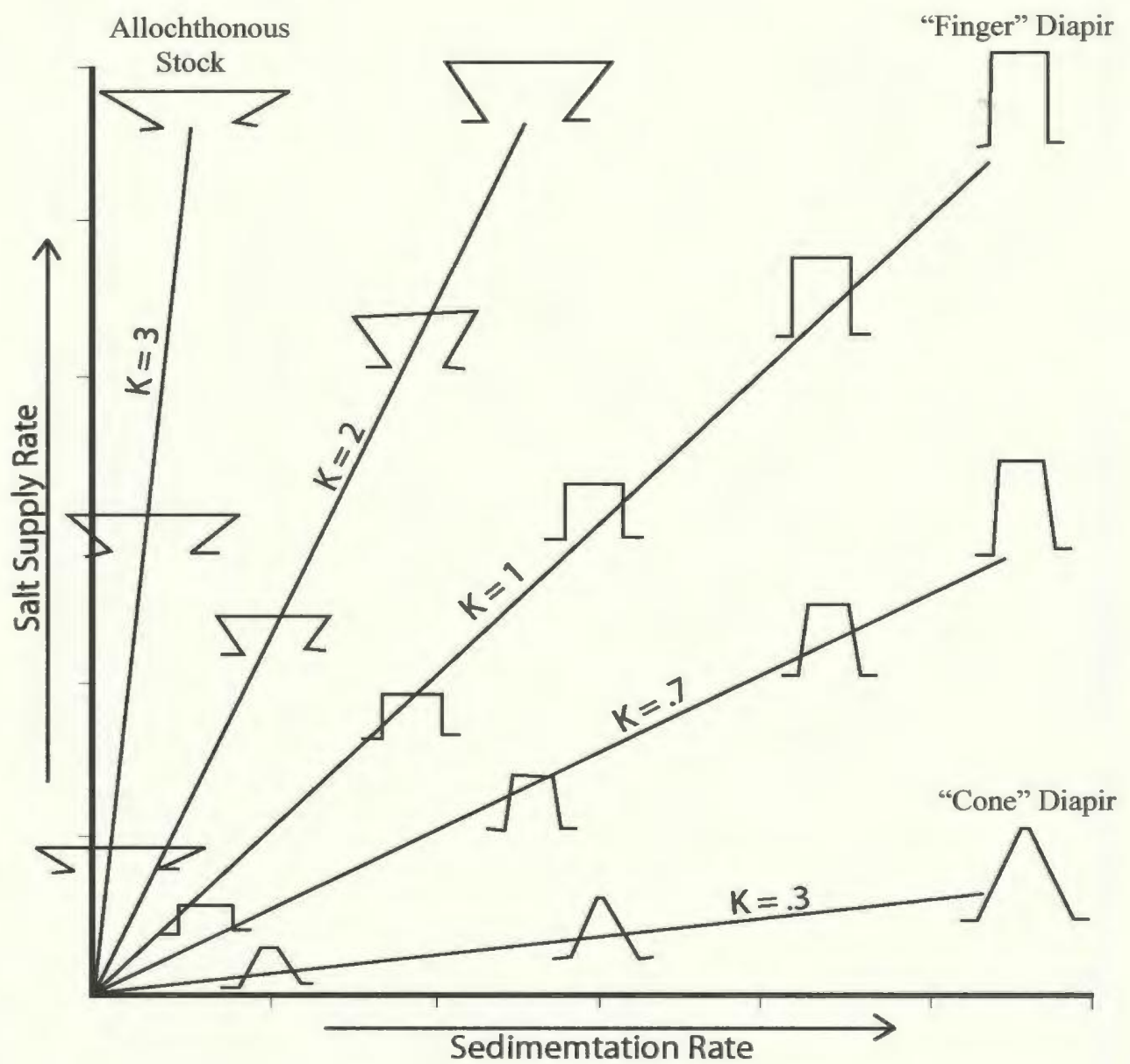


Figure 5-9: Salt diapir and allochthonous stock geometries as controlled by salt supply and sedimentation.  $K$  = slope of linear relationship. Figure modified from McGuinness and Hossack, 1993)

expand laterally. Inversely, if sedimentation is relatively faster than the rate of salt flow the diapir will progressively taper in width. A diapir will continue to grow passively until its source layer is depleted (welded), at which time the diapir will no longer grow and will be buried by subsequent sedimentation.

Contraction uniquely affects diapir shape and greatly influences diapir evolution and adjacent stratal architecture. In gravity driven contractional regimes, such as the lower slope region of the Scotian Slope, the zone of shortening is formed due to a combination of gravity gliding of up-slope sediments and gravity spreading of the salt layer (Galway, 1986; Figure 5-2). Down-dip salt diapirs, being the weakest part of the rock volume, will preferentially accommodate shortening. The salt body narrows and the overburden folds, with salt displaced from the diapir filling the core of the overlying fold. Initial shortening results in broad, low relief symmetrical folds in the lower slope region, continued shortening results in an increase in fold amplitude.

Within the map area on the Scotian Margin, the Diapiric association predominates the architecture of the middle and lower slope regions. The location and orientation of diapiric structures coincide closely with basement-involved faults, with most diapirs located directly over basement-involved faults (Figures 5-10 and 5-11) and most salt wells trending southwest-northeast, parallel to the faults. Primary welds are commonly located adjacent to the diapiric structures. These welds are associated with the evacuation of autochthonous salt and are exclusively contained within Late Triassic to Early Jurassic stratigraphy. In such areas the Tr2 Sequence Boundary represents a primary salt weld.



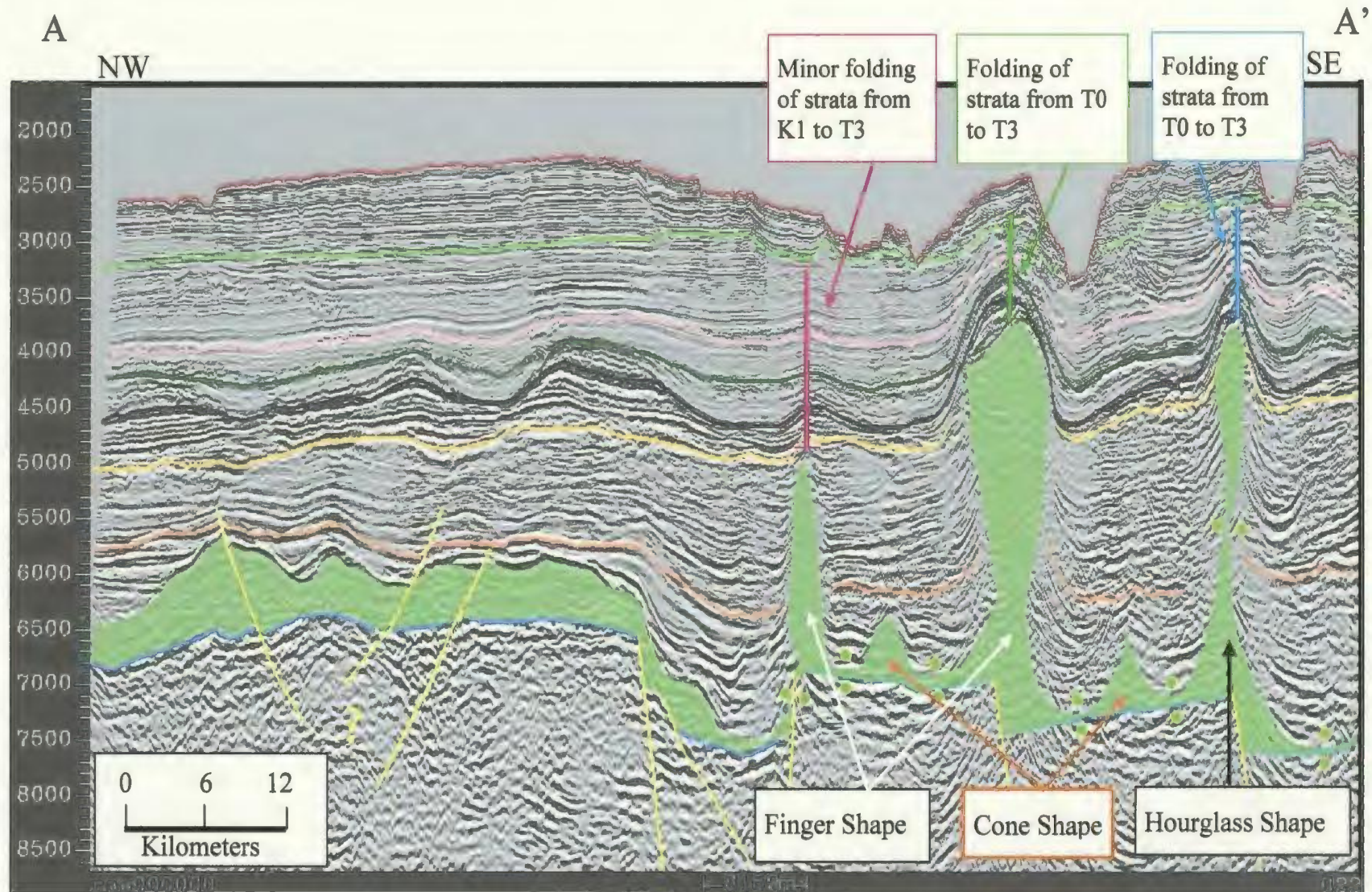


Figure 5-10: Southwest-northeast seismic strike line A-A'. Note the location of diapirs directly over basement-involved faults. Also note the cone shape of small diapirs, the finger shape of tall diapirs, and the presence of an hourglass shaped diapir. Also note the association between diapirs and folded overburden (located in the crests of anticlinal folds) and the association between bathymetric channels and synclinal Tertiary folds at the flanks of diapirs. Note the lack of both diapirs and bathymetric channels in the southwest. Paired dots represent salt welds. Vertical scale is TWT (ms). See Figure 5-4 for location.



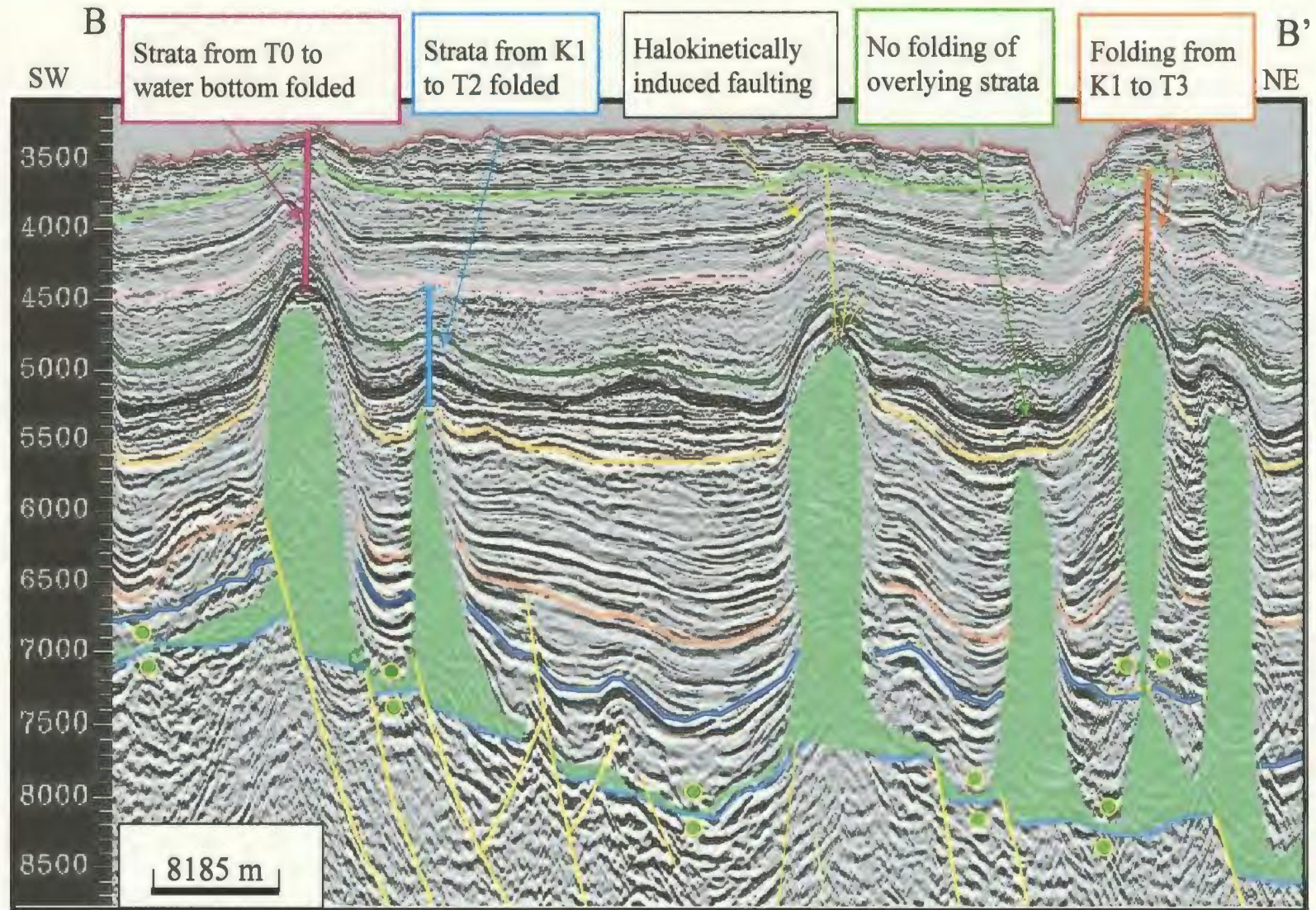


Figure 5-11: Southwest to northeast seismic strike section B-B'. The diapirs lie directly over basement-involved faults. Note the uniform “finger” shape of diapirs, with the exception of the second most diapir from the northeast which has an hourglass shape, and the association between folding and diapirism, with most diapirs located within the crest of the folds. Also note the variation in the timing of folding. Paired dots represent salt weld. Vertical scale is TWT (ms). See Figure 5-4 for location.

Diapirs commonly intersect the K1 Sequence Boundary, but do not often intersect the T0 Sequence Boundary indicating that the autochthonous source layer feeding these structures was regionally depleted (welded) by the Late Cretaceous (Figures 5-10 to 5-13).

Both the concentration and structural complexity of the diapirs increase basinward. In the eastern map area, the landward limit of the Diapiric association is a southwest-northeast lineament, parallel to the shelf break, that occurs at the upper portion of the middle slope region (Figures 5-4, 5-5 and 5-10). In the western map area the landward limit of the Diapiric association is also parallel to the shelf-break, but it is located farther basinward at the center of the middle slope region (Figure 5-4, 5-5 and 5-11). The western and eastern landward limits of the Diapiric Association are offset by a 15 kilometer-long lineament orientated northwest-southeast, perpendicular to the shelf break. One explanation for this map pattern is that the lineament is a sinistral transfer fault or fault zone (see Section 4.2.6). However, this fault is not imaged on the seismic data used in this study, and thus this interpretation is speculative.

Diapirs located in the landward portions of the Diapiric association commonly occur as solitary structures with shapes ranging from “cone” to “finger”. The diapirs vary greatly in height ranging from 500 to 3500 ms TWT. Width ranges from 2 to 6 kilometers in strike sections and 2 – 20 kilometers in profile sections (Figure 5-10, 5-11). In general, smaller diapirs, less than 1000 ms TWT in height, have a cone shape and do not intersect the J2 Sequence Boundary (Middle to Late Jurassic in age). Their tapered



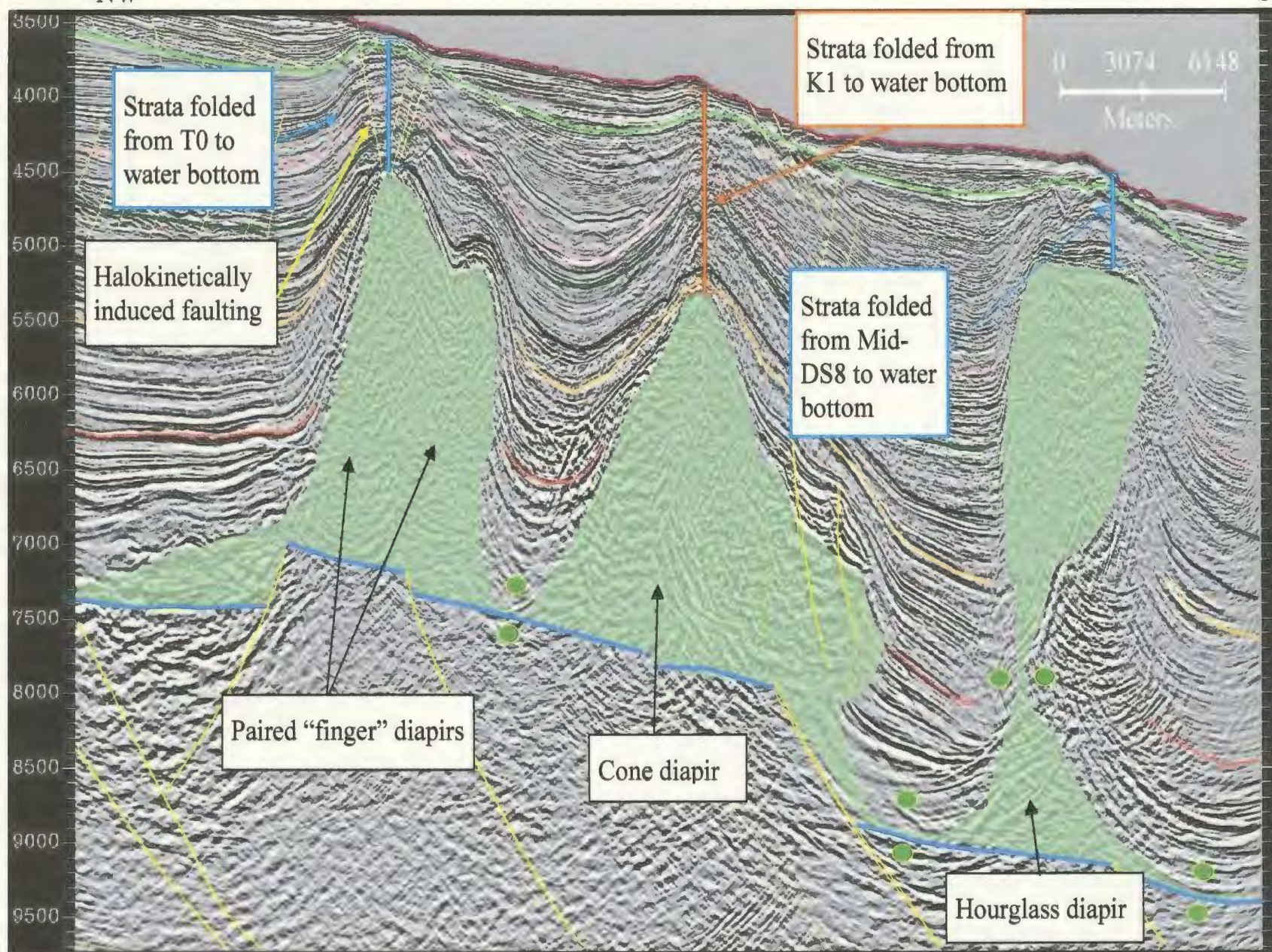
C  
NWC'  
SE

Figure 5-12: Seismic profile C-C' from the western middle to lower slope region. Note the relationship between diapirism and folding with diapirs located in the crest of folds. Also note the synchronous timing of folding. Paired dots represent salt welds. Vertical scale is TWT (ms). See Figure 5-4 for location.



D  
NW

SE D'

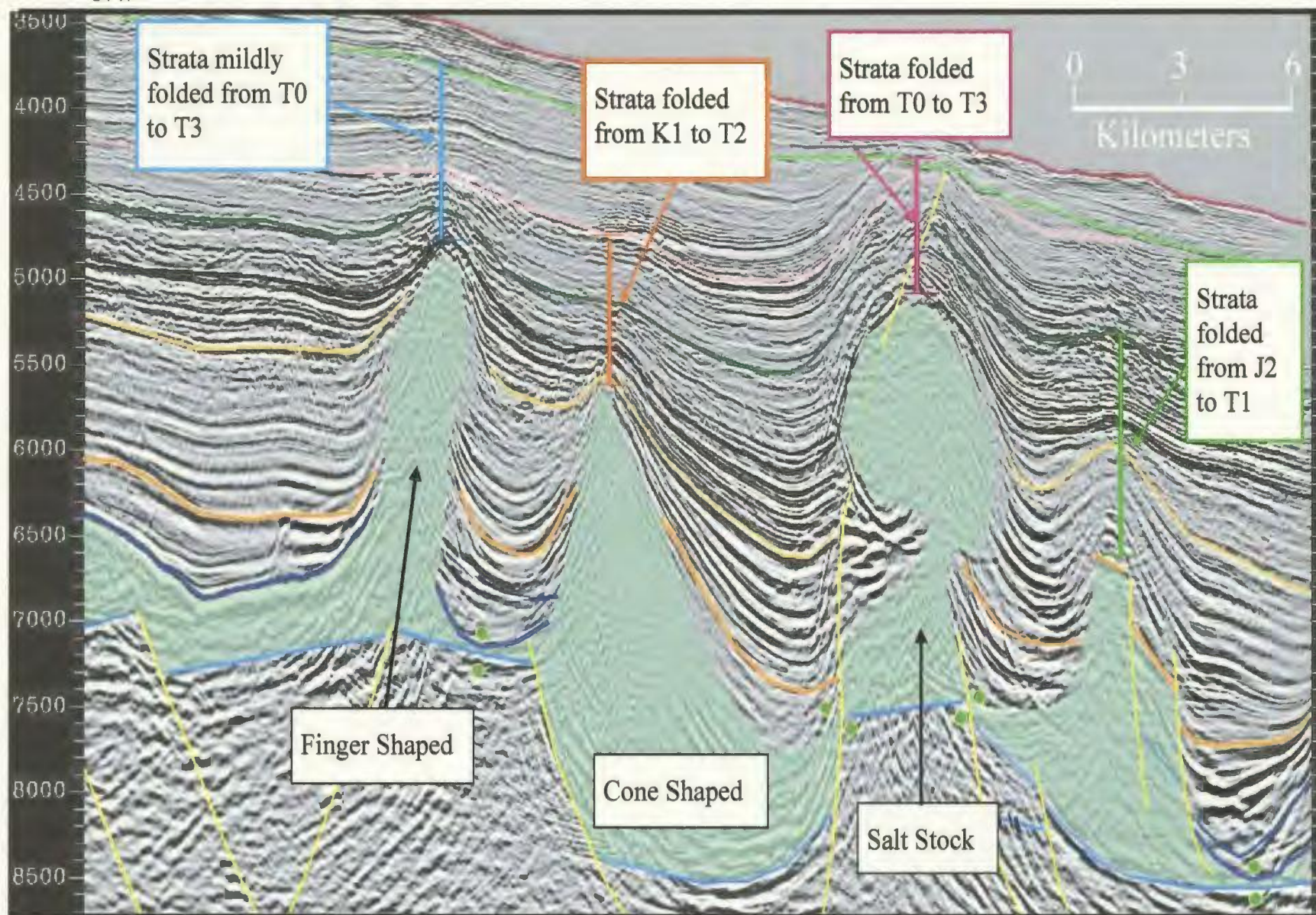


Figure 5-13: Seismic profile D-D'. Note the variation in diapir shape and age of folding of the overburden. Paired dots represent salt welds. See Figure 5-4 for location. Vertical scale is TWT (ms).



shape indicates that they were formed during a time in which sedimentation progressively increased relative to salt flow (Figures 5-9 and 5-10).

The shape of diapirs in strike sections becomes more uniform in a basinward direction. Here, most diapirs have a “finger-like” shape, with their width ranging from 2-6 kilometers. In profile sections, these structures have a highly variable shape and are up to 2-20 kilometers wide. Profile shapes range from finger-like to cone (Figures 5-9, 5-12 and 5-13).

Within the map area, diapirs have a close association with folds, in that most diapirs are located in the crests of anticlinally folded overburden (Figures 5-10 to 5-13). Tertiary stratigraphy from the T0 to T3 sequence boundary is commonly folded over diapiric structures. Strata overlying the T3 sequence boundary are commonly unstructured, indicating that folding terminated prior to the Quaternary. A likely explanation for the relationship between fold and diapir location is that the diapir predates the folding, thereby controlling the location of the folds because of the inherent weakness of salt. A salt diapir will preferentially accommodate shortening, being the weakest part of the rock column. Once isolated from autochthonous salt by evacuation and welding, the diapir ceases to grow and becomes buried. Post-halokinetic deposition over the salt body will be folded by continued contraction with salt displaced from the diapir filling the core of the overlying fold (Rowan, 2002). This process is known as diapir rejuvenation (Figure 5-14). Although it appears as though the salt has actively raised the overburden (active diapirism) it has in reality just responded passively to the imposed tectonic force. If buoyancy were the only force driving diapir growth there



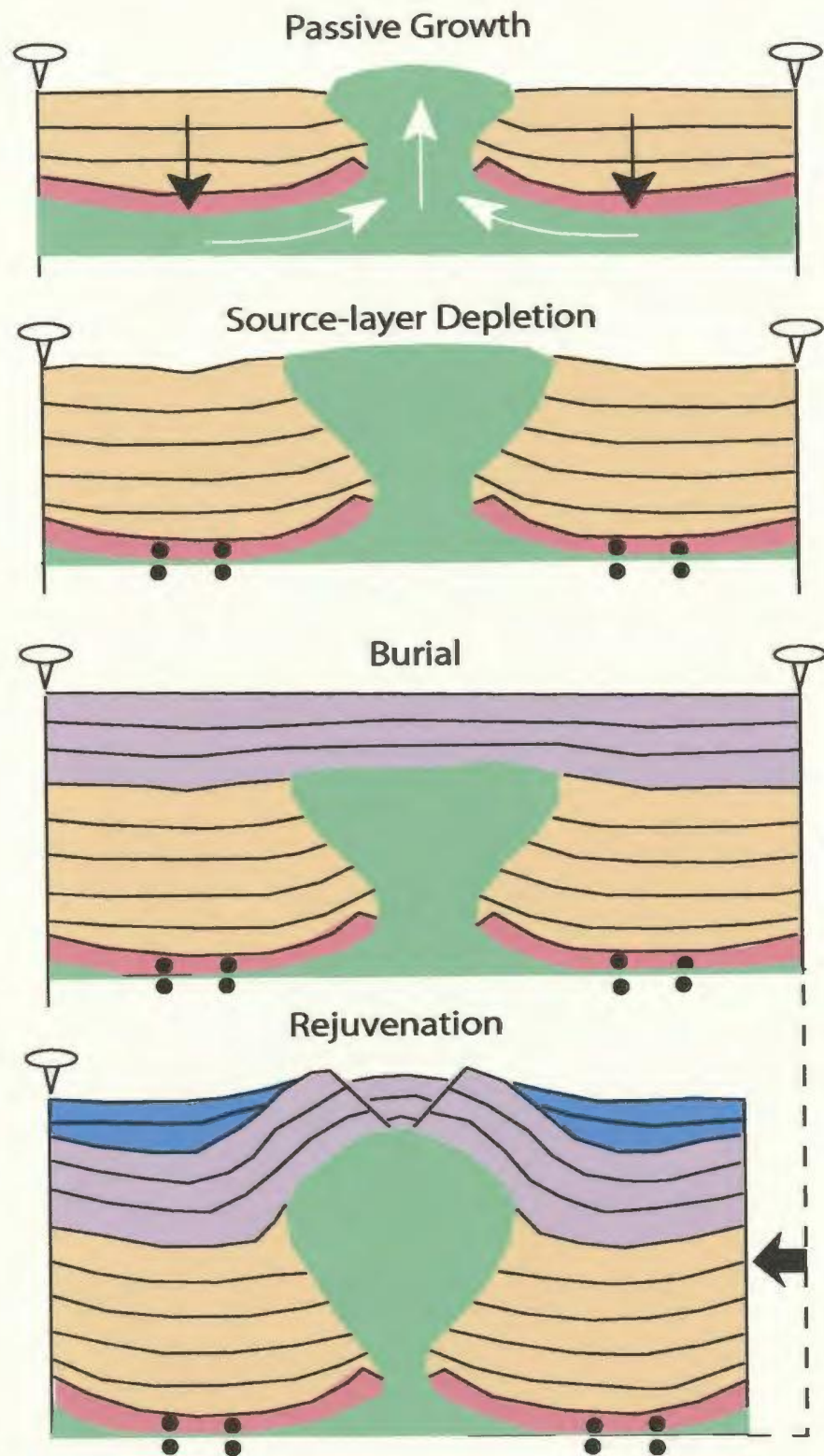


Figure 5-14: Diapir rejuvenation during contraction. Paired dots represent salt welds. Figure modified from Vendeville and Nilsen, 1995.

would not be any buried or dead diapirs, and all diapirs would reach the surface. In the diapiric association of the Scotian Margin, the overall consistent thickness of folded Tertiary and Quaternary strata attests to the pre-kinematic deposition of the folded section.

The crests of anticlinal folds over diapirs commonly contain normal faults (Figures 5-12 and 5-13). In this study, these faults have been grouped into the Halokinetically Induced Fault Family (see Section 4.2.5). These faults may form due to two processes: 1) evacuation of the salt from the diapir and thus collapse of the folded crest overlying the diapir, or 2) local extension of the brittle strata overlying the anticlinal crest in order to accommodate folding (i.e. outer arc extension). The lack of growth strata overlying the crest of diapirs indicates that diapir subsidence was not the process responsible for faulting. Thus, normal faults overlying the flanks of diapirs formed in response to local extension at the crest of the anticlines due to regional folding.

There is a close association between bathymetric channel location and diapir and fold crest location. Firstly, the landward limit of diapirism occurs further up slope in the eastern map area where large bathymetric channels shape the seafloor. No diapirs are located in the adjacent western portion of this region where the seafloor is flat (Figure 5-10). Secondly, all bathymetric channels observed directly overlie synclines adjacent to the anticlinal folds overlying diapiric structures, indicating that the synclinal folds have some control on channel location (Figure 5-10).

#### 5.3.4 The Secondary Weld Association

The Secondary Weld association is distributed within discrete zones scattered throughout the middle and lower slope region (blue in Figure 5-5). In map pattern, it is often enclosed within random areas dominated by the Diapiric association, and/or commonly located directly landward of the Allochthonous Salt association. Secondary welds are contained within Jurassic and Cretaceous successions and were not observed within the Tertiary succession.

Vertical welds commonly occur as the central section of rejuvenated diapirs that have been “squeezed” into an hourglass shape (Figures 5-10, 5-11, 5-12, 5-15). The hourglass diapirs have a relatively wide base that tapers up into a central section that is has been vertically welded, before widening toward the top of the structure in a “tear drop” or “inverted triangle” shape. Hourglass diapirs with central vertical welds are always located in the crest of folded overburden.

Inclined secondary welds occur less commonly in the study area than vertical secondary welds. Inclined welds have a very strong relationship with the Allochthonous Salt Association in that they are commonly located immediately landward of allochthonous salt structures. Inclined welds are always tilted basinward and constitute the stems of basinward tilted diapirs and/or lateral salt bodies (allochthonous salt) (Figure 5-16). The inclined welds represent relic feeders to these salt structures. Salt structures with inclined secondary weld feeders are also commonly located in the crest of folded overburden



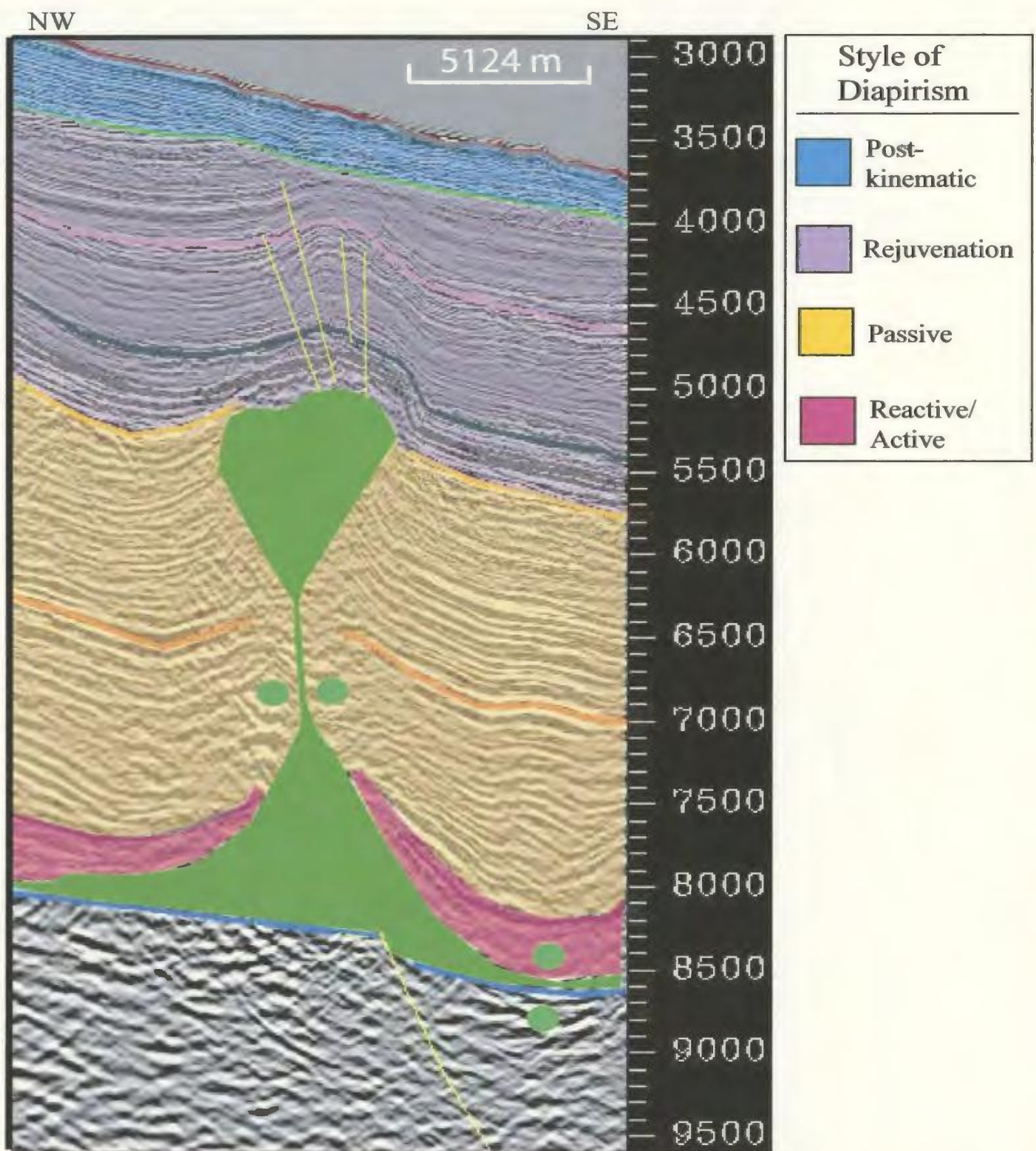


Figure 5-15: Example of rejuvenated “hourglass” shaped diapir with secondary weld at the middle stem. Autochthonous salt adjacent to diapir is also welded (primary weld). Seismic profile section is from the lower slope region, western map area. Paired dots represent salt welds. Vertical scale is TWT (ms).

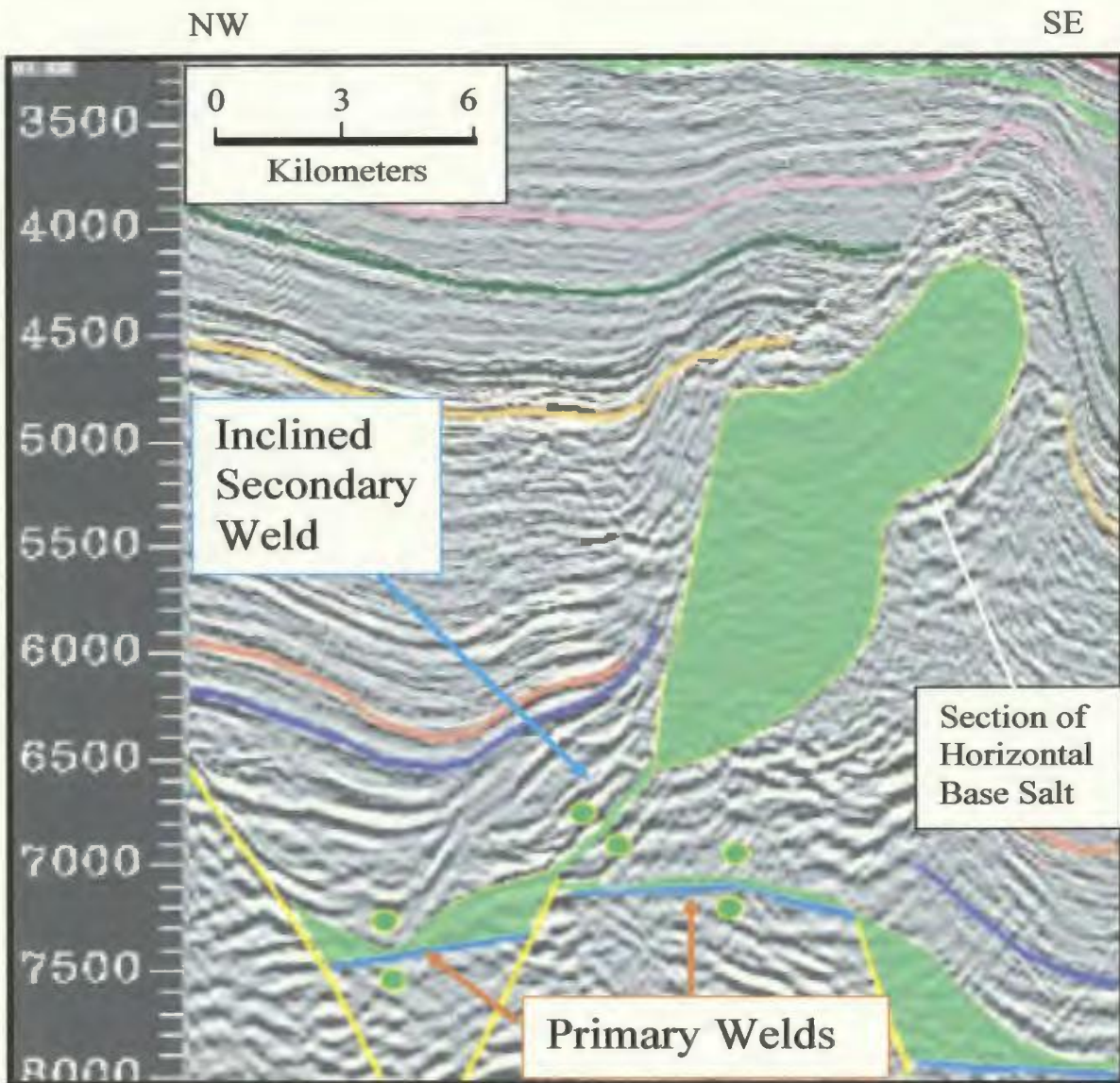


Figure 5-16: Portion of northwest-southeast seismic profile from the central middle slope region with example of inclined secondary salt weld. Note the location of secondary weld over basement-involved fault. Secondary weld is the feeder to a basinward tilted salt diapir with a small region of horizontal allochthonous base salt. Vertical scale is TWT (ms).



The diapir-fold-secondary weld family of structures is an unequivocal indicator of contraction. The location of the structures on the lower slope suggests that shortening resulting from up-dip gravity gliding and/or spreading caused the diapir to be squeezed, narrowing the diapir and forcing internal salt upward. The flanks of the diapir eventually meet and form a secondary weld, thereby disconnecting the top of the diapir from autochthonous salt. A key implication of the proposed explanation is that shortening can be one of the major causes of salt extrusion in areas where the source layer has not yet been depleted. Squeezing of a diapir greatly increased salt flow rates, and this favored extrusion of allochthonous salt. If enough salt is extruded it may grow laterally on the sea floor forming an allochthonous salt layer. This model also explains the map association between the Secondary Weld association and the Allochthonous Salt association, with secondary welds commonly located landward of allochthonous salt.

#### 5.3.5 The Allochthonous Salt Association

Within the map area the Allochthonous Salt Association is restricted to the eastern middle slope region and the lower slope region (pink in Figure 5-5). The basinward boundary of this association lies beyond the southeastern limit of the seismic grid. The association is bounded in a landward direction by the Secondary Weld association or the Diapiric association. Allochthonous salt structures with intervening sediment-filled minibasins and underlying primary salt welds dominate the structural style of this association, but the structures are complex and show considerable variation in geometry and orientation.



An allochthonous salt structure is any lateral or sheet-like salt body emplaced at a stratigraphic level above the autochthonous source layer (Jackson and Talbot, 1991). These structures form when the rate of salt flowage or expulsion is greater than that of sedimentation (Figure 5-9). Thus, the critical difference between a diapir and allochthonous salt sheet is the ratio of the rate of sedimentation relative to the rate of salt flow. The timing of allochthonous sheet emplacement is synchronous to the stratigraphic level adjacent to the base of the salt sheet.

There are three end member styles of allochthonous salt: asymmetric salt tongues, radial bulb-shaped salt stocks, and salt nappes (Rowan, 2002; Figure 5-17). A salt suture is a junction between individual allochthonous salt structures that have coalesced laterally. A second-cycle salt structure is a structure that rises by reactivation of allochthonous salt. It is sourced from an allochthonous salt layer and has onlapping adjacent strata.

Within the study area, allochthonous salt is contained in salt tongues or stocks with a few examples of second-cycle salt structures (Figure 5-18). No salt nappes were mapped, indicating that allochthonous salt formation happened relatively quickly over a short time interval (conducive to stalk and tongue formation) rather than slowly and continuously (which is conducive to nappe formation) (Rowan, 2002). However, the absence of nappes in the study area may be a function of limited seismic coverage, as the basinward limit of salt is not imaged. Models of salt movement on passive margins commonly predict that nappes, when present, form the basinward limit of salt (Rowan, 2002).

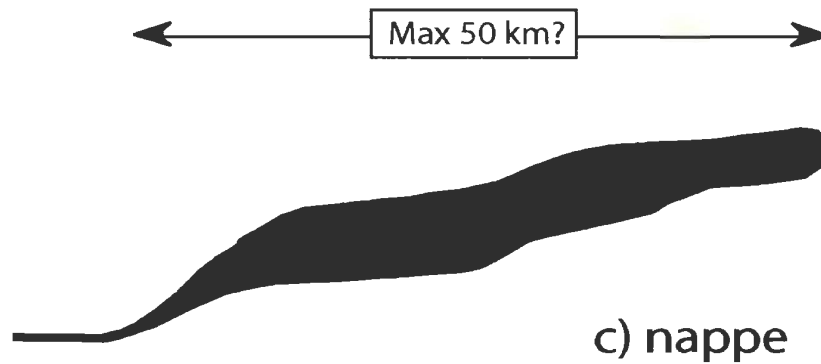
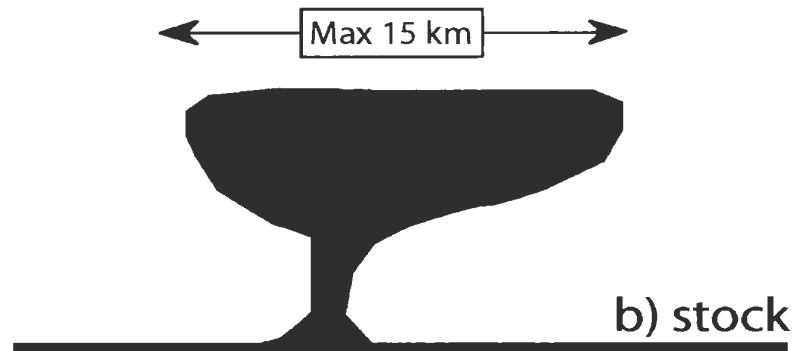
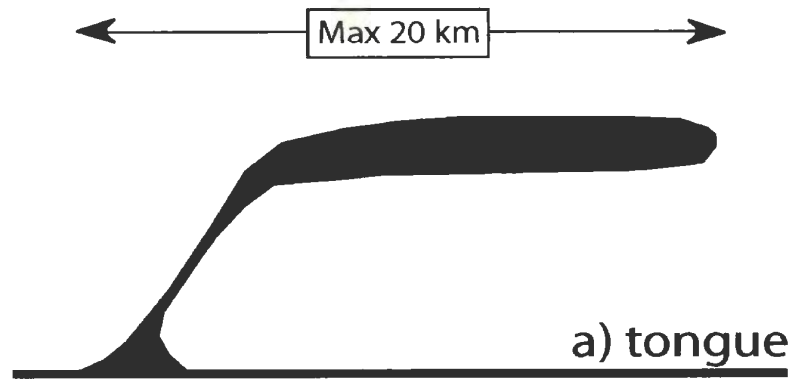


Figure 5-17: End member geometries of allochthonous salt systems: a) asymmetric salt tongues, b) radial bulb-shaped salt stocks and c) salt nappe. (Figure modified from Rowan, 2002)

### Salt Stocks

A salt stock is characterized by a narrow vertical feeder that sources a radial or slightly asymmetrical bulbous top. Within the Allochthonous Salt association, salt stocks have an average diameter ranging from 5 to 7 kilometers (Figures 5-18, and 5-19). They are occasionally symmetrical, but more often asymmetric with no apparent pattern in the direction of asymmetry. The age of the strata directly underlying the base of the bulb of a salt stock represents the timing of allochthonous salt formation. Within the map area, the base of allochthonous salt stocks is most commonly contained within DS4 (Middle to Late Cretaceous) but may also be located in DS5 (Late Cretaceous) (Figures 5-18 and 5-19). This indicates that during the Late Cretaceous on the Scotian Slope there was a major increase in the rate of salt flow relative to the rate of sedimentation. This change in rates coincides with the Late Cretaceous demise of the Sable Delta depositional system. Vertical thickness of salt stocks ranges from 1200 to 2100 ms TWT, with the top of these salt structures located in DS5 (Late Cretaceous) or DS6 (Eocene), indicating that salt flow had ended by this time.

No salt stock canopies have been mapped within the study area. However, the “mirror image” paired geometry of some salt stocks suggests the structures in question are actually joined in a semi-circle shape out of section as part of the one larger structure (Figure 5-19).



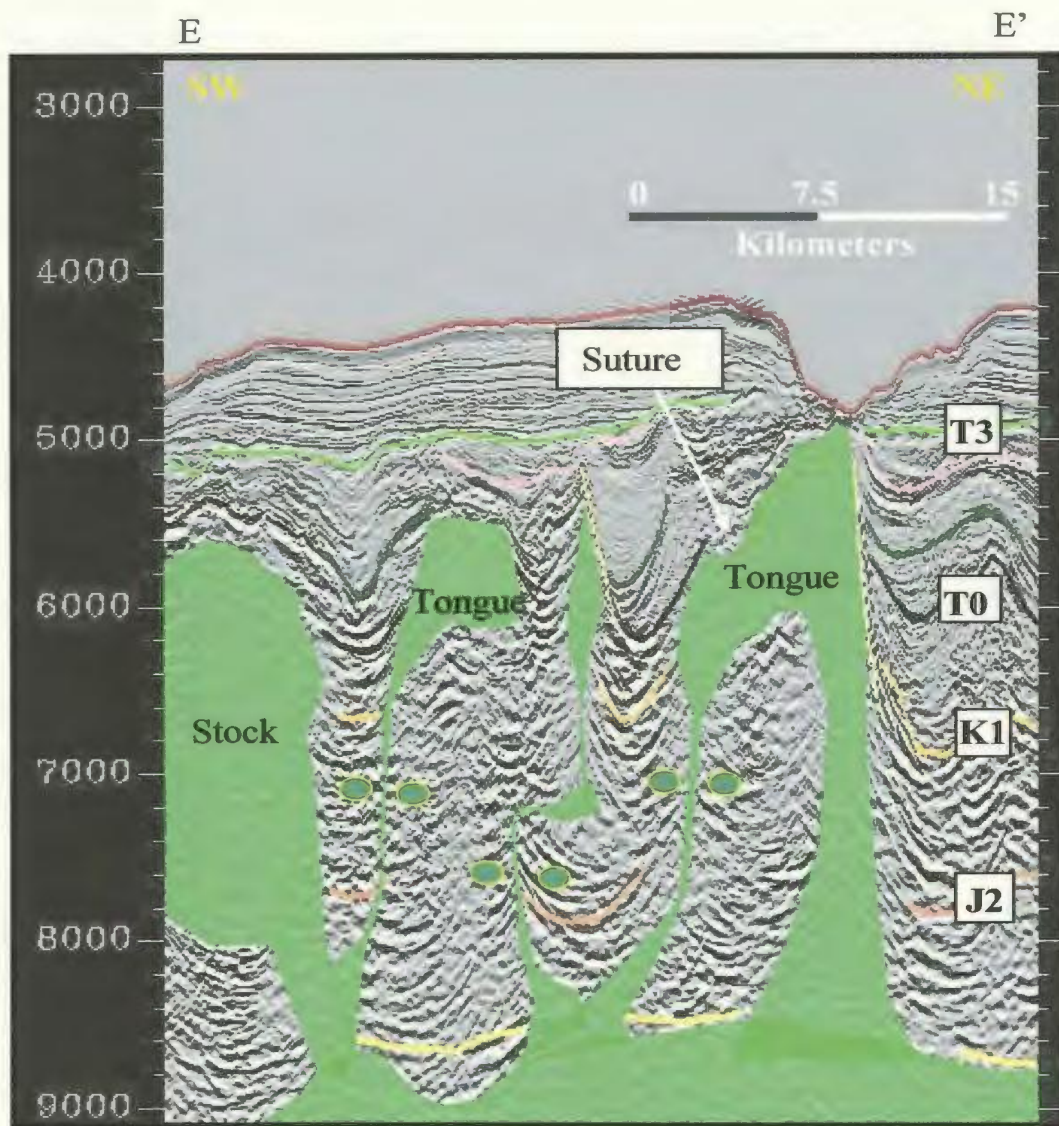


Figure 5-18: Seismic strike line E-E' showing vertical or secondary salt welds (noted by paired dots), salt stock and salt tongues. Salt welds are marked by a structural discordance of reflectors. Note that salt movement has structured all successions below the T3 Sequence Boundary. Reflectors above T3 are regularly layered, sub-parallel and concordant with the T3 Sequence Boundary. Vertical scale is TWT (ms). See Figure 5-4 for location.



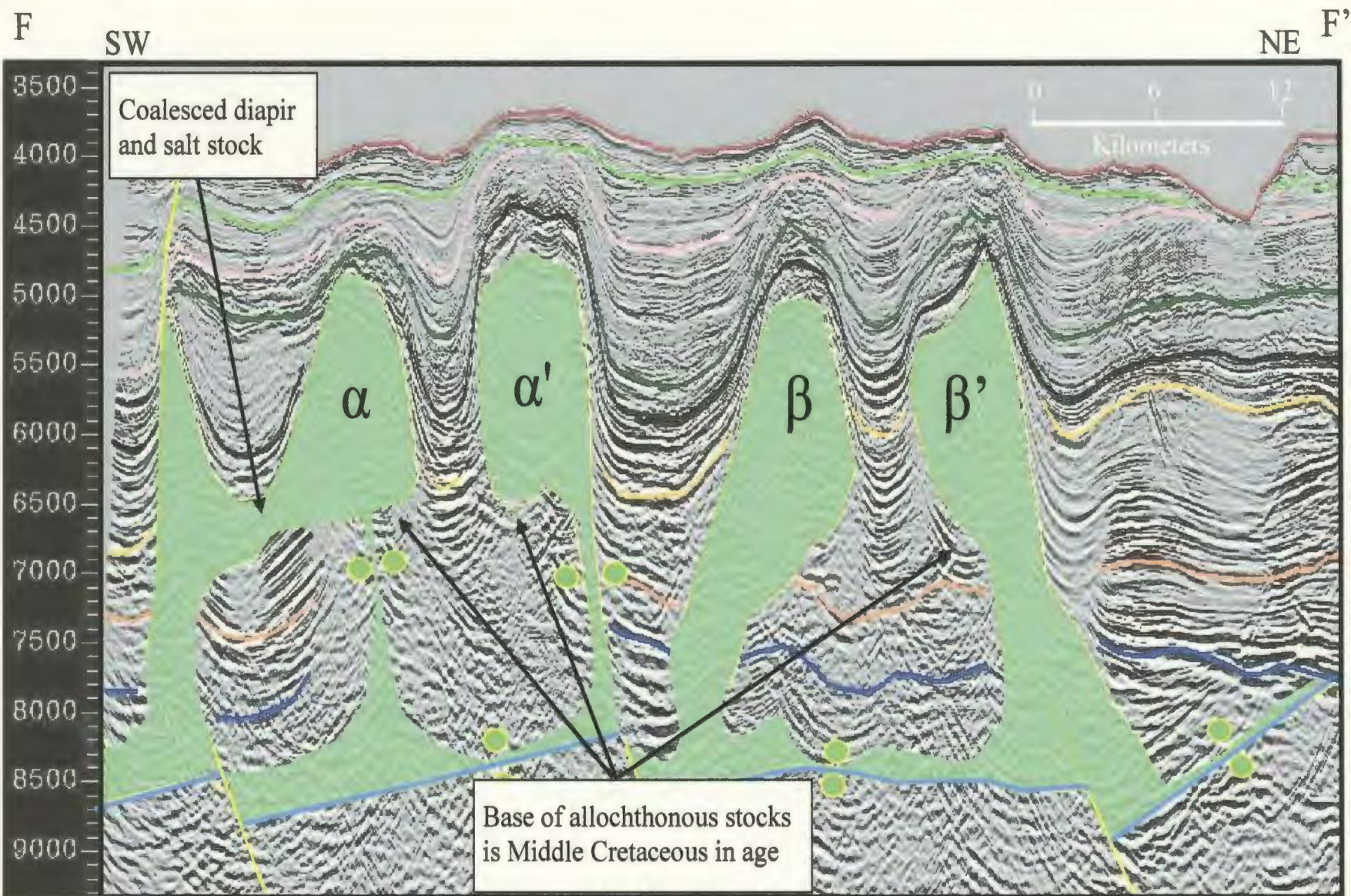


Figure 5-19: Southwest-northeast seismic strike line F-F'. Salt structures are allochthonous salt stocks, with emplacement of allochthonous sheets occurring within DS4 (Early to Middle Cretaceous). Note the association between the salt stocks and folding of the overlying Tertiary through Quaternary successions. Also note the paired geometry of the structures  $\alpha$ ,  $\alpha'$  and  $\beta$ ,  $\beta'$  suggesting the pairs are actually sourced from the same layer and joined in a semi-circular shape out of the plane of section section. Paired dots represent salt welds. Vertical scale is TWT (ms). See Figure 5-4 for location.



### Salt Tongues

Salt tongues are asymmetric sub-horizontal allochthonous salt structures with a basinward sub-vertical or inclined feeder (Figure 5-17a). They form when a basin-leaning diapir extrudes salt laterally. The extrusion is asymmetric so that the feeder is located at the landward edge of the tongue (Rowan, 2002). Salt tongues can evolve to two end member styles: stepped counterregional and roho. The evolution of a salt tongue into a steppe counterregional system vs. a roho system is a function of the loading history above the allochthonous salt, and the down dip length of the salt sheet (Rowan, 2002). A relatively long sheet will have enough gravity head to cause basinward translation and roho-style evacuation, whereas the overburden above a short sheet will not move laterally and thus forms a counterregional system.

Within the Allochthonous Salt association, there are examples of both stepped counterregional and roho salt-tongue systems. Stepped counterregional systems are characterized by a basinward-leaning feeder, that extrudes laterally to form a tongue (Figure 5-20). Upon the exhaustion of the autochthonous salt source, the tongue collapses, resulting in a basinward dipping and thickening sedimentary growth wedge, and landward-dipping secondary diapir.

Stepped counterregional systems have been mapped within all areas containing the Allochthonous Salt association. They range in profile length from 5 to 20 kilometers and in strike width from 2 to 10 kilometers (Figure 5-20). The vertical thickness ranges from 600 to 1500 ms TWT. The base of stepped counterregional systems, and thus the timing of lateral salt emplacement, ranges from the middle of DS4 (middle Cretaceous) to



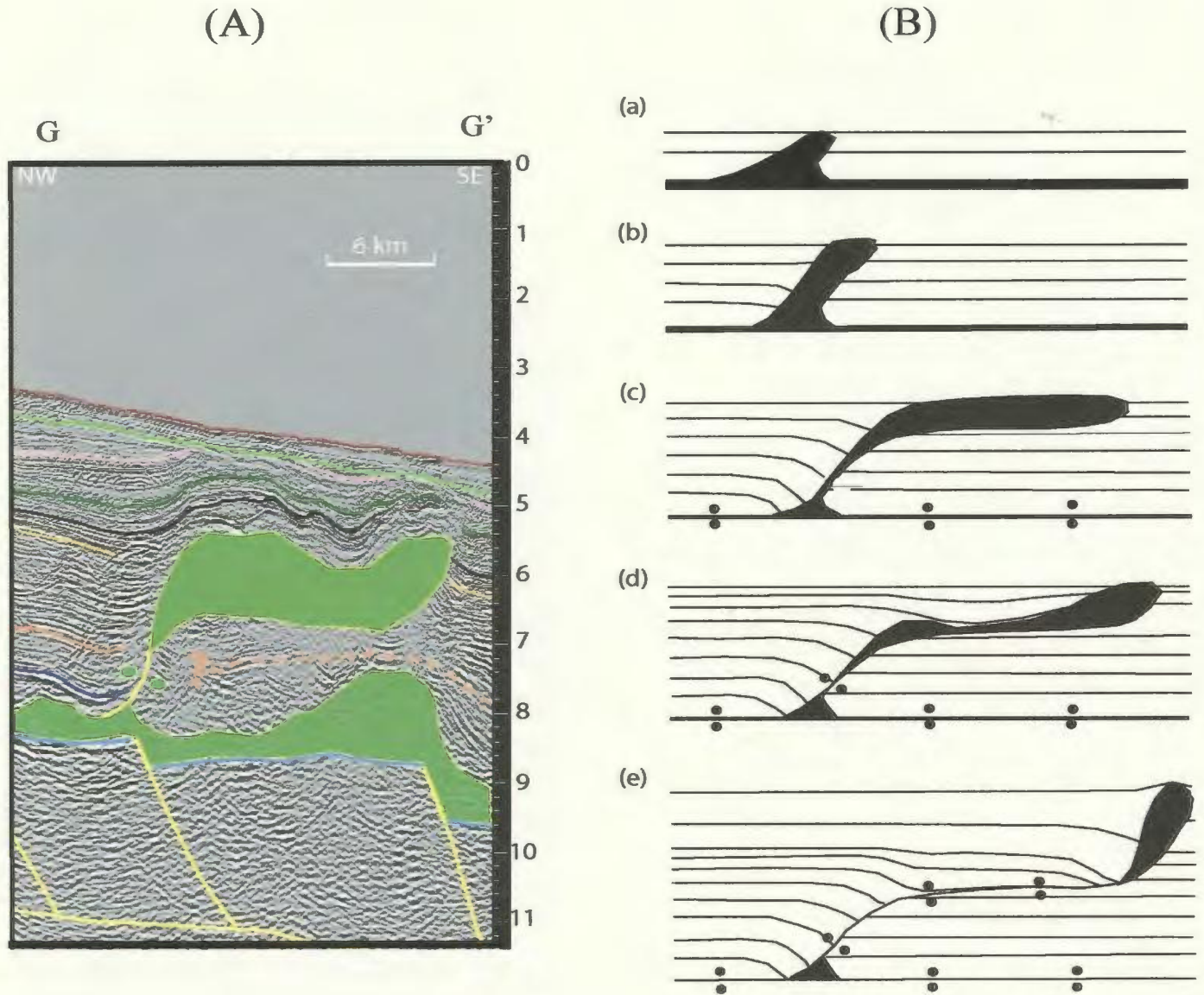


Figure 5-20: (A) Northwest-southeast seismic profile G-G' with example of allochthonous salt tongue. Vertical scale is TWT (s). See Figure 5-5 for location. (B) Schematic evolution of a stepped counterregional tongue system (Rowan, 2002). (a) and (b) passive growth of basinward leaning diapir, (c) diapir extrudes laterally to form allochthonous tongue, autochthonous source salt is welded, (d) inclined feeder is welded resulting in collapse of central tongue and development of basinward-dipping and thickening growth wedge, (e) formation of secondary landward dipping secondary diapir or equivalent weld. Note that example (A) is at stage (d) of diagram (2).

synchronous to the K1 Sequence Boundary (Late Cretaceous). The top of counterregional steppe systems, and thus timing of the end of allochthonous salt emplacement, ranges from intra DS6 (Eocene) to intra DS7 (Miocene-Oligocene).

Because of their geometrical complexity, roho salt-tongue canopy systems are not easily mapped in detail in two-dimensional seismic grids. They are characterized by extensional basinward dipping growth faults that detach within the allochthonous canopy (Figure 5-21). Roho systems are also commonly associated with contractional toe structures along the basinward edge, and strike-slip structures along the margins, both indicating basinward translation of the overburden.

Figure 5-22 is one of two seismic profile lines from the easternmost study area containing a possible roho salt-tongue system. Roho systems have not been mapped anywhere else in the study area. The possible roho system contains a landward salt tongue structure, approximately 10 km in length, with its base situated at the K1 Sequence Boundary (Late Cretaceous), and top within DS7 (Oligocene-Miocene). Reflectors underlying this salt structure, from the J1 Sequence Boundary (Early Jurassic) to, and including, the base of the salt structure are folded into a broad fold towards a large basinward dipping listric fault. Between the fault and the salt tongue is a mini-basin with divergent reflectors (growth strata) from the K1 Sequence Boundary to the T1 Sequence Boundary (top Eocene). The proximity of the mini-basin to the growth fault and the age of the growth strata suggests that this minibasin formed in response to creation of accommodation space by extension and rotation of the hanging wall strata above the

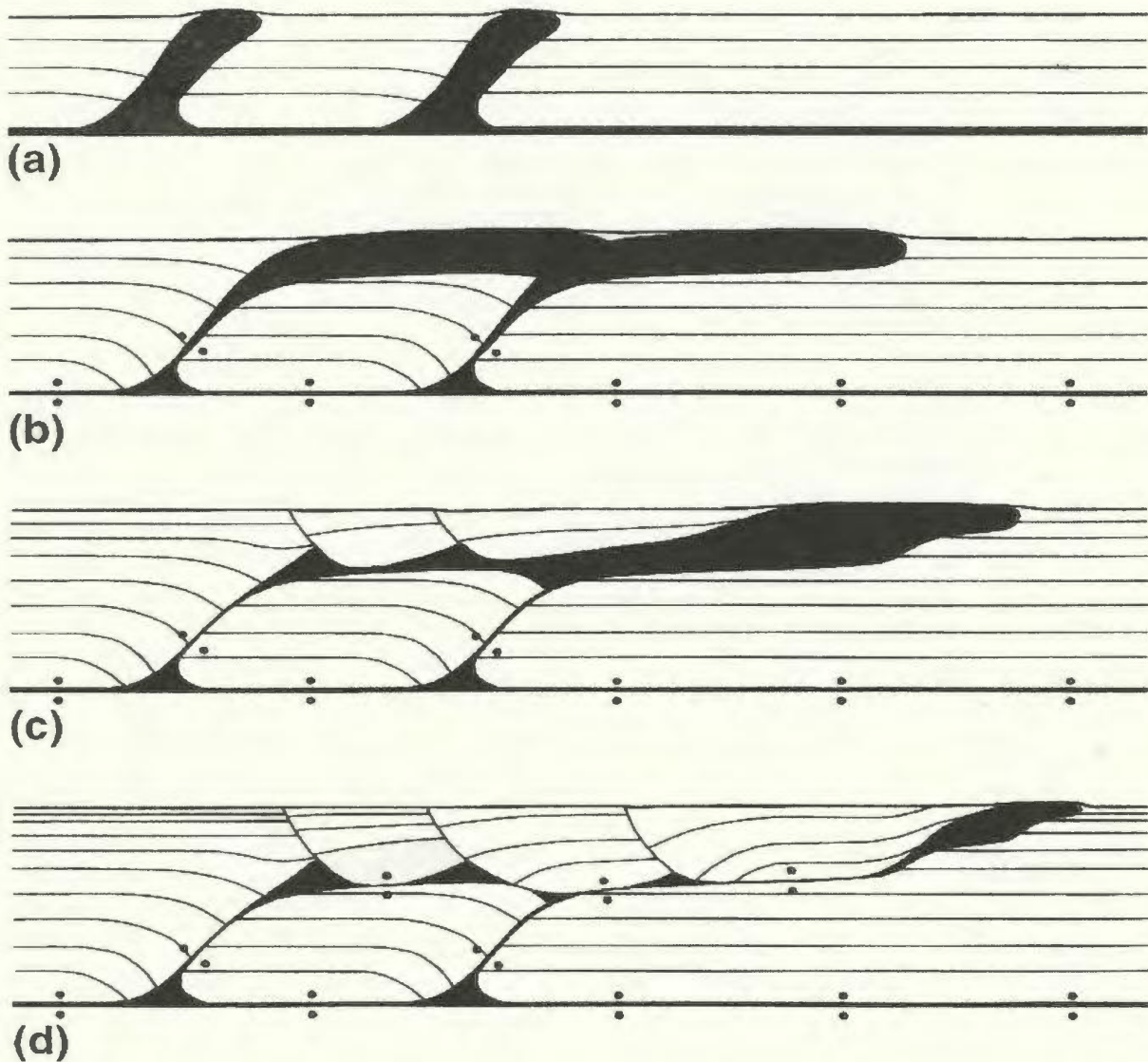


Figure 5-21: Schematic evolution of roho system (Rowan, 2002). a) passive growth of basinward leaning diapir, b) amalgamation of salt tongues to form sub-horizontal salt-tongue canopy, c) basinward evacuation of salt facilitated by the development of basinward-dipping listric faults that sole into the canopy, and d) extrusion of displaced salt to form secondary diapirs or shallower salt tongues.



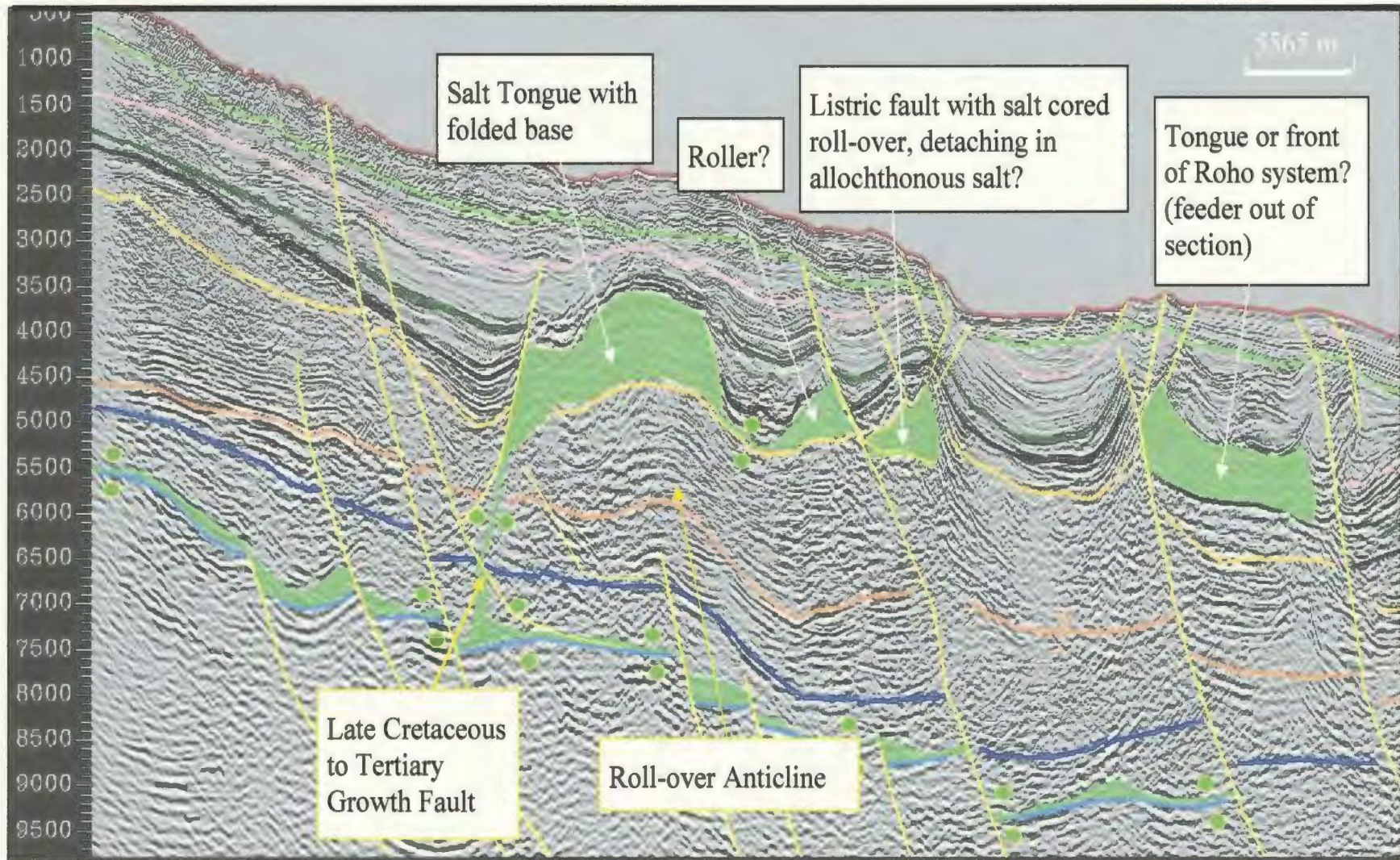
H  
NWH'  
SE

Figure 5-22: Northwest-southeast seismic profile H-H' with allochthonous salt tongue and potential roho system. Note the presence of a basinward dipping normal listric growth fault that detaches in allochthonous salt, and the presence of an allochthonous salt roller in the footwall of the fault. . See Figure 5-5 for location. They system is cut by a number of reactivated basement-involved faults. Vertical scale is TWT (ms). See Figure 5-5 for location.



listric fault, causing the development of the roll-over anticline. The timing of folding was thus Late Cretaceous to Eocene, coeval with the expulsion of salt to form the salt tongue.

The salt tongue pinches in a basinward direction to a horizontal weld at the K1 Sequence Boundary. The weld connects to two triangular shaped salt bodies that are separated by a normal, basinward dipping down-to-basement fault, and K1 to T1 mini-basins. Growth strata in the mini-basins have an asymmetric geometry with thickening in a landward direction, suggesting the presence of a listric growth fault that detaches in the allochthonous salt layer. If this interpretation is correct, the more landward of the two triangular salt bodies is an allochthonous salt roller, and the more basinward one is a salt core in a roll-over anticline. This structural architecture would classify the structure as a (partial) roho system. Basinward of the roho system is an allochthonous salt body approximately 8 kilometers in length and 700 ms TWT in height. No feeder to this body is imaged in the seismic data. The geometry of the structure is typical of a salt tongue, suggesting that there is likely a landward feeder lying out of the plane of section of the seismic line. Although this system has some of the criteria required to classify it as a roho system, it is missing contractional toe structures along the basinward edge which are commonly associated with roho systems. Also absent are strike-slip structures along the margins. However, the lack of recognition of such structures might be due to the coarse grid spacing, and the ambiguity associated with identifying strike-slip faults on seismic data.

## 5.4 Kinematic Analysis of Salt Structures

### 5.4.1 Introduction

Sedimentary successions proximal to salt bodies often contain halokinetic sequences that record the interaction between salt movement and sedimentation. The sequences consist of relatively conformable successions of growth strata genetically influenced by near-surface or extrusive salt movement and are locally bounded at the top and base by angular unconformities that become disconformable to conformable with increasing distance from the causative salt structure (Giles et. al., 2003).

Halokinetic sequences differ from traditional depositional sequences in scale and mechanism of formation. Unlike depositional sequences that may be traceable across an entire sedimentary basin, halokinetic sequences are discordant only within a few kilometers of a diapir. Halokinetic sequences form due to temporal variations in bathymetric relief over the diapir, whereas depositional sequences form as accommodation rate varies relative to regional sediment accumulation rate.

Angular unconformities bounding the halokinetic sequences form when the net rate of diapiric rise exceeds the rate of local sediment accumulation, allowing diapiric inflation at the surface to generate steep, unstable slopes upon which subjacent growth strata are truncated by either slope failure or erosion (Giles et. al., 2003). Increasing the local sediment accumulation rate relative to net diapiric rise rate results in onlap and overstep of strata onto the diapir. These burial processes suppress diapiric surface topography and erosion. Halokinetic sequence boundaries correspond to periods either of major increase in net salt rise rate or decrease in local net sediment accumulation rate



regardless of depositional setting and potentially independent of regional base-level changes (Giles et al., 2004).

Halokinetic sequences display differences in stratal and structural architecture that reflect the rate in salt-body rise relative to adjacent sediment-accumulation rate (Giles, 2003). These differences can be used as kinematic indicators from which the timing of salt movement can be inferred. Kinematic indicators are any structural or sedimentary architecture that demonstrates there has been movement of one feature relative to another. They not only record the current configuration of salt, faults and sediment but also often provide a record of the intermediate steps that occurred during the evolution of the salt structure. Based on stratal and structural architecture, halokinetic sequences can be categorized into three temporal divisions; pre-halokinematic, syn-halokinematic and post-halokinematic. These divisions relate to the timing of sedimentation relative to the timing of salt movement.

Pre-halokinematic sediments are those sediments that existed before salt movement or deformation. These sediments are generally of constant thickness, and are situated directly above the evaporite unit and below syn-kinematic sediments. In cases where salt movement commenced very shortly after evaporite deposition, the thickness of a pre-halokinematic sedimentary package may be very thin and below the limit of seismic resolution.

Syn-kinematic sediments are those that were deposited coeval with salt movement. Jackson and Talbot (1991) define a syn-kinematic layer as “strata interval, typically overlying the pre-kinematic layer, showing local stratigraphic thickening (above

structures such as withdrawal basins that subside faster than their surroundings) or thinning (above relatively rising structures). Changes in thickness can also be recorded by onlap or truncation at all levels of the syn-kinematic layer. The syn-kinematic layer records sedimentation during salt flow or during any other type of deformation". Post-kinematic strata is described by Jackson and Talbot (1991) as "strata interval overlying the syn-kinematic layer and recording sedimentation after salt flow or any other deformation has ceased. Basal post-kinematic strata can onlap or truncate an underlying, uneven deformation surface but show no thickness changes ascribed to local deformation".

The definition of syn-kinematic strata by Jackson and Talbot (1991) fails to consider those sedimentary packages that were deposited coeval to salt movement during times when sedimentation was equal to, or out paced diapir growth and there was no major evacuation of directly underlying autochthonous salt resulting in the creation of accommodation space and deposition of growth strata. In this case the sequence, though syn-kinematic, would show no thickening or thinning, and thus would not meet the criteria of syn-kinematic strata as defined by Jackson and Talbot (1991). Such a sequence would be considered "post-kinematic" by Jackson and Talbot (1991). By this definition syn-kinematic and post-kinematic units may repeat or occur "out of sequence" within the temporal stratigraphic succession in areas of multi-stage or variable rate salt movement. However, experiments by Vendeville and Jackson (1992) proved that salt cannot punch its way through brittle overburden without influence from an external process (i.e., tectonism). Since we know that diapirs grow passively on the sea floor, and that passive

growth will continue until the source salt layer is depleted at which time the diapir will cease to grow and get buried by further sedimentation, the definition of syn-kinematic growth as defined by Jackson and Talbot (1991) must be revised.

Here, syn-kinematic strata will be defined as any sedimentary package that is intersected by a salt structure. Syn-kinematic strata can therefore be divided into two classes; syn-kinematic growth strata defined by thinning and thickening of section, and syn-kinematic passive strata which shows no thickness variation, but are intersected by a salt structure. Post-kinematic successions will here be defined as the stratigraphic succession that overlies the highest point of a salt body and is not intersected by the salt body. Post-kinematic strata can be grouped into two classes on the basis of deformation that post-dates diapir growth; 1) those that have not been deformed; and 2) those that have been folded by compressional forces that postdate diapir formation, a process known as rejuvenation (see Section 5.3.5)

#### 5.4.2 Salt Movement and Sedimentation

Halokinematic analysis was conducted in order to date the various phases of salt movement and deduce the nature of the interaction between salt and sedimentation during the evolution of the basin. Basin fill was divided into pre-kinematic, syn-kinematic and post-kinematic successions on the basis of stratal and structural architecture of sediments in relation to salt structures. This analysis was conducted throughout the seismic grid, but only a limited number of seismic lines with kinematic analysis are presented in this



section (Figures 5-23 to 5-25). Throughout the seismic grid there is a commonality in the phases and style of salt movement through time with fine scale variations.

#### *Pre-kinematic*

Within the study area pre-kinematic successions lie directly above allochthonous salt (Figures 5-23 to 5-25). The successions are characterized by their consistent thickness, and fragmented nature due to subsequent faulting and salt movement. Here, pre-kinematic successions are generally very thin (less than 200 ms TWT). Occasionally, there is no pre-kinematic succession imaged. The relative thinness or absence of pre-kinematic successions indicates that within the study area salt movement commenced very shortly after its deposition by accumulation.

#### *Syn-kinematic*

Within the study area, syn-kinematic successions directly overlie pre-kinematic successions where pre-kinematic successions are imaged on seismic data. Where pre-kinematic successions are not imaged on seismic data, either due to their absence in the stratigraphic column or due their vertical thinness being below the limits of seismic resolution, syn-kinematic successions overly autochthonous salt (Figures 5-23 to 5-25). Syn-kinematic successions are characterized by their spatial relationship with salt structures, whereby reflectors contained in syn-kinematic successions onlap onto salt structures.

Salt structures with onlapping syn-kinematic reflectors have been consistently mapped within DS3 (Middle to Late Jurassic) and DS4 (Early to Middle Cretaceous). Locally the top of salt structures and adjacent onlapping syn-kinematic reflectors may be located anywhere between an intra-DS3 horizon and an intra-DS8 horizon. Most commonly however, the top of the syn-kinematic succession is the T0 Sequence Boundary. This indicates that most of the Mesozoic basin fill within the study area is syn-kinematic with salt movement.

Within the map area, some individual syn-kinematic halokinetic sequences thicken away from the salt structure and thin towards it. Thickening is commonly subtle. The location of the thickest portion of a halokinetic sequence represents the location of the local depocenter at the time of deposition (Figure 5-23). Syn-kinematic peripheral sink salt minibasins are commonly composed of numerous stacked halokinetic sequences. The thickest portion of each individual sequence represents the location greatest accommodation space at the time of deposition. Paleo-depocenters are commonly offset laterally due to a shift in the location of maximum accommodation through time. This offset is evidence that the evacuation of autochthonous salt and subsequent primary welding evolved in definitive phases due to differential loading of the salt layer by local syn-kinematic depocenters.

Turtle structures are syn-kinematic growth strata packages mounded between salt diapirs and having a flat base and rounded crest over a sedimentary thick. A turtle structure forms once a weld forms beneath the center of a subsiding minibasin when the flanks of the minibasins which are still underlain by salt collapse. A new flanking

depocenter forms thus inverting the original depocenter into a turtle structure. A turtle structure is an indicator of at least two generations of salt movement. The age of the turtle structure is defined as the age of the touchdown of the initial basin and the start of the flank collapse. Turtle structures have been commonly mapped within the middle slope region of the map area (Figures 5-24 and 5-25). They have been only identified on seismic strike lines, indicating that the structures are not four way closures. Turtle structures range in strike length from 10 to 15 kilometers, and in height from 800 to 1500 ms TWT. The age of turtle structures within the map area ranges from synchronous with the J2 Sequence Boundary (Late Jurassic) to intra-DS4 (Early Cretaceous).

Syn-kinematic successions with uniform thickness have commonly been mapped within the study area. These successions represent times of passive diapir growth where the rate of salt movement was approximately equal to the rate of sedimentation, with no major evacuation of salt from the underlying autochthonous source layer. The occurrence of syn-kinematic successions with uniform thickness generally increases with height in the stratigraphic column (Figures 5-24 and 5-25), however these successions may occur anywhere within the syn-kinematic succession (Figure 5-23). In general, syn-kinematic successions with thickening dominate below the J2 Sequence Boundary, whereas above the J2 Sequence Boundary syn-kinematic successions with uniform thickness dominate.

### Post-Kinematic

Post-kinematic successions directly overlie syn-kinematic successions. Post – kinematic successions overlie, but do not onlap onto salt structures. Within the study area



the base of post-kinematic stratigraphy may vary in age from intra-DS3 to intra-DS8, but is most commonly synchronous with the T0 Sequence Boundary.

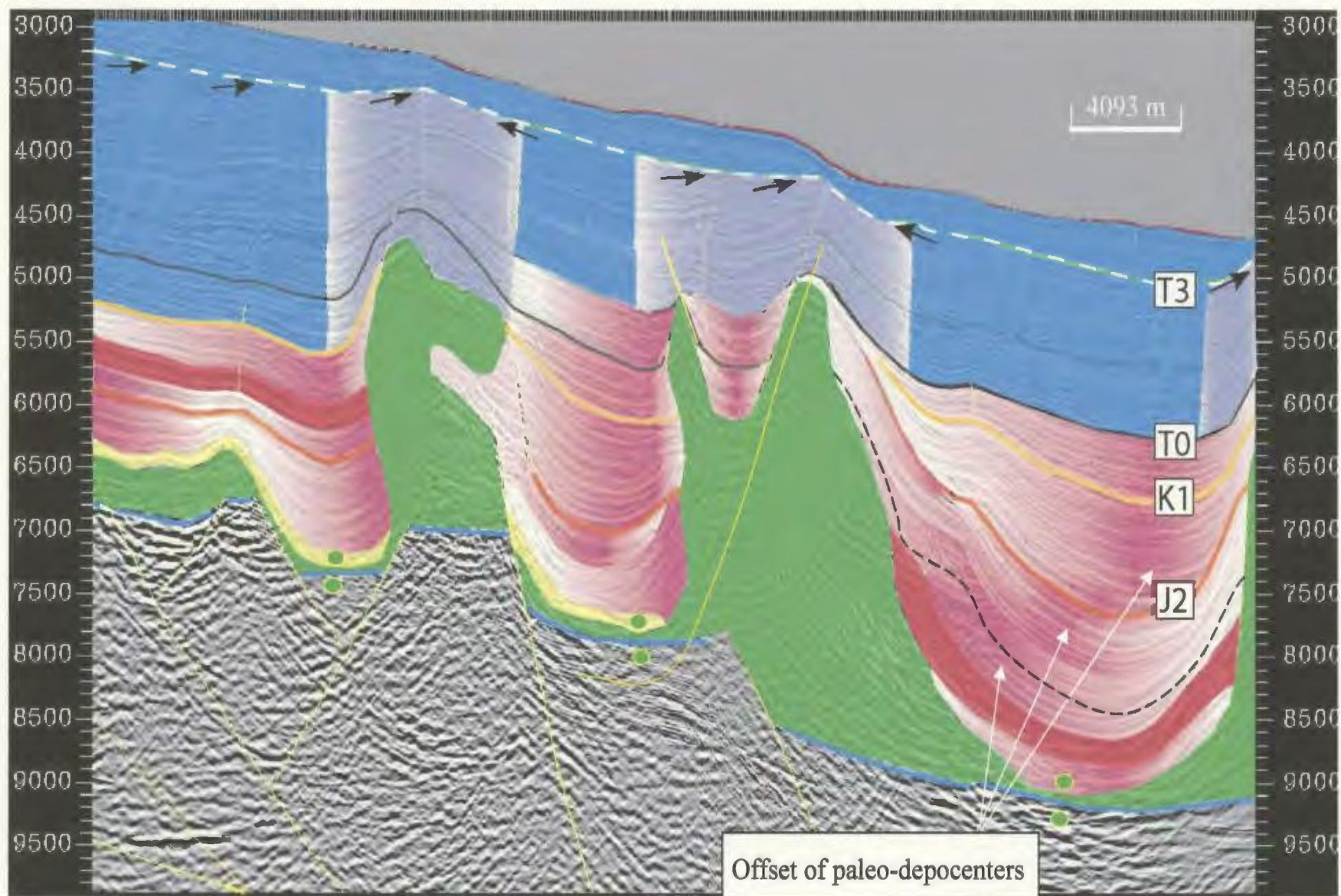
Post-kinematic reflectors are commonly concordant with the top of the syn-kinematic succession. However, locally in areas where the top of the syn-kinematic succession has relief (either erosional or structural) post-kinematic reflectors commonly onlap on to it.

A special kind of post-kinematic succession, the rejuvenated succession, is very common within the study area. In areas of rejuvenation post-kinematic reflectors are folded over salt structures as a result of post-(halo)kinematic shortening due to gravity gliding and spreading (see Section 5.3.5). An angular unconformity generally marks the top of the post-kinematic rejuvenation package. In seismic lines with diapirs of different ages, each diapir has an associated rejuvenation package. Four halokinetic sequence boundaries marking the end of major episodes of diapir rejuvenation have been mapped: 1) Intra-DS4 (Early Cretaceous), 2) T1 Sequence Boundary (top Eocene), T3 (top Pliocene) and 4) the water bottom. The T3 halokinetic Sequence boundary has the most erosional relief, and thus marks the top of the most significant stage of diapir rejuvenation.

Figure 5-23: Northwest-southeast seismic profile from the western study area with temporal kinematic stages associated with diapir evolution highlighted. Black arrows indicate direction of successive reflector truncation, white dashed line represents angular unconformity (Sequence Boundary T3) marking the top of a halokenitic sequence of diapir rejuvenation. Bathymetric relief of the water bottom over each diapir indicates that the region is currently experiencing diapir rejuvenation and causative shortening. Vertical scale is TWT (ms).

NW

SE



Salt  
 Pre-kinematic

Syn-kinematic (no growth)  
 Syn-kinematic with growth  
 (pink = thickening, white = thinning)

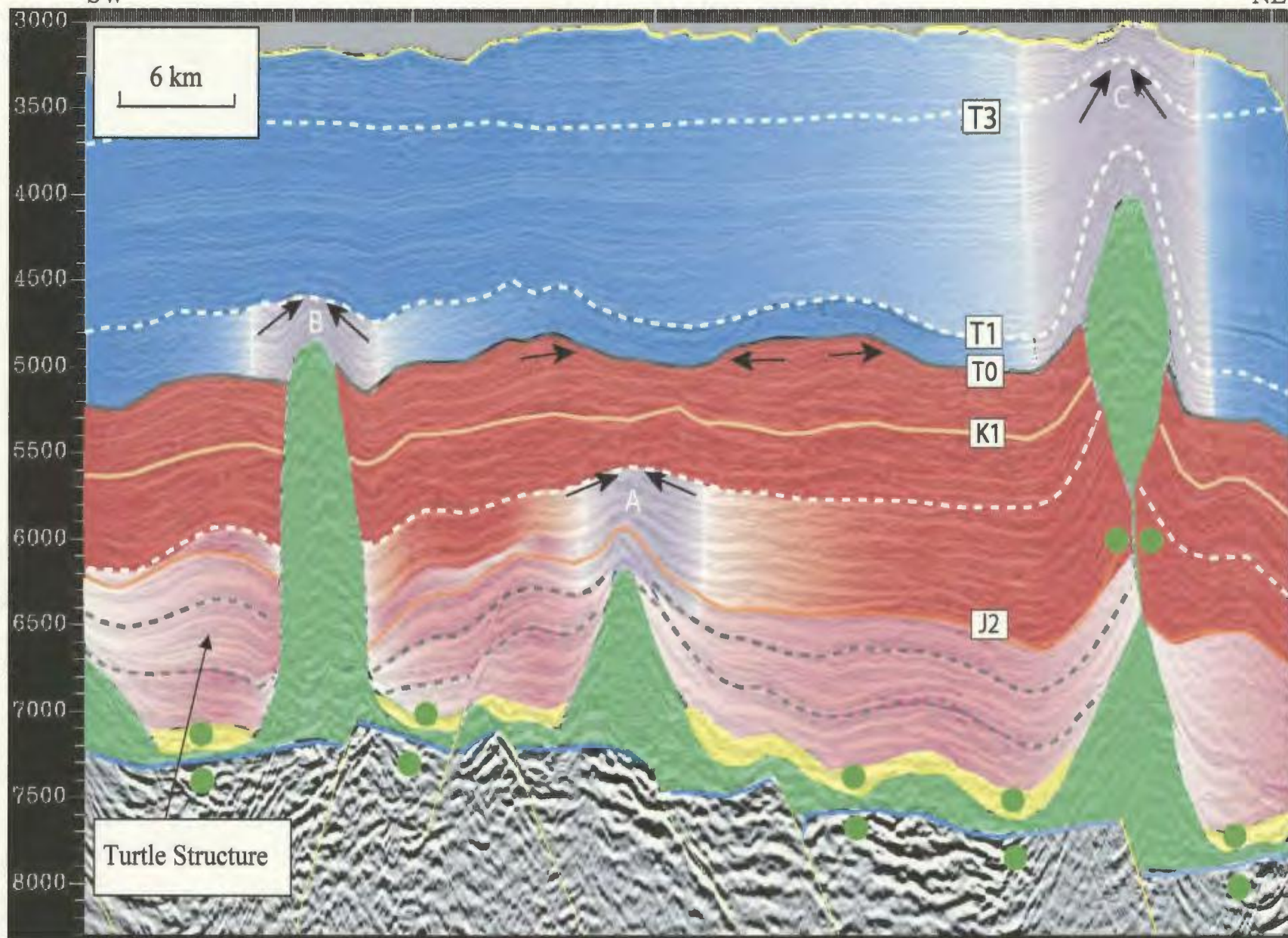
Post-kinematic (rejuvenated)  
 Post-kinematic (not rejuvenated)



Figure 5-24: Southwest–northeast seismic strike section through the central slope region with temporal kinematic stages associated with diapir evolution highlighted. Black arrows represent direction of truncated of reflectors, white dashed lines angular unconformity and co-relative conformities marking the top of halokenitic sequences associated with diapir rejuvenation: A) intra-DS4, B) Sequence Boundary T1 and C) Sequence boundary T3. Bathymetric relief of the water bottom over each diapir indicates that the region is currently experiencing diapir rejuvenation and causative shortening. Black arrows underlying T0 represent truncation due to canyon development, not salt related. Vertical scale is TWT (ms).

SW

NE



Salt

Pre-kinematic

Syn-kinematic (no growth)

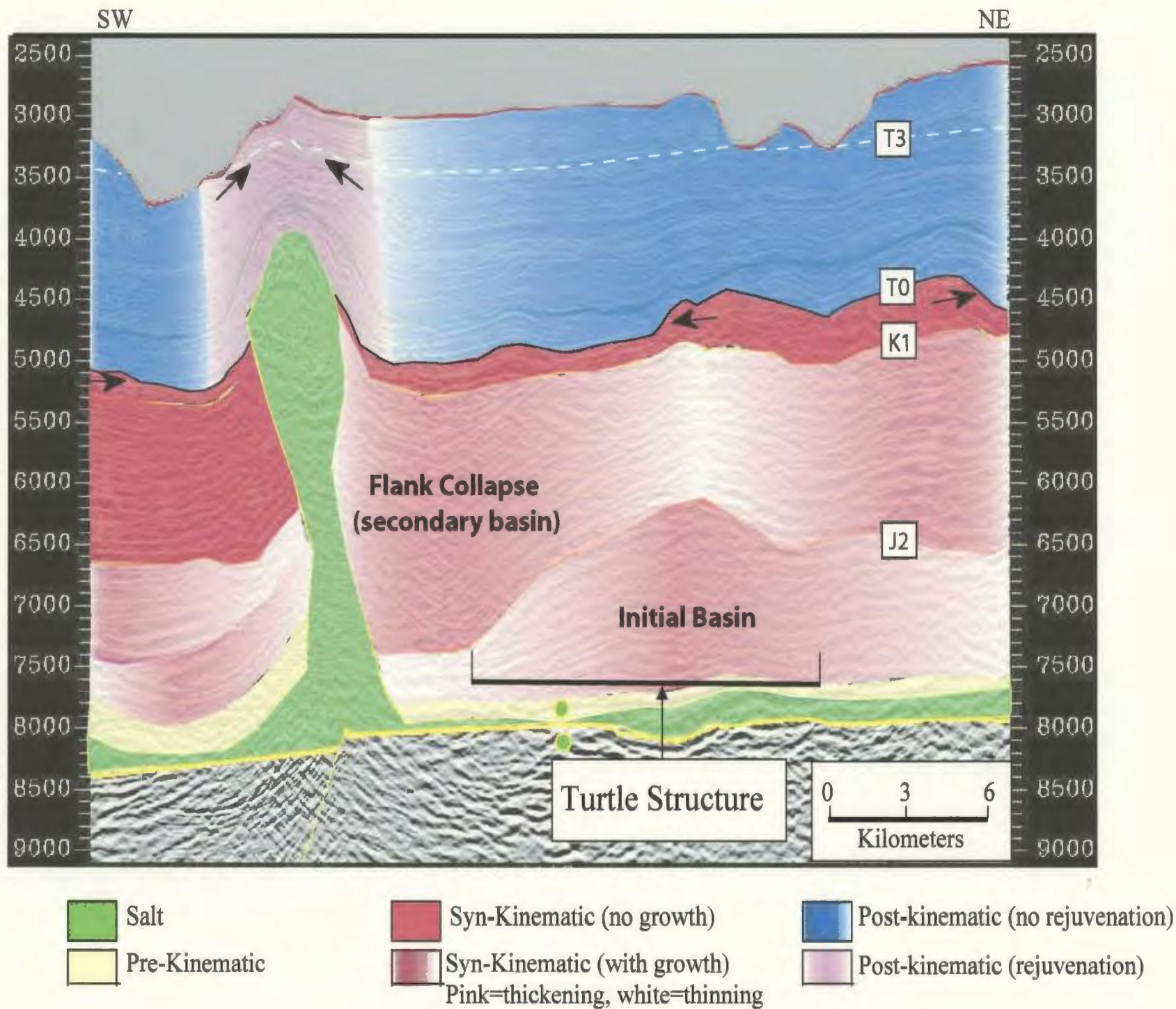
Syn-kinematic growth  
(pink = thickening, white = thinning)

Post kinematic (not rejuvenated)

Post kinematic (rejuvenated)

Figure 5-25: Southwest–northeast seismic strike line from the eastern central slope with temporal kinematic stages associated with diapir evolution highlighted. Note example of turtle structure. Black arrows indicate direction of successive truncation of reflectors. White dashed line represents angular unconformity and co-relative conformity (Sequence Boundary T3) associated with diapir rejuvenation. Vertical scale is TWT (ms).





## Chapter 6

### Evolution of the Scotian Slope Basin: Discussion

#### 6.1 Evolution of the Scotian Slope Basin

The Scotian Slope Basin records a complex tectono-stratigraphic history. This is indicated by the variable and complex nature of the sedimentology, stratigraphy and structural geology of the basin fill in both time and space. The present study, based on 2D seismic interpretation and well correlation, documents the evolution of the central Scotian Slope and reveals the primary influences on Mesozoic and Cenozoic stratigraphic, tectonic and halotectonic structure. Basin stratigraphy can be divided into six tectono-stratigraphic mega-sequences on the basis of seismic characters, differing styles of sedimentation, regional tectonism and halotectonism. In ascending order the ages of these mega-sequences are: Pre-Mesozoic, Late Triassic to Early Jurassic, Middle Jurassic to Late Jurassic, Cretaceous, Tertiary, and Quaternary (Figures 6-1 and 6-2).

##### 6.1.1 Pre-Mesozoic

The Pre-Mesozoic Mega-sequence is bounded at its top by the Tr2 Sequence Boundary. The base of the mega-sequence is not definable in the seismic data. The mega-sequence includes pre-Mesozoic basement rocks of the Meguma Group and prerift sedimentary rocks of Depositional Sequence 1. None of the wells on the seismic grid used in this study penetrated pre-Mesozoic basement. Basement composition is extrapolated from two wells northwest of the map area that bottomed in Cambro-

Figure 6-1: Seismic profile from the western map area with the 6 tectono-stratigraphic mega sequences outlined by white dashed lines. In ascending order the ages of these mega sequences are: A) Pre-Mesozoic, B) Late Triassic to Early Jurassic, C) Middle Jurassic to Late Jurassic, D) Cretaceous, E) Tertiary and F) Quaternary. The profile has been kinematically analyzed and highlighted accordingly. Vertical scale is TWT (ms).



NW

SE

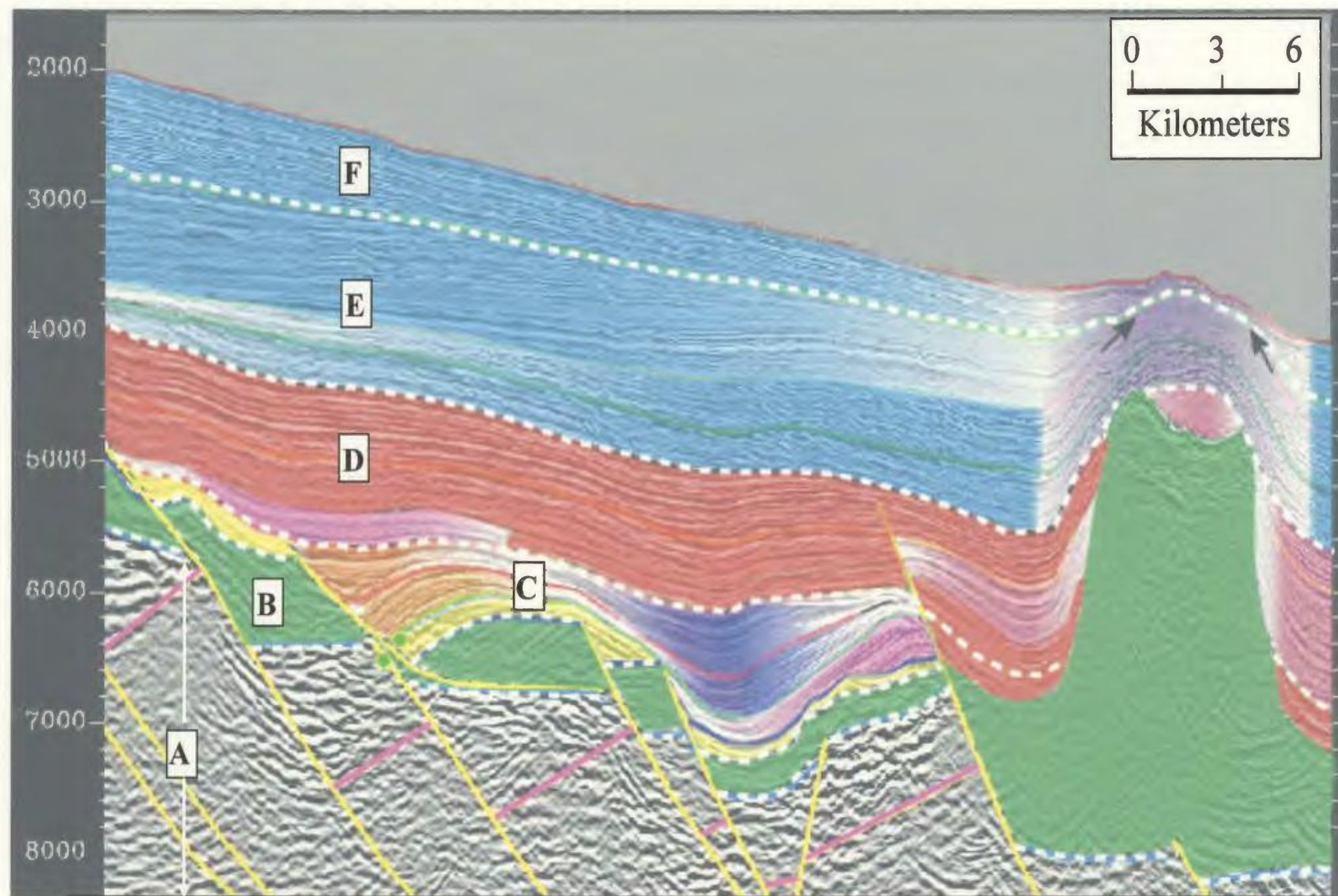
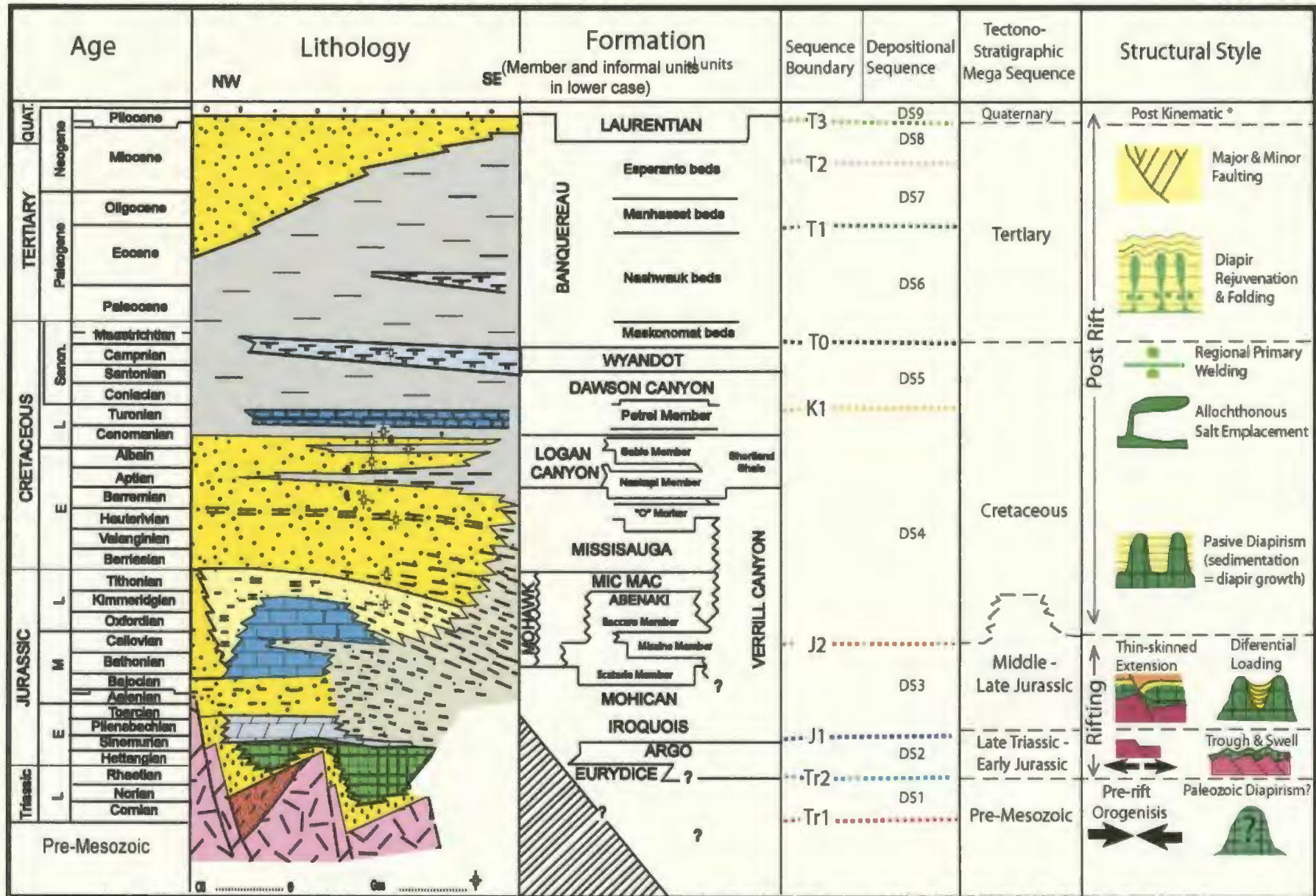


Figure 6-2: Tectono-stratigraphic compilation chart of the Scotian Basin summarizing lithology, lithostratigraphy, sequence boundaries and depositional sequences, tectono-stratigraphic mega-sequences, and associated structural styles. Lithology and formation data from Welsink et al. (1989). Asterisk in Structural Style column indicates minor diapir rejuvenation and minor gravity faulting







Ordovician metasedimentary rocks of the Meguma Group and coarse grained granite (see Section 3.3.1). Within the study area, the top of basement stratigraphy represented by a weak event imaged deep in the seismic data. The marker does not yield strong reflections, but is characterized by a change in seismic character, indicating a small impedance contrast at the top of basement (A in Figure 6-1). Due to the low impedance contrast and the stratified nature of the metasedimentary Meguma Group, the exact top of basement is often difficult to define and may locally represent an intra-basement or pre-rift pick.

Packages of reflectors directly overlying and concordant with the top basement marker are interpreted as Paleozoic pre-rift deposits of Depositional Sequence 1 (DS1). Due to the low map confidence in the top basement pick, these reflectors may also locally represent the upper portions of the Meguma Group. Sporadically within rotated basement fault blocks there are anomalous geometries associated with DS1 reflectors (see Section 4.2.2). The reflectors are uplifted relative to adjacent sections and have a domed rather than rotated reflection pattern that would be typical of rotational faulting. The geometry suggests the local presence of a Paleozoic salt body contained within DS1. Although Paleozoic salt has not been recognized within the Scotian Basin, there are numerous Paleozoic basins along the eastern Canadian continental margin where such salt has been documented (i.e. the Georges Banks region, Cape Breton Island, and the Magdalen Basin). This potential Paleozoic salt, however, has not exerted a fundamental control on Mesozoic basin sedimentation patterns, or structural architecture within the study area.

### 6.1.2 Late Triassic to Early Jurassic

The Late Triassic to Early Jurassic mega-sequence is bounded at its base by the Tr2 Sequence Boundary and at its top by the J1 Sequence Boundary. The mega-sequence is characterized by stratigraphy and structure associated with the intra-continental onset of rifting of the Pangean Supercontinent and initial stages in the formation of the North Atlantic Ocean. Within the Scotian Basin, rifting resulted in the formation of a number of northeast-southwest trending basement involved normal faults and northwest-southeast trending transfer faults which define the boundaries of a set of sub-basins. Within the study area all seismically imaged basement faults are normal extensional in nature. The presence of a sinistral transfer fault in the central part of the map area is implied by a change in the orientation of sedimentary faults and the offset of the landward limit of diapiric salt structures across the central map area (Figure 6-3; Section 4.2.6). The seismic signature of this potential transfer fault is not sufficiently clear on the data grid to allow detailed mapping and description.

Extension associated with initial rifting was accommodated by the development of a fault array that evolved into a dominant listric basement-involved (thick-skinned) fault fan system. This Slope Basin-Bounding Fault Family accounted for the bulk of crustal extension and proved a major influence on subsequent structural development of the margin (see Section 4.2.1). The bounding faults dip southeast and appear to sole into a deep-seated fault imaged in the footwall of the most inboard faults of the Basin-Bounding slope fan (Figure 6-3). Due to limited seismic coverage, the upper portion of the footwall fault is not imaged in the TGS N-OPEC seismic data set, but can be traced

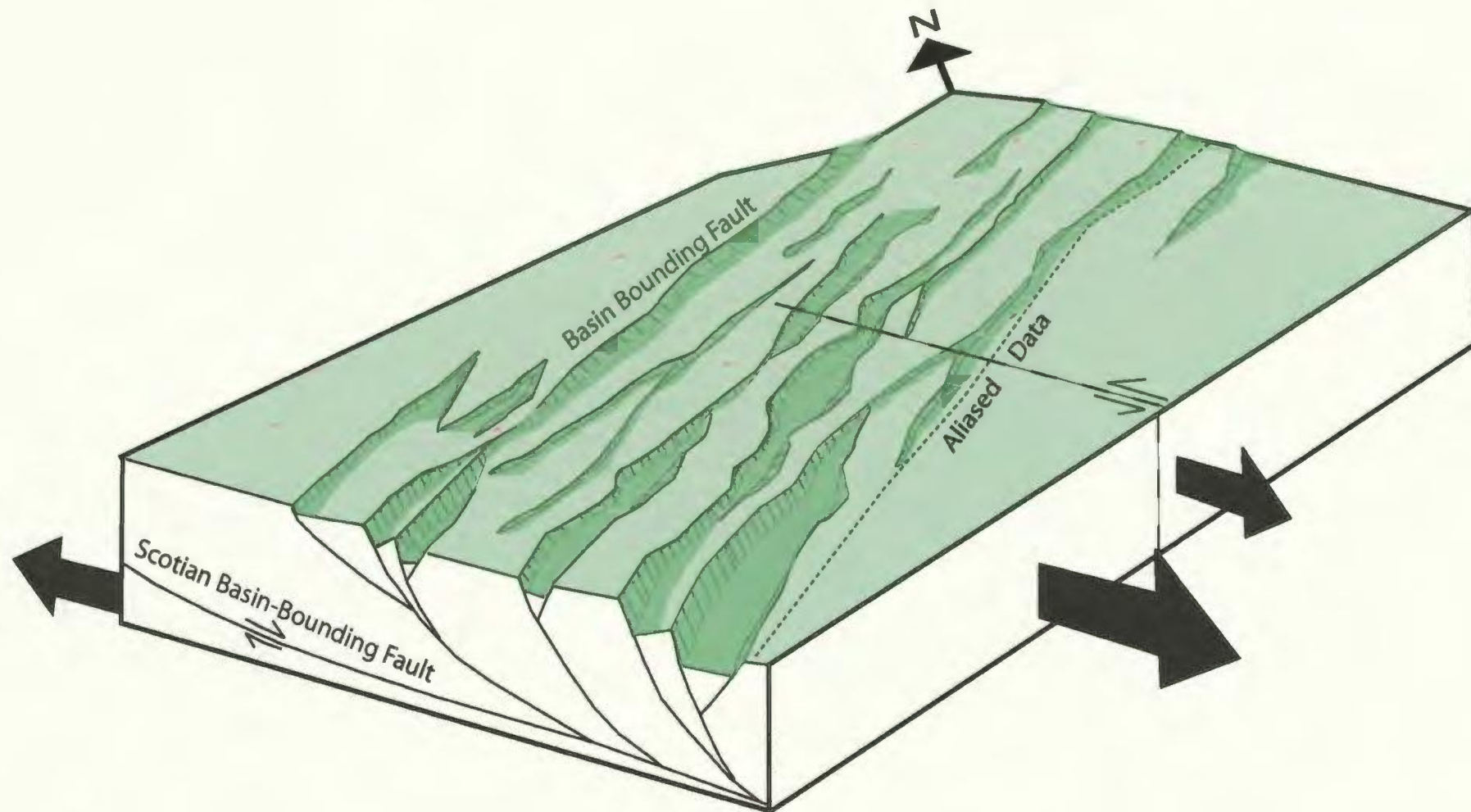


Figure 6-3: Schematic block diagram of the structure of the study area during the Early Jurassic. Dashed line represents the location of a potential sinistral transfer fault. Black arrows represent direction of extension, size of arrows represent the discrepancy in the relative amount of movement that would have caused the development of a transfer fault. Light green represents evaporite deposition. Dark green represents areas that would have been structural lows during evaporite deposition, and thus areas where original evaporite thickness may have been greater than regional. Seismic grid in white, exploration wells in pink.



onto the shelf in the Lithoprobe 88-1 deep seismic line. The fault links with the regional seaward-dipping Scotian Basin bounding fault system described on the Scotian Shelf by Welsink et al. (1989).

Faults of the Basement-Involved Fault Family are located in the hanging wall of and sole into the Basin-Bounding Fault Family (4.2.2). They form a listric fan of synthetic and antithetic faults that accommodated regional extension during rifting. The faults of this family delineate the major structural units in the map area by sub-dividing the hanging wall side of the Basin-Bounding Fault Family into: a) asymmetric half-grabens filled with syn-rift sediments, b) symmetric grabens filled with syn-rift sediments, and c) horsts with onlapping syn-rift sediments. Syn-rift sedimentation patterns and structural styles were greatly influenced by the rift architecture of the Basin-Bounding and Basement-Involved fault families.

Synrift sedimentation was characterized by red bed deposits of the Eurydice Formation and evaporites of the Argo Formation. The two formations, here grouped into Depositional Sequence 2 (DS2), are commonly interfingered and locally indistinguishable on seismic data (B in Figure 6-1). Due to its present depth and extensive flowage through time, neither the original depositional thickness nor initial distribution of the salt is known. The syn-rift nature of evaporite deposition suggests that its original thickness was not evenly distributed through the basin, but rather concentrated in elongated lows formed by basement-involved faults (Figure 6-2). All salt contained within DS2 has been deformed (i.e. a horizontal top salt was rarely observed). The most common salt structures of this age are troughs and swells. There is a strong association

between the location of salt swells and basement-involved faults with most swells located directly over basement faults. This indicates that the distribution of early salt structures was controlled by basement structure (Figure 6-4). Where present, pre-halokinematic stratigraphy is very thin (less than 200 ms TWT), indicating that salt movement commenced shortly after deposition of the evaporites.

### 6.1.3 Middle to Late Jurassic

The Middle to Late Jurassic tectono-stratigraphic mega-sequence is bounded by the J1 Sequence Boundary (breakup unconformity) at its base and either the J2 Sequence Boundary or Top Abenaki Marker at its top (C in Figure 6-1; Figure 6-2). The sequence is composed of shallow marine dolostones of the Iroquois Formation, tidally influenced siliclastics of the Mohican Formation and deepwater marls and muds of the Verrill Canyon Formation which are collectively grouped into Depositional Sequence 3, and shelf carbonates of the Abenaki Formation. The mega-sequence directly overlies red bed and autochthonous evaporite deposits of Depositional Sequence 2.

The Abenaki Formation has limited areal extent within the study area. It is present on the shelf and extends only locally onto the upper slope in the western map area near the Acadia K-62 well. The Slope Basin-Bounding Fault Family fan is the primary control on the local distribution of the Jurassic carbonate bank. The most predominant faults within the fan mark the seaward limit of the bank and generally tip at the top Abenaki Formation seismic marker.

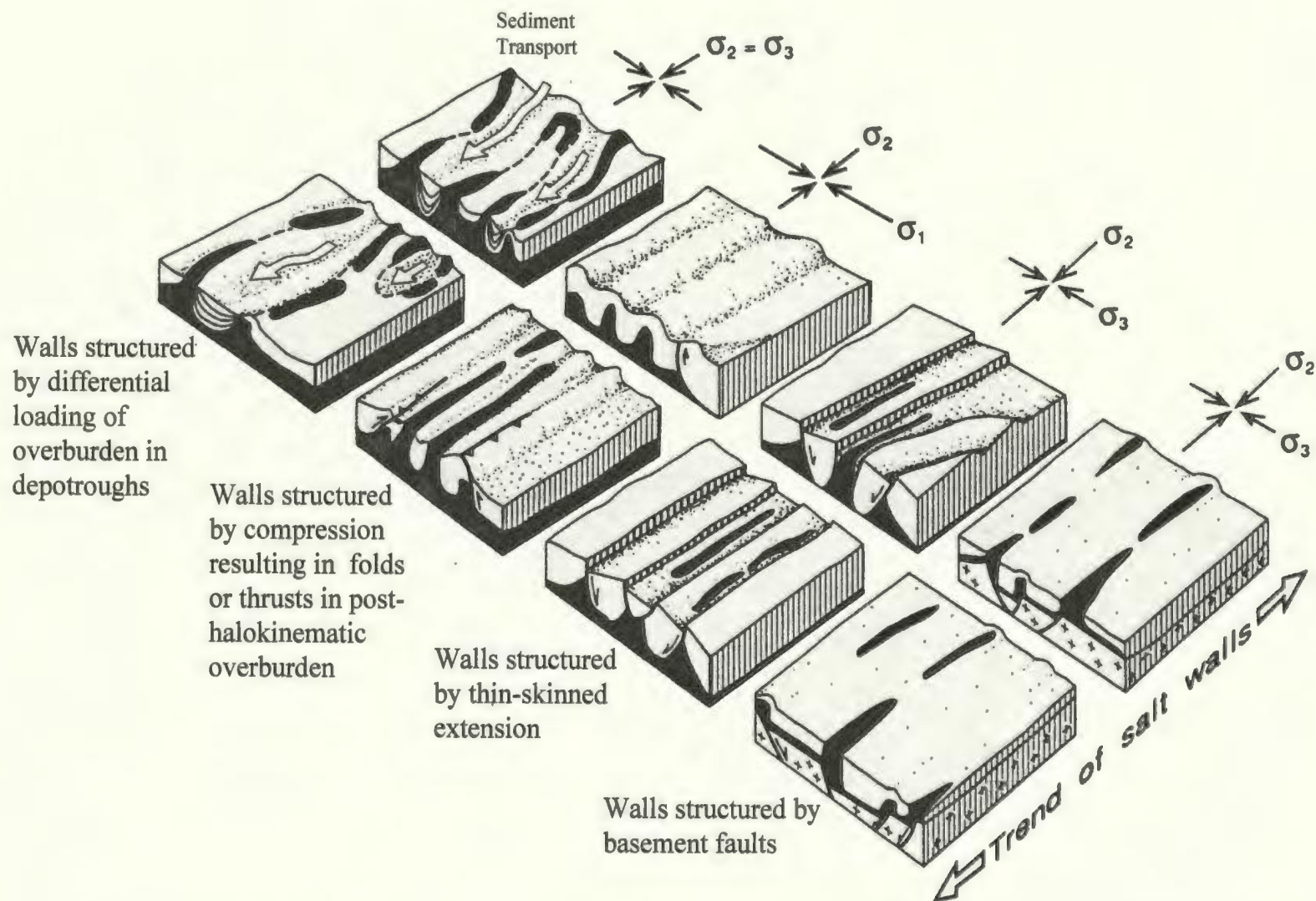


Figure 6-4: Structuring of salt walls by four types of stress regimes.  $\sigma_1$ ,  $\sigma_2$ , and  $\sigma_3$  are the maximum, intermediate and minimum principal stresses. Modified from Jackson and Talbot, 1991.



On the slope, the Late to Middle Jurassic mega-sequence is composed of Depositional Sequence 3 (DS3). It has an overall thickening trend toward the southeast that is commonly disrupted by small, localized thickness variations. Locally thickened packages extend 2 to 20 kilometers in diameter and may be up to 1800 ms thick (TWT). Thickness variations are related to complex interactions between the Basement-Involved Fault Family (thick-skinned), the Listric Growth Fault Family (thin-skinned) and salt tectonics during the Middle to Late Jurassic (Figure 6-1).

Basement-Involved faults generally tip at the J1 Sequence Boundary indicating crustal extension was ongoing until the end of the Early Jurassic. However, local Middle to Late Jurassic mega sequence growth architectures within large basement grabens indicate that crustal readjustment and tectonic subsidence continued until the Late Jurassic (Figure 6-1). Tectonic and thermal subsidence resulted in the development of a regional tilt during the Middle to Late Jurassic. The developing gravity gradient resulted in thin-skinned extension. Listric growth faults commonly formed in the upper and middle slope regions above the hanging wall of basement faults, and soled into the evaporite unit. Rotation and continued extension of listric faults was driven by synchronous crustal readjustment and deposition of growth strata in the hanging wall of the listric fault. The unequal distribution of sediment load in basement grabens and in hanging walls of listric faults resulted in salt evacuation from these areas due to differential loading, and thus the further creation of accommodation space through salt movement. Thinning of the sedimentary overburden through listric faulting resulted in reactive and active diapirism. Thus, Middle to Late Jurassic halotectonics was

simultaneously influenced by three differing stress regimes related to basement structure, thin-skinned extension, and differential loading of the overburden (Figure 6-4).

#### 6.1.4 Cretaceous

The Cretaceous tectono-stratigraphic mega-sequence is bounded at its base by either the J2 Sequence Boundary or the Top Abenaki Formation Marker, and at its top by the T0 Sequence Boundary (d in Figure 6-1; Figure 6-2). The sequence is composed of clastic deposits of the Logan Canyon, Mic Mac, Mississauga and Verrill Canyon formations of Depositional Sequence 4, and shale and chalk deposits of the Dawson Canyon and Wyandot formations of Depositional Sequence 5.

The base of the Cretaceous mega-sequence marks a major change in the character of sedimentation patterns within the map area. Within the study area the thickness distribution of the Cretaceous mega sequence is fairly predictable. There is an overall gradual thickening of the sequence towards the northeast in proximity to the paleo-Sable Delta. In dip oriented seismic sections there is very little change in the thickness of this mega sequence, thus indicating that sedimentation during the Cretaceous was strongly influenced by the Sable delta.

There is no significant fault related growth strata contained within the Cretaceous mega sequence. This suggests that crustal readjustment terminated by the Early Cretaceous, making the Cretaceous the first true post-kinematic tectono-stratigraphic mega sequence.

Listric growth faults typically tip at the base of the Cretaceous mega-sequence. Only once within the map area was a listric fault observed propagating through Cretaceous stratigraphy. The lack of growth strata associated with listric faulting within the Cretaceous also marks a major change in the style and distribution of Cretaceous sedimentation relative to that of the Middle to Late Jurassic.

Salt diapirism was primarily passive during the Cretaceous. The "finger-like" shape of most Cretaceous diapirs suggests that the relative rate of sedimentation was approximately equal to diapir growth. However, the presence of a few cone shaped diapirs suggests that locally, the rate of relative sedimentation exceeded diapir growth.

The local presence of salt withdrawal growth strata adjacent to diapiric structures in the lower portions of the Cretaceous mega sequence suggests that evacuation of salt by differential loading fueled diapir growth during the early Cretaceous (Figure 6-4). In the middle to upper portions of the mega sequence there is little growth related to salt movement, indicating that salt evacuation generally kept pace with sedimentation during this time.

Most diapirs within the study area do not intersect the T0 Sequence Boundary, indicating that the autochthonous salt source feeding the diapirs was regionally depleted (primary welding) by the late Cretaceous. Secondary (vertical) welds commonly occur in the Cretaceous. Their presence is an unequivocal sign of gravity induced regional compression. Most secondary welds are located in the middle and lower slope region, suggesting that compression was driven by up-dip gravity gliding or spreading. The squeezing of diapirs resulted in an increased rate of salt flow relative to sedimentation,



and commonly the lateral expulsion of salt on to the sea floor commencing the development of allochthonous salt structures. The timing of expulsion is coincident with the base of allochthonous salt, which is most often situated within the upper portions of the Cretaceous mega sequence. There are a few mapped allochthonous salt structures whose base is located within Depositional Sequence 9 (Eocene). The expulsion of allochthonous salt during the Late Cretaceous to Early Tertiary indicates that there was a major increase in the relative ratio of salt flow to sedimentation at this time. This change was likely due to a combination of 1) diapir squeezing as a result of contraction and 2) a decrease in the rate of sedimentation due to the demise of the Sable Delta during the Late Cretaceous.

#### 6.1.5 Tertiary

The Tertiary tectono-stratigraphic mega sequence is bounded at the base by the T0 Sequence Boundary and at the top by the T3 Sequence Boundary (e in Figure 6-1). The entire Tertiary sedimentary succession is included in the Banquereau Formation (Figure 6-2). The base of the Tertiary mega-sequence is an undulating surface of erosion with significant relief and a slope dip parallel (north-west to south-east) orientated fabric. The large erosional troughs and flanking crests of the T0 Sequence Boundary have been interpreted as sub aqueous canyons and levees associated with the transport of sediments from the shelf to the lower slope. The canyons can be mapped over the upper and middle slope region, but not over the lower slope region where diapiric structures commonly intersect the T0 Sequence Boundary. It is likely that canyons fed into lobe complexes in

this diapiric region. However, it was not possible to map mounds that might be associated with lobe deposition. This may be due to the coarse grid spacing of seismic data.

Within the Tertiary mega-sequence there are two unconformity surfaces with significant erosional relief, here termed the T1 and T2 sequence boundaries respectively. Reflectors overlying the base of the mega sequence, the T0 Sequence Boundary, as well as those overlying the two intra-mega sequence unconformity surfaces successively onlap their respective unconformities in a landward direction. This reflection termination pattern indicates that relative sealevel was rising throughout the Tertiary.

Within the Tertiary mega sequence, large sub-aqueous canyons with significant erosional relief repeatedly carved deep into underlying strata. The canyons are situated at differing levels within Tertiary stratigraphy. The canyons can be confidently mapped on the shelf and upper slope. In the middle to lower slope regions the relief of most canyons has decreased significantly making basinward mapping difficult.

Seismic reflectors within the Tertiary mega-sequence are broken by major and minor sedimentary faults. These faults generally trend southwest-northeast parallel with both the Slope Basin-Bounding Fault trend, and the shelf break. Within the Tertiary, minor faults commonly occur in discrete fault packages that detach on distinct bedding parallel slip surfaces. Fault style and dip patterns change across slip surfaces, reflecting differences in mechanical behavior of lithology during the development of the fault systems. These faults appear to occur as a result of gravitational tension, and form in areas bounded by canyons which have deeply eroded the youngest successions.

Few salt structures intersect the T0 Sequence Boundary, indicating that the autochthonous salt source feeding most diapirs was significantly depleted by the Early Tertiary. Salt very seldom intersects the T1 Sequence Boundary, and never the T2 Sequence Boundary. Most salt structures contained within Tertiary stratigraphy are allochthonous in nature with only a few examples of diapirs. Within Tertiary stratigraphy salt is most common in the eastern portion of the lower map area where structural complexity is high.

Most Tertiary-aged salt structures within the map area have associated folded overburden. The folding is an unequivocal sign of contraction, and occurs in order to balance the up-dip extension associated with gravity gliding and spreading. The folds are usually polyharmonic because of the increasing overburden thickness with time. The presence of allochthonous roho and stepped counterregional systems is also indicative down dip lateral transfer of sediment load during the Tertiary.

#### 6.1.6 Quaternary

The Quaternary tectono-stratigraphic mega sequence is composed entirely of Depositional Sequence 9. It bounded at its base by Sequence Boundary T3, and at its top by the water bottom (F in Figure 6-1; Figure 6-2). Sequence Boundary T3 is a continuous angular unconformity surface that sequentially truncates underlying reflectors in a basinward direction, or toward the crest of anticlinal folds overlying salt structures. The T3 Sequence Boundary is generally undeformed except locally where it is gently folded over salt diapirs. Reflectors within this the Quaternary mega-sequence are



characteristically concordant with the T3 Sequence Boundary, except where they are truncated by Quaternary and bathymetric canyons. The Quaternary tectono-stratigraphic mega sequence is predominantly post kinematic to both tectonics and salt tectonics with minor exceptions.

Gentle folding of the Quaternary mega-sequence over diapirs indicates Quaternary through Recent up dip gravity spreading. There is a close association between the location of Quaternary and bathymetric canyons and rejuvenated diapirs and their folded overburden, with most canyons located above the synclinal fold located on the flank of the diapir. This association indicates that folding plays a strong influence on sedimentation patterns.

The Quaternary mega-sequence is cut by a number of minor sedimentary faults. The faults show a wide range of shapes and forms varying from curved and listric to planar and domino-style and have only minor vertical offset (less than 100ms TWT). Growth strata associated with these faults is not imaged on the seismic data used in this study. The faults are commonly associated with triangular depressions at the tip point of the fault. These depressions have been interpreted as pock-marks controlled by a network of syn-sedimentary minor faults acting as potential conduits for fluid flow. The spatial distribution of the pockmarks is impossible to determine due to the coarse seismic grid spacing. However, in view of their association with minor faults it is likely that in plan view, these pock-marks are either linear anomalies caused by leakages along faults or circular anomalies caused by point leakages at the intersection of two faults. Some

Quaternary faults have structural relief on the sea floor suggesting that they are still active in certain areas of the basin.

## 6.2 Implications for a Scotian Slope Petroleum System

A petroleum system is a natural geologic assemblage that encompasses active hydrocarbon producing source rock and all related quantities of oil and gas. A “working” petroleum system is one which has produced commercial accumulations of hydrocarbons. For petroleum system to “work” it must include all elements (source rock, reservoir and seal) and processes (trap formation, burial, hydrocarbon generation, and migration) that are necessary for hydrocarbon accumulation. The relative timing of the elements and processes within a petroleum system, in particular the formation of a trapping mechanism before the generation and migration of hydrocarbons, is essential if the system is to accumulate hydrocarbons.

Numerous large structural traps have been mapped within the study area. However, due to the limited well control in the Scotian Slope Basin and lack of regional geochemical studies, the presence of each of the other elements and process required for working petroleum system is mostly speculative.

### *Reservoir*

The presence of reservoir rock on the Scotian Slope can be predicted by extrapolation of known Scotian Shelf lithostratigraphy and analogy of slope seismic sequences to other related basins in the world. Play types on the Scotian Slope are

typical of passive margins modified by salt tectonics driven by sediment loading, and requiring deep water turbidite sands for reservoir (Kidston et al., 2002).

Within the central slope map area several major submarine canyons are observed on the seafloor and several channels and paleo-valleys can be mapped in the subsurface, particularly within the Late Cretaceous and Tertiary depositional sequences 5-9 (See Chapter 3). These channels may have provided conduits for coarse grained turbidite fan deposits or may themselves contain sand rich levees or fill.

Turbidite channels with levees are mapped within the upper and middle slope regions. The shape of the channels, with moderate levee height and width to depth ratio, suggests these channels were depositional and transported sand to mud sized sediment (Figure 6-4; Galloway, 1998). The channels cannot be mapped through the lower slope diapiric province. It is possible that they extend through this area as bypass channels, but are not imaged due to aliasing (relatively small size of the channels as compared to the coarse seismic grid spacing) or poor seismic resolution within the diapiric province. Alternatively, the channels may not bypass the diapiric province, but rather spill in to lobe deposits, possibly concentrated in areas of negative relief on seafloor within salt withdrawal minibasins. The latter model is preferred since leveed channels, typically formed up dip from channel/lobe complexes, are mapped within the middle slope region and suggest the presence of depositional lobes immediately down dip (Figure 6-4). Late Cretaceous to Early Tertiary turbidite channels and associated lobe deposits concentrated within salt mini-basins are considered one of the most promising reservoir targets on the Scotian Slope (Kidston et al., 2002).



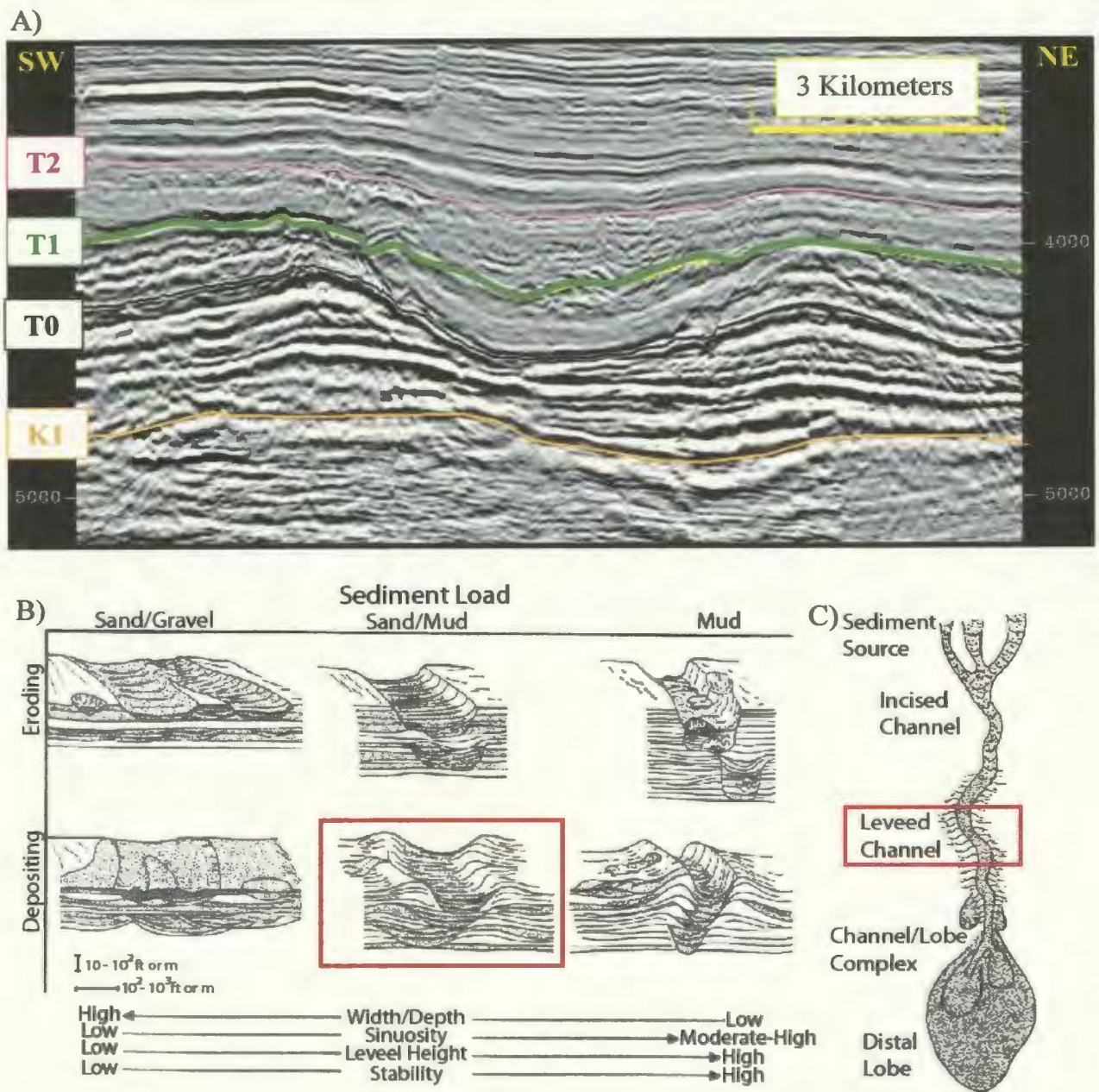


Figure 6-5: A) Portion of seismic strike line from the central middle slope region with example of channel and levee. B) Spectrum of turbidite channels contrasting the geometric and depositional attributes of erosional and depositional types as a function of texture and sediment transport (Galloway, 1998). The shape of the channel/levee (A), with moderate levee height and width to depth ratio indicates that the channel was depositional, and likely transported a sand/mud mixture. C) Geomorphic elements of a turbidite channel/lobe complex (Galloway, 1998). The presence of the depositional leveed channel complex (A) suggests the presence of a channel/lobe complex down dip.

Source

Kidston et al. (2002) identified 6 potential source rocks contained in the Scotian

Slope Basin:

1. Logan Canyon Formation: Cretaceous (Albian – Cenomanian; Upper DS4)
2. Verrill Canyon Fm: Cretaceous (Berriasian – Valanginian; Middle DS4)
3. Verrill Canyon Formation: Jurassic (Kimmeridgian – Oxfordian; Lower DS4)
4. Misaine Member /Abenaki Fm: Jurassic (Callovian; Upper DS3)
5. Mohican Fm (Lacustrine): Jurassic (Toarcian – Bajocian; Middle DS3)
6. Early Syn-rift and Post-rift Lacustrine: Triassic (Carnian – Norian; DS1) and Jurassic (Toarcian – Bajocian; Middle DS3)

The first three intervals are well documented from wells in the Sable Sub-Basin.

The Jurassic Verrill Canyon Formation is the most important source for the sub-basin (Kidston et. al., 2002). It contains terrestrially derived Type III organic matter, and has a relatively low organic richness ranging from 0.55% to 2.25% (Powell, 1982). The Misaine Member, Abenaki Formation has been identified through drilling as a source rock on the shelf and correlated to its deepwater equivalent from results of the Deep Sea/Ocean Drilling Projects elsewhere in the Atlantic basin (Kidston et al., 2002). The remaining 2 source rock intervals are conceptual (Kidston et al, 2002) and based on regional geology correlations.

#### *Timing of Maturation*

Geochemical analysis and 1D modeling by Mukhopadhyay (2002) indicate the potential for multiple source rock intervals on the Scotian Slope. Burial history plots



place the mature oil window at 5000-6000 m burial depth and main gas generation window beginning at ~ 6250 m (Figure 6-6). This analysis indicates that the main expulsion event for hydrocarbons within the Central Scotian Slope occurred from 90 to 60 Ma during the Late Cretaceous period of increased rate of thermal subsidence. The two conceptual intervals, the early-middle Jurassic Mohican Formation and Triassic syn-rift lacustrine, are modeled as prolific hydrocarbon producers if they are present. The Misaine Member of the Abenaki Formation as well as two Verrill Canyon Formation intervals, all have the potential to generate significant hydrocarbons. The model shows the Late Cretaceous Logan Canyon as immature.

An isochron map of the J2 Sequence Boundary to the Water Bottom was constructed to roughly estimate the hydrocarbon potential of the mapped study area (Figure 6-7). The J2 Sequence Boundary was used as the base of the isochron because it approximately coincides with the Kimmeridgian Verrill Canyon Formation, the proven source rock of the adjacent Sable sub-basin (Figure 6-2). A velocity of three kilometers/second was used to depth convert the isochron map to an isopach map. This value is in the range of average velocity for the Kimmeridgian on the slope and shelf of North Atlantic Canadian Basins (Enachescu, 2004). This depth conversion is intended only as a first approximation to highlight the most probable area for source rock maturation.

The general thickness distribution pattern demonstrates an overall thickening toward the northeast and thinning toward the southwest. Based on Mukhopadhyay's (2002) assessment of hydrocarbon generation on the slope vs. depth of burial, the mapped



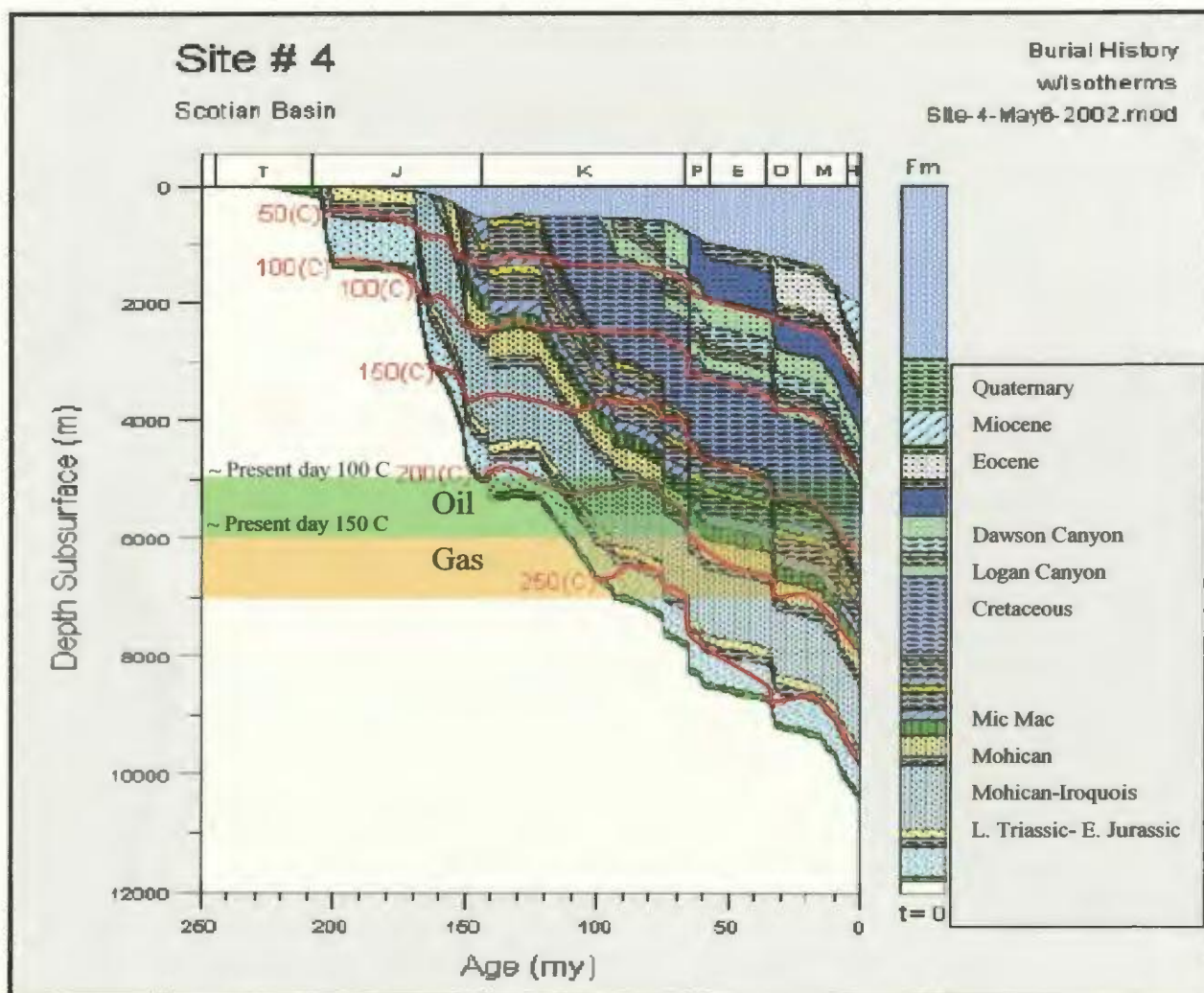


Figure 6-6: Burial history profile for the western-central Scotian Slope. Isotherms are in 50 C increments (modified form Mukhopadhyay, 2002)

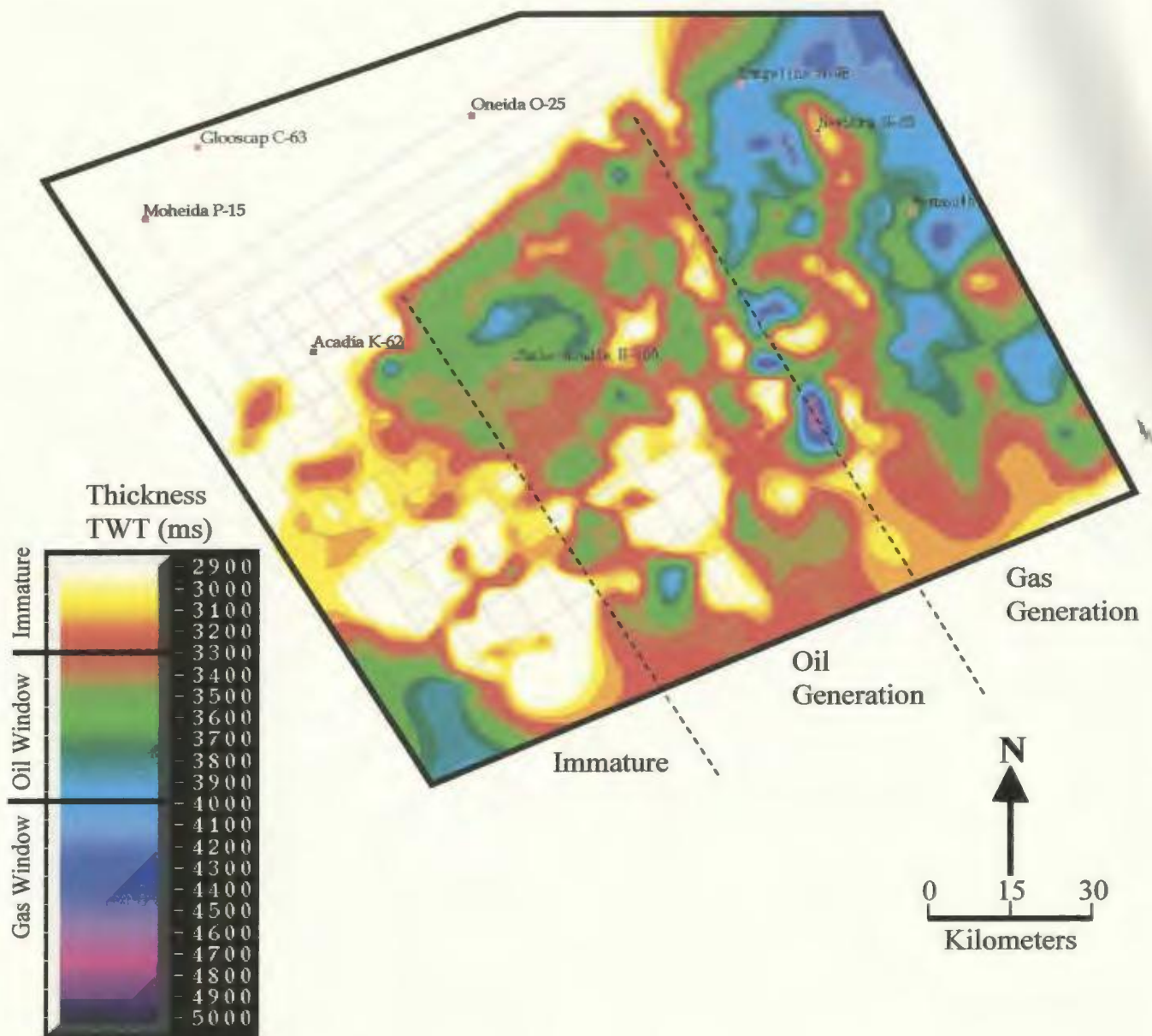


Figure 6-7: Isochron map of Sequence Boundary J2 to Water Bottom. The Vertical scale is in TWT (ms). A tentative depth conversion using a velocity of 3 km/s indicates areas where hydrocarbons would be generated if: < 5000 m = Immature, 5000 – 6000 m = oil window, and > 6000 m = gas window (hydrocarbon generation depth after Mukhopadhyay, 2002)

area can be divided into three slope perpendicular fairways on the basis of the potential for hydrocarbon generation: 1) the western map area appears to be immature, 2) the central is within the oil generating window, and 3) the east within the gas generating window.

Upon comparing the J2 Sequence Boundary-Water Bottom isochron map to the individual isochron maps of depositional sequences 4-9 (see Chapter 3) it is apparent that the major control on the depth of burial of the J2 Sequence Boundary is the thickness and distribution pattern of Depositional Sequence 4 (Cretaceous). DS4 generally thickens to the east in proximity to the Sable Delta. Thus in accordance with Figure 6-7, the closer to the Sable Delta, the thicker the J2 Sequence Boundary overburden, and the more mature the potential Kimmeridgian-Oxfordian (and older) source rock. Also, the closer to the Sable Delta, the better the chance to encounter coarse turbidite sands on the slope.

#### *Timing of Structural Trap Formation*

Within the mapped area of the central Scotian Slope Basin there is a great variety in the size, shape, and genesis of tectonic and halotectonic structures (see chapters 4 and 5). The structures, however, can be collectively classified according to their timing of formation into one of the six tectono-stratigraphic mega-sequences defined in section 6.1 (Figure 6-2):

- Pre-Mesozoic structures were primarily formed by orogenesis. Potential Paleozoic salt structures are imaged in the seismic data, but do not affect the Mesozoic basin fill.



- Late Triassic to early Jurassic structures constitute folded and onlapping strata over basement structures
- Middle to Late Jurassic structures are characterized by rollovers anticlines and growth strata associated with listric faulting and turtle structures associated with episodic salt withdrawal.
- Cretaceous structures are formed by allochthonous salt sheets emplaced at that time.
- Tertiary structures were formed due to diapir rejuvenation, and consist of anticlinal folded Tertiary strata located over salt diapirs, and upturned Cretaceous strata that flank the squeezed diapir.
- Quaternary structures are generally negligible and consist of anticlinal folded strata over salt diapirs in response to minor diapir rejuvenation and/or minor gravity faulting

Upon considering the ages of potential source rock intervals and the timing of hydrocarbon generation as calculated by Mukhopadhyay (2002) four tectono-stratigraphic mega-sequences were identified as containing potential hydrocarbon traps. Only those structures that formed subsequent to the deposition of the oldest potential source rock (Triassic Carnian – Norian) *and* prior to the conclusion of hydrocarbon generation and migration (Late Cretaceous) would be potential successful hydrocarbon traps.

Pre-Mesozoic structures are not considered potential structural traps as they are older than and lie stratigraphically below the earliest source rock interval, thus would not be on the migration pathway of rising hydrocarbons. All other tectono-stratigraphic mega-sequences are younger than the potential Triassic source rock, and therefore could theoretically trap hydrocarbons generated from this interval.

All structures formed as a result of Tertiary diapir rejuvenation including anticlinal folded Tertiary strata located over salt diapirs, and Cretaceous strata flanking squeezed diapir that was upturned during the Tertiary, were formed subsequent to hydrocarbon generation and thus would not have the potential to trap hydrocarbons generated during the Cretaceous. Rare Tertiary allochthonous salt sheets were also not emplaced until after the main episode of hydrocarbon generation and thus would not have been able to trap migrating Cretaceous hydrocarbons.

Late Triassic to early Jurassic basement related structures, Middle to late Jurassic rollovers anticlines and growth strata associated with listric faulting and turtle structures associated with episodic salt withdrawal all formed prior to hydrocarbon generation and thus, on the criteria of timing alone would constitute good traps. The potential of Late Cretaceous allochthonous salt sheets to act as traps is dependent on the exact timing of salt emplacement in relation to the generation and migration of hydrocarbons. Most allochthonous salt was emplaced during the Late Cretaceous and therefore would have been able to trap subsequent hydrocarbons that migrated during the "later" Cretaceous.

### *The Potential Hydrocarbon System*

Considering all the elements and processes necessary for working hydrocarbon system, the most likely plays within the mapped study area consist of: 1) a reservoir of Cretaceous to Tertiary turbidite channel, levee or lobe sands, 2) a source rock most likely within the Kimmeridgian Verrill Canyon Formation (possible contribution from Jurassic Mohican Formation or Late Triassic to Early Jurassic early Syn-rift and/or Post-rift Lacustrine deposits, 3) a seal of Verrill Canyon Formation , Dawson Canyon or Banquereau shale (see Figure 6-2) or allochthonous salt, and 4) structural, tectonic and/or halokinetic traps ranging from Triassic to Cretaceous in age.

Due to the increased Jurassic overburden thickness toward the east (in proximity to the paleo-Sable Delta) the area of presently mature oil source rock would be located within the central map area, and mature gas source rock to eastern map area (Figure 6-7). Finally, as the main expulsion event for hydrocarbons within the Central Scotian Slope occurred from 90 to 60 Ma during the Late Cretaceous period, the targeted structural traps should be Late Triassic to Early Jurassic folded, draped, or and onlapping strata over basement related structures, Middle to Late Jurassic rollover anticlines and growth strata associated with Middle to Late Jurassic listric faulting, turtle structures associated with episodic salt withdrawal, or Late Cretaceous sub-salt traps.

The validity of a Scotian Slope hydrocarbon system within the study area has been tested twice in recent years by the Newburn H-23 and Weymouth A-45 exploration wells. Both wells were drilled in the eastern portion of the study area, and both came out dry. The main reason for the failure (from personal communications) was lack of



reservoir. The well locations were chosen by their respective oil companies based on high quality 3D seismic surveys. Lithological prediction and AVO studies were most likely conducted prior to drilling indicating the presence of reservoir. Failure to discover hydrocarbons in the wells may point to the limitations of seismic resolution to predict reservoirs within the late Jurassic-Early Cretaceous successions. It also shows that drilling on the Scotian Slope is high risk exploration; that more regional studies are needed, better correlation of seismic with lithologies encountered in the wells, etc.

## Chapter 7

### Conclusions and Recommendations for Future Work

#### 7.1 Justification for the Study

The continental shelf and slope of Nova Scotia is underlain by a number of interconnected rift sub-basins that collectively form the Scotian Basin. Petroleum exploration companies have been moderately successful on the shelf region of the basin, close to Sable Island, where several significant hydrocarbon discoveries have lead to the development of Sable Project. This success has sparked interest in exploration of the adjacent frontier slope region within water depths between 200 and 2500m.

In the Scotian Slope Basin there have been limited regional studies on the structural, tectonic and stratigraphic framework of the area. Results of the half dozen exploration wells drilled recently on the slope and abandoned without economic discoveries, have just recently been made public or are still confidential. Therefore no integration of modern well results and seismic data exists at this time. Present accounts of the Scotian Slope are largely extrapolated from shelf descriptions and/or modeled after play types and depositional systems typically associated with deep water exploration in other Atlantic margin areas such as the Gulf of Mexico and West Africa (Figure 1-2). The most complete geological papers on the Scotian Slope structure and seismic-stratigraphy are by Kidston et. al (2002) and Loudon (2002). Both papers are regional accounts of the entire Scotian Slope Basin and were used as the primary references in this thesis. However, regional generalization made in the papers often fails to account for the detailed stratigraphic and structural character, relationships and architectures observed in the mapped study area of this thesis.

## 7.2 Key Conclusions

Geological Evolution - Scotian Basin development commenced in the Late Triassic to Early Jurassic with rifting of the Pangean Supercontinent and separation of North America and Africa. Red bed and evaporate deposition characterized the rift phase, while the drift phase started in Mid Jurassic was characterized by clastic progradational with periods of carbonate deposition (Figure 2-3). A prominent carbonate bank developed in the western part of the basin during the Late Jurassic, the eastern extent of which was limited by a Late Jurassic to Early Cretaceous major deltaic depocenter located in the Sable Island. Major transgressive sequences were deposited as relative sea level rose throughout the Late Cretaceous and Tertiary. This overall transgression was punctuated by major sea level drops resulting in the deposition of regressive lowstand sequences partially comprising turbidite deposits.

Seismic Stratigraphy- A TGS NOPEC 6 by 6 kilometer seismic grid and well information were used in this study. Ten major sequence boundaries were identified by their reflection character and termination patterns. They divide the Mesozoic through Cenozoic Scotian Basin fill into nine depositional sequences (DS1-DS9; Figure 3-4). There is a major change in the style and thickness distribution patterns of the depositional sequence through time.

- *Depositional sequences 1-3* (Late Triassic to Late Jurassic) are contained in local, deep mini-basins primarily related to basement structure and salt movement.
- *Depositional Sequence 4* (Early to Late Cretaceous) has a fairly uniform thickening trend towards the east in proximity of the paleo-Sable Delta.



- The thickness distribution pattern of *Depositional Sequence 5* (latest Cretaceous) has a slope parallel fabric, and is primarily controlled by sub aqueous channels associated with the base Tertiary unconformity that marks the top of the sequence.
- *Depositional sequences 6-9* have regional paleo depocenters that successively overstep each other in a landward direction. These sequences are characterized by large paleo-channels.

Tectonics - Five fault families are defined within this study on the basis of their regionality, duration of movement and depths of detachment (Figure 4-2).

- *The Slope Basin-Bounding Fault Family* consists of a series of normal, downthrown to the basin, extensional faults located beneath the hinge zone of the Scotian Margin. Faults within this fault family mark the seaward limit of the Jurassic carbonate bank and generally tip at the Top Abenaki Formation seismic marker or Sequence Boundary J2.
- *The Basement-Involved Fault Family* is located in the hanging wall of, and soles into, the Basin-Bounding Fault Family. Faults of this family tip at or below the J2 Sequence Boundary. Basement-Involved Faults delineate the structural units in the map area by sub-dividing the basin into: a) asymmetric half-grabens filled with syn-rift sediments, b) symmetric grabens filled with syn-rift sediments, and c) horsts, bounded by onlapping sediments.
- *The Listric Growth Fault Family* consists of a series of normal sense listric faults that sole into the top of or within the autochthonous evaporite unit. These faults

exclusively deform Late Triassic to Late Jurassic stratigraphy, and tip at or below the J2 Sequence Boundary.

- *Major and minor sedimentary faults* strike southwest- northeast, vary in shape from slightly curved to listric and dip either basinward or landward. These faults are commonly spatially associated with and trend parallel to, basin-bounding and basement-involved faults and are contained within Tertiary and Quaternary stratigraphy where they may be associated with pockmarks.
- *Halokinetically induced faults* form due to the protracted movement of salt and may occur in any level of basin fill.
- The existence of a sixth fault family, the Transfer Fault Family, is implied by a change in major fault lineament orientation through the center of the map area, and by the offset of the landward limit of diapiric salt structures across the central map area. The signature of this potential transfer fault is not clear enough on the available seismic data to allow for confident mapping.

Salt Tectonics - The complete spectrum of salt structures typical of passive margins have been identified and mapped within the study area. Five halotectonic structural associations with variable areal distributions have been identified (Figure 5-5). These associations are: *the Trough and Swell Association, the Intra-Salt Detachment Association, the Diapiric Association, the Secondary Weld Association, and the Allochthonous Salt Association.*

- Most observed salt structures, regardless of their “association”, are located over basement faults indicating that initial salt movement was largely controlled by basement structure.
- The map distribution of salt associations indicates that gravity process related to the tilting of the slope played a major factor in the style and distribution of salt structures.
  - The Trough and Swell and the Intra-Salt Detachment associations characterize the extensional strain domain of the upper slope region.
  - The Diapiric, Secondary Weld and Allochthonous Salt associations characterized the compressional stress domain of the lower slope region.
  - The middle slope contains styles typical of all associations and is considered a transition zone between extensional and compressional domains.
- The general lack of syn-halokinematic growth strata indicates that diapirism was primarily passive, and the relative rate of diapir growth approximately equal to the relative rate of sedimentation.
- The strong association between diapirs and folded overburden, with diapirs located in the crest of folds indicates that there was a significant episode of post-halokinematic diapir rejuvenation.

#### The Potential Hydrocarbon System

Considering all the elements and processes necessary for working hydrocarbon system, the most likely plays within the mapped study area consist of:



- A reservoir of Cretaceous to Tertiary turbidite channel, levee or lobe sands
- A source rock most likely within the Kimmeridgian Verrill Canyon Formation (possible contribution from Jurassic Mohican Formation or Late Triassic to Early Jurassic early Syn-rift and/or Post-rift Lacustrine deposits)
- A seal of Verrill Canyon Formation , Dawson Canyon or Banquereau shale (see Figure 6-2) or allochthonous salt
- Structural, tectonic and/or halokinetic traps ranging from Triassic to Cretaceous in age.
- The area of presently mature oil source rock is located within the central map area, and mature gas source rock in the eastern map area (Figure 6-5).
- As the main expulsion event for hydrocarbons within the Central Scotian Slope occurred during the Late Cretaceous period, the targeted structural traps should be Late Triassic to Early Jurassic folded draped or and onlapping strata over basement related structures, Middle to Late Jurassic rollover anticlines and growth strata associated with Middle to Late Jurassic listric faulting, turtle structures associated with episodic salt withdrawal, or Late Cretaceous sub-salt traps.
- Failure to discover hydrocarbons in recent slope exploration wells may point to the limitations of seismic resolution to image reservoirs within the late Jurassic- Early Cretaceous successions, and shows that drilling on the Scotian Slope is high risk exploration; that more regional studies are needed, better correlation of seismic with lithologies encountered in the wells must be performed after well data becomes public, eventually using the new 3D coverage existing in the area.

### 7.3 Recommendations for Future Work

There are several areas in which future work could significantly enhance the results of this project.

1) A seismic facies analysis of the seismic sequences defined in Chapter 3 to better delineate the depositional environments of the slope and provide a basis for prediction of potential reservoir facies. Seismic data used in this study should be reprocessed pre-stack data and tied to all slope wells.

2) Balanced 2D structural restorations of select seismic lines to provide additional constraints on the seismic interpretations presented in this project. These constrictions would better illustrate the influence of tectonics and halotectonics on depositional patterns throughout the evolution of the basin.

3) Seismic interpretation presented in this project should be checked against newly available well data. Namely, the Newburn H-23 well, located in the eastern map area, which becomes publicly available in fall, 2004, and the Weymouth A-45 well also located in the eastern map area, which becomes publicly available the spring of 2006.

4) A petroleum geology study, including geochemical analysis using samples from slope wells, followed by basin modeling using adequate seismic sequences dating and true thicknesses.

## References

- Alsop, G. I., Brown, J.P., Davison, I. D, and Gibling, M. R., 2000: The geometry of drag zones adjacent to salt diapirs, *Journal of the Geological Society, London*, vol. 157, p. 1019-1029.
- Ascoli, P., 1988, Mesozoic-Cenozoic foraminiferal, ostracod, and calpoinellid zonation of the north Atlantic margin of North America: Georges Banks – Scotian basins and northeastern Grand Banks (Jeanne d’Arc, Carson and Flemish Pass basins). Biostratigraphic correlation of 51 wells: Geological Survey of Canada, Open File 1791, 41 p.
- Barrett, D. L., Berry, M, Blanchard, J. E., and Keen, M. J., 1964: Seismic studies on the eastern seaboard of Canada: the Atlantic Coast of Nova Scotia, *Canadian Journal of Earth Science*, vol. 1, p. 10-22.
- Bell, J.S., and Campbell, G.R., 1990: Petroleum resources, Chapter 12 *in* *Geology of the continental margin of Eastern Canada*, M.J. Keen and G.L. Williams (ed); Geological Survey of Canada, no. 2, 677-720 (also Geological Society of America, *The Geology of North America*, vol.I-1).
- Berry, J. A., and Piper, D. J. W., 1993: Seismic stratigraphy of the central Scotian Rise: a record of continental glaciation, *Geo-Marine Letters*, vol. 13, p. 197-206.
- Bhattacharyya, B. K., and Raychaudhuri, B., 1967, Areomagnetic and geological interpretation of a section of the Appalachian belt in Canada, *Canadian Journal of Earth Science*, vol. 4, p. 1015-1037.
- Bower, M. E., 1962: Sea magnetometer surveys off southwestern Nova Scotia, from Sable Island to St. Pierre Bank, and over Scatarie Bank, Geological Survey of Canada. Paper 62-6, p. 13.
- Bujak Davies Group Limited, 1988, Palynological analysis of the Scotian Shelf wells, Geological Survey of Canada, Open Files, 1857 to 1868.
- Carvalho, J., Sr. and Kuilman, W. K., Sr., 2003, Deepwater Angola; seafloor pock-marks as hydrocarbon indicators?, Abstract, 2003 AAPG International Conference & Exhibition Technical Program, [http://aapg.confex.com/aapg/barcelona/techprogram/paper\\_83568.htm](http://aapg.confex.com/aapg/barcelona/techprogram/paper_83568.htm), (20 May 2004).
- Canada-Nova Scotia Offshore Petroleum Board, 2004, Maps: Active Exploration Licenses in the Nova Scotia Offshore Area, [http://www.cnsopb.ns.ca/maps/pdf/web\\_map\\_full\\_size.pdf](http://www.cnsopb.ns.ca/maps/pdf/web_map_full_size.pdf) (2 April 2004)



- Dehler, S. A., and Keen, C. E., 2001, Magnetic signature of a non-volcanic margin transition off Atlantic Canada. American Geophysical Union, Eos Transactions, 82 (47), Fall Meeting Supplement, Abstract T52A-0910 (AGU Fall Annual Meeting, San Francisco)
- Dehler, S. A., and Keen, C. E., 2002, A fresh look as the evolution of the continental margin off Nova Scotia, Canadian Society of Petroleum Geologists Diamond Jubilee Convention, June 2002, Calgary AB (Extended Abstract)
- Diegel, F. A., Karlo, J. F., Schunster, D. C., Shoup, R. C., and Tauvers, P. R., 1995, Cenozoic structural evolution and tectono-stratigraphic framework of the northern Gulf Coast Continental Margin, *in* M. P. A., Jackson, D. G., Roberts, and S. Snelson, eds., Salt Tectonics: a global perspective: AAPG Memoir 65, p. 109-151.
- Dolph, D. A., Hogg, J.R., Harland, N.J., Syhlonyk, G. E., Mackidd, D. G., 2001: An overview of petroleum systems in the Scotian Basin, offshore Nova Scotia, Canada, AAPG Annual Meeting Abstract, June 3-6, 2001, Denver Colorado.
- Drake, C. L, Worzel, J. L., and Beckman, W. C., 1954: Geophysical investigations in the emerged and submerged Atlantic coastal plain. Pt. IX, Gulf of Maine. Geological Society of America, Bulletin 65, p. 957-970.
- Emery, K. O., and Uchupi, J. D., 1965: Structure of the Georges Bank, Marine Geology, vol. 3, 532 p.
- Emery, K. O., Uchupi J, D., Phillips, J. D., Bowin, C. O., Bruce, E. T., and Knott, S. T., 1970: Continental rise off Eastern North America, American Association of Petroleum Geology, vol. 54, p. 44-108.
- Enachescu, M. E., 1987, Tectonic and structural framework of the Northeast Newfoundland Continental Margin, *in* Beaumont, C. and Tankard, A. J. (Eds.), Sedimentary basins and basin-forming mechanisms, Canadian Society of Petroleum Geologists, Memoir 12 (1987), p. 117-146.
- Enachescu, M. E., 2004, personal communication.
- Galloway, W. E., 1986, Growth faults and fault-related structures of retrograding terrigenous clastic continental margins, Transactions-Gulf Coast Association of Geological Studies, vol. XXXVI, p.121-128.
- Galloway, W.E, 1998, Siliciclastic slope and base-of-slope depositional systems: component facies, stratigraphic architecture, and classification, AAPG Bulletin, vol. 82, p. 596-595.

- Gauley, B. J., 2001, Lithostratigraphy and sediment failure on the central Scotian Slope, unpublished M.Sc. thesis, Dalhousie University.
- Geological Survey of Canada, 1991, East Coast Basin Atlas Series: Scotian Shelf, Atlantic Geoscience Centre, 152 p.
- Ge, H., Jackson, M. P. A., and Vendeville, B. C., 1997, Kinematics and dynamics of salt tectonics driven by progradation: The American Association of Petroleum Geologists Bulletin, vol. 81, no. 3, p. 398-423.
- Giles, K. A., Lawton T. F., Rowan. M. G., 2003, Halokinetic sequences, Geological Society of America Abstracts with Programs, vol. 35, no. 6, September 2003, p. 642.
- Giles, K. A., Lawton, T. D., and Rowan, M. G., 2004, Halokinetic sequences within a depositional sequence stratigraphic framework, 2004, AAPG Annual Meeting 2004 Abstract.
- Hardy, I. A., 1975, Lithostratigraphy of the Banquereau Formation of the Scotian Shelf: offshore geology of Eastern Canada, Volume 2 – Regional Geology, Geological Survey of Canada, paper 74-30, p.163-174.
- Hill, P. R., and Bowen, A. J., 1983, Modern sediment dynamics at the shelf slope boundary, Nova Scotia, *in* The shelf break, critical interface on continental margins, ed. D. J. Stanley and G. T. Moore. Society of Economic Palaeontologists and Mineralogists Special Publication no. 33, p. 265-276.
- Hongxing, G, Jackson, M.P.A, and Vendeville, B.C, 1997, Kinematics and dynamics of salt tectonics driven by progradation, AAPG Bulletin, vol. 81, no. 3, p. 398-423.
- Hogg, J.R., 2000, An overview of exploration trends in the Scotian Basin offshore Nova Scotia, Canada, AAPG Eastern Section Meeting Abstract, September 24-26, 2000, London Ontario, Canada.
- Hogg, J. R., 2003, Exploration offshore Nova Scotia Canada: recent exploration drilling and future potential, Abstract, AAPG Annual Convention, Salt Lake City, Utah, May 11-14, 2003
- Hogg, R. H., Dolph, D. A., Mackidd, D., Michel, K., 2001, The Scotian Salt Province, and unexplored deepwater salt basin, AAPG Annual Meeting Abstract, June 3-6, 2001, Denver, Colorado.
- Howie, R. D., and Barss, M. S., 1975, Upper Palaeozoic rocks of the Atlantic provinces,



- Gulf of St. Lawrence and adjacent continental shelf; *in* Offshore Geology of Eastern Canada, Volume 2, Regional Geology, ed. W. J. M. van der Linden and J. A. Wade; Geological Survey of Canada, Paper 74-30, vol.2, p. 35-50.
- Hood, P., 1966a, Magnetic surveys of the continental shelves of Eastern Canada: in Continental Margins and Island Arcs; ed, W. H. Poole; Geological Survey of Canada, Paper 66-15, p. 19-32.
- Hood, P., 1966b, Ship and airborne magnetometer results from the Scotian Shelf, Grand Banks, and Flemish Cap, Maritime Sediments, vol. 2, p. 15-19
- Jackson, M. P. A., 1995, Retrospective salt tectonics, *in* M. P. A. Jackson, D. G. Roberts, and S. Snelson, eds., Salt tectonics: a global perspective: AAPG Memoir 65, p. 1-28.
- Jackson, M. P. A., and Cramez, C., 1989, Seismic recognition of salt welds in salt tectonic regimes: SEPM Gulf Coast Section Tenth Annual Research Conference Program with Abstracts, Houston, Texas, p. 66-71.
- Jackson, M. P. A., and Talbot, C. J., 1986, External shapes, strain rates, and dynamics of salt structures: Geological Society of America Bulletin, vol. 97, p. 305-328.
- Jackson, M. P. A., and Talbot, C. J., 1991, A glossary of salt tectonics, Bureau of Economic Geology, Geological Circular 91-4
- Jackson M. P. A., and Vendeville, B. C., 1994, Regional extension as a geologic trigger for diapirism: Geological Society of America Bulletin, vol. 106, p. 57-73.
- Jansa, L. F. and Wade, J. A., 1975, Geology of the continental margin off Nova Scotia and Newfoundland: offshore geology of Eastern Canada, Volume 2 – Regional Geology, Geological Survey of Canada, paper 74-30, p.51-106.
- Keen, C. E., and Loncarevic, B. D., 1966, Crustal structure on the eastern seaboard of Canada: studies on the continental margin; Canadian Journal of Earth Science, vol.3, p. 65-76.
- Keen, C. E., and Kay, W. A., 1991, Deep seismic reflection data from the Bay of Fundy and Gulf of Maine: tectonic implications for the northern Appalachians, Canadian Journal of Earth Science, vol.28, p. 1096-1111.
- Keen, C. E., MacLean, B. C., and Kay, W. A., 1991, A deep seismic profile across the Nova Scotia continental margin, offshore Eastern Canada, Canadian Journal of Earth Science, vol. 28, p. 1112-1120.



- Keen, C. E., and Potter, D. P., 1995, Formation and evolution of the Nova Scotia rifted margin: evidence from deep seismic reflection data, *Tectonics*, vol. 14, p. 918-932.
- Kidston, A. G., Brown, D. E., Altheim, B., and Smith, B. M., 2002, Hydrocarbon potential of the deep-water Scotian Slope, Canada-Nova Scotia Offshore Petroleum Board report, October 2002, Version 1.0.
- King, L.H. and MacLean, B., 1970, A diapiric structure near Sable Island-Scotian Shelf. *Maritime Sediments* 6, p. 1-4.
- Larson, P. H., 1988, Relay structures in a Lower Permian basement-involved extensional system, east Greenland: *Journal of Structural Geology*, vol. 10, p. 3-8.
- Letouzey, J., Colletta B., Vially, R., and Chermette, J. C., 1995, Evolution of salt-related structures in compressional settings, *in* M. P. A. Jackson, D. G. Roberts, and S. Snelson, eds., *Salt Tectonics: a global perspective: AAPG Memoir 65*, p. 41-60
- Lister, G. S., Etheridge, M. A., and Symonds, P. A., 1986, Detachment faulting and the evolution of passive continental margins, *Geology*, vol. 14, p. 246-250.
- Louden, K., 2002, Tectonic evolution of the east coast of Canada, *CSEG Recorder*, February, 2002, p. 37-48.
- MacLean, B. C., and Wade, J. A., 1993, East coast basin atlas series: seismic markers and stratigraphic picks in Scotian Basin wells. Atlantic Geoscience Centre, Geological Survey of Canada, 276 p.
- Magnusson, D. H., 1973, The Sable Island deep test of the Scotian Shelf; in *Earth Science Symposium on Offshore Eastern Canada*, ed P. J. Hood; Geological Survey of Canada, paper 71-23, p. 253-266.
- McGuinness, D. B., and Hossack, J. R., 1993, The development of allochthonous salt sheets as controlled by the rates of extension, sedimentation and salt supply, *in* Armentrout, J. M., Bloch, R., Olsen, H. C., and Perkins, B. F., eds., *Rates of Geological Process: Fourteenth Annual Research Conference, Gulf Coast Section, SEPM Foundation, Program with Papers*, p. 127-139
- McIver, N. L., 1972, Cenozoic and Mesozoic stratigraphy of the Nova Scotia shelf. *Canadian Journal of Earth Science* 9, p 54-70.
- Mitchum, R. M., Jr., Vail, P. R., and Sangree, J. B., 1977, Seismic stratigraphy and global changes of sea level, Part 6: Stratigraphic interpretation of seismic reflection patterns in depositional sequences, *Seismic Stratigraphy: Applications*

to Hydrocarbon Exploration. C. E. Payton, American Association of Petroleum Geologists, Tulsa. AAPG Memoir 26, p. 117-133.

Mukhopadhyay, P. K., 1995, Organic petrography and kinetics of Jurassic/Cretaceous shales and geochemistry of selected liquid hydrocarbons, Scotian Basin. Geological Survey of Canada Open File Report no. 3284.

Mukhopadhyay, P. K., 2002, Evaluation of petroleum systems of five dummy wells from various seismic sections of the Scotian Slope, Offshore Nova Scotia, based on one-dimensional numerical modeling and using geochemical concepts, Canadian-Nova Scotia Offshore Petroleum Board confidential internal report *in* Kidston, A. G., Brown, D. E., Altheim, B., and Smith, B. M., 2002, Hydrocarbon potential of the deep-water Scotian Slope, Canada-Nova Scotia Offshore Petroleum Board report, October 2002, Version 1.0.

Mukhopadhyay, P. K. and Wade, J. A., 1990, Organic facies and maturation of sediments from three Scotian Shelf Wells. Bulletin of Canadian Geology, vol. 38, no. 4, p 407-424.

Mukhopadhyay, P.K., Wade, J.A., Kruge, M.A., Samoun, A., Harvey, P. J., 2002 Deepwater petroleum system of Jurassic-Tertiary sediments of the Scotian Basin, offshore Nova Scotia, eastern Canada, AAPG Annual Meeting Abstract, March 10-13, 2002, Houston, Texas

Officer, C. B., and Ewing, M., 1954, Geophysical investigations in the emerged and submerged Atlantic coastal plain. Part III. continental shelf, continental slope and continental rise south of Nova Scotia. Geological Society of America. Bulletin 65: 653-670.

Peel, F. J., Travis, C. J., and Hossack, J. R., 1995, Genetic structural provinces and salt tectonics of the Cenozoic offshore U.S. Gulf of Mexico: A preliminary analysis, *in* M. P. A. Jackson, D. G. Roberts and S. Snelson, eds., Salt Tectonics: a global perspective: AAPG Memoir 65, p. 153-175.

Pickrill, R., Piper, D. J. W., Collins, J., Kleiner, A., Gee, L., 2001, Scotian Slope mapping project: The benefits of an integrated regional high-resolution multibeam survey, paper presentation, Offshore Technology Conference, Houston, Texas, 30 April – 3 May, 2001.

Piper, D. J. W. , Farre, J. A. and Shor, A. N., 1985, Late Quaternary slumps and debris flows on the Scotian Slope, Geological Society of America Bulletin 96: 1508-1517.

Piper, D.J.W., Skene, K.I., and Morash, N., 1999, History of major debris flows on the



- Scotian Rise, Geological Survey of Canada Current Research.  
 Press, F., and Beckmann, W., 1954, Geophysical investigations in the emerged and submerged Atlantic costal plain. Part VIII. Grand Banks and adjacent shelves. Geological Society of America. Bulletin 65: 299-314.
- Powell, T. G., 1982, Petroleum Geochemistry of the Verrill Canyon Formation: a source for the Scotian Shelf hydrocarbons. Bulletin of Canadian Petroleum Geology, vol. 30, p. 167-770.
- Rowan, M. G., 1993, A systematic technique for the sequential restoration of salt structures: Tectonophysics, vol. 288, p. 331-348.
- Rowan, M. G., 1995, Structural styles and evolution of allochthonous salt, central Louisiana outer shelf and upper slope, *in* M. P. A. Jackson, D. G. Roberts and S. Snelson, eds., Salt Tectonics: a global perspective: AAPG Memoir 65, p. 199-228.
- Rowan, M.G., 2002, Practical salt tectonics, Rowan Consulting, Inc. short course, Petroleum Society CIM- Halifax Section, Oct 7-8, 2002, Halifax, Nova Scotia
- Sherwin, D. F., 1973, Scotian Shelf and Grand Banks *in* Future petroleum provinces of Canada, Canadian Society of Petroleum Geologists, Memoir 1, p. 519-559.
- Swift, S. A., 1987, Late Cretaceous-Cenozoic development of the outer continental margin, Southwestern Nova Scotia: The American Association of Petroleum Geologists Bulletin, vol. 71, no. 6, p. 678-701.
- Tankard, A.J., and Balkwill, H.R., 1989, Extensional tectonics and stratigraphy of the North Atlantic: Introduction, AAPG Memoir 46, 1-5.
- Tankard, A.J., and Welsink, H.J., 1989, Mesozoic extension and styles of basin formation in Atlantic Canada, AAPG Memoir 46. 175-195.
- Thomas, F. C., 2001, Cenozoic Micropaleontology of three wells, Scotian Shelf and Slope, Geological Survey of Canada, Open File Report 4014, 36 p.
- Uchupi, E., 1965, Maps showing relation of land and submarine topography, Nova Scotia to Florida, U.S. Geological Survey. Miscellaneous Geology Inventory Map I-451, scale 1:1,000,000, 3 sheets  
 1968, Atlantic continental shelf and slope of the United States – Physiography. United States Geologic Survey, Professional Paper 529-C, 30 p.  
 1969, Marine geology of the continental margin off Nova Scotia, Canada. New York Academy of Science Transactions, Series 2, vol. 31, p. 56-65



- Vail, P. R., R. M. Mitchum, Jr., et al. (1977a). Seismic stratigraphy and global changes in sea level, part 3: Relative changes of sea level from coastal onlap. *Seismic Stratigraphy: Applications to Hydrocarbon Exploration*. C. E. Payton, American Association of Petroleum Geologists, Tulsa. AAPG Memoir 26: 49-62.
- Vail, P. R., R. M. Mitchum, Jr., et al. (1977b). Seismic stratigraphy and global changes in sea level, part 4: Global cycles of relative changes in sea level. *Seismic Stratigraphy: Applications to Hydrocarbon Exploration*. C. E. Payton, American Association of Petroleum Geologists, Tulsa. AAPG Memoir 26: 83-97.
- Vendeville, B. C., and Jackson, M. P. A., 1992a, The rise of diapirs during thin-skinned extension: *Marine and Petroleum Geology* vol. 9, p. 331-353.
- Van Wagoner, J. C., Posamentier, H. W., Mitchum, R. M., Vail, P. R., Sarg, J. F., Loutit, T. S., and Hardenbol, J., 1988, An overview of sequence stratigraphy and key definitions, in Wilgus, C. K., Hastings, B. S., St. Kendall, C. G., Posamentier, H. W., Ross, C. A., and Van Wagoner, J. C., eds., *Sea-level Changes: An integrated approach*, Society Economic Paleontologists and Mineralogists, Tulsa, Oklahoma, Special Publication No. 42, p.39-45.
- Van Wagoner, J. C., Mitchum, R. M., Campion, K.M., and Rahmanian, V.D., 1990, Siliclastic Sequence Stratigraphy in Well Logs, Cores, and Outcrops: Concepts for high-resolution correlation of time and facies, AAPG Methods in Exploration Series, No.7, The American Association of Petroleum Geologists, p. 55.
- Vendeville, B. C., and Jackson, M. P. A., 1992b, The fall of diapirs during thin-skinned extension: *Marine and Petroleum Geology* vol. 9, p. 354-371.
- Wade, J. A., and MacLean, B. C., 1990, The geology of the southeastern margin of Canada, Chapter 5, Part 2: Aspects of the geology of the Scotian Basin from recent seismic and well data. *In: Geology of the Continental Margin of Eastern Canada*. M. J. Keen and G. L. Williams (eds.). Geological Survey of Canada, *Geology of Canada*, no. 2, p. 190-238.
- Wade, J.A., MacLean, B.C. and Williams, G. L., 1995, Mesozoic and Cenozoic stratigraphy, eastern Scotian Shelf: new interpretations, *Canadian Journal of Earth Science*, vol. 32, p.1462-1473.
- Wade, J. A., and Sherwin, D. F., 1990, Offshore schedule of wells: east coast offshore (Nova Scotia/Gulf of St. Lawrence), Davis Strait, Hudson Bay & Hudson Strait, West Coast offshore. Energy, Mines and Resources Canada – Indian and Northern Affairs Canada, Ottawa.

- Welsink, H.J., Dwyer, J.D., and Knight, R.J., 1989, Tectono-stratigraphy of the passive margin of Nova Scotia, AAPG Memoir 46, p. 215-231.
- Williams, H., 1984, Miogeoclines and suspect terrains of the Caledonian-Appalachian orogen: tectonic patterns in the North Atlantic region: Canadian Journal of Earth Sciences, vol. 21, p.887-901.
- Williamson, M. A. and Smyth C., 1992, Timing of gas overpressure generation in the Sable Basin offshore Nova Scotia: implications for gas migration dynamics: Bulletin of Canadian Petroleum Geology, vol. 40, no 2 (June, 1992), p. 151-169.
- Willmore, P. L., and Tolmie, R., 1956, Geophysical observations on the history and structure of Sable Island. Transactions of the Royal Society of Canada, Series 3. Canadian Commission of Oceanography 50, p. 13-20.
- Winker, C. D., 1996, High-resolution seismic stratigraphy of a late Pleistocene submarine fan ponded by salt-withdrawal mini-basins on the Gulf of Mexico continental slope: Offshore Technology Conference Program with Abstracts, p. 619-628.

